TOP SECRET – RUFF

H FILE NO. 4.12

HANDLE VIA TALENT-KEYHOLE CONTROL SYSTEM ONLY

# MISSION 1201

# SENSOR SUBSYSTEM POST FLIGHT ANALYSIS REPORT

## PHOTO RECONNAISSANCE SYSTEMS DIVISION
## OFFICE OF SPECIAL PROJECTS

TCS 354016-71

GROUP 1
Excluded from automatic downgrading and declassification

TOP SECRET – RUFF

## Warning

This document contains information affecting the national security of the United States within the meaning of the espionage laws U.S. Code Title 18, Sections 793 and 794. The law prohibits its transmission or the revelation of its contents in any manner to an unauthorized person, as well as its use in any manner prejudicial to the safety or interest of the United States or for the benefit of any foreign government to the detriment of the United States. It is to be seen only by U. S. personnel especially indoctrinated and authorized to receive information in the designated control channels. Its security must be maintained in accordance with regulations pertaining to the designated controls.

Published By

HQ AIR FORCE SPECIAL PROJECTS PRODUCTION FACILITY

# MISSION 1201

# SENSOR SUBSYSTEM

# POST FLIGHT ANALYSIS REPORT

30 SEPTEMBER 1971

This report consists of 286 pages.

Series B
TCS 354016-71
Cy 16 of 31 Cys

## SECURITY NOTIFICATION

Your attention is directed to the fact that this document contains domestic photography and therefore classified "NOFORN."

POST FLIGHT ANALYSIS REPORT
1201

PUBLICATION REVIEW

This report has been reviewed and is approved.

ROBERT J. KOHLER
PFA Chairman

# FOREWORD

This report was prepared for and by direction of the Director, Photo Reconnaissance Systems, Office of Special Projects. This report constitutes Volume II of the final mission report. Volume I is entitled Performance Evaluation Team, Mission 1201, BYE 15285-71.

The preparation, collection, and reduction of the data in this report has been a joint effort of the Post Flight Analysis (PFA) Team. Major contributors to this report include:

Sections I and II - PFA Team
Section III - Sensor Subsystem Contractor
Section IV - BRIDGEHEAD and AFSPPF
Section V - National Photographic Interpretation Center
Section VI - Sensor Subsystem Project Office and AFSPPF
Section VII - PFA Team

The majority of the raw data collection was accomplished at, and by, AFSPPF. The PFA Team is indebted for the excellent support received from Colonel William E. Callanan, Commander, and his staff.

## TABLE OF CONTENTS

# Introduction

SECTION I

INTRODUCTION

1.1 BACKGROUND

Mission 1201 was launched on 15 June 1971 at 1841Z. This was the first flight mission in the KH-9 Series. The KH-9 is a search and surveillance camera system designed to provide high resolution with large area coverage. Mission statistics, camera and RV recoveries are summarized in Tables 1-1 thru 1-3.

This report details the technical evaluation of the performance of the cameras employed on this flight. Important aspects of the satellite vehicle performance, post recovery handling, and exploitation of the product are also included. The report is the consensus view of the Post Flight Analysis (PFA) Team, which consists of representatives from the Sensor Subsystem Project Office (SSPO), the System Project Office (SPO), and Sensor Subsystem Contractor (SSC), the National Photographic Interpretation Center (NPIC), the BRIDGEHEAD Processing Facility, and the Air Force Special Projects Production Facility (AFSPPF).

The KH-9 development program was initiated in the Fall of 1966. The first flight camera (SV-1) was shipped to the System Vehicle Integrating Contractor (SVIC) on 19 October 1970 for integration with the space vehicle. The performance of the SV-1 cameras (SN-003), as determined from preflight testing, was detailed in the "Flight Model (SN-003) Acceptance Team Report", BYE 15285-70. This report was published on 6 November 1970. At SVIC schedule delays were encountered due, primarily, to the need to replace the slit and shutter mechanisms to preclude a known potential catastrophic on-orbit failure. This change necessitated removal and reinstallation of the platens which required one additional test of SV-1 in Photographic Test Chamber A-2. The first Chamber A-2 test was conducted in February 1971 and the second in May 1971. The results of the photographic tests, as well as a review of the readiness of SV-1 for launch were published in the "SV-1 (SN-003) Flight Readiness Report", BYE 15264-71. This report was published on 9 June 1971.

The flight system was shipped to Vandenberg AFB on 1 June 1971 where it was mated with the booster. After completing the normal flight readiness checks, the system was launched on 15 June 1971.

1.2 ON-ORBIT PERFORMANCE

The PFA Team convened at the processing site and evaluated the performance of the camera system from the imagery and available telemetered data after recovery of each reentry vehicle (RV). Mission segment 1201-3 was not recovered due to a chute failure and at present is lost at sea. Search and recovery attempts are continuing.

During the course of the PFA meetings several actions were taken in attempts to improve photographic quality. These actions are summarized in Table 1-4.

TABLE 1-1

MISSION STATISTICS

Mission Number - 1201

Launch Date - 15 June 1971

Launch Time - 1841Z

Satellite Vehicle - SV-1 (8001)

Sensor Subsystem - SN-003

Orbit Inclination - 96.39°

Initial Perigee - 99.3NM

Initial Apogee - 165.0NM

Argument of Perigee - 165.4°

Initial Period - 89.38 min.

Range of Photo Altitudes - 1201-1, 99-138NM;
1201-2, 98-126NM;
1201-4, 99-151NM

Range of Beta Angles - +20° to +22°

TABLE 1-2

CAMERA STATISTICS

| | Forward-looking | Aft-looking |
|---|---|---|
| Camera Designations | A | B |
| Film | 1414 | 1414 |
| Focal Length | 60.005 inches | 59.984 inches |
| Filter Type | W/2E | W/12 |
| Initial Focus Setting* | 79μ | 52μ |
| Supply Footage | 99,100 ft. | 99,267 ft. |
| Supply Spool No. | 5022 | 5030 |
| Supply Film Weight | 790.3 lbs. | 783.9 lbs. |
| Optical Set Nos. | 013 | 017 |
| Initial Pneumatics | 33.5 lbs | |
| Remaining Pneumatics | 14.4 lbs | |

* Focus was changed twice on the Forward-looking Camera and once on the Aft-looking Camera, see Section III.

TABLE 1-3

RV RECOVERY STATISTICS

| | RV-1 | RV-2 | RV-3 | RV-4 |
|---|---|---|---|---|
| Recovery Date | 20 June 71 | 26 June 71 | - | 16 July 71 |
| Recovery Time | 2144Z | 2140Z | - | 2222Z |
| Comment | Water Pickup (chute partially torn) | Air Catch (chute damaged) | Sank (chute failure due to premature dereefing) | Air Catch |

TABLE 1-4

SIGNIFICANT ON-ORBIT CAMERA ADJUSTMENTS

Forward-looking Camera

1. Rev 129, the focus position was advanced by 8 microns to a new platen position of 71 microns.
2. Exposure was decreased by .06 log E on Rev 135 for acquisitions above 10 degrees solar altitude.
3. Rev 231, the focus position was advanced by an additional 8 microns to a new platen position of 64 microns.

Aft-looking Camera

1. Rev 129, the focus position was advanced by 6 microns to a new platen position of 46 microns.
2. Exposure was decreased by .06 log E on Rev 135 for acquisitions above 10 degrees solar altitude.

# Summary



Approved for Release: 2022/03/03 C05132845

# SECTION II

# SUMMARY

## 2.1 CAMERA OPERATIONS

Mission 1201, the first flight of the KH-9 Camera System, must be classified as a remarkable success. The KH-9 Camera was an extremely complex engineering task. It combines near diffraction-limited optics, with state-of-the-art servo-systems that have required the best in both optical and electronic technology. Many developmental difficulties have been experienced with the camera and the problems of film tracking and synchronization are far from ended. Rewind will continue to require restriction on Mission 1202.

### 2.1.1 Performance Anomalies

From an engineering point of view, Mission 1201 provided significant insight into the performance of the KH-9 Camera and the problems that need to be addressed. In summary, the two major image quality problems were the out-of-focus conditions and image smear. Both cameras were initially flown out-of-focus, with the Forward-looking Camera being the most significantly affected. A single focus change of -6 microns was necessary on the Aft-looking Camera, and two focus changes totaling -16 microns were necessary on the Forward-looking Camera to obtain image quality near optimum. These focus adjustments were deemed necessary thru the evaluation of the thru focus engineering tests which proved invaluable to the PFA Team. The ability to use thru focus tests to fine tune the camera on-orbit, and noticeably improve the photographic results, is clearly useful. The real difficulty with this problem is that there is, at this point in time, no understanding of why the cameras were not properly focused at the beginning of the mission. Focus is set based on a careful evaluation of thru focus resolution and edge focus targets taken in a vacuum chamber. The temperature and pressure environment of the optics, platen, and film plane are sufficiently similar between orbit and the test chamber, that no significant focus differences should occur. There are uncertainties in focus setting due to the subjectivity necessary to properly balance the performance across the field. However, it was estimated and recorded in the SV-1 Flight Readiness Report that this uncertainty would be aprx 4-8 microns. The Aft-looking Camera was within this range, the Forward-looking Camera was not. Further discussion of this problem is contained in Section III. Specific conclusions and recommendations for future action are presented in Section VII.

Before launch it was known, based on chamber testing, that the film synchronization errors were greater than desired. Analysis of the photography confirms that the imagery was affected by smear, and that the magnitude of the smear errors was at least as great as predicted thru preflight testing. In fact, there is some evidence from line target analysis to indicate that smear, particularly on the Forward-looking Camera, was worse than expected. This issue is discussed in greater detail in Sections III and change was implemented during Op 125, Rev 135 of 1201-2. No gross camera exposure difficulties were apparent throughout the mission.

2.1.6 Specular Reflections

Specular reflections were severe on the Forward-looking Camera at approximately 35° to 40° latitude at a +20° scan. The specular reflections were, however, predictable with the "Crystal Ball" Program. For future missions, an analysis of the optimum launch time should be conducted to minimize the effect of specular reflections on priority targets.

2.2 EXPLOITATION SUITABILITY

2.2.1 Photointerpretation (PI) Quality

In spite of the focus and film synchronization errors, the PI suitability of the mission was good. This does not mean that the focus and smear problems were inconsequential, but simply indicates that the photointerpreters were pleased with the product returned from this first KH-9 mission. In addition, it is not always possible to correlate PI judgments with known camera problems as, in this instance, target readout is done in stereo. This condition is forgiving to a poor performing camera since the stereo view will favor the higher quality photograph.

Examination of the PI quality ratings of the OAK targets showed that the majority of the targets were rated in the fair and good categories. Mission 1201 statistics are summarized in Table 2-1.

TABLE 2-1

SUMMARY OF PI QUALITY

(percentage)

| | Ratings | | | |
|---|---|---|---|---|
| Mission | Excellent | Good | Fair | Poor |
| 1201-1 | 0.8 | 29.8 | 47.8 | 21.6 |
| 1201-2 | 1.6 | 27.6 | 45.6 | 25.5 |
| 1201-4 | 0.5 | 10.4 | 50.5 | 38.6 |

The National Photographic Interpretation Center (NPIC) reported that the imagery obtained at high obliquity did not contain the details of that acquired near scan nadir. In many instances, detailed readout of order of battle targets, particularly ground order of battle, was difficult beyond ±45° of scan. NPIC further reported, however, that interpretation related to area search could be performed at the high scan angles.

2.2.2 Mission Information Potential (MIP)

The MIP is a rating given by NPIC, and is intended to be indicative of the best photography acquired by the camera system within each mission segment. MIP chips for the 1200 series mission were made from KH-7 photography with the best chip assigned a rating of 155. The numbering system was an extension of the KH-4 MIP system, with the highest KH-4 MIP chip assigned a rating of 125. The MIP value of 155 equates to a ground resolved distance (GRD) of approximately 1.8 feet, whereas 125 equates to approximately 4.0 feet. The MIP values assigned to Mission 1201 are summarized in Table 2-2.

TABLE 2-2

MISSION 1201 MIP RATINGS

| | Cameras | |
|---|---|---|
| Mission | Forward-looking | Aft-looking |
| 1201-1 | 125 | 140 |
| 1201-2 | 135 | 135 |
| 1201-4 | 145 | 140 |

The high MIP values, of 145 and 140, demonstrate that the camera system is basically capable of meeting its design goal of providing KH-7 quality with KH-4 coverage.

## 2.3 PROCESSING AND REPRODUCTION

There were no major problems experienced during defilming, processing, or reproduction. The Optical Titling System operated successfully with over 99% of all frames being titled completely. Predicted and actual film weights showed good correlation.

A duplication study conducted by NPIC revealed that on the basis of sixteen CORN targets analyzed from the three buckets of Mission 1201 that there is no significant loss in resolution as a result of the duplication process. Although special printing aided the photointerpreters, in most instances the standard SO-192 reproductions were found to be satisfactory for first phase readout.

## 2.4 VISUAL EDGE MATCHING

The visual edge match (VEM) technique was used extensively in the evaluation of Mission 1201. This was the first intensive use of this technique for system performance analysis work. It was extremely useful in all phases of performance assessment and promises to be a major addition to the photo evaluation field. The major problem areas with VEM are the calibration (in conversion of edge number to resolving power), and the edge selection procedures. The VEM technique demonstrated a good ability to quantize focus changes, performance as a function of field and scan angles, frame-to-frame variability, etc. For engineering assessment it has proven a most useful tool.

## 2.5 CRYSPER PROGRAM

The predicted values of ground resolved distance (GRD) generated by the CRYSPER orbital photographic acquisition model, were well correlated with GRD values read from CORN target acquisitions and PI ratings of image quality.

The model indicated that the system, in terms of overall performance, was operating somewhat lower in resolution than anticipated. In-track predictions were better correlated with the CORN readings than were the cross-track predictions. This is consistent with the aforementioned observations made about smear.

Aside from the accurate estimate of general performance provided by the model, the comparison with PI ratings gives promise of providing a valuable derivative tool to determine limiting GRDs associated with particular target types.

## 2.6 SATELLITE VEHICLE PERFORMANCE SUMMARY

The overall performance of the satellite vehicle was excellent and all mission objectives except the recovery of RV-3 were met. The operational mission lasted 31 days, followed by a 21 day solo operation. This solo operation was an engineering test performed after separation of the final RV and was terminated by a commanded deboost of the vehicle. The overall SV performance for the ascent phase and each of the four mission segments is summarized below:

### 2.6.1 Ascent

Ascent events were nominal and stabilization of the SV allowed deployment of the solar arrays on Rev 1. Apparent contamination of Aft Section thermal control surfaces during ascent caused an over-temperature condition in the battery module which remained constant throughout the mission.

### 2.6.2 1201-1

By Rev 16, all subsystem health checks had been completed and operational photography began on Rev 24. On Rev 82, RV-1 was successfully separated with a total film load of 40,000 feet. Damage to the aerial retrieval target cone was observed which led to the decision to allow the RV to water impact. The RV was recovered from the water with no damage to the payload.

### 2.6.3 1201-2

Operational photography continued on Rev 88 using RV-2. On Rev 179, RV-2 was successfully separated with a total film load of 52,000 feet. Main parachute damage again occurred but aerial recovery of the RV was successful.

### 2.6.4 1201-3

Operational photography continued on Rev 185 using RV-3. On Rev 405, RV-3 was successfully separated but was neither sighted nor recovered. Major damage to the main parachute apparently occurred during deployment. As a result of this malfunction, the film load of 54,000 feet was lost.

### 2.6.5 1201-4

Following some difficulties with camera Emergency Shut Downs (ESDs), operational photography was resumed on Rev 470. The premature degradation of the pyro batteries led to the decision to separate

RV-4 on Rev 502. Separation and aerial retrieval of RV-4 was normal and 26,000 feet of film was recovered.

# Camera Operations

# SECTION III

# CAMERA OPERATIONS

## 3.1 INTRODUCTION

This section presents an analysis of camera performance from both a photographic and engineering standpoint. In assessing the photographic performance, resolution, focus, and exposure were examined and an extensive data base developed from visual edge matching (VEM) measurements and mobile CORN target readings. This data base coupled with an assessment of the VEM technique itself enabled an objective evaluation of focus and resolution. The performance from an engineering point of view is discussed on the basis of the anomalies that occurred during the mission and evaluation of the down-link telemetry signals. For historical purposes, considerable care has been taken to record all key profiles and configurations for Mission 1201.

The launch and mission operation of SV-1 culminated approximately a year and a half of ground testing at all levels of sensor assembly. During this period, photographic and engineering evaluation of performance was a continuing effort involving some very difficult and puzzling performance anomalies. The analyses herein attempt to correlate ground test and predicted performance recorded on-orbit. These analyses were performed on the basis that ground test data of follow-on sensors may more easily be understood as related to the ultimate flight required performance.

## 3.2 ON-ORBIT OPERATIONS

### 3.2.1 Launch and Orbital Conditions

Satellite Vehicle (SV-1) was launched from Vandenberg AFB on 15 June 1971. The configuration of the sensor system is presented in Table 3-1.

TABLE 3-1
LAUNCH CONFIGURATION

| | |
|---|---|
| Mission Operation - 1201 | Intra-Range Operation - 8709 |
| Sensor System SN-003 | Satellite Vehicle (SV-1) - 8001 |

| | Forward-looking | Aft-looking |
|---|---|---|
| Filter Type | W-2E | W-12 |
| Focal Length (inches) | 60.005 | 59.984 |
| Focus Setting (microns) | 79 | 52 |
| Film Type | 1414 | 1414 |
| SU & TU Film On-Board (feet) | 100,826 | 100,502 |
| Film Weight (pounds) | 790.3 | 783.9 |
| Film in TU-1 (feet) | 1,726 | 1,235 |
| Spool Number | 5022 | 5030 |
| Pneumatics Loaded (pounds) | 16.8 | 16.7 |

Initial flight conditions as compared with planned parameters are listed in Table 3-2. Basic orbital parameters throughout the operational portion of the mission are shown in Appendix B. The orbital inclination remained constant at 96.39 degrees.

TABLE 3-2
LAUNCH PARAMETERS

| | Planned | Actual |
|---|---|---|
| Launch Time (GMT) | 1841 - 2041 | 1841 |
| SVT Launch Time (seconds) | 67.0 | 67.0 |
| Inclination (degrees) | 96.38 | 96.39 |
| Initial Perigee (NM) | 100.8 | 99.3 |
| Initial Apogee (NM) | 164.6 | 165.1 |
| Argument of Perigee (degrees) | 159.8 | 165.4 |
| Initial Period (minutes) | 89.38 | 89.38 |

### 3.2.2 Sequence of Significant Events

The satellite vehicle was launched from VAFB, SLC-4E, at 1841 GMT on 15 June 1971. The countdown and lift-off were performed without incident. The sensor system uncaged in a nominal manner after BV/SV separation, this event was verified from the tape recorder data at Rev 1, POGO. Health checks were performed during the first day to verify sensor system functional performance. A summary of the revs and the amount of film for each RV is presented in Table 3-3.

#### 3.2.2.1 Rev 4

The first attempt to transport film was during a constant velocity run, Sequence (Seq) 208, performed over POGO. The sensor system functioned properly, verifying that the film was aligned within the film path. Steerers, tensions, takeup and supply summed errors were well within limits. The film chute and supply pressures had stabilized after ascent and were measured as 0.7 and 0.8 psi respectively prior to the pneumatics on command.

#### 3.2.2.2 Rev 8

The Sensor System Health Check, Sequence 203, was performed over COOK. All sensor executed commands were functionally verified including all tested bits of the variable commands. Focal plane position and the focus sensor (LSFS) output indicated 79 and 95 microns, respectively, for the Forward-looking Camera and 52 and 45 microns, respectively, for the Aft-looking Camera. Preflight predictions for the LSFS at the corresponding focal plane positions were 88 and 36 microns, for the Forward and Aft Cameras respectively.

#### 3.2.2.3 Rev 14

A manual operation (MOP) was executed over BOSS and was nominal. Fifty frames were commanded and executed, a total of 458 feet of film was transported. The focal plane position and LSFS remained unchanged from the previous operation at Rev 8 COOK.

3.2.2.4 Rev 16

A second MOP was executed over COOK. All camera parameters were nominal. Data obtained via the Microwave-Link was also evaluated and verified the accuracy of the Augie Mode processing and calibration techniques. A total of 58 frames were commanded and executed during the MOP with 533 feet of film transported.

3.2.2.5 Further Events Thru RV-1 Recovery

Rev 16 - Sensor system completed all health checks and was considered operational.

Rev 24 - Sensor system engineering, Sequence 209.

Rev 31 - Thru focus Test (MOP*F), Sequence 190.

Rev 32 - Thru $V_y$ Test (MOP*VY), ±0.00336 rad/sec.

Rev 40 - Sensor system engineering, Sequence 209.

Rev 47 - Thru Exposure Test (MOP*E), ±1 stop.

Rev 48 - MOP*F, Sequence 190.

Rev 55 - Variable block erase (VBE) of programmable memory unit 1, aborted because of fire in station.

Rev 64 - VBE to station contacts. Analyst calculated predicted Data Interface Unit (DIU) counter in error and took immediate contingency action when actual counter value disagreed with predicted.

Rev 73 - Sensor system engineering, Sequence 209.

Rev 78 - RV-1 to RV-2 transfer.

Rev 82 - RV-1 separated.

3.2.2.6 Events Thru RV-2 Recovery

Rev 88 - Sensor system engineering, Sequence 209.

Rev 96 - Thru Focus Test, Sequence 190.

Rev 104 - Sensor system engineering, Sequence 209.

Rev 113 - MOP.

Rev 121 - Sensor system engineering, Sequence 209.

Rev 129 - Advanced focal plane position 8μ on Forward and 6μ on Aft Cameras; MOP*F, Sequences 215 and 216.

Rev 137 - Sensor system engineering, Sequence 209.

Rev 145 - MOP*F, Sequence 217; MOP*VY, -.002088 to -0.003364 rad/sec.

Rev 153 - Sensor system engineering, Sequence 209.

Rev 160 - MOP*F, Sequence 217.

Rev 169 - Sensor system engineering, Sequence 209.


Approved for Release: 2022/03/03 C05132845

Rev 175 - RV-2 to RV-3 transfer.

Rev 179 - RV-2 separated.

3.2.2.7 Events Thru RV-3 Separation

Revs 185, 201 and 217 - Sensor system engineering, Sequence 209.

Rev 231 - Advanced focal plane position 8μ on Forward Camera.

Rev 234 - Sensor system engineering, Sequence 209.

Rev 242 - MOP*VY, -0.003248 to +0.003132 rad/sec.

Rev 250 - Sensor system engineering, Sequence 209.

Rev 258 - MOP*F, ±8μ, Forward Camera only.

Rev 266 - Sensor system engineering, Sequence 209.

Rev 274 - MOP.

Rev 282 - Sensor system engineering, Sequence 209.

Rev 290 - MOP.

Rev 298 - Sensor system engineering, Sequence 209.

Rev 306 - MOP.

Rev 314 - Sensor system engineering, Sequence 209; ESD occurred on Op 5, see para 3.3.1.

Rev 322 - Constant Velocity Test (CVT), Sequence 208.

Rev 323 - Sensor system engineering, Sequence 209, normal stereo operation was resumed.

Rev 337 - CVT, Sequence 208.

Rev 401 - RV-3 to RV-4 transfer.

Rev 402 - ESD occurred during PREP 2, see para 3.3.2.

Rev 405 - RV-3 separated.

3.2.2.8 Events Thru RV-4 Recovery

Revs 411 and 417 - Creep CVT, Aft Camera side, Sequence 185.

Rev 419 - CVT, Sequence 208, normal stereo operation was resumed.

Rev 420 and 435 - MOP.

Rev 445 - ESD occurred at start of 4th op, see para 3.3.3.

Rev 452 - Mini-Creep CVT Test, Aft Camera side, Sequence 185.

Rev 459 - OB cycle, Sequences 191 and 192.

Rev 465 - Two Mini-Creep CVTs, Aft Camera side, Sequence 185.

Rev 466 - Two Mini-Creep CVTs, Aft Camera side, Sequence 185.

Rev 468 - High Speed CVT, Aft Camera side, Sequence 194.

Rev 470 - Mono Forward Camera Engineering Test, Sequence 182.

Rev 472 - Mono Aft Camera Engineering Test, Sequence 183.

Rev 476 - Sensor system engineering, Sequence 209.

Rev 477 - Normal stereo operation was resumed.

Rev 484 - MOP.

Rev 492 - ESD occurred at start of 2nd op, normal stereo operation was resumed with the 4th op.

Rev 497 - Mono Aft Camera MOP 1; Mono Aft Camera MOP 2, max allowable RWV = 35 inches/sec, shutter disable; Mono Aft Camera MOP 3, max allowable RWV = 55 inches/sec, shutter disabled.

Rev 502 - RV-4 separated.

TABLE 3-3

SUMMARY BY RECOVERY VEHICLE

| RV | Active Period (revs) | Take Up Camera | Take Up Film (feet) |
|---|---|---|---|
| 1 | 0-82 | A (Fwd) | 20,469 |
| | | B (Aft) | 20,033 |
| 2 | 82-179 | A (Fwd) | 26,094 |
| | | B (Aft) | 26,164 |
| 3 | 179-405 | A (Fwd) | 26,983 |
| | | B (Aft | 27,100 |
| 4 | 405-501 | A (Fwd) | 13,044 |
| | | B (Aft) | 12,753 |

### 3.2.3 Camera Operations Summary

Appendix C lists the total camera operations of Mission 1201, identifying the amount of photography acquired at the various operating conditions of scan angle and scan center. The operational employment can be assessed by summarizing Appendix C in terms of percentage of scan angle operations, see Table 3-4. The predominance of photography acquired at the shorter scan angles was spooled on RV-3 which at this time has not been recovered.

TABLE 3-4

SCAN ANGLE OPERATIONS SUMMARY

| Scan Angle (degrees) | Percentage of Mission (%) |
|---|---|
| 120 | 3 |
| 90 | 27 |
| 60 | 36 |
| 30 | 34 |

3.2.4 Solo Activities

The Solo phase of the mission began after the separation of RV-4. The following experiments were planned for this flight.

3.2.4.1 System Command and Control (SCC)

SCC-2 was selected on Rev 588 and the remainder of the flight was performed in this mode.

3.2.4.2 Optical Bar (OB) Bearing Life

The OBs were operated for long durations to evaluate bearing life and electronic temperature profiles. The system was operated for approximately 5.5 hours over 23 orbital revolutions. There was no indication of increased torque, however, the platen drive motor temperatures did increase 12 degrees.

3.2.4.3 Low Voltage Test

The low voltage test was deleted to insure adequate power for the duration of Solo.

3.2.4.4 Monoscopic (Mono) Operations

Mono operations were not accomplished during the Solo phase since partial completion of the test objective was accomplished during the operational phase as a result of the ESD on Rev 445. Forward Camera Mono operations were executed over the Rev span 472 - 476 and three Mono Aft Camera operations were programmed during Rev 497. All mono operations were normal.

3.2.4.5 Slit Width Test (SWT)

The SWT was successfully commanded throughout its mechanized range on Rev 599.

3.2.4.6 Focal Plane Servo Test

This test was initiated on Rev 587. The focal plane on each camera was commanded through its mechanized range. The focal planes of both cameras were retreated to their positive stops. The focal planes were then advanced to the full negative positions, each focal plane mechanism was commanded past the maximum of the internal camera assembly. When subsequent retreat commands were executed, the Forward Camera focal plane mechanism recovered from the negative position; however, the Aft Camera focal plane mechanism bound at the -206μ focal plane position and the mechanism was unable to recover by moving over the maximum of the internal camera assembly. Additional attempts were made to recover the Aft Camera focal plane drive mechanism but all were unsuccessful.

3.2.4.7 Optical Bar Logic Test

The OB Logic Test was deleted in order to conserve electrical power.

3.2.4.8 Optical Bar Thermal Effects

Both OBs were positioned to nadir for two orbital revs to determine thermal effects. The temperature of each corrector plate decreased 20° during this test.

3.2.4.9 System Health Test

This test, (Sequence 203), was executed just prior to SV deboost to evaluate functional operation after an extended time in orbit. The sensor operated successfully.

### 3.2.5 Command Sequence Definition

The command sequences utilized in the Mission 1201 data base are defined in Table 3-5.

TABLE 3-5

COMMAND SEQUENCES

| Seq No. | Description | Purpose |
|---|---|---|
| 49 | RV Take up Prep | This sequence in conjunction with the trim and seal sequences prepares RV-1 thru RV-3 for separation; and RV-2 thru RV-4 for operation. |
| 50 | Redundant RV Take up Prep | Contains redundant off commands for Sequence 49. |
| 120 | Sensor Subsystem ON/OFF Stereo | Sets up and shuts down the camera system for stereo operation per target requirements. |
| 121 | Optical Bar ON/OFF | Starts and stops the OB of the SS. |
| 122 | Film Transports ON/OFF | Starts and stops the film transports. |
| 123 | Vx/h Update | Updates the value of Vx/h as a function of the ephemeris. |
| 124 | Vy/h Update | Updates the value of Vy/h as a function of the ephemeris. |
| 125 | Slit Width Update | Updates the value of slit width settings as a function of exposure requirements. |
| 126 | Redundant End-of-Rev Initialization | Redundant off commands following last sensor system operation on a rev. |
| 127 | Redundant End-of-Rev Initialization with ESD Disable | Contingency sequence for providing redundant off commands following last SS operation on a rev, and also incorporating an ESD disable command. |
| 128 | Focus Retreat | Updates focus settings as computed by automatic focus adjust. |
| 129 | Focus Advance | Updates focus settings as computed by automatic focus adjust. |
| 130 | Variable Parameter | Vx/h, Vy/h, Vs and slit updates for merged sequences. |
| 131 | Monoscopic Operation, Aft-looking Camera | This sequence operates the Aft Camera only, and uses the same variable parameter inputs employed by Sequence 120 (stereo op). |
| 132 | Monoscopic Operation, Forward-looking Camera | This sequence operates the Forward Camera only, and uses the same variable parameter inputs employed by Sequence 120 (stereo op). |
| 133 | End-of-Rev Initialization | This sequence loads Sequence 126 (redundant "off" commands) into the opposite PMU. |

TABLE 3-5 (CONT'D)

COMMAND SEQUENCES

| Seq No. | Description | Purpose |
|---|---|---|
| 134 | Both Transport, Aft-looking Camera | Contingency sequence whereby system can operate both transports with Aft Camera only. |
| 135 | Both Optical Bars, FT Forward-looking Camera | Contingency sequence whereby system can operate both OBs with Forward Camera film transport only. |
| 180 | Constant Velocity Sequence, Forward-looking Camera | Verifies proper tracking in Forward Camera film path (refer Seq 208). |
| 181 | Constant Velocity Sequence, Aft-looking Camera | Verifies proper tracking in Aft Camera film path (refer Seq 208). |
| 182 | Mono A, Engineering Test | Mono engineering test to monitor Forward Camera system integrity. |
| 183 | Mono A, Engineering Test | Mono engineering test to monitor Aft Camera system integrity. |
| 184 | ESO Creep, Forward-looking Camera | Diagnostic sequence which transports Forward Camera film at 3 ips. Used after an ESD. |
| 185 | ESO Creep, Aft-looking Camera | Diagnostic sequence which transports Aft Camera film at 3 ips. Used after an ESD. |
| 186 | Pneumatic B Tank Isolate | Isolates Aft pneumatic tank. |
| 187 | Pneumatic System B Isolate | Provides low pressure pneumatics isolation for Aft Camera. |
| 188 | Thru Focus, $\pm 12/\pm 4\mu$ | Flight test sequence to determine plane of best focus. |
| 189 | Thru Focus, $\pm 20/\pm 10\mu$ | Flight test sequence to determine plane of best focus. |
| 190 | Thru Focus, $\pm 16/\pm 8\mu$ | Flight test sequence to determine plane of best focus. |
| 191 | Solo OB Bearing Test - Power On | Power On Sequence for extended duration of OB rotation. Used after RV-4 separation to provide thermal test data. |
| 192 | Solo OB Bearing Test - Power Off | Power Off sequence used with Sequence 191. |
| 193 | Shutter Enable/Disable | Enables/disables one or both camera shutters. |
| 200 | Take up 2 Enable | Transfers active take up functions to take up 2. |
| 201 | Take up 3 Enable | Transfers active take up functions to take up 3. |
| 202 | Take up 4 Enable | Transfers active take up functions to take up 4. |
| 203 | SS Health Check | Dynamic stereo op performed over station to ascertain the integrity of the sensor system. |

TABLE 3-5 (CONT'D)

COMMAND SEQUENCES

| Seq No. | Description | Purpose |
|---|---|---|
| 204 | Uncage SS | Uncages sensor system using primary uncaging command, and operates SCC-1 and SCC-2. |
| 205 | Redundant, Uncage | Redundant uncage stored in opposite PMU. |
| 207 | Wrap | Provides double wrap on next take up prior to trim and seal functions. |
| 208 | Constant Velocity Sequence | Verifies proper film tracking. Used after uncage, TU transfer, RV separate, and for operations analysis as required. |
| 209 | Cook - SS Engineering Data Pass | Used on Rev 8 Cook and a subsequent night pass each day to monitor system integrity. |
| 210 | Pneumatic A Tank Isolate | Isolates A pneumatic tank. |
| 211 | Pneumatic System A Isolate | Provides low pressure pneumatics isolation for Forward Camera. |
| 212 | Supply Pressurization | This sequence is used to pressurize the supply. |
| 213 | OB Aft-looking Camera Stow | Stows Aft Camera bar. |
| 214 | OB Forward-looking Camera Stow | Stows Forward Camera bar. |
| 215 | Thru Focus Advance | Focus test whereby film plane moves toward field group and returns. |
| 216 | Thru Focus Retreat | Focus test whereby film plane moves away field group and returns. |
| 217 | Thru Focus Advance/Retreat | Thru focus test whereby film plane moves away and toward field group. |
| 221 | RV-1 Inlet Trim and Seal | Prepares RV-1 for separation. |
| 222 | RV-2 Inlet Trim and Seal | Prepares RV-2 for separation. |
| 223 | RV-3 Inlet Trim and Seal | Prepares RV-3 for separation. |
| 224 | RV-4 Inlet Trim and Seal | Prepares RV-4 for separation. |
| 225 | RV-2 Outlet Trim and Seal | Prepares RV-1 for separation. |
| 226 | RV-3 Outlet Trim and Seal | Prepares RV-2 for separation. |
| 227 | RV-4 Outlet Trim and Seal | Prepares RV-3 for separation. |

## 3.3 ANOMALIES

This section is compiled to identify the anomalies that occurred during Mission 1201 and provide an analysis of the probable cause(s) for such occurrences.

### 3.3.1 Aft-looking Camera ESD at Brake Release on Rev 314

There was an ESD at brake release on the 5th operation of Rev 314. The telemetry data indicated a jam in the fine film drive system of the Aft Camera. The looper carriage executed the ESD circuitry when it was pulled to the stop on the take up side. A constant velocity run was made on Rev 322 and observed in real time during the COOK pass. After the ESD the tension in the system normalized and the looper repositioned, therefore, the ESD circuitry was reset with the camera power ON command. The constant velocity run was proper so a six frame engineering sequence was run in real time on the Rev 323 COOK pass. This sequence was performed satisfactorily and subsequently normal payload operations were resumed. Inspection of the film was not possible since this ESD occurred while operating during Mission 1201-3.

3.3.2 Aft-looking Camera ESD at Constant Velocity on Rev 402

Subsequent to the RV-3 to RV-4 transfer sequence, a CVT was performed during which an ESD occurred on the Aft Camera. Telemetry (TM) data showed that approximately 15 seconds after film movement the Aft Camera coarse tensions decreased, followed by the take up summed error and integrated output indicating the take up servo motor was exerting a much greater torque than normal. It was also noted that a ripple or chatter appeared and remained on the input drive, output drive, output coarse tensions take up summed error, and take up tachometer. Except for the take up signals, the other signals returned to their normal DC level. Following the issuance of the film transports off command, while the film speed was decreasing, the input and output tensions decreased causing the ESD condition. The take up summed error went to its maximum value and the input and output drives exhibited a large error. An ESO mini-creep was performed during Rev 411, COOK pass, and the tensions returned to their normal level. At Rev 417, BOSS, another mini-creep was performed; the data indicated the system was responding normally. At Rev 419, COOK, a 104 second creep test was performed successfully. It appears that the ESD resulted from a restriction in the film path between the looper output and take up. A previous anomaly which occurred during SV-1 factory testing exhibited signatures similar to those of the flight anomaly. The cause of the test anomaly was a physical drag on the material due to epoxy chips which were wedged between the film and the idler roller in the take up.

Examination of the processed film between and adjacent to Ops 376 and 377 indicated no physical damage that would indicate the exact location and cause of the ESD. The start up of the ESO mini-creep that reestablished proper tensions tends to confirm the conclusion reached from the TM data. It appears that the scuffing of the material by the output drive capstan, the embossing by the input drive capstan, and the aprx 2" wide fog mark of the slit were all caused by the tension normalizing. The scuffing was considered to be minimal. During this period of time the output capstan would have turned very little but material would have been transported prior to the take up removing the slack in the output looper causing the scuffing on the material. The film path between the supply and the slit would have been under tension and not moving initially causing the embossing. A metallic-like chip that has the appearance of a piece of scrap from a manufacturing operation was discovered embedded in the base side of the film 17" toward the take up from the slit. The metal chip was metallurgically analyzed as aluminum with traces of zinc, copper and magnesium. Until the source of the metal chip is identified, the location of the chip on the film is not necessarily meaningful. The source of the metal chip has not been identified.

3.3.3 Aft-looking Camera ESD at Brake Release on Rev 445

An ESD occurred at the time of brake release on the 4th operation of Rev 445. TM data indicated the film was not being driven properly through the fine film drive system causing the looper to be driven to the stop on the take up side, generating the ESD. An abbreviated mini-creep was performed and observed in real time on the Rev 452 COOK pass. This data indicated that, although a small amount of film moved through the fine film drive, the input drive capstan was not rotating.

In an attempt to free the suspected jam in the input drive several sequences were programmed. On the Rev 450 COOK pass, the OBs were operated to cycle the platen, however, this operation was unsuccessful as the looper remained at the take up side limit switch. Four additional abbreviated mini-creeps were run on Revs 465 and 466 on the POGO and BOSS passes, however, they did not remedy the ESD condition. On the Rev 468 COOK pass a 20 inches/sec constant velocity operation was performed for a 5.4 seconds duration. This operation successfully transported film through the fine film drive system but did not free the drive capstan. On Rev 472 a monoscopic Aft run was undertaken. The TM data indicated that the looper moved from the ESD position and tensions had normalized at the beginning of this run. On the Rev 476 COOK pass a stereo engineering sequence was run. TM data showed the Aft input drive capstan to be operating properly. Normal stereo payload operations were resumed on Rev 477.

Detailed analysis of the processed film indicated no physical damage on the material. There were no tears, foldovers, dimpling, scuffing, embossing, or scratching to indicate a mistracking or hangup that would cause an ESD due to the film web itself. Film in the region of the platen at the time of the ESD showed some plus-density markings indicating the twister was oscillating but the material was not moving. Approximately 26 feet of film showed extremely faint plus-density streaks, that matched the input drive capstan lands and grooves, which could only be observed by grazing light. The exposure started at the beginning of the 2nd of the 4 mini-creeps and continued through the first 165 feet of the Mono Aft operation. Measurements made on the processed film confirmed the TM data. On the operation on which the ESD occurred, the film only moved 5" past the slit tending to confirm that the output looper was driven against its stop. The lack of plus-density banding or physical damage on the material for the ESO run and the first of the 4 mini-creeps could be due to a lower tension since the supply provided 31" of film on the operation that shut the system down. As the mini-creeps were run, more film was transported past the slit than was provided by the supply, possibly increasing the tension but not sufficiently to do more than pressure expose the emulsion.

3.3.4 System ESD on Rev 492

On Rev 492 the system experienced an ESD on the Forward-looking and Aft-looking Cameras because of incompatible Vx and Vs commands. The Extended Command System failed to input the required Vs for the second of a three operation nested sequence. This caused the third operation to be missed because there was no camera power off (C-) command until the end of the operation. With the camera power on (C+) command at the fourth operation, the ESD circuitry was reset and subsequent operation was normal. During Op 2, the sensor system was commanded from 60° to a 120° scan angle configuration. Due to a logic design error in the Extended Command System the Vs command required for the 120° scan angle was decoded incorrectly as a "Decoder A ON" command, and the coarse film speed was not changed from the previous operation. The resulting incompatibility between the coarse and fine film speeds was too great for looper compensation, and the ESD occurred when the looper was driven against the stops.

In their present configuration, the Decoders will not allow the commands listed in Table 3-6 to be executed. These long variable stored program commands use Decoder A and end in the octal characters 640, 641, 642, and 643. Of these commands, those beginning with 11EV21, 11EV22, 11EV23, and 12EV4 are not presently mechanized. The Command System Contractor has indicated that those in the list beginning with 12EV6 are not configured as logical command sequences and, as a result, are not used. The remaining commands are 11EV20640, 11EV20641, and 11EV20643, which correspond to commanded coarse film speeds of 53.5190 ips, 53.6475 ips, 53.7760 ips, and 53.9045 ips respectively. In the event a redesign to the command system cannot be implemented prior to future missions, use of these commands must be avoided. The illegal Vs commands noted above will, at present, be sent only during an operation which requires a scan angle of 120° and a Vx/h of .0417 rad/sec. If the mission requires one of the illegal commands, the software could be made to set a malfunction flag in the command message to identify the problem. Upon recognition of such a flag, the message could be manually altered in either of two ways. One way would be to switch to SCC-2 which would not exhibit the Vs problem because Decoder B would be used to execute the commands. The other way would be to change the Vs command to a legal value as close as possible to the correct value. The new value would, at most, be two steps away from the correct value. Such a variation would not degrade photography and would not cause a system shutdown.

TABLE 3-6

ILLEGAL SV-1 LONG VARIABLE STORED PROGRAM COMMANDS

| | | |
|---|---|---|
| 11EV20640 | 12EV40640 | 12EV60640 |
| 11EV20641 | 12EV40641 | 12EV60641 |
| 11EV20642 | 12EV40642 | 12EV60642 |
| 11EV20643 | 12EV40643 | 12EV60643 |
| 11EV21640 | 12EV41640 | 12EV61640 |
| 11EV21641 | 12EV41641 | 12EV61651 |
| 11EV21642 | 12EV41642 | 12EV61642 |
| 11EV21643 | 12EV41643 | 12EV61643 |
| 11EV22640 | 12EV42640 | 12EV62640 |
| 11EV22641 | 12EV42641 | 12EV62641 |
| 11EV22642 | 12EV42642 | 12EV62642 |
| 11EV22643 | 12EV42643 | 12EV62643 |
| 11EV23640 | 12EV43640 | 12EV63640 |
| 11EV23641 | 12EV43641 | 12EV63641 |
| 11EV23642 | 12EV43642 | 12EV63642 |
| 11EV23643 | 12EV43643 | 12EV63643 |

3.3.5 Displaced Ancillary Data (Anomaly 1201-2-009)

Start of frame, scan angle, and SVT marks were displaced along the film edge on both cameras to the extent that some SVT marks were completely off the edge of the film. Most severe displacement occurred on the Forward Camera.

On the Forward Camera, Op 75, Frame 023, the film displacement with respect to the slit was such that the format on the untitled edge was shifted up 3/8", thereby placing the scan angle marks on the titled edge less than 3/64" from the edge. As Op 75 continued, the film track was reestablished and the SVT word was imaged properly. The SVT displacement is due to film offset within the coarse-fine film path interface, which in turn is reflected as film wander in the focal plane. This condition which has the character of a constant bias over long periods as well as an AC component is similar to that which was experienced in test.

3.3.6 Plus-Density Markings (Anomaly 1201-2-008)

Raindrop-like plus-density marks across the full web occurred on both cameras on a cyclic basis. These marks form a definite pattern across the full web and are most evident for the entire length of Ops 64-66, the initial footage in RV-2. The number of occurrences was greatly reduced as the mission continued; however, the pattern remained the same for each occurrence. Ops 64-68 contain scratching along the major axis of the web which appears to occur inversely proportional to the plus-density marks and are likely related. The anomaly does not occur on RV-4 film, and the cause is not yet understood.

3.3.7 Electrostatic Discharge (Anomaly 1201-1-006)

Plus-density marking were detected on the Aft Camera in the format areas. These plus-density electrostatic discharge markings occurred randomly through the mission with the greatest frequency occurring on Op 9, Frames 020, 021, and 022. The marks are diffuse and of such low density that image quality is not significantly degraded. Similar markings were observed on chamber test material and are considered to be characteristic.

3.3.8 Dither Markings (Anomaly 1201-1-002)

Intermittent pressure and plus-density marks also appeared across the width of the format at the beginning and end of frames on the Forward Camera. System design of servo motor electronics causes a "hunting" at zero velocity. This in turn causes oscillations of the metering capstans and resulted in plus-density marks on the film. The density and frequency of the "dither" marking is considered minor and not degrading to the imagery. This condition was also present on ground test material with the same intermittent frequency. This anomaly due to dither during the recycle pause is a characteristic of system behavior and will be present on future mission material.

3.3.9 Inter-Op Slit Exposure (Anomaly 1201-1-001)

A narrow cross-web band characteristically appears on the between ops footage. During optical bar start up, the capping shutter remains open which resulted in the fogging of the film situated over the slit. A design change is being developed to eliminate this anomaly.

3.3.10 Fog in Inter-Op Spacing (Anomaly 1201-2-010)

The inter-op spacing of the Forward Camera between Ops 64 and 65 was excessively long and contained a fogged area. At some time during the rampup for Op 65, the capping shutter opened and closed, exposing a frame-like format. In addition, the characteristic slit exposure was imaged four times in the inter-op spacing. The occurrence of this anomaly is a function of OB position when the stow command is given as part of the CV run. During a constant velocity sequence the OBs are rotating or creeping at a very slow rate. When the stow sequence is commanded following a CV mode, the capping shutter will open for one OB rev, or any portion of a rev, until the capping shutter is reset.

3.3.11 Slit Exposure on Photography (Anomaly 1201-1-005)

An area within the frame format with dimensions equal to the length of the slit and 0.5" in width was observed on the last frame of Op 63 on the Aft Camera. With a 30° scan mode, a Vs lower than 20 inches/sec and a rewind constant (RWC) of minus 5", an insufficient length of film was transported during recycle and rampdown. This condition placed the last exposed frame at the slit. Consequently, the slit was imaged because the capping shutter remains open for the first OB rev prior to film transports ON. This anomaly is characteristic of 1201 and SN-002 with the effect that operational photography equal to the slit area will be destroyed when operating at 30° scan angles and moderate Vx/h, for which the shutdown ramp is shorter than the last recycle reversal. When system rewind of greater than -5 in/sec is incorporated, this condition will occur at scan angles greater than 30° depending on those scan angles used prior to and after shutdown.

3.3.12 Skew Angle Design Limitation (Anomaly 1201-2-013)

Excessive in-track smear was apparent on the Aft Camera, Op 80, Rev 102, Frame 001. It is the only such occurrence in the mission photography. It also appears to a lesser degree in the corresponding frame of the Forward-looking Camera. A review of the TM data and command list just prior to this frame failed to show excessive attitude rates or a vehicle maneuver. Investigation isolated the cause to be improper generation of skew angle modulation, a known logic design limitation. The anomaly will occur on off-center 30° and 60° scan modes on the Forward Camera for positive scan centers and on the Aft Camera for negative scan centers. Assuming an early shutter open/close of 5°, maximum velocity errors (Vx/h = .040) introduced are 30/±45, 0.75 ips; 30/±30, 0.70 ips; 60/±30, 0.55 ips; and 30/15, 0.41 ips. The P mode is generated by the SCC when the OB passes -69.5° (first forward transition prior to the first photo frame). For off-center scan sectors where forward transition occurs after -69.5°, the generation of P mode is delayed. Skew angle modulation is generated primarily by counting pulses emanating from a cosine bit density track on the OB encoder. The pulses are not gated into the counter (in the modulation computer) until the start of P mode; therefore, when P mode is generated late, bits are not counted and skew angle is erroneously generated.

3.3.13 Scratching (Anomalies 1201-1-007 and 011)

A severe scratch located on the emulsion side 1.5 inches from the timing track edge occurred during Ops 19 and 48. This scratching stays parallel to the film edge and was not detected on any other footage from subsequent buckets. Although the cause has not been pinpointed, emulsion dust buildup on the crossover assembly is suspect.

A continuous fine scratch was noted intermittently, sometimes through and sometimes slightly above the time word. Although inadequacy of clearance from the aperture block was initially suspect, its clearance (200μ minimum) is not at all restrictive considering the film thickness is 50 microns. Also, if the block were the cause, there would be a fixed relationship between the scratch and the time word. In addition, any cause in the fine film path would produce three scratches because it involves recycle footage. The most likely cause at this time is the skew bars in the supply exit vestibule.

3.3.14 Tears and Pickoffs (Anomalies 1201-1-003 and 004)

Irregular film tears and emulsion pickoffs occurred on Op 64, Frames 004 and 005. These defects were introduced during despooling. The film apparently contacted moisture which had originated from external recesses of the recovery vehicle. Presplicing procedures have been modified to prevent recurrence, see Section IV for further details.

Emulsion pickoff occurred at the format center for most of the frames of Op 62. The marks are clearly defined without the streaking that is usually associated with the air bar. This is the only op within the mission affected by this anomaly. Being the second-to-last operation in RV-1, the anomaly is possibly associated either with on-orbit bucket transfer or initial despooling. The specific cause has not yet been identified.

## 3.4 ON-ORBIT PERFORMANCE

### 3.4.1 Engineering Tests

#### 3.4.1.1 Optical Performance

The sensor system was subjected to a series of engineering tests to evaluate optical performance and to determine plane of best focus. The tests are listed in Table 3-7. These tests can be separated into the following categories.

A. Manual Operations (MOP)

These tests were performed to obtain CORN target and cultural imagery for photographic quality evaluation.

B. Thru Focus Tests

The thru focus tests performed during RV-1 and the initial part of RV-2 exercised the focal plane ±16 microns in increments of 8 microns. Approximately six frames were programmed at the extreme focal plane positions and six at the nominal settings. After the focal plane evaluation was completed from RV-1, subsequent thru focus tests were programmed to exercise the focal plane ±8 microns in increments of 8 microns. Again, six frames were executed at each extreme and the nominal focal position setting. On Rev 258, a thru focus test was planned for the Forward Camera at the request of the PFA Team. See paragraph 3.4.2 for the detailed analyses of system focus.

C. Thru Exposure Tests

These tests, which biased the slit position approximately ±1 Stop in one-half Stop increments were performed in order to assist in the evaluation of the exposure criteria. Only two tests were executed, both during 1201-1. The exposure criteria was modified slightly during 1201-2 portion of the mission. See paragraph ~~3.4.3~~ 3.10 for exposure analysis.

D. Thru V/y Tests

An experiment to evaluate the cross-track smear contribution was attempted by modifying the V/y command in increments of ±4 steps (±0.028 inch/sec). The tests were performed three times. The success of these tests was limited due to the lack of culture on a continuous frame basis compatible to the commanded V/y change. The objective was to determine cross-track DC smear by analyzing the resultant imagery for quality on the second series of tests. Analysis revealed that the exposure time (order of 1 millisecond) arrested image motion sufficiently to detect cross-track DC smear magnitude dependency on the V/y command. It is recommended that wide slit thru V/y testing be conducted during Mission 1202 and the flight ops be planned to acquire cultural detail.

TABLE 3-7

ENGINEERING TEST SUMMARY

| Rev | Test | Degrees N Lat ON | Degrees N Lat OFF | Specifics |
|---|---|---|---|---|
| 14 | MOP | 48.9 | 39.8 | - |
| 16 | MOP | 44.2 | 33.8 | - |
| 31 | Thru Focus | 46.3 | 32.1 | ±16 microns |
| 32 | V/y Test | 45.1 | 31.8 | ±0.003364 rad/sec |
| 47 | Thru Exposure | 44.4 | 34.6 | ±1 Stop in 1/2 Stop increments |
| 48 | Thru Focus | 44.1 | 31.4 | ±16 microns |
| 63 | Thru Exposure | 42.0 | 36.0 | ±1 Stop in 1/2 Stop increments |
| 96 | Thru Focus | 40.7 | 32.8 | ±16 microns |
| 113 | MOP | 38.8 | 37.6 | - |
| 129 | Thru Focus | 39.9 | 34.1 | ±8 microns |
| 145 | Thru Focus | 38.8 | - | ±8 microns |
| 145 | V/y Test | - | 32.9 | -0.002088 to -0.003364 rad/sec |
| 160 | Thru Focus | 39.5 | 34.6 | ±8 microns |
| 242 | V/y Test | 41.1 | 36.5 | -0.00324 to +0.003132 rad/sec |
| 258 | Thru Focus (Forward Camera only) | 38.8 | 35.4 | ±8 microns |
| 274 | MOP | 36.0 | 32.3 | - |
| 290 | MOP | 36.8 | 33.1 | - |
| 306 | MOP | 36.7 | 31.6 | - |
| 420 | MOP | 38.1 | 36.2 | - |
| 435 | MOP | 33.0 | 31.4 | - |
| 484 | MOP | 39.5 | 37.7 | - |

3.4.1.2 Operational Engineering Test

Additional engineering tests were run at completion of the scheduled 1201-4 Mission, Rev 497. The purposes of these tests were to: (a) verify operation of the shutter disable box on the Aft Camera, inhibiting the normal shutter operation to a full open position; and (b) verify system rewind operation at 35 and 55 inches/sec. Three Aft Camera mono ops were run during Rev 497 over South America, each with the shutter operation inhibited. The conditions for each op are listed in Table 3-8.

TABLE 3-8

OPERATIONAL ENGINEERING TEST

| Rev | Operation No. | Scan Angle (degrees) | Rewind (inches/sec) | Aft Camera Frames |
|---|---|---|---|---|
| 497 | 428B | 120 | 5 | 058 |
| 497 | 429B | 90 | 35 | 084 |
| 497 | 430B | 60 | 55 | 061 |

The results of these tests verified operation of the shutter disable box. Additionally, the mono runs verified film tracking during the variable command of rewind velocities. It was also determined that in the event of a shutter failure during subsequent missions, activation of the disable box as a backup mode would enable acquisition of useful photography. In this test, photography was degraded from three sources: (a) double exposure that occurred primarily as a function of recycle during normal interframe spacing; (b) smear occurring as a result of image exposure during normal recycling of the platen assembly; and (c) increased base fog due to diffuse lighting. Although lack of culture and predominance of cloud cover precluded an exact assessment of the amount of photography degraded, it was evident that a higher percentage of useful photography was acquired than had been initially determined through analytic techniques. The reason for this is that the higher base fog areas still provided useful imagery.

3.4.1.3 Solo Tests

Solo covers the sensor activities which were performed following separation of RV-4. The original inputs for Solo were incorporated into the Field Test Force (FTF) Profile Addendum which was modified to add additional tests. Tables 3-9 and 3-10 identify the Solo tests that were run by the appropriate Flight Profile Addendum (FPA) and the schedule of the executed tests.

TABLE 3-9

SOLO TESTS

| | Test | FPA Acronym |
|---|---|---|
| A | Sequencer Block II | P/L - 1 |
| B | Optical Bar Life | P/L - 2 |
| C | Low Voltage | P/L - 3 |
| D | Monoscopic Operation | P/L - 4 |
| E | Slit Width Range | P/L - 5 |
| F | Focal Plane Servo | P/L - 6 |
| G | Optical Bar Logic Check | P/L - 7 |
| H | Maximum Rewind | P/L - 8 |
| J | Optical Bar Corrector Plate Exposure | P/L - 9 |
| K | Final System Health Check | P/L - 10 |

TABLE 3-10

SENSOR SYSTEM SOLO TEST

| Rev | PCM Format | Booster Vehicle | EV | Aprx Duration (min) | Test Type |
|---|---|---|---|---|---|
| 582.4H | B | 599880 | 600012 | N/A | H |
| 583.4 | C | 605044 | 606284 | 20 | B |
| 584.4 | C | 610386 | 611626 | 20 | B |
| 585.4 | C | 615728 | 616246 | 8 | B |
| 586.4 | C | 621070 | 621590 | 8 | B |
| 587.4 | C | 626413 | 626933 | 8 | B F |
| 588.4 | C | 631750 | 632274 | 8 | A B |
| 589.4 | C | 637096 | 637856 | 12 | B F |
| 590.4 | C | 642437 | 643197 | 12 | B |
| 591.4 | C | 647778 | 648538 | 12 | B |
| 592.4 | C | 653119 | 653879 | 12 | B |
| 593.4 | C | 658460 | 659220 | 12 | B |
| 594.4 | C | 663800 | 664560 | 12 | B |
| 595.4 | C | 669374 | 670134 | 12 | B |
| 596.4 | C | 674479 | 675239 | 12 | B |
| 597.4 | C | 680171 | 680931 | 12 | B |

TABLE 3-10 (CONT'D)

SENSOR SYSTEM SOLO TEST

| Rev | Format | Booster Vehicle | EV | Aprx Duration (min) | Test Type |
|---|---|---|---|---|---|
| 598.4 | C | 685158 | 686398 | 20 | B |
| 599.4H | B | 690618 | 690808 | N/A | E |
| 599.5 | C | 691101 | 692040 | 15 | B |
| 600.4 | C | 694836 | 696776 | 15 | B |
| 601.5 | C | 701924 | 702864 | 15 | B |
| 602.4 | C | 706513 | 707453 | 15 | B |
| 603.4 | C | 711851 | 712791 | 15 | B |
| 604.4 | C | 717189 | 718129 | 15 | B |
| 605.1K | B | 720780 | 720850 | N/A | B |
| 606.2 | C | 726958 | 929398 | 40 | B |
| 610.3 | C | 748975 | 749323 | 7 1/2 | J |
| 612.3 | C | 759612 | 759808 | N/A | N/A |
| 685.4 | C | 310721 | 310785 | N/A | B F |
| 831.C | B | 254332 | 254728 | N/A | KF |

Each test of the Solo mode is further explained in the following paragraphs:

A. Test A

Block II of the sensor system was selected on Rev 588 and the remainder of Solo was performed using this mode. All command functions were executed properly.

B. Test B

The original intent of the Optical Bar Life Test was to activate the OBs over long periods of time (possibly multi-rev durations) in order to evaluate bearing life performance, and also to monitor thermal and electrical characteristics over extended operation intervals. Unfortunately, power system limitations precluded long runs except when solar array power was available. The Life Test was modified to a series of separate long operations (one per rev) commencing on Rev 583 and terminating on Rev 606. The final operation (40 minutes on Rev 606) approximated a sun-up to sun-down operation. No apparent indication of bearing seizure was obvious. Thermal data are plotted on Figures 3-1 and 3-2 for the thermal sensors monitoring the Forward and Aft Cameras platen motor temperatures.

C. Test C

The Low Voltage Test was deleted to insure adequate power for all systems for the duration of Solo.

FIGURE 3-1

FORWARD-LOOKING CAMERA PLATEN MOTOR TEMPERATURE

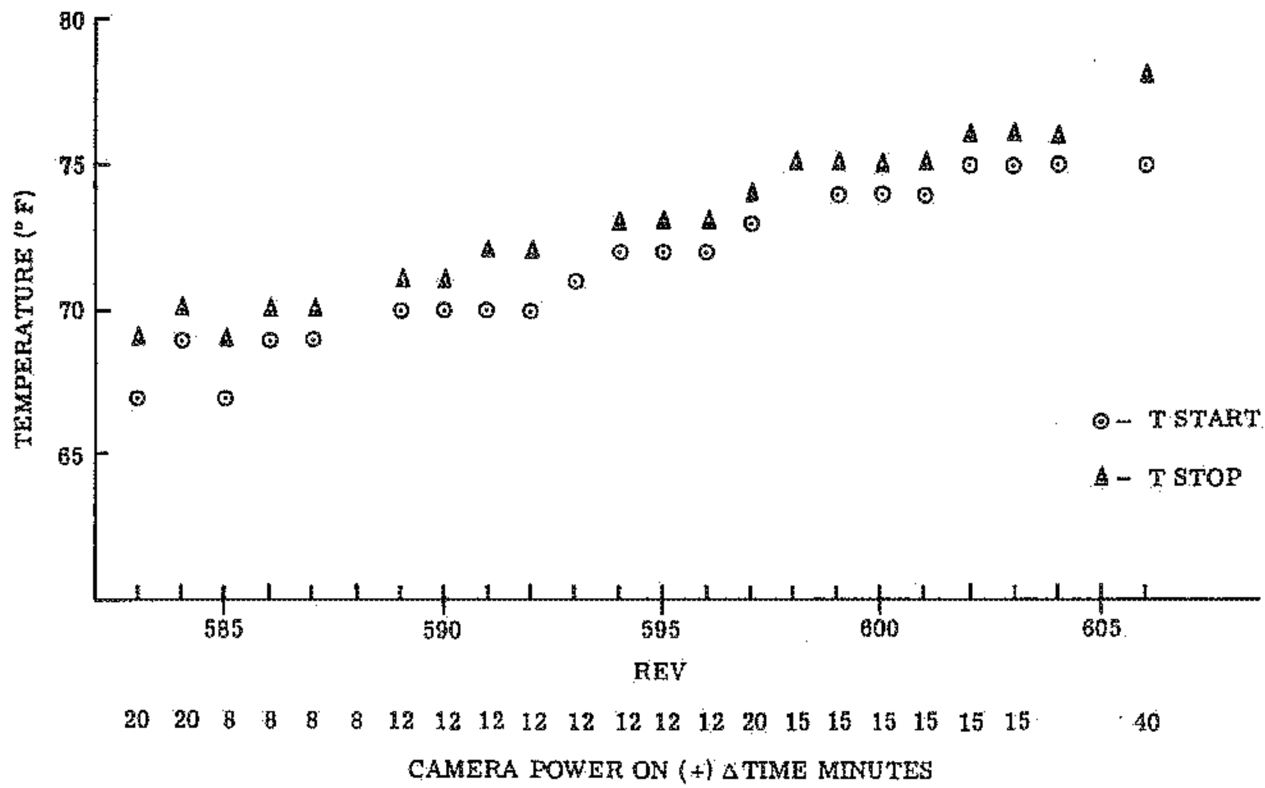

AFT-LOOKING CAMERA PLATEN MOTOR TEMPERATURE

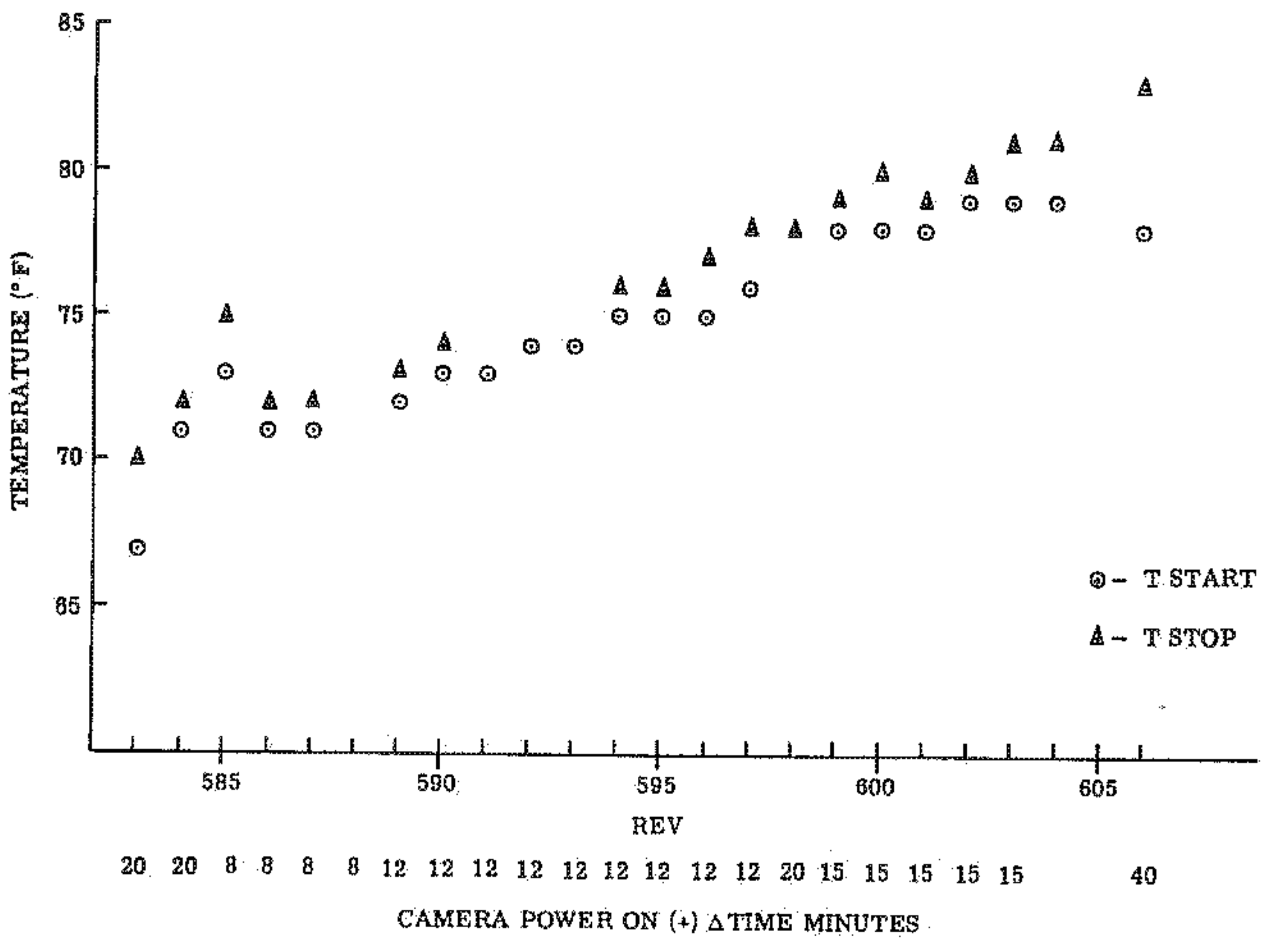


FIGURE 3-2

D. Test D

An unscheduled ESD on the Aft Camera resulted in mono operations (Revs 472-476) which exceeded the Forward Camera OB requirement of this test. Subsequent efforts (Rev 497) to equalize the RV-4 P/L stacks prior to recovery, satisfied the mono B requirement. The mono A with both OBs was not performed due to the expedited recovery of RV-4. All operations were normal.

E. Test E

The Slit Width Range Test was successfully performed on Rev 599. This single operation fulfilled the total test requirement.

F. Test F

The Focal Plane Servo Test was initially performed on Revs 587, 589, and 685. The first and second tests were designed to exercise the focal plane through its maximum range, and when the second exercise resulted in a "hung" condition on the Aft Camera mechanism, the third test was to attempt a recovery of the constrained assembly.

The initial focal plane positions were +64μ, for the Forward, and +64μ for the Aft Camera. Figure 3-3 plots the executed commands, FP-A position data (P423) and LSFS-A (P425) for the two sets of test sequences completed during Revs 589 and 591. Figure 3-4 plots FP-B (P424), LSFS-B (P426) and the executed commands for the Aft Camera focal plane test.

The first test sequence performed was a 79 retreat command execution for each side, the commanding interval was 0.2 sec. FP-A came to rest at its positive stop, +203μ, with 10 retreat commands executed following the time FP-A came to rest, see Figure 3-4. FP-B came to rest at its positive stop, +171μ, with a 16 retreat command executed following the time FP-B came to rest.

Without removal of camera power, 99 advance commands were executed on both FP-A and FP-B. Both sides responded to the commands executed to within 1% of the calculated position, FP-A now at 2μ and FP-B at -22μ. LSFS responded in direct correlation to the FP position. The second test sequence was 110 advance commands for each side, commanding interval was 0.2 sec. FP-A reached a maximum at -188μ then moved positive to -182μ indicating that the command had driven the FP-A past the maximum limit of the focus adjust mechanism. The LSFS reacted in direct correlation to the FP. FP-B reached its maximum of -223μ but at -195μ (LSFS was at -155μ), the LSFS changed direction and repositioned at -69μ. The FP-B final position was -218μ. Again the data indicated that the FP-B had been commanded past the maximum limit of the focus adjust mechanism.

Without removal of camera power 100 retreat commands were executed on both FP-A and FP-B. The FP-A responded with a movement of 200μ coming to a new position of 12μ, the LSFS responded directly. The FP-B began to respond to the command execution but stopped all movement at a position of -206μ, the LSFS during the FP-B movement from -223 to 206μ moved from -69 to -144μ. The data indicates that during this second test the FP-B went sufficiently past the maximum limit of the

FORWARD CAMERA FOCAL PLANE

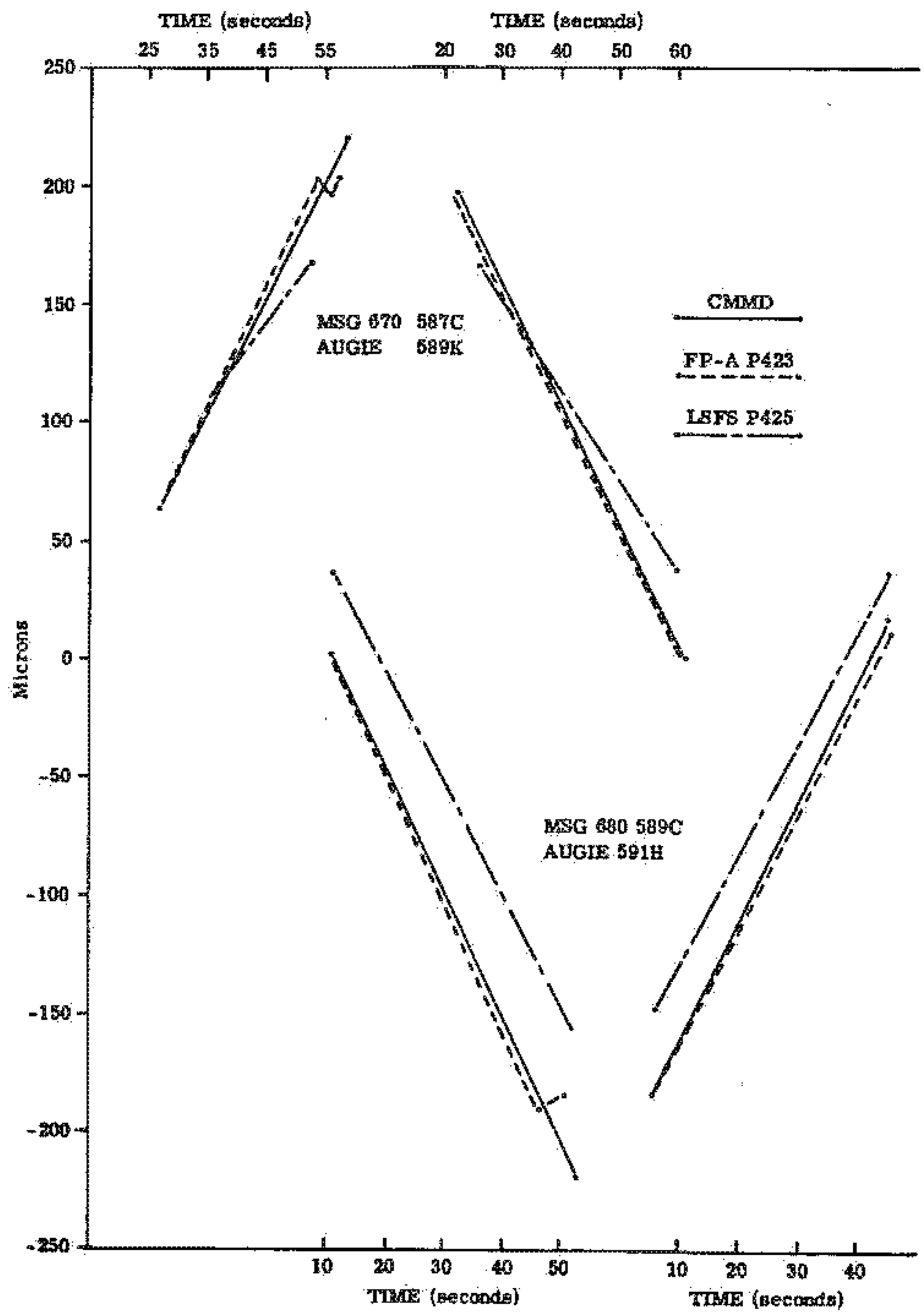


FIGURE 3-3

AFT CAMERA FOCAL PLANE

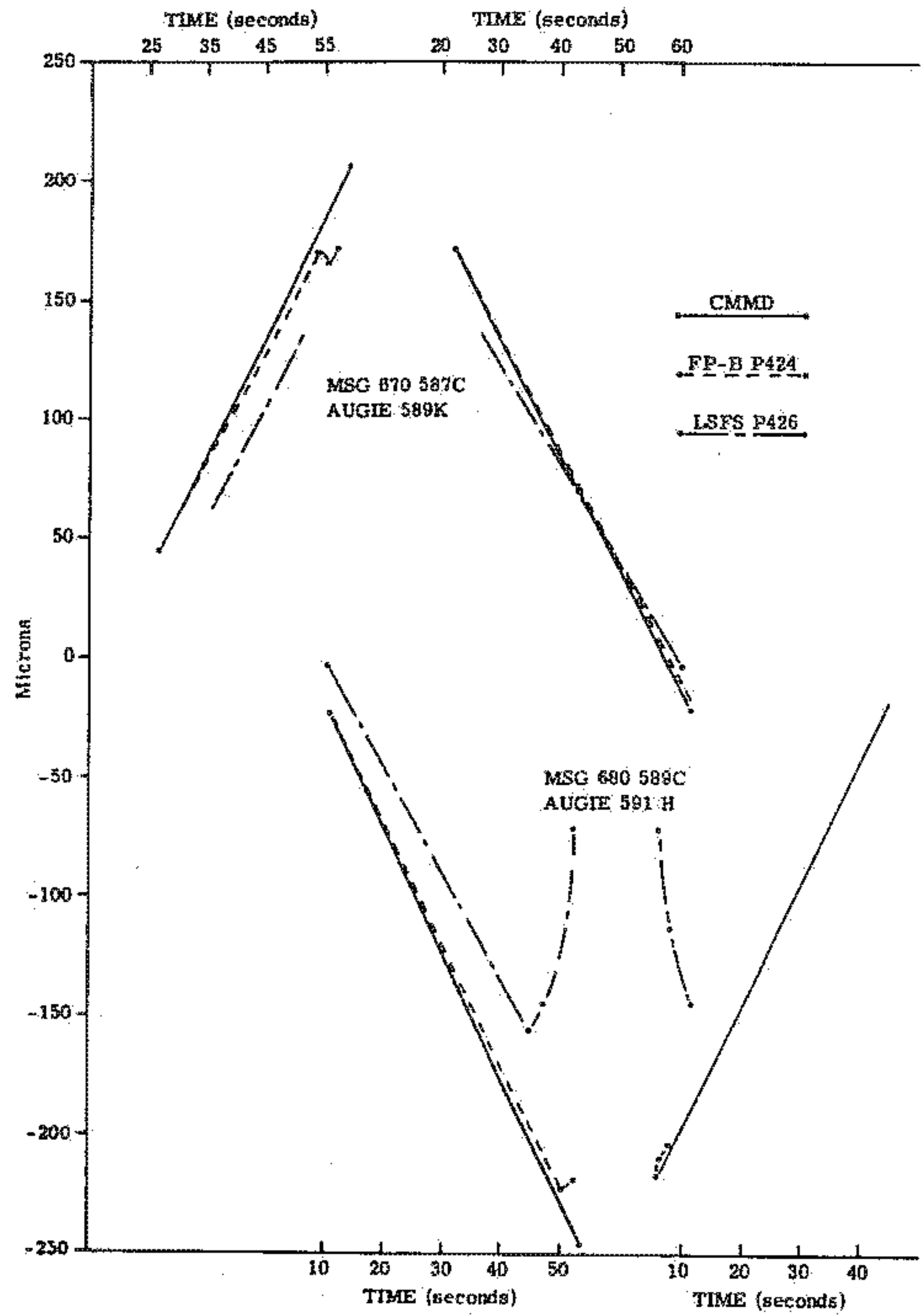


FIGURE 3-4

focus adjust mechanism so as to cause the pivot arms and flexures which transmit cam radius diameter into FP movement to become jammed, bent, or misaligned, preventing further movement of the focal plane.

Focal plane instrumentation is implemented so the FP position monitors (P423, P424) are actually relating platen position. The LSFS monitors (P425, P426) are monitoring the position of the FP referenced to the predicted PBF. With the above taken into consideration, the data substantiates that the camera position responded properly to the executed commands, whereas the FP responded at first properly, then made a rapid movement opposite to the executed commands. This opposite movement indicated that the pivot arms and/or flexures had become bent or misaligned when the commanded position was beyond the maximum position of the camera. The data from the second portion of the test verified an attempt by the camera to follow the executed commands but was incapable of completing the movement when the focal plane moved opposite to the command direction. Again the opposite motion of the focal plane indicates that a jammed condition of the pivot arms and flexures had occurred.

The focal plane tests completed during Revs 685 and 831 continue to substantiate the conclusion stated before. FP-A position -P423 and LSFS P425 monitors indicated that the camera responded properly to the executed commands, but the LSFS P426 was erratic in its response showing a trend towards moving in a direction opposite to that commanded.

G. Test G

The Optical Bar Logic Check was deleted due to uncertainty as to instrument shutdown capability, and the affects of same on system power requirements.

H. Test H

A maximum velocity rewind was conducted after separation of RV-4 to remove the film from the film path. This does not fulfill the objective of the maximum rewind experiment which is to determine if the film path would operate after the rewind.

I. Test J

The Optical Bar Corrector Plate Exposure Test was initiated on Rev 610.3 and was terminated on Rev 611.9. It consisted of creeping each camera for 450 seconds, shutting off power, and monitoring temperatures with the corrector plate exposed for two revs. Both cameras were then stowed. Both corrector plates decreased approximately 20° F from the stowed equilibrium level.

J. Test K

A final System Health Check was performed on Rev 831. The results indicated that the system was operating, with the exception of the Aft Camera output drive. The output drive tachometer and summed error telemetry data indicated the drive was not moving. This was not a system failure, but was instead the result of the film which does not allow the looper position to coincide with a normal operation, see Test H. The looper position is an input to the output drive servo system.

## 3.5 CORN TRIBAR ANALYSIS

### 3.5.1 Introduction

Thirty four readable CORN tribar target images were acquired during Mission 1201. They were distributed among the three mission segments in groups of 14 from RV-1, 13 from RV-2 and 7 from RV-4. The data from these targets is utilized to evaluate the system performance in terms of film synchronization (smear) and resolution. Since the images were obtained under varying conditions of contrast and focus, a normalization was required to provide a valid basis for comparison. The normalization procedures used are explained in detail in the following paragraphs.

The purpose of the tribar data is to provide an evaluation of the system performance after recovery of each RV and allow system adjustments to improve the performance. It is also possible to determine trends in system performance by normalizing all data for focus and contrast; however, this was not done on this system.

The results of this analysis in terms of image motion are that the Aft Camera performance was as anticipated, whereas the Forward Camera had a greater amount of smear than was anticipated from ground testing. The Forward Camera performance was sensitive to the platen position in terms of the amount of defocus, while the Aft Camera was closer to its desired platen position.

### 3.5.2 Contrast Reduction Adjustments

The acquired tribar targets were obtained under a variety of haze conditions. In order to gain a perspective into system performance, it is of practical significance to normalize resolution to what it would have been if the target contrast at the entrance pupil had been 2:1. The MTF/AIM intercept concept is employed to accomplish this resolution normalization.

Microdensitometer traces on the original negatives were made of CORN edge targets adjacent to tribar displays. The effective scan slit dimension was 1 x 40 microns, and the optical system numerical apertures were 0.35 influx and 0.25 efflux. Resultant delta densities were converted to contrast via transformation through a microdensity/log exposure response curve. Because the exact response under the measurement conditions is not yet known, a best estimate D log E curve was used, see Curve 1 in Figure 3-5. This best estimate curve was taken from unpublished data provided by the processing contractor and is for 10μ line exposures on dual gamma processed SO-236 Film.

The edge contrast value thus obtained is combined with the edge and tribar ground reflectance values in order to obtain the tribar contrast at the entrance pupil. This value was computed through the following equation:

$$M_R = \frac{(C_E - 1)(R_H - R_L)}{(C_E - 1)(R_H + R_L) + 2(r_H - C_E r_L)}$$

Where

$M_R$ = Tribar target modulation

$C_E$ = Edge target contrast.

$R_H$ = High reflectance value of ground tribar target.

$R_L$ = Low reflectance value of ground tribar target.

$r_H$ = High reflectance of ground edge target.

$r_L$ = Low reflectance of ground edge target.

From which, tribar target contrast is given by

$$C_R = \frac{1 + M_R}{1 - M_R}$$

These reflectance values were determined for each CORN deployment location group by integrating measured radiometric traces over the spectral transmissions of each differently filtered camera.

3.5.3 Defocus

The amount of defocus for each tribar acquisition was estimated by assuming that the final platen position was an optimum average over scan and field for each camera. The final platen positions were 64 microns for the Forward and 46 microns for the Aft Camera. The corresponding polychromatic MTFs, previously generated from test chamber data, were used with the specification AIM curve to obtain normalized resolution for each target.

3.5.4 Tribar Smear Estimate

The procedure for estimating the magnitude of (assumed) linear smear occurring when the target was exposed is as follows.

A. The difference in modulation between the intersection of the selected PMTF with the specification AIM curve, which is adjusted for the tribar contrast at the entrance pupil, and the point of read resolution is found. This modulation difference is used to calculate the magnitude of linear smear, whose sinc transfer function, when multiplied by the PMTF, will have a modulation equal to that of the AIM curve, at the read resolution in cycles/mm.

B. The intersection point of the PMTF with linear smear component is then intersected with the AIM curve for 2:1 contrast to obtain the 2:1 normalized resolution. The accuracy of this technique, for the normalization of resolution, is more dependent on using the correct tribar contrast at the entrance pupil than it is on selecting the correct AIM curve or PMTF. This is valid as long as the PMTF and AIM curve slopes are approximately correct within the spatial frequency range of interest. However, the accuracy of estimating the magnitude of linear smear is strongly dependent on selecting the correct optical system PMTF and film AIM curve.

As calculated by the method discussed, the average magnitude of smear for each camera, and the average values from two of the line analysis programs are presented in Table 3-11.

TABLE 3-11

SMEAR

(microns)

| | In-Track | | | Cross-Track | | |
|---|---|---|---|---|---|---|
| Camera | MTF/AIM | Line Analysis Case 1 | Line Analysis Case 8 | MTF/AIM | Line Analysis Case 1 | Line Analysis Case 8 |
| Forward | 4.0 | 3.0 | 5.4 | 6.7 | 6.1 | 6.7 |
| Aft | 1.7 | 2.5 | 4.5 | 2.9 | 2.8 | 5.2 |

NOTES:

1. MTF/AIM - linear smear is assumed via sine function multiplication with PMTF.
2. Line Analysis (Case 1) - parabolic smear (or linear smear in limiting case) is assumed, "old" smear model.
3. Line Analysis (Case 8) - parabolic smear (or linear smear in limiting case) is assumed, "new" smear model.

The Aft Camera is very well behaved as far as the mean value of smear is concerned and is in good agreement with the predicted 1 to 2 microns smear as presented in Figure 4-7 of the SN-003 Flight Readiness Report. The Forward Camera, however, exhibited a higher in-track and cross-track mean than had been anticipated from ground testing, specifically 4 to 7 microns as compared to the 1 to 2 microns anticipated. The line analysis smear models employed in this evaluation are discussed in detail in Section VI of this report.

3.5.5 Resolution by Target

The raw and normalized CORN target data for the Forward Camera is presented in Table 3-12 and for the Aft Camera in Table 3-13.

3.5.6 Normalized Resolution Average by Platen Position

Although the sampling is somewhat small, the 2:1 normalized mobile CORN resolution values tabulated as a function of platen position show a trend compatible with the on-orbit platen change decisions made on 1201, see Table 3-14. It can be seen from this table that only the in and cross-track between $79\mu$ and $71\mu$, and $79\mu$ and $64\mu$ show with 80% confidence a significant resolution difference.

3.5.7 Contrast Adjustments

The D log E curve presented as Curve 1 in Figure 3-5 which was used in this study was considered at the time to be the most applicable to obtain edge contrast at the entrance pupil. However further analysis has been accomplished. Table 3-15 shows the variation in tribar contrast at the entrance pupil for several frames which were calculated by different methods and utilized both D log E curves, see Figure 3-5.

TABLE 3-12

FORWARD CAMERA CORN TARGET DATA

| Op | Frame | Platen Position (microns) | Tribar Contrast at Entrance Pupil | In-Track Read Resolution (c/mm) | In-Track Resolution 2:1 Contrast Normalized (c/mm) | Cross-Track Read Resolution (c/mm) | Cross-Track Resolution 2:1 Contrast Normalized (c/mm) | Scan Angle (degrees) | Field Position (degrees) |
|---|---|---|---|---|---|---|---|---|---|
| 5 | 029 | 79 | 1.96 | 102 | 103 | 63 | 63 | -5.9 | -2.2 |
| 5 | 048 | 79 | 2.04 | 164 | 163 | 121 | 121 | 19.5 | 0.7 |
| 16 | 007 | 79 | - | 185 | - | 108 | - | 6.7 | -0.2 |
| 17 | 008 | 79 | 2.09 | 126 | 124 | 84 | 83 | 6.7 | -0.2 |
| 17 | 055 | 79 | 1.93 | 192 | 196 | 132 | 135 | 5.3 | -0.2 |
| 35 | 055 | 79 | - | 170 | - | 114 | - | 3.5 | -0.5 |
| 65 | 008 | 79 | 1.80 | 100 | 103 | 76 | 78 | -14.4 | 1.4 |
| 120 | 018 | 79 | 1.85 | 114 | 117 | 91 | 93 | 9.7 | 1.5 |
| 120 | 025 | 79 | 2.05 | 112 | 111 | 99 | 98 | 53.0 | 1.7 |
| 120 | 026 | 79 | 2.05 | 113 | 112 | 78 | 76 | 53.5 | 1.7 |
| 145 | 012 | 71 | 1.33 | 133 | 192 | 118 | 182 | 10.3 | -1.3 |
| 165 | 015 | 71 | 2.03 | 182 | 181 | 137 | 136 | -21.6 | 0.8 |
| 165 | 022 | 71 | 2.40 | 127 | 122 | 97 | 93 | -23.0 | -1.1 |
| 384 | 002 | 64 | 1.60 | 216 | 250 | 172 | 208 | -18.0 | 0.8 |
| 409 | 001 | 64 | 1.62 | 150 | 173 | 103 | 112 | -10.8 | 2.5 |
| 409 | 001 | 64 | 1.75 | 126 | 133 | 94 | 98 | -8.2 | 2.9 |
| 409 | 002 | 64 | 1.75 | 160 | 173 | 88 | 91 | -8.1 | -3.0 |

TABLE 3-13

AFT CAMERA CORN TARGET DATA

| Op | Frame | Platen Position (microns) | Tribar Contrast at Entrance Pupil | In-Track: Read Resolution (c/mm) | In-Track: Resolution 2:1 Contrast Normalized (c/mm) | Cross-Track: Read Resolution (c/mm) | Cross-Track: Resolution 2:1 Contrast Normalized (c/mm) | Scan Angle (degrees) | Field Position (degrees) |
|---|---|---|---|---|---|---|---|---|---|
| 5 | 029 | 52 | 1.81 | 172 | 181 | 126 | 132 | -5.1 | -0.1 |
| 5 | 049 | 52 | 2.12 | 171 | 167 | 133 | 130 | 20.4 | 1.8 |
| 16 | 008 | 52 | - | 152 | - | 115 | - | 7.6 | 2.5 |
| 17 | 009 | 52 | 2.30 | 188 | 178 | 144 | 137 | 22.8 | -0.3 |
| 17 | 056 | 52 | 1.81 | 142 | 149 | 137 | 146 | 8.6 | 2.9 |
| 35 | 020 | 52 | - | 152 | - | 97 | - | 22.1 | 0.1 |
| 35 | 055 | 52 | - | 123 | - | 77 | - | 4.4 | -2.5 |
| 35 | 056 | 52 | - | 156 | - | 103 | - | 4.4 | 2.9 |
| 120 | 019 | 52 | 1.62 | 179 | 209 | 146 | 173 | 10.8 | 0.9 |
| 120 | 026 | 37 | 1.77 | 167 | 180 | 127 | 134 | 53.8 | -1.4 |
| 120 | 027 | 37 | 1.77 | 167 | 180 | 146 | 157 | 53.4 | 1.5 |
| 145 | 012 | 46 | 1.42 | 133 | 171 | 125 | 173 | 11.1 | -2.0 |
| 165 | 016 | 46 | 1.94 | 149 | 151 | 113 | 114 | -20.5 | 2.3 |
| 165 | 022 | 46 | 1.37 | 157 | 229 | 117 | 166 | -22.4 | -1.1 |
| 384 | 003 | 46 | 1.52 | 148 | 179 | 134 | 165 | -16.8 | 2.3 |
| 409 | 002 | 46 | 1.57 | 200 | 241 | 113 | 128 | -9.9 | 0.5 |
| 409 | 002 | 46 | 1.71 | 181 | 201 | 106 | 112 | -7.3 | 0.1 |

FIGURE 3-5

SENSITOMETRIC CURVES FOR MICRODENSITOMETRIC ANALYSIS

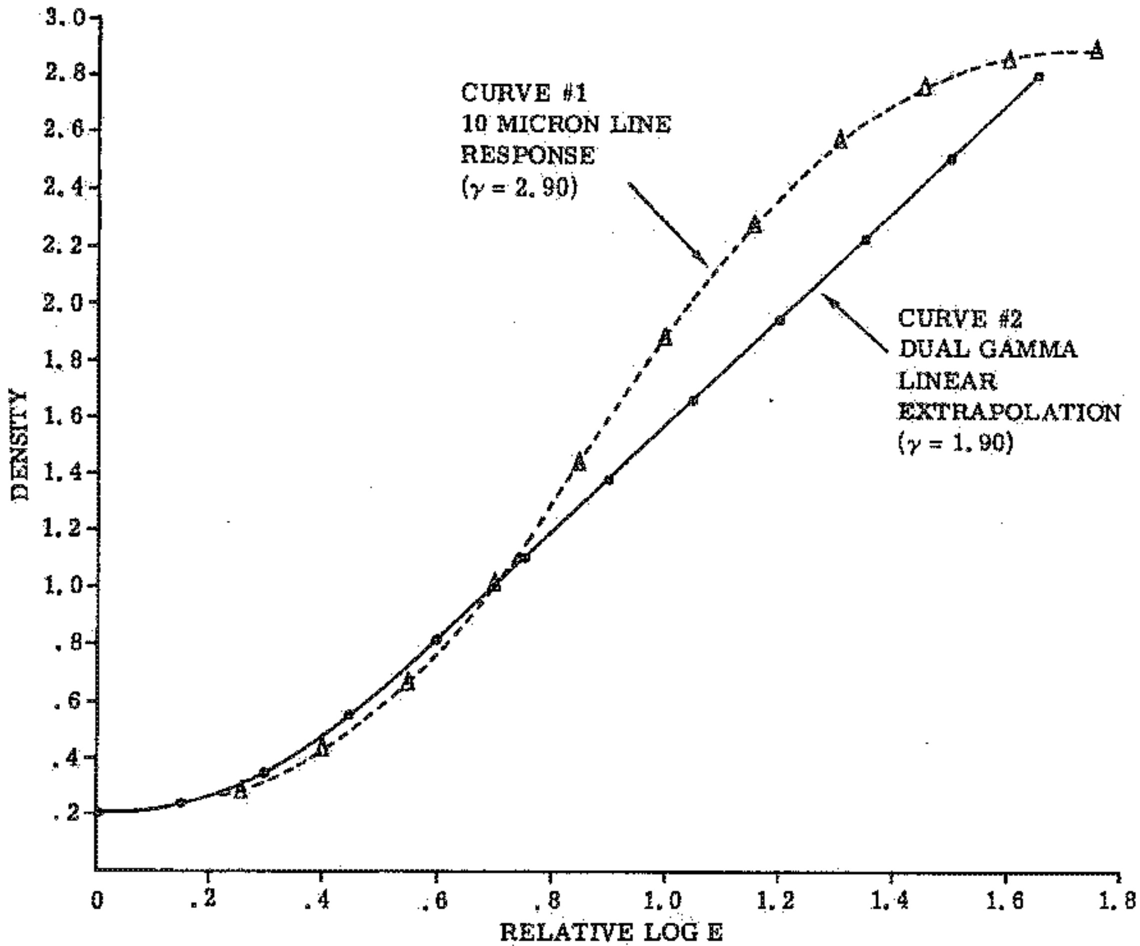




TOP SECRET RUFF

Handle via Talent Keyhole Controls Only

Approved for Release: 2022/03/03 C05132845

TABLE 3-15

TRIBAR CONTRAST AT THE ENTRANCE PUPIL

CALCULATED FIVE WAYS

| Method 1 | Method 2 | Method 3 | Method 4 | Method 5 |
|---|---|---|---|---|
| 1.85 | 1.87 | 1.80 | 2.41 | 2.09 |
| 2.05 | 1.69 | 1.75 | 2.14 | 2.03 |
| 1.62 | 1.74 | 1.90 | 2.06 | 1.92 |
| 1.75 | 1.61 | 1.69 | 2.30 | 2.39 |
| 1.77 | 1.73 | 1.40 | 2.22 | 1.54 |
| 1.57 | 1.57 | 1.64 | 1.99 | 1.99 |

NOTES:

1. D log E 1 refers to Curve 1 and D log E 2 to Curve 2 to Figure 3-5, page 3-29.
2. Methods 2 and 3 used AFSPPF microdensitometric trace data, while Method 1 used BRIDGEHEAD microdensitometric data.
3. Methods 1, 2, and 4 calculated contrast using tribar contrast equations in the text, while Methods 3 and 5 used the line trace area to get tribar contrast.

From the rather large range of values representing the same ground tribar target in a given row, it is clear that further study in this area is warranted. Specifically, the most relevant D log E curve to use would be one generated by exposing a series of edges approximately 100μ in size. By making each edge have a 2:1 contrast, a frequency spectrum which goes out to aprx 150 cycles/mm, and a typical operational background density, the pronounced adjacency effects should be almost the same for the mission edges and D log E curve edges exposed onto mission material. This should result in the most accurate conversion of mission film density to edge contrast at the entrance pupil.

## 3.6 FOCUS ANALYSIS

### 3.6.1 Introduction

The purpose of this section is to assess the effectiveness of the platen position adjustments made on-orbit. As detailed in paragraph 3.4, six thru focus runs were acquired over the ZI. Because of difficulties which included cloud cover and lack of cultural detail, most of these were only marginally useful in the determination of focus adequacy. The most critical thru focus runs are those collected in RV-1 because they constitute the only information base upon which to decide whether to change focus, and by how much and in what direction. Subsequent runs in later buckets are for verification or fine tuning. The Mission 1201 operational film acquired at different platen positions constitutes the major source of focus information. The operational platen positions and where in the mission they were affected, are given in Table 3-14. There were three platen positions (79μ, 71μ, and 63μ) on the Forward Camera and

## TABLE 3-14

### 2:1 NORMALIZED CORN TARGET RESOLUTION

#### FORWARD CAMERA

| Platen Position (microns) | In-Track (c/mm) | Standard Deviation (c/mm) | No. of Targets | Cross-Track (c/mm) | Standard Deviation (c/mm) | No. of Targets | Geo Mean (c/mm) |
|---|---|---|---|---|---|---|---|
| 79 (Lift-off) | 129 | 33.3 | 8 | 93 | 24.2 | 8 | 110 |
| 71 (First Change) | 165 | 37.6 | 3 | 137 | 44.5 | 3 | 150 |
| 64 (Final) | 182 | 48.9 | 4 | 127 | 54.5 | 4 | 152 |

#### AFT CAMERA

| Platen Position (microns) | In-Track (c/mm) | Standard Deviation (c/mm) | No. of Targets | Cross-Track (c/mm) | Standard Deviation (c/mm) | No. of Targets | Geo Mean (c/mm) |
|---|---|---|---|---|---|---|---|
| 52 (Lift-off) | 177 | 21.9 | 5 | 144 | 17.6 | 5 | 160 |
| 46 (Final) | 195 | 34.9 | 6 | 143 | 28.1 | 6 | 167 |
| 37 (Thru Focus) | 180 | 0 | 2 | 146 | 16.3 | 2 | 162 |

NOTE: Although the decision to choose 0 defocus PMTF for platen positions of 64μ on the Forward Camera and 46μ on the Aft Camera somewhat influences the trend in Table 3-14, it was found that the unnormalized resolution values follow the same trend. Averages are over field and scan positions.

two (52μ and 46μ) on the Aft Camera that were used progressively during the mission.

3.6.2 Synopsis of PFA Messages from BRIDGEHEAD

Upon the return of the 1201-1 film, initial post flight analysis determined that both cameras were out-of-focus in the same direction (film behind focal plane) and that the imagery of the Forward Camera was more degraded than that from the Aft. The effects of field curvature and focal plane tilt were evidenced as quality variations in the imagery from both cameras. After platen position adjustments, the quality of photography from both cameras appeared to have improved, with the Aft film web almost uniform in quality, and at best focus. After another platen position adjustment on the Forward Camera side only, its image quality appeared to have improved to the point of being superior to that from the Aft Camera. In fact, an anomolous loss in quality seemed evident on the Aft film from RV-4.

After the above reports were made, additional in-depth analysis with both controlled tribar image ZI acquisitions, and VEM analysis of urban/industrial clusters in the operational photography, has to a great degree substantiated these initial impressions. As a result more details have become available on the degree of performance improvement with operational focal plane adjustments and the changing profiles of field curvature. This analysis, however, showed that there was no apparent image quality loss on the Aft Camera product from RV-4.

3.6.3 Mobile CORN Tribar Target Data

Mobile CORN tribar acquisitions normalized for 2:1 incident contrast (paragraph 3.5) produce reliable resolution data which is useful in focus analysis. The fundamental limitation to this evaluation technique is the sparcity of sampling. However, when this data is grouped according to platen position, a mission focus history evolves which is not unlike that arrived at by the PFA Team during the mission, see Table 3-16. This is true despite the fact that differences in field and scan locations are not taken into account.

TABLE 3-16

FOCUS HISTORY

| Camera | Operation No. | Frame | Mission Segment | Platen Posn (microns) | Platen Posn (microns) |
|---|---|---|---|---|---|
| | 1 | 1 | RV-1 | 79 | - |
| Forward | 121 | 1 | RV-2 | 71 | -8 |
| | 240 | 1 | RV-3 | 63 | -8 |
| | | | | | -16 Total |
| Aft | 1 | 1 | RV-1 | 52 | - |
| | 120 | 31 | RV-2 | 46 | -6 |

According to the in-track resolution data alone, at the initial focal positions, the Forward Camera (129 c/mm) did not perform as well as the Aft (177 c/mm). With the first focus adjustment on-orbit, each side improved performance. The 8μ change on the Forward Camera produced a 28% increase in resolution while the 6μ change on the Aft Camera resulted in only a 10% increase. After the additional 8μ adjustment on the Forward Camera there was an additional 10% resolution increase, but the performance remained slightly inferior to that of the Aft Camera.

It is in the last case that this description differs from the original impressions. The tribar deployments reveal no loss of Aft Camera image quality in RV-4 recovered film. In addition, one deployment acquired on successive Aft Camera frames at 37μ indicates that the 46μ setting was indeed near optimum.

This mission focus history is not told by comparing the geometric mean resolution values because the cross-track values are consistently low. The indication here is that the values have been saturated by some sort of cross-track smear limitation, (paragraph 3.5).

3.6.4 Visual Edge Match (VEM) Data

VEM data collected at random throughout the mission within the 45 format cells was grouped together into camera and platen position categories as an overall attempt to characterize the image quality in terms of its focus history. This data includes samplings of field and scan locations, slit widths, scan mode and center, matrix, and reader. The results of this summarization are given in Figure 3-6. For the Forward Camera, a performance improvement with each of the 8μ platen position adjustments is evident. For the Aft Camera, no performance difference is evident from the data with the focus change. This is not unreasonable since the VEM resolution data has a variability and since measurements are included from both RV-2 and 4. This could explain the balancing of RV-2 improvement and RV-4 degradation originally suspected by the PFA Team. All five data points have a standard deviation of ±30 c/mm associated with them.

In Figure 3-6, there is a disturbing discrepancy between the Forward and Aft performance levels in general. The fact that the Aft Camera values are much higher is suspicious. Considering the difficulties in VEM resolution calibration at this stage of its use, there could be errors in this area. For example, if the Aft Camera values are reduced 16% to account in a rough way for the calibration differences between the two cameras, the measured results look more like what was expected to happen in an absolute sense. To clarify this, predicted average resolution values for these conditions are included in Figure 3-6. These predictions were made by assuming that the final focus settings were exactly optimum on each camera and that smear was constant at 2μ in both directions and linear. In this way, MTF's for each camera individually were combined for the 0 and ±2.5 field position and intersected with a 2:1 contrast AIM curve to produce the average predicted values listed in Table 3-17 and shown in Figure 3-6. There is remarkable agreement between the Forward and Aft Cameras.

FIGURE 3-6

GRAND AVERAGE VEM RESOLUTION FOR OPERATIONAL PLATEN POSITIONS

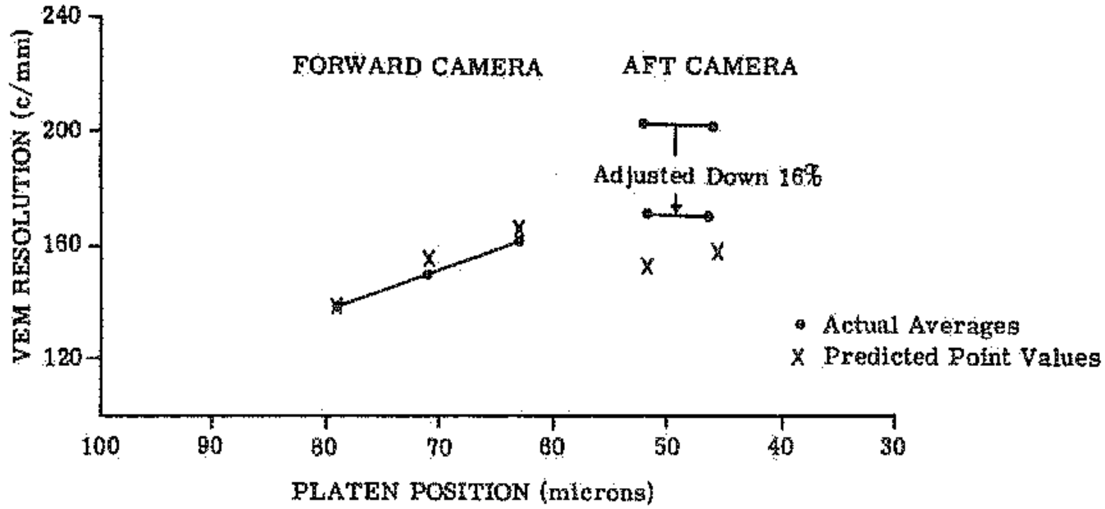


NOTE: Adjusted down 16% due to possible calibration error.

TOP SECRET RUFF

Handle via Talent-Keyhole Controls Only



Approved for Release: 2022/03/03 C05132845

TABLE 3-17

AVERAGE AND PREDICTED RESOLUTION FOR OPERATIONAL PLATEN POSITION

| Camera | Sequence | Platen Position (microns) | Approximate Sample Size | Average Resolution (c/mm) | Predicted Resolution (c/mm) | Percent Difference (%) |
|---|---|---|---|---|---|---|
| Forward | First | 79 | 500 | 138 | 139 | +.7 |
| | Second | 71 | 700 | 150 | 155 | +3.3 |
| | Final | 63 | 1400 | 162 | 165 | +1.9 |
| Aft | First | 52 | 1000 | 203(171)* | 153 | -24.6(-10.5)* |
| | Final | 46 | 700 | 202(170)* | 158 | -21.8(-7.1)* |

*Adjusted down 16% due to possible calibration error.

A more detailed view of focus adjustment effects is afforded by geometric mean minor axis profiles averaged for all available scan positions. This presentation is made in Figure 3-7. For the Forward Camera, the first focus change indicates an across the web performance improvement while the second focus change reflects an improvement each side of center. For the Aft Camera, the initial platen setting has resulted in a profile superior to that of the Forward Camera. With the platen shift, the resulting profile suggests either similar or possibly better performance.

Finally, in an attempt to isolate more finely the quality effects of the mission's focus adjustments, minor axis profiles for center of format data only were generated. Also, the profiles are restricted to a range of narrow slits (.150" and .175") to minimize degrading effects due to image smear and film dynamics. In Figures 3-8, 3-9, and 3-10, the determined profiles in terms of geometric mean resolution values (in and cross-track) are given for the operational platen positions. For the initial photography the Forward Camera profiles oscillate at aprx the 140 cycles/mm level. This essentially flat response suggests that a fairly significant degree of defocus was in effect at that time. At the same time, the Aft Camera profile also suggests defocus, but to a lesser degree. There is a discernible center peak at 200 cycles/mm, falling off on either edge to 190 cycles/mm.

After the first focal adjustment, both platen positions were closer to their OBs. No effect of the $-8\mu$ change on the Forward side is detected with this criterion, whereas the $-6\mu$ adjustment on the Aft Camera apparently produced an outstanding improvement. The second additional platen position change of $-8\mu$ on the Forward side seemed to have improved the situation significantly, though the performance is still not as good as that of the Aft Camera.

Extending this approach a little further, sufficient data was collected at one additional platen position on each side to determine comparative profiles. These profiles are compared to the operational platen position profiles in Figures 3-11 thru 3-13. On the Aft side the focus is for $35\mu$, a platen position

MEAN OF MINOR AXIS PROFILES FROM ALL SCAN, IN-TRACK AND CROSS-TRACK DATA FOR THE FIVE OPERATIONAL PLATEN POSITIONS

FORWARD CAMERA

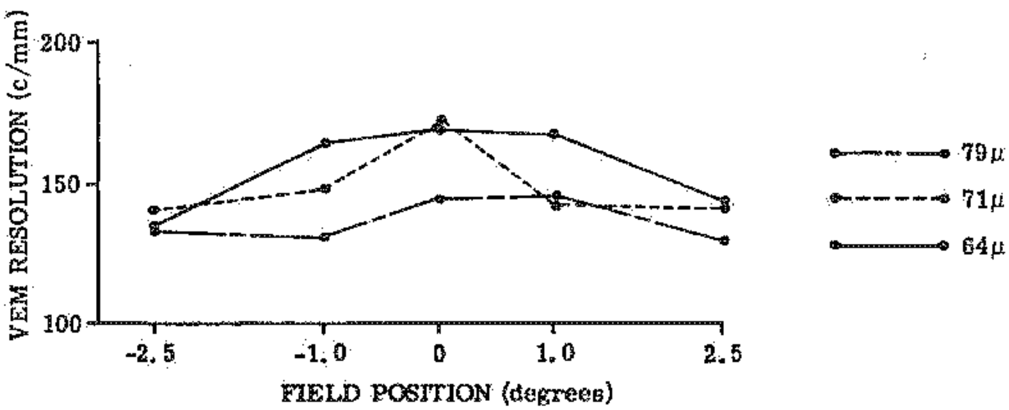


AFT CAMERA

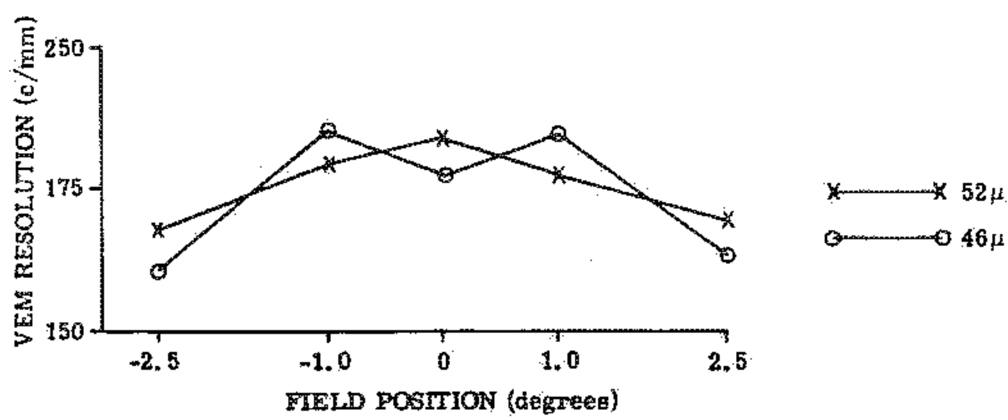


FIGURE 3-7

GEOMETRIC MEAN CENTER FORMAT MINOR AXIS PROFILES

FOR THE FIVE OPERATIONAL PLATEN POSITIONS

FORWARD CAMERA

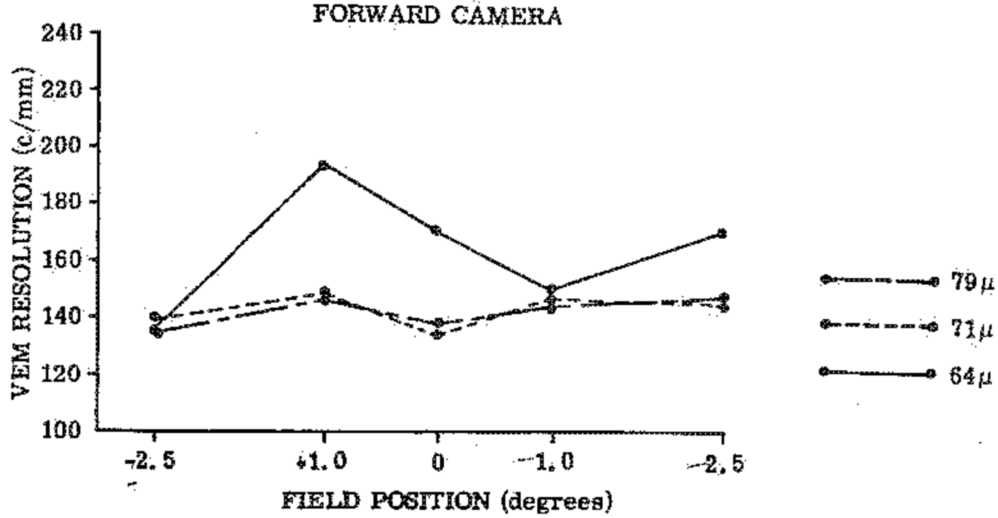


AFT CAMERA

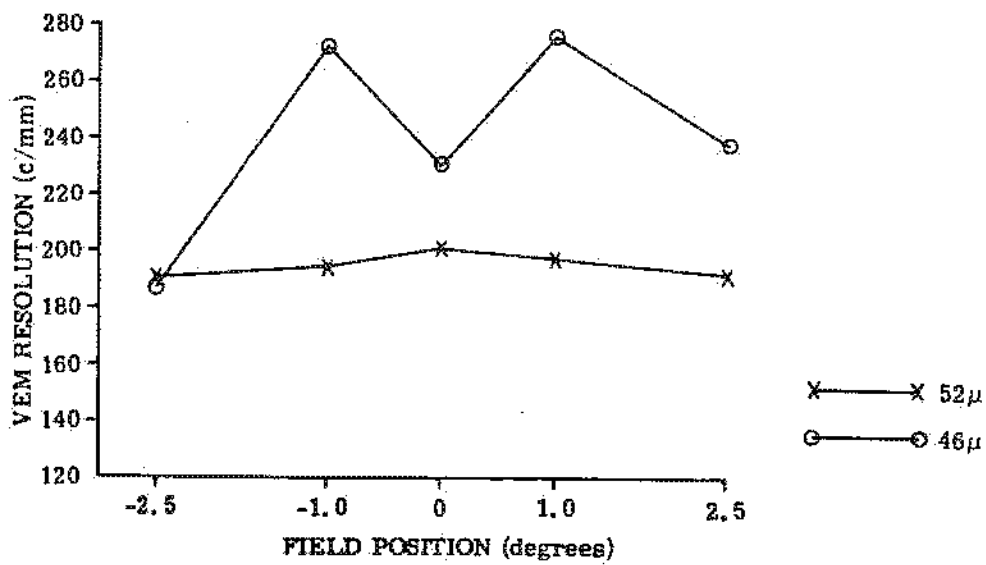


NOTES:

| | FORWARD | AFT |
|---|---|---|
| INITIAL PLATEN POSN | 79μ | 52μ |
| SECOND PLATEN POSN | 71μ | NA |
| FINAL PLATEN POSN | 64μ | 46μ |

FIGURE 3-8

FORWARD CAMERA IN AND CROSS-TRACK CENTER FORMAT MINOR AXIS PROFILES FOR THE FIVE OPERATIONAL PLATEN POSITIONS

IN-TRACK

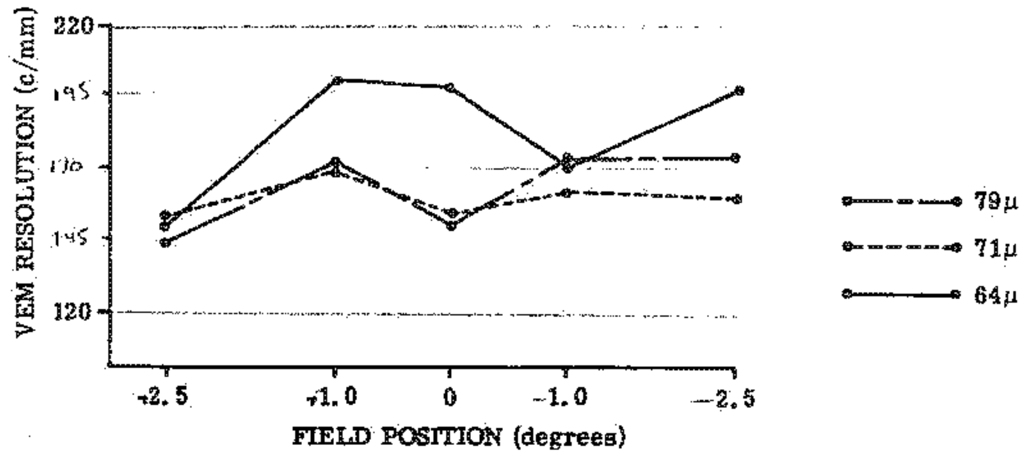


CROSS-TRACK

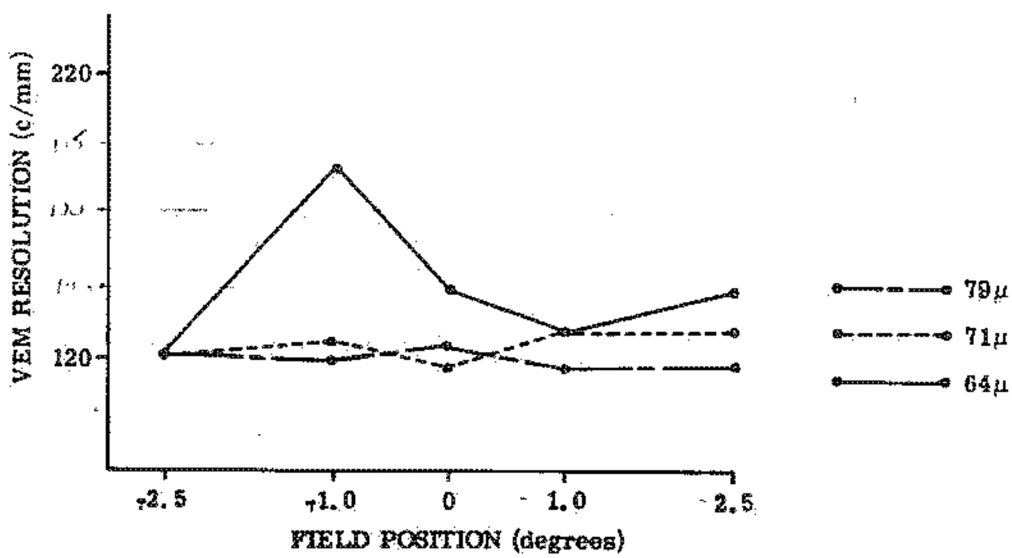


FIGURE 3-9

AFT CAMERA IN AND CROSS-TRACK CENTER FORMAT MINOR AXIS PROFILES

FOR THE FIVE OPERATIONAL PLATEN POSITIONS

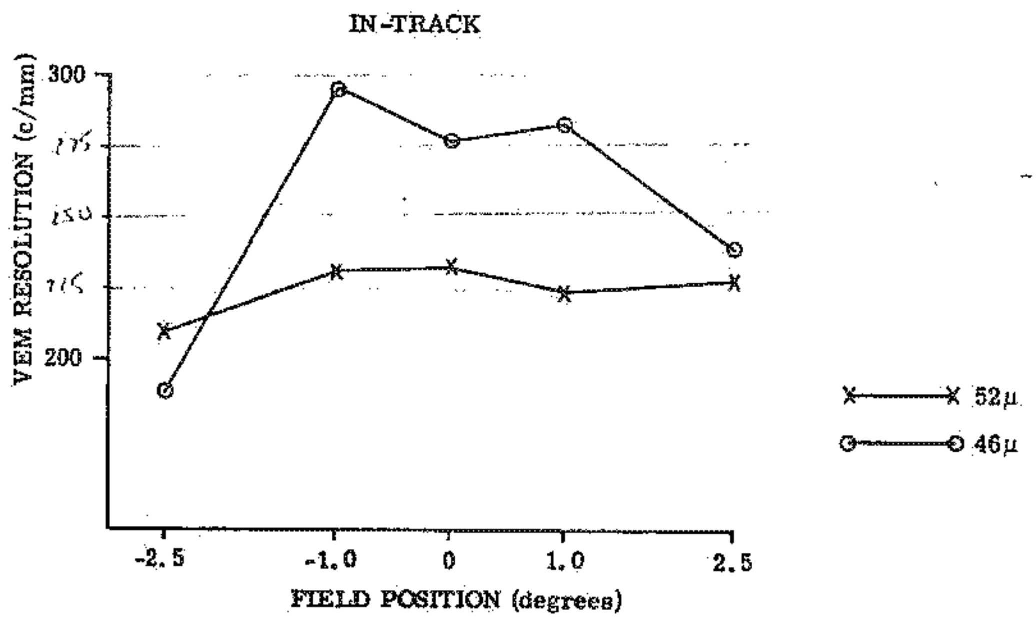


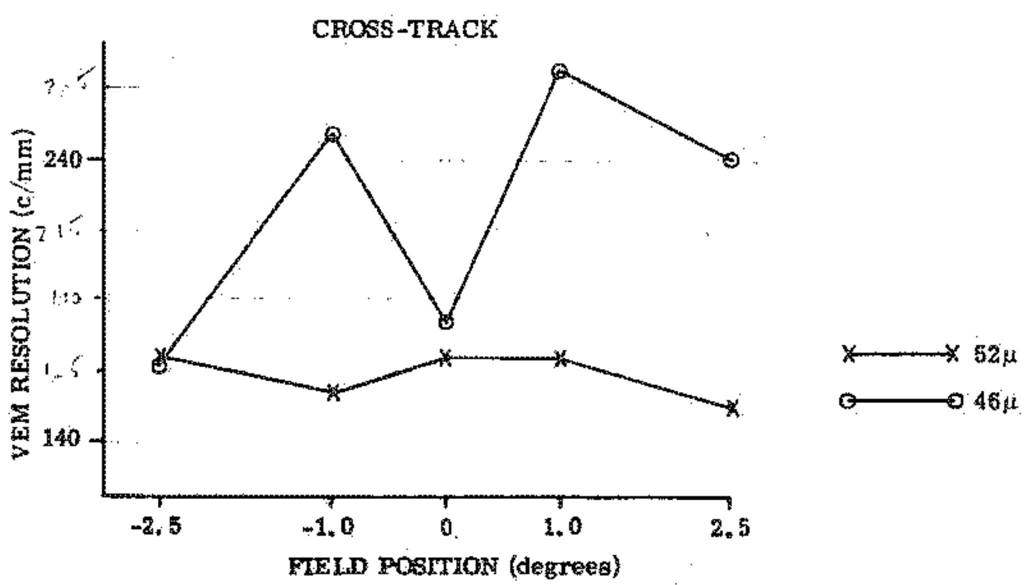


FIGURE 3-10

GEOMETRIC MEAN CENTER FORMAT MINOR AXIS PROFILES

FOR THRU FOCUS PLATEN POSITIONS

FORWARD CAMERA

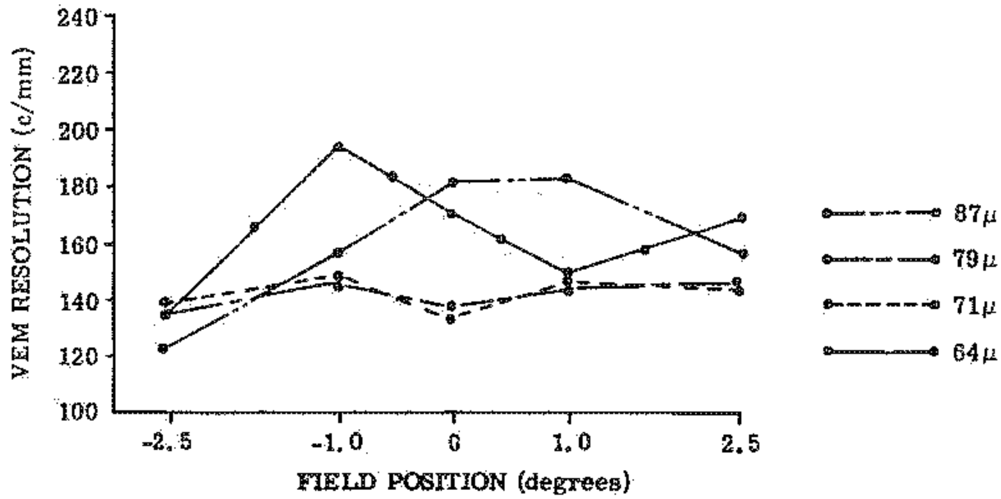


AFT CAMERA

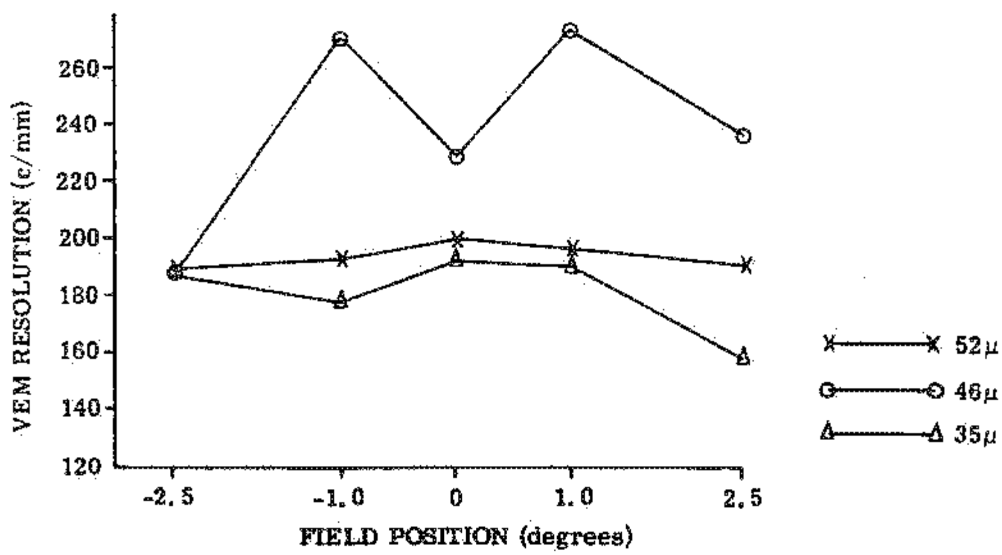


NOTES:

| | FORWARD | AFT |
|---|---|---|
| INITIAL PLATEN POSN | 79μ | 52μ |
| SECOND PLATEN POSN | 71μ | NA |
| FINAL PLATEN POSN | 64μ | 46μ |

FIGURE 3-11

FORWARD CAMERA CENTER FORMAT MINOR AXIS PROFILES
FOR THRU FOCUS PLATEN POSITIONS

IN-TRACK

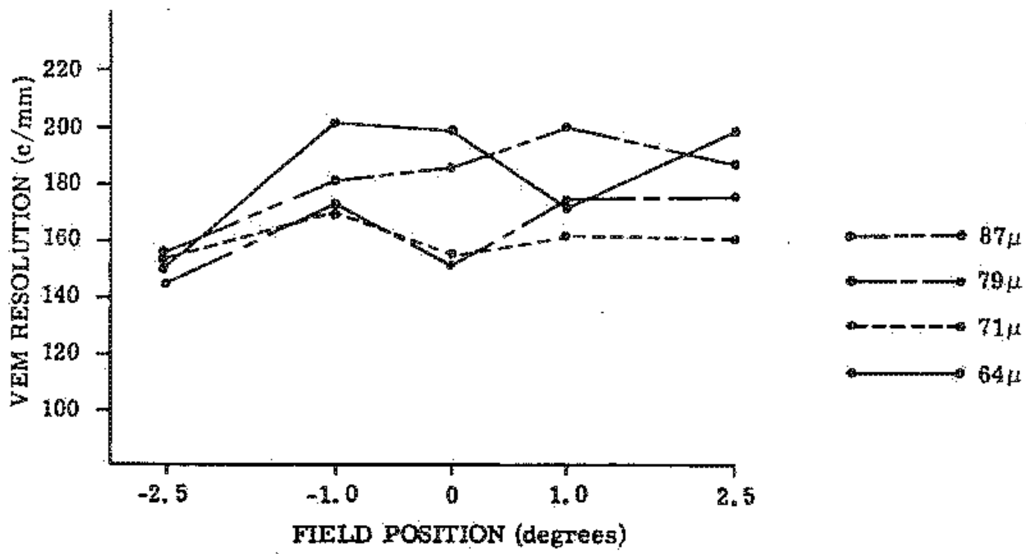


CROSS-TRACK

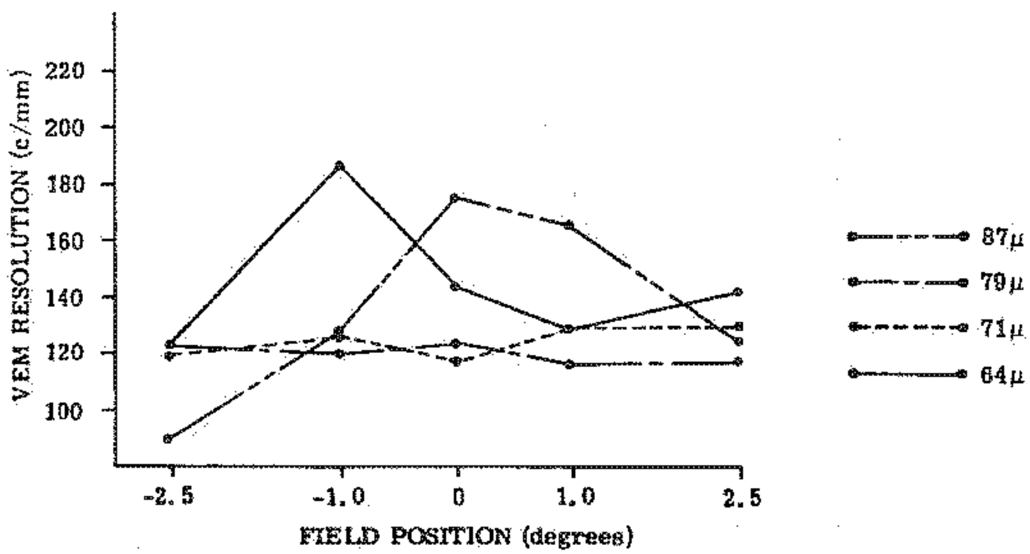


FIGURE 3-12



Approved for Release: 2022/03/03 C05132845

AFT CAMERA CENTER FORMAT MINOR AXIS PROFILES

FOR THRU FOCUS PLATEN POSITIONS

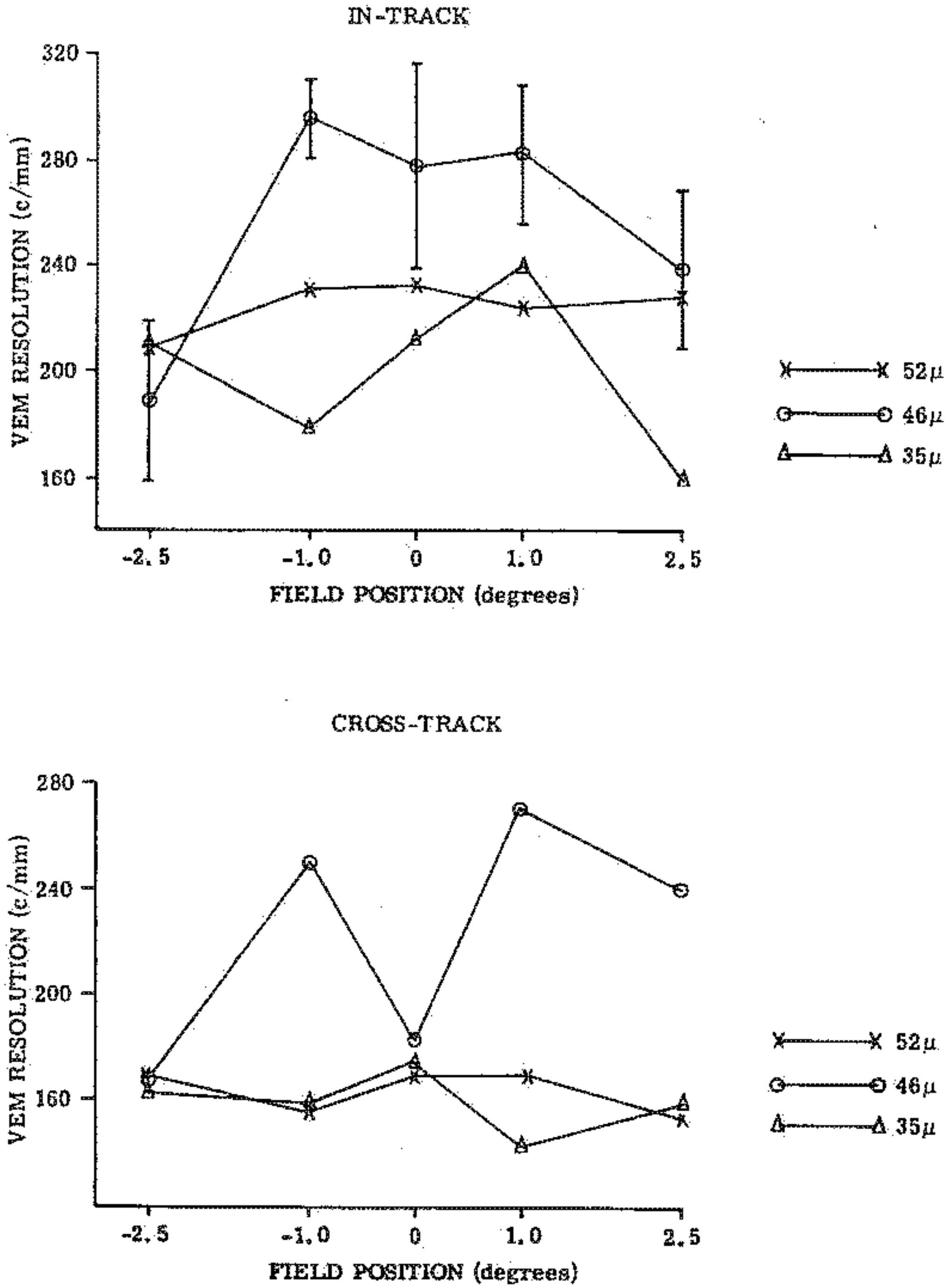


FIGURE 3-13

which is closer to the OB than the final operational setting. The indicated performance is down slightly below the 52μ profile, which isolates the 46μ setting as very close to peak performance. On the Forward side, however, the situation becomes more confusing. Although there wasn't any data for another position closer to the OB, there was for one further away from the OB (87μ) than the initial position. From the progression shown in Figure 3-8, it is expected that the 87μ profile would be lower than the 71/79μ profiles, since the 63μ profile is highest. But in fact the 87μ profile is comparable to that of the final focus setting 23 microns away, see Figure 3-11. The data for both the extended range profiles, however, is sparse and, therefore, cannot be considered as valid as the operational profiles.

3.6.5 Conclusions

A. The on-orbit focus adjust decisions made by the PFA Team during the mission were good.

B. The Aft Camera finally operated close to maximum resolution.

C. The Forward Camera could possibly have been further improved by another platen position change in the minus direction.

3.6.6 Summary

If all of the conclusions are indeed true, it is not understood where in preflight chamber testing procedures this discrepancy between cameras, which amounts to aprx 12μ of focus setting, should be found.

## 3.7 CAMERA RESOLUTION PERFORMANCE

### 3.7.1 Introduction

An extensive analysis of operational photography was performed using the visual edge matching (VEM) technique in order to relate orbital resolution performance to that achieved during laboratory testing. Of particular interest are the contrasts which assess the entire format resolution, resolution as a function of field angle (minor axis), and resolution as a function of scan angle (major axis). Each of these topics will be addressed in the following section.

Although thousands of operational edges were matched and resolution values derived during the post flight analysis, it was not possible to collect enough data to make as many concrete statements about camera performance as desired. It should be noted that this is the first time a camera performance program using primarily the visual edge matching technique has been used to assess an operational system.

### 3.7.2 Overall Resolution

Tables 3-18 and 3-19 present the equivalent 2:1 contrast resolution as determined by VEM. The data is divided by Forward and Aft Cameras and presented as a function of scan and field angle for both the in and cross-track directions. The superscripts for each resolution value represent the number of frames which were analyzed, while each resolution value is the average of the number of frames analyzed. The focus positions (64μ Forward and 46μ Aft) chosen were those which were considered to be best focus

## TABLE 3-18

### FORWARD CAMERA VEM RESOLUTION FORMAT DISTRIBUTION

PLATEN POSITION = 64 MICRONS BEST

In-Track

| Field Position (degrees) | Scan Angle (degrees) -60 | -45 | -30 | -15 | 0 | 15 | 30 | 45 | 60 |
|---|---|---|---|---|---|---|---|---|---|
| +2.5 | 219 (1) | 223 (1) | 126 (2) | 141 (5) | 152 (4) | 151 (7) | 165 (8) | 168 (1) | 217 (1) |
| +1.0 | 243 (1) | 149 (1) | 146 (3) | 177 (5) | 201 (2) | 195 (9) | 192 (8) | 247 (1) | 231 (1) |
| 0.0 | 243 (1) | 179 (1) | 147 (3) | 192 (4) | 198 (3) | 197 (7) | 196 (5) | 259 (1) | 243 (1) |
| -1.0 | 140 (1) | 142 (2) | 137 (2) | 214 (4) | 170 (1) | 154 (6) | 185 (4) | 215 (1) | 227 (1) |
| -2.5 | 130 (1) | 105 (1) | 150 (2) | 158 (3) | 164 (3) | 178 (5) | 179 (7) | 140 (1) | 217 (1) |

Cross-Track

| Field Position (degrees) | -60 | -45 | -30 | -15 | 0 | 15 | 30 | 45 | 60 |
|---|---|---|---|---|---|---|---|---|---|
| +2.5 | 155 (1) | 178 (1) | 116 (2) | 139 (5) | 122 (4) | 133 (7) | 148 (8) | 169 (1) | 160 (1) |
| +1.0 | 192 (1) | 149 (1) | 120 (3) | 151 (5) | 187 (2) | 169 (9) | 170 (8) | 213 (1) | 171 (1) |
| 0.0 | 217 (1) | 120 (1) | 123 (3) | 187 (4) | 143 (3) | 183 (7) | 185 (5) | 243 (1) | 193 (1) |
| -1.0 | 135 (1) | 123 (2) | 104 (2) | 192 (4) | 129 (1) | 152 (6) | 171 (4) | 209 (1) | 177 (1) |
| -2.5 | 98 (1) | 105 (1) | 112 (2) | 158 (3) | 130 (3) | 129 (5) | 128 (7) | 81 (1) | 146 (1) |

NOTE: Numbers in parentheses indicate the number of frames which were analyzed.

## TABLE 3-19

### AFT CAMERA VEM RESOLUTION FORMAT DISTRIBUTION

PLATEN POSITION = 46μ BEST

In-Track

| Field Position (degrees) | Scan Angle (degrees) -60 | -45 | -30 | -15 | 0 | 15 | 30 | 45 | 60 |
|---|---|---|---|---|---|---|---|---|---|
| -2.5 | - | - | 184 (2) | 219 (2) | 189 (1) | 240 (1) | 252 (1) | 219 (1) | - |
| -1.0 | - | - | 216 (2) | 233 (2) | 295 (1) | 251 (1) | 271 (1) | 259 (1) | - |
| 0.0 | - | - | 215 (2) | 192 (3) | 259 (1) | 259 (1) | 256 (1) | 261 (1) | - |
| +1.0 | - | - | 236 (2) | 171 (2) | 282 (1) | 257 (1) | 264 (1) | 258 | - |
| +2.5 | - | - | 201 (3) | 187 (1) | 238 (1) | 193 (1) | 212 (1) | 173 (1) | - |

Cross-Track

| Field Position (degrees) | -60 | -45 | -30 | -15 | 0 | 15 | 30 | 45 | 60 |
|---|---|---|---|---|---|---|---|---|---|
| -2.5 | - | - | 151 | 193 | 167 | 212 | 209 | 189 | - |
| -1.0 | - | - | 143 | 219 | 251 | 177 | 252 | 216 | - |
| 0.0 | - | - | 170 | 129 | 215 | 207 | 226 | 243 | - |
| +1.0 | - | - | 218 | 146 | 270 | 242 | 191 | 221 | - |
| +2.5 | - | - | 158 | 151 | 240 | 184 | 151 | 145 | - |

NOTE: Numbers in parentheses indicate the number of frames which were analyzed.

on-orbit. Two general observations can be immediately made which are consistent with the expected camera performance. They are (a) on both cameras the cross-track resolution is lower than the in-track resolution; and (b) in the vast majority of instances the in and cross-track resolution decreases from the center of the format to the edges of the format (minor axis).

Comparing the overall resolution of the Forward to the Aft Camera presents an inconsistency with the predicted performance that would have been expected from laboratory tests in Chamber A-2. The SN-003 Flight Readiness Report indicates that the geometric mean of the Forward Camera (scan angle 0°, field angle 0.0) would be 200 cycles/mm and the Aft Camera would be 165 cycles/mm. The VEM results, however, show the opposite, namely the Forward Camera yields a geometric mean of 168 cycles/mm and the Aft Camera 237 cycles/mm. It is true that the sample size collected for the VEM analysis is small in particular on the Aft Camera, however, the trend is clear. Tribar data was collected during domestic operations and although small in sample size it also indicates that the Aft Camera performed slightly better than the Forward Camera. The geometric mean as determined from tribar data is 152 cycles/mm for the Forward and 167 cycles/mm for the Aft Camera, see paragraph 3.5 for the complete analysis. The tribar data tends to confirm the VEM analysis although the VEM values for the Aft Camera appear to be too high. This discrepancy is probably due to the calibration procedure employed to convert VEM edge matrix numbers to camera resolution.

Off-axis laboratory measurements are made at -45° and +55° scan on the Forward Camera, while on the Aft Camera they are at +45° and -55° scan. Although Table 3-20 is presented as a comparison between laboratory and orbit performance, not many conclusions can be drawn due to the lack of a significant number of VEM data points. However, the axial position of the Forward Camera does show good agreement.

### 3.7.3 Minor Axis Resolution Profile

The minor axis resolution profile was analyzed to see how the optical field curvature and focal plane tilt affect performance. The data collected on the Forward Camera at +15° scan angle was large enough to permit analysis. Table 3-21 gives a statistical summary for each of the five cells across the web at +15°. This data differs slightly from that in Table 3-18 because each data cell which usually contains six in-track and six cross-track VEM readings per frame was used to typify a single format position.

TABLE 3-20

LABORATORY VERSUS ORBITAL PERFORMANCE

Forward Camera

| | -45°/-2.5° | | 0°/0° | | 55°/+2.0° | |
|---|---|---|---|---|---|---|
| Direction | Lab | Orbit | Lab | Orbit | Lab | Orbit |
| In-Track | 150 | 105 (1) | 200 | 198 (3) | 182 | 217 (1) |
| Cross-Track | 170 | 105 (1) | 190 | 143 (3) | 190 | 142 (1) |

Aft Camera

| | +45°/-2.5° | | 0°/0° | | -55°/+2.0° | |
|---|---|---|---|---|---|---|
| Direction | Lab | Orbit | Lab | Orbit | Lab | Orbit |
| In-Track | 140 | 219 (1) | 200 | 259 (1) | 170 | - |
| Cross-Track | 120 | 189 (1) | 150 | 215 (1) | 120 | - |

NOTES:

1. A one to one correlation between orbital resolution and chamber resolution cannot be expected at off-axis positions (+45° . -2.5° and -55°/+2.0°). The chamber test is run with IMC disabled, and does not include fixed known orbital image motion errors.
2. Numbers in parentheses indicate the number of frames which were analyzed.

TABLE 3-21

FORWARD CAMERA MINOR AXIS PROFILE

64μ PLATEN POSITION, SCAN ANGLE +15°

| Field Posn (degrees) | Mean Res (c/mm) | | Standard Deviation | | No. Samples | |
|---|---|---|---|---|---|---|
| | In-Track | Cross-Track | In-Track | Cross-Track | In-Track | Cross-Track |
| +2.5 | 150.6 | 133.4 | 36.3 | 26.2 | 42 | 42 |
| +1.0 | 191.7 | 170.6 | 44.3 | 49.2 | 49 | 49 |
| 0.0 | 205.1 | 197.5 | 45.7 | 48.8 | 34 | 33 |
| -1.0 | 154.0 | 152.2 | 40.7 | 45.4 | 36 | 36 |
| -2.5 | 179.9 | 129.3 | 37.7 | 26.4 | 26 | 26 |

NOTE: The standard deviation was determined from the total number of edges matched at each field position.

Figure 3-14 is a graphical representation of the minor axis profile for the conditions mentioned. The associated ±one sigma values are also presented. This figure shows that under these conditions there is no significant difference between in and cross-track resolution. Figure 3-15 shows the mean resolution with its standard deviation for these same conditions. Superimposed on Figure 3-15 are predicted orbital resolutions for various amounts of smear. Taken into account is both the field curvature and focal plane tilt which were measured during laboratory testing. It can be concluded from this plot that the agreement between laboratory and orbital operation is good. This is true for smear values in the cross-track direction up to 6 microns and also for small values of in-track smear. Such a comparison could not be made for the Aft Camera at best focus. Even for positions other than best focus it would be difficult to compare due to the high VEM readings recorded on the Aft Camera.

### 3.7.4 Major Axis Resolution Profile

The major axis profile of resolution was examined for the purpose of determining resolution changes with scan angle. The things that should affect resolution as a function of scan angle are image motion and focus. Focus is a symmetric function and should affect both sides of scan angle equally. Both cameras' image motions were measured during preflight and acceptance testing. The expected on-orbit fixed known motions are shown in Table 3-22. This table shows the start of scan to be minus 60° for the Forward Camera and +60° for the Aft. One would expect in-flight to see the start of frame resolution on each camera to be lower than the rest of the frame. Figures 3-16 thru 3-19 show the major axis resolution obtained from VEM. The circles are the average values and the ±one sigma spread in the data is shown. Noted above each spread is the number of frames in the sample. Points beyond ±30° have no more than one data point. The cross-track resolution shows a tendency to be lower at the start of scan on both cameras. These results agree with Table 3-22. The in-track resolution on both cameras show some of the same trend but not as strongly as the cross-track direction. These observations are made with caution since the sample sizes are so small and the ±one sigma values large. Tables 3-23 and 3-24 give the geometric means for all field positions. A 52 microns platen position was used for the Aft Camera because more data existed than for the platen position at 46μ.

TABLE 3-22

CHAMBER A-2 MAJOR AXIS SMEAR

Forward Camera

| Direction | Scan Angle (degrees) -45 | 0 | 55 |
|---|---|---|---|
| In-Track | .003 | -.018 | .029 |
| Cross-Track | -.062 | -.012 | -.035 |

Aft Camera

| Direction | Scan Angle (degrees) +45 | 0 | 55 |
|---|---|---|---|
| In-Track | -.066 | -.024 | .032 |
| Cross-Track | -.093 | -.043 | -.061 |

NOTE: The smear values are presented in inches per second.

TABLE 3-23

FORWARD CAMERA GEOMETRIC MEAN FORMAT DISTRIBUTION

64μ PLATEN POSITION

| Field Posn (degrees) | Scan Angle (degrees) -60 | -45 | -30 | -15 | 0 | 15 | 30 | 45 | 60 |
|---|---|---|---|---|---|---|---|---|---|
| +2.5 | 184 (1) | 199 (1) | 121 (2) | 140 (5) | 136 (4) | 142 (7) | 156 (8) | 168 (1) | 186 (1) |
| +1.0 | 216 (1) | 149 (1) | 132 (3) | 163 (5) | 194 (2) | 182 (9) | 181 (8) | 229 (1) | 199 (1) |
| 0.0 | 230 (1) | 147 (1) | 134 (3) | 189 (4) | 168 (3) | 190 (7) | 190 (5) | 251 (1) | 217 (1) |
| -1.0 | 137 (1) | 132 (2) | 119 (2) | 203 (4) | 148 (1) | 153 (6) | 178 (4) | 212 (1) | 200 (1) |
| -2.5 | 112 (1) | 105 (1) | 130 (2) | 157 (3) | 155 (3) | 152 (5) | 151 (7) | 106 (1) | 178 (1) |

NOTE: Numbers in parentheses indicate the number of frames which were analyzed.

FORWARD CAMERA MINOR AXIS RESOLUTION PROFILES
(64μ PLATEN POSITION, 15° SCAN ANGLE)

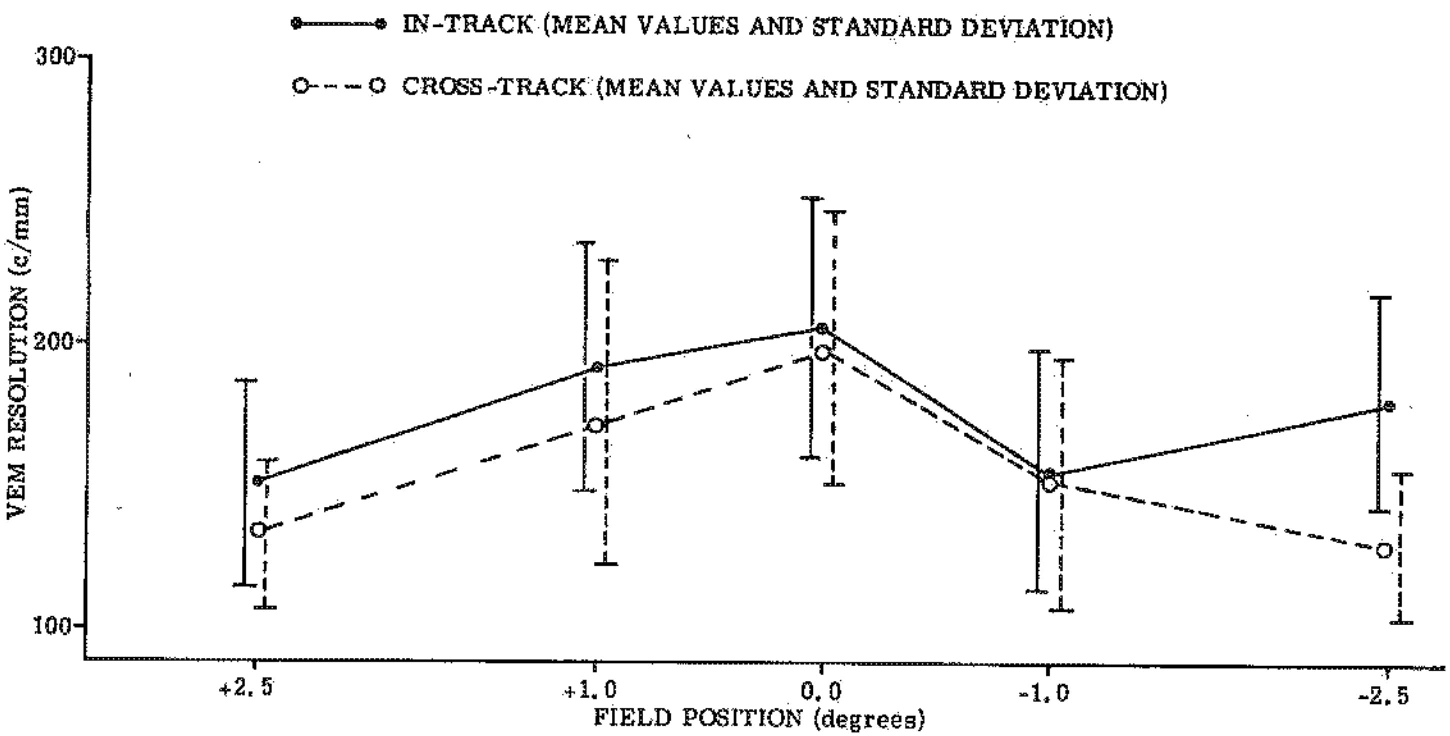


FIGURE 3-14

TOP SECRET RUFF

Handle via Talent-Keyhole Controls Only



Approved for Release: 2022/03/03 C05132845

FIGURE 3-15

FORWARD CAMERA MINOR AXIS GEOMETRIC MEAN RESOLUTION PROFILE
(64μ PLATEN POSITION, 15° SCAN ANGLE)

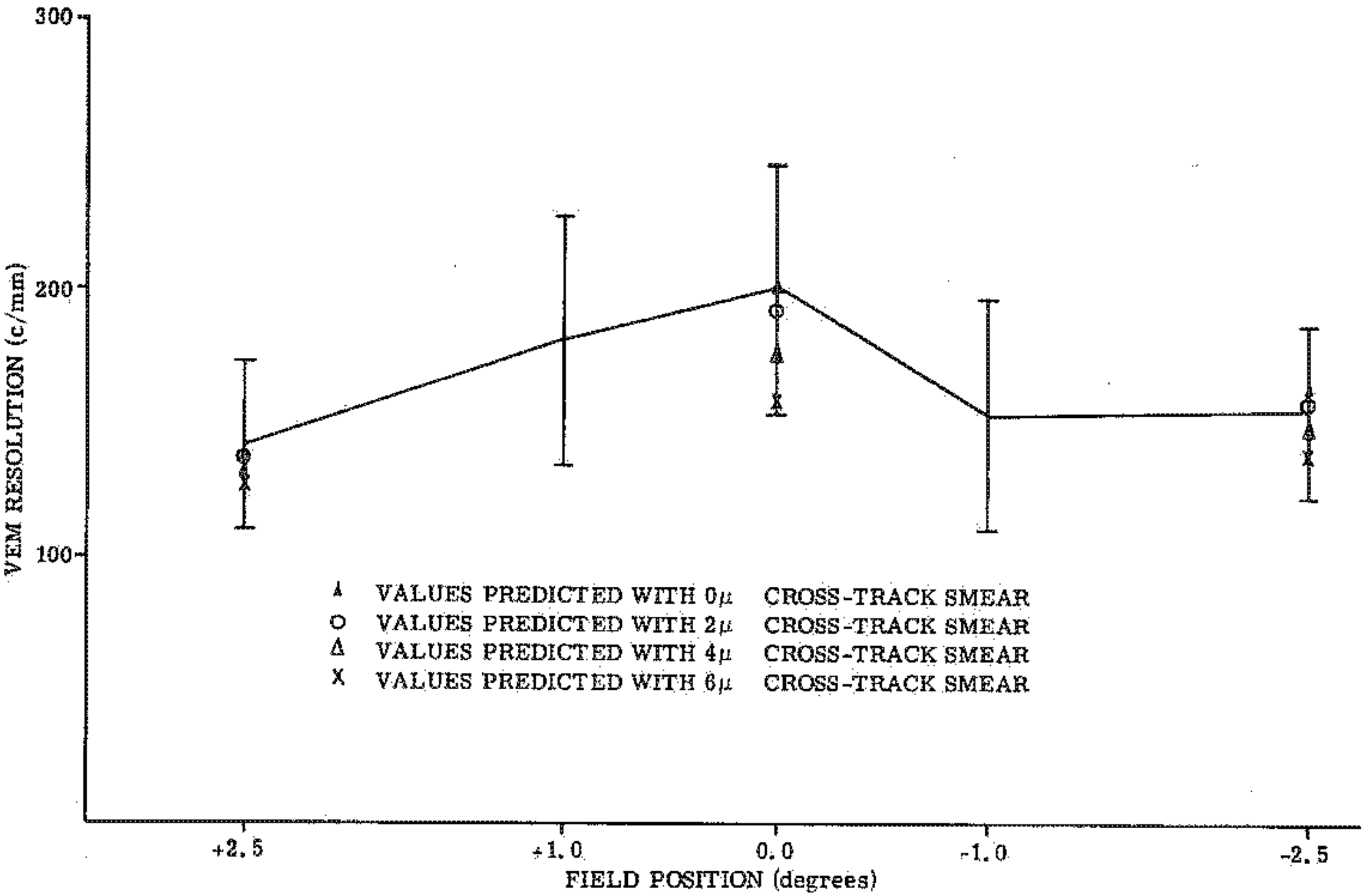

FIGURE 3-16

FORWARD CAMERA MAJOR AXIS PROFILE AT 0° FIELD POSITION

IN-TRACK

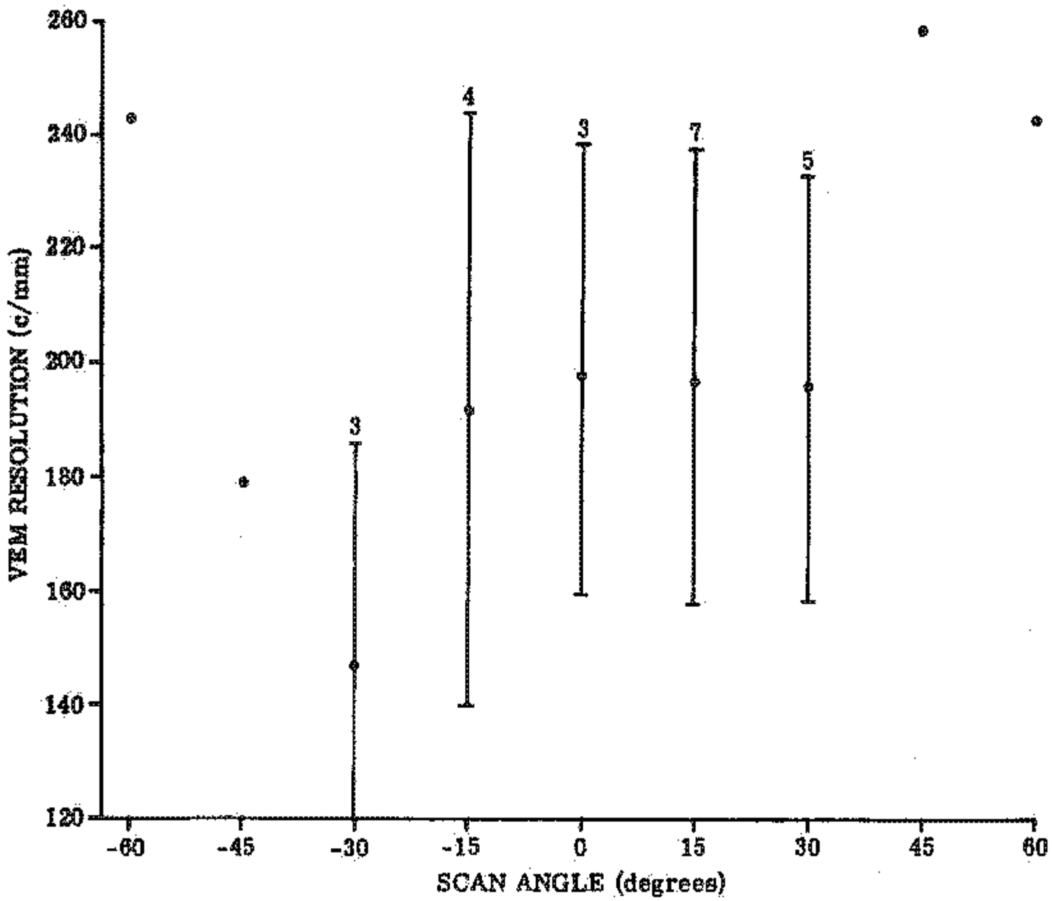

FORWARD CAMERA MAJOR AXIS PROFILE AT 0° FIELD POSITION

CROSS-TRACK

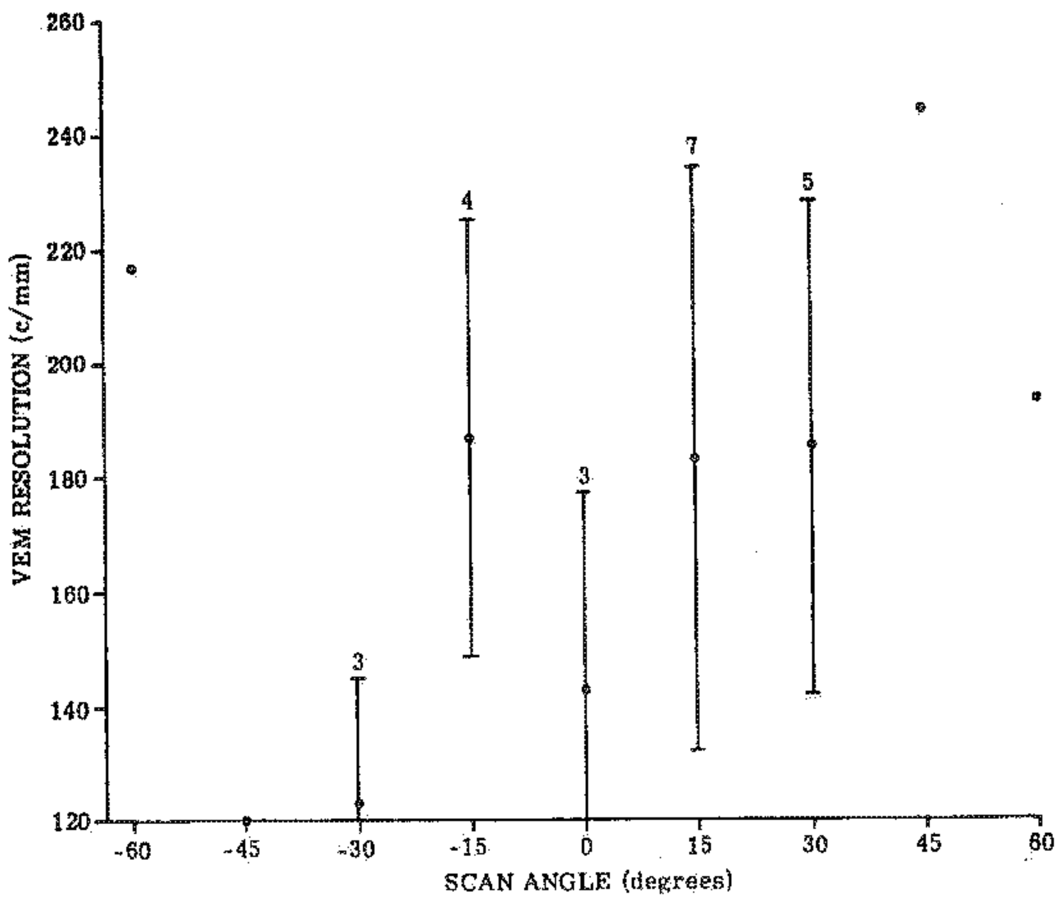


FIGURE 3-17





Approved for Release: 2022/03/03 C05132845

AFT CAMERA MAJOR AXIS PROFILE AT 0° FIELD POSITION

IN-TRACK

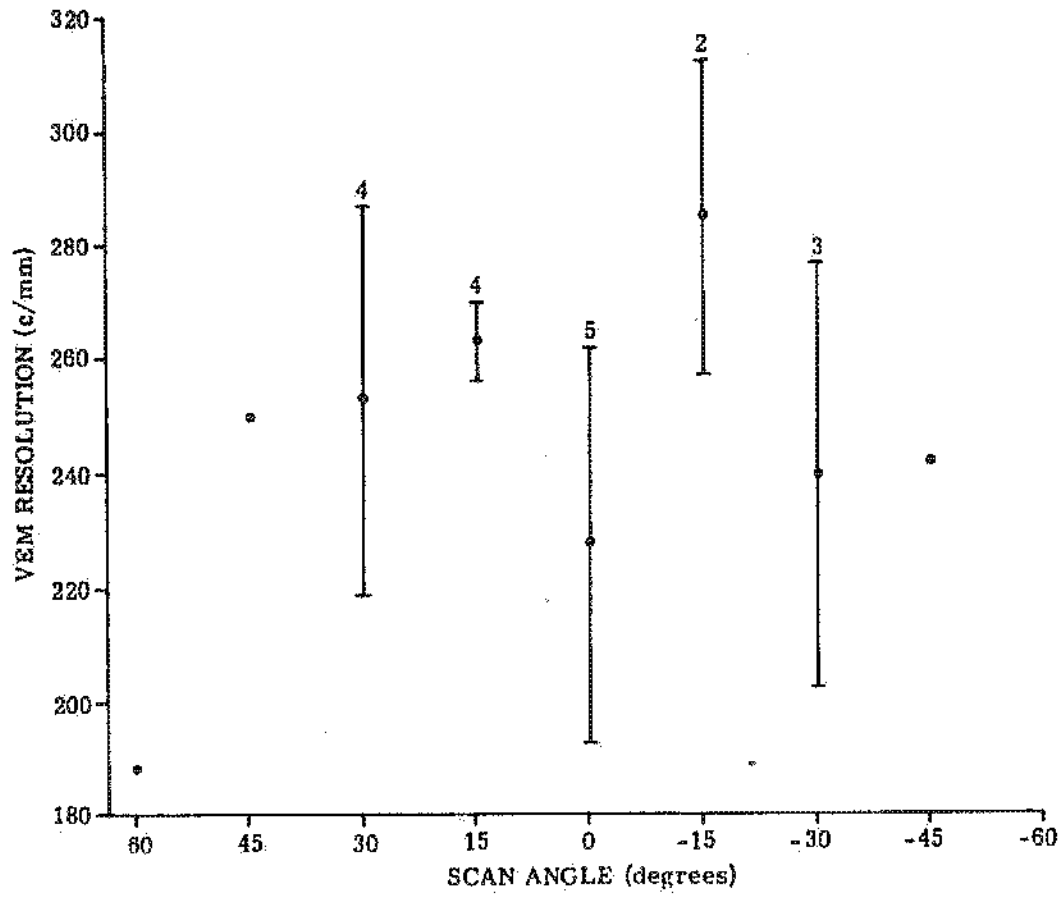


FIGURE 3-18

AFT CAMERA MAJOR AXIS PROFILE AT 0° FIELD POSITION

CROSS-TRACK

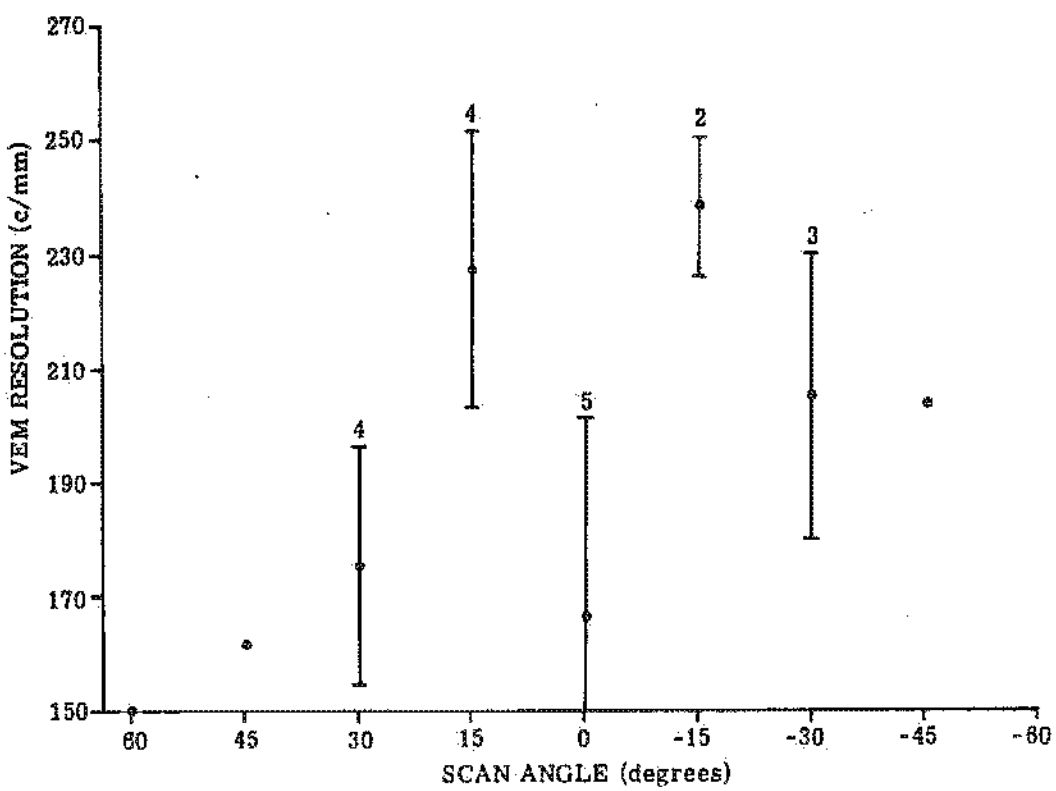


FIGURE 3-19

Handle via Talent-Keyhole Controls Only

TABLE 3-24

AFT CAMERA GEOMETRIC MEAN FORMAT DISTRIBUTION

52μ PLATEN POSITION

| Field Posn (degrees) | Scan Angle (degrees) | | | | | | | | |
|---|---|---|---|---|---|---|---|---|---|
| | -60 | -45 | -30 | -15 | 0 | 15 | 30 | 45 | 60 |
| +2.5 | 130 (1) | 186 (1) | 197 (2) | 202 (3) | 193 (4) | 207 (4) | 191 (4) | 210 (1) | 142 (3) |
| +1.0 | 139 (1) | 201 (1) | 215 (4) | 227 (4) | 201 (9) | 222 (1) | 236 (1) | 214 (1) | 177 (1) |
| 0.0 | 168 (1) | 201 (1) | 210 (4) | 244 (4) | 195 (5) | 260 (2) | 222 (3) | 222 (1) | - |
| -1.0 | 176 (1) | 173 (1) | 216 (2) | 219 (3) | 209 (4) | 241 (3) | 202 (2) | - | - |
| -2.5 | - | 171 (2) | 203 (2) | 199 (3) | 184 (9) | 193 (2) | 192 (1) | 156 (1) | 141 (1) |

NOTE: Numbers in parentheses indicate the number of frames which were analyzed.

### 3.7.5 Conclusions

A. In general the VEM technique was quite useful in showing relative performance and trends in performance. There is, however, some question as to the absolute value of resolution obtained.

B. Assessment of field curvature and tilt is amenable to VEM analysis.

C. Comparisons between in-track and cross-track performance within a camera can be made and have been shown to agree with laboratory measurements.

### 3.7.6 Summary

Visual edge matching was used as a measure of resolution performance. The initial approach in analyzing the mission was to fill in as much of the format with resolution values as possible. This led to a sparsity of data at the extreme scan angles. This sparsity was also due to how the camera was operated; namely there were few 120 degree scans and many scan sectors which lacked extreme scan information. Based upon these observations, VEM measurements on Mission 1201 should be continued. Format positions which correspond to test chamber results should be stressed in collecting VEM data. Finally, the calibration of the VEM matrices should be examined in detail. A critique of the VEM method is given in greater detail in Section VI.

## 3.8 IMAGE QUALITY VARIABILITY

### 3.8.1 Introduction

Two Forward Camera (64μ) and one Aft Camera (46μ) operations were chosen for a study of frame-to-frame variability. They were chosen because of the amount of available VEM data from the frames within these operations.

For each operation, the mean in and cross-track resolution values were determined. This represented the total range of resolution for a particular VEM cell, operation, direction, and camera.

Tables 3-25, 3-26 and 3-27 present the range of means calculated for each cell throughout the three operations measured.

TABLE 3-25

FORWARD CAMERA FRAME-TO-FRAME VARIABILITY

64μ PLATEN POSITION, OP 398

| VEM Cell | | In-Track | | Cross-Track | |
|---|---|---|---|---|---|
| Field Posn (degrees) | Scan Angle (degrees) | Minimum (c/mm) | Maximum (c/mm) | Minimum (c/mm) | Maximum (c/mm) |
| +2.5 | +15 | 146 | 206 | 103 | 147 |
| +2.5 | +30 | 142 | 168 | 99 | 150 |
| +1.0 | +15 | 124 | 183 | 99 | 204 |
| +1.0 | +30 | 160 | 202 | 147 | 235 |
| 0 | +15 | 155 | 253 | 100 | 235 |
| -1.0 | -15 | 121 | 182 | 131 | 176 |
| -1.0 | +15 | 137 | 237 | 118 | 155 |
| -1.0 | +30 | 160 | 228 | 130 | 202 |
| -2.5 | -15 | 103 | 118 | 141 | 146 |
| -2.5 | 0 | 143 | 146 | 99 | 105 |
| -2.5 | +15 | 121 | 202 | 106 | 156 |
| -2.5 | +30 | 126 | 165 | 95 | 165 |

NOTE: Frames at the -2.5°/-15° and -2.5°/0° positions could not be determined with 80% confidence.

TABLE 3-26

FORWARD CAMERA FRAME-TO-FRAME VARIABILITY

64μ PLATEN POSITION, OP 420

| VEM Cell | | In-Track | | Cross-Track | |
|---|---|---|---|---|---|
| Field Posn (degrees) | Scan Angle (degrees) | Minimum (c/mm) | Maximum (c/mm) | Minimum (c/mm) | Maximum (c/mm) |
| 2.5 | -15 | 167 | 167 | 167 | 200 |
| 2.5 | +15 | 167 | 193 | 125 | 140 |
| 2.5 | +30 | 120 | 226 | 110 | 140 |
| 1.0 | -45 | 140 | 144 | 105 | 140 |
| 1.0 | -15 | 226 | 239 | 197 | 215 |
| 1.0 | +30 | 178 | 200 | 135 | 167 |
| 0 | -15 | 220 | 252 | 184 | 226 |
| 0 | +15 | 230 | 235 | 199 | 235 |
| 0 | +30 | 178 | 226 | 135 | 226 |

TABLE 3-26 (CONT'D)

FORWARD CAMERA FRAME-TO-FRAME VARIABILITY

64μ PLATEN POSITION, OP 420

| VEM Cell | | In-Track | | Cross-Track | |
|---|---|---|---|---|---|
| Field Posn (degrees) | Scan Angle (degrees) | Minimum (c/mm) | Maximum (c/mm) | Minimum (c/mm) | Maximum (c/mm) |
| -1.0 | +15 | 204 | 235 | 206 | 243 |
| -1.0 | +30 | 130 | 226 | 150 | 200 |
| -2.5 | -15 | 174 | 175 | 139 | 145 |
| -2.5 | +30 | 206 | 213 | 167 | 217 |

NOTE: Frames at the 2.5°/+15°, 1.0°/-15°, 1.0°/+30°, and -2.5°/-15° positions could not be determined with 80% confidence.

TABLE 3-27

AFT CAMERA FRAME-TO-FRAME VARIABILITY

46μ PLATEN POSITION, OP 383

| VEM Cell | | In-Track | | Cross-Track | |
|---|---|---|---|---|---|
| Field Posn (degrees) | Scan Angle (degrees) | Minimum (c/mm) | Maximum (c/mm) | Minimum (c/mm) | Maximum (c/mm) |
| 2.5 | -30 | 193 | 211 | 125 | 177 |
| 1.0 | -30 | 222 | 249 | 172 | 265 |
| 1.0 | -15 | 124 | 217 | 115 | 177 |
| 0 | -30 | 210 | 220 | 140 | 200 |
| 0 | -15 | 172 | 212 | 124 | 138 |
| -1.0 | -30 | 189 | 243 | 115 | 172 |
| -1.0 | -15 | 172 | 295 | 177 | 261 |
| -2.5 | -30 | 166 | 201 | 125 | 177 |
| -2.5 | -15 | 182 | 256 | 151 | 235 |

NOTE: All differences between frames were determined with 80% confidence.

### 3.8.2 Considerations and Theory

In order to determine whether or not there is a significant shift in resolution between frames (at a given location) due to the KH-9 System variability, one must take into account (a) the variability of the VEM measuring technique; (b) the inherent error of assuming a VEM cell to have a constant image quality throughout an area 6 inches x 1/2 inch; and (c) the frame-to-frame variability of the duplicate positive contact printing process.

The first two combined sources of variability are given by the sample standard deviation associated with reading six edges in one VEM cell, on one frame, in one direction, i.e., the standard deviations associated with the mean resolution values given in Tables 3-25, 3-26 and 3-27. It was found that, on the average, this sample standard deviation is 17% of the mean resolution level. It should be noted that this average standard deviation of 17% being an average itself also has a standard deviation associated with it. In this case the standard deviation applied to the 17% is 7.7%. A subjective analysis of individual VEM cells also indicates that there is a variability of image quality within one cell. The third source of variability, the duping process, was not analytically considered here, but is generally thought to be "small", see paragraph 5.6 of this report.

With a known sample size of six and standard deviation of 17% of the mean (1 cell, 1 direction), it turns out that there is an 80% chance of detecting a real change in mean resolution of 25% or greater, between frames for a given cell. A larger percentage change (i.e., higher confidence) of detecting a smaller percentage change (<25%) in mean resolution between frames, cannot be achieved with the known sample size of six and standard deviation of 17% of the mean. With this statistical information, the "Student t" test can be utilized in order to answer the following question with 80% confidence: Is there a statistically significant change in mean resolution between frames, for one VEM cell, in one direction, due mainly to the KH-9 System variability?

3.8.3 Statistical Analysis

The "Student t" test was therefore run on each pair of mean resolution values given in Tables 3-25, 3-26 and 3-27. The results show that with 80% confidence there is a statistically significant change in the mean resolution, in 68% of the cases studied. To illustrate the procedure used, an example is given below:

Example: Forward Camera, Op 398, 64μ Platen Position, -2.5° Field Position x 15° cell

Frame 011 - mean of 6 in-track VEM edges = 121 c/mm
standard deviation = 17% of 121 c/mm = 20.6 c/mm

Frame 015 - mean of 6 in-track VEM edges = 202 c/mm
standard deviation = 17% of 202 c/mm = 34.3 c/mm.

The "Student t" test is an equation which considers the two mean resolutions (121 c/mm and 202 c/mm), the two standard deviations (20.6 c/mm and 34.3 c/mm), and the two sample sizes (6 and 6) to arrive at the following conclusions: The two mean resolutions are different, or the two mean resolutions are the same. The conclusion is always based on a particular confidence which is always less than 100%, in any real case when the variability (standard deviation) is not zero. Applying this test to the example, the conclusion is that the two means are significantly different with 80% confidence, i.e., since the two means differed by more than 25%, one can be 80% sure that the conclusion is correct.

For an indication of the variability between operations, at the various mission platen position settings, see Figures 3-20 and 3-21. These figures in the 0° scan, 0° field VEM cell mean resolution, in and cross-track directions, are plotted from several operations throughout Mission 1201. These figures show that there is a significant difference between the two end points and the lowest resolution value in the in and cross-track directions.

Dynamic resolution testing of SN-003 in the final Chamber A-2 environment produced some measure of image quality variability. General indications were that the Aft Camera produced more variable resolution than the Forward Camera. By summarizing overall variability from Tables 3-25, 3-26, and 3-27, the indication is that the Aft Camera was perhaps slightly more variable than the Forward on Mission 1201. This characterization was done by calculating the percentage variation of the means in each cell and computing the average. Results are shown in Table 3-28.

TABLE 3-28

PERCENT VARIABILITY COMPARISON

| Camera: | Forward | Aft |
|---|---|---|
| Operation: | 398 and 420 | 383 |
| Cells: | 49 | 18 |
| Avg Variability (%): | 36 | 43 |

Looking at the cameras more closely, the variations depicted in Figures 3-20 and 3-21 are not unlike those produced in the Chamber A-2 testing as typified by the Forward Camera data depicted in Figure 3-13 on page 3-19 of the SN-003 Flight Readiness Report. For the Aft Camera, although the variations are about the same, the resolution levels for Chamber A-2 are much lower than the flight resolutions. These comparisons are shown in Table 3-29.

TABLE 3-29

RANGE OF RESOLUTION VARIABILITY BETWEEN TEST AND FLIGHT

Forward Camera

| Direction | Mission 1201 | Chamber A-2 |
|---|---|---|
| In-Track (c/mm) | 150-240 | 190-250 |
| Cross-Track (c/mm) | 120-190 | 150-210 |

Aft Camera

| Direction | Mission 1201 | Chamber A-2 |
|---|---|---|
| In-Track (c/mm) | 210-275 | 110-180 |
| Cross-Track (c/mm) | 145-225 | 50-170 |

FIGURE 3-20

FORWARD CAMERA FRAME-TO-FRAME VARIABILITY
(Mean Resolution, 0° Field, 0° Scan Cell)

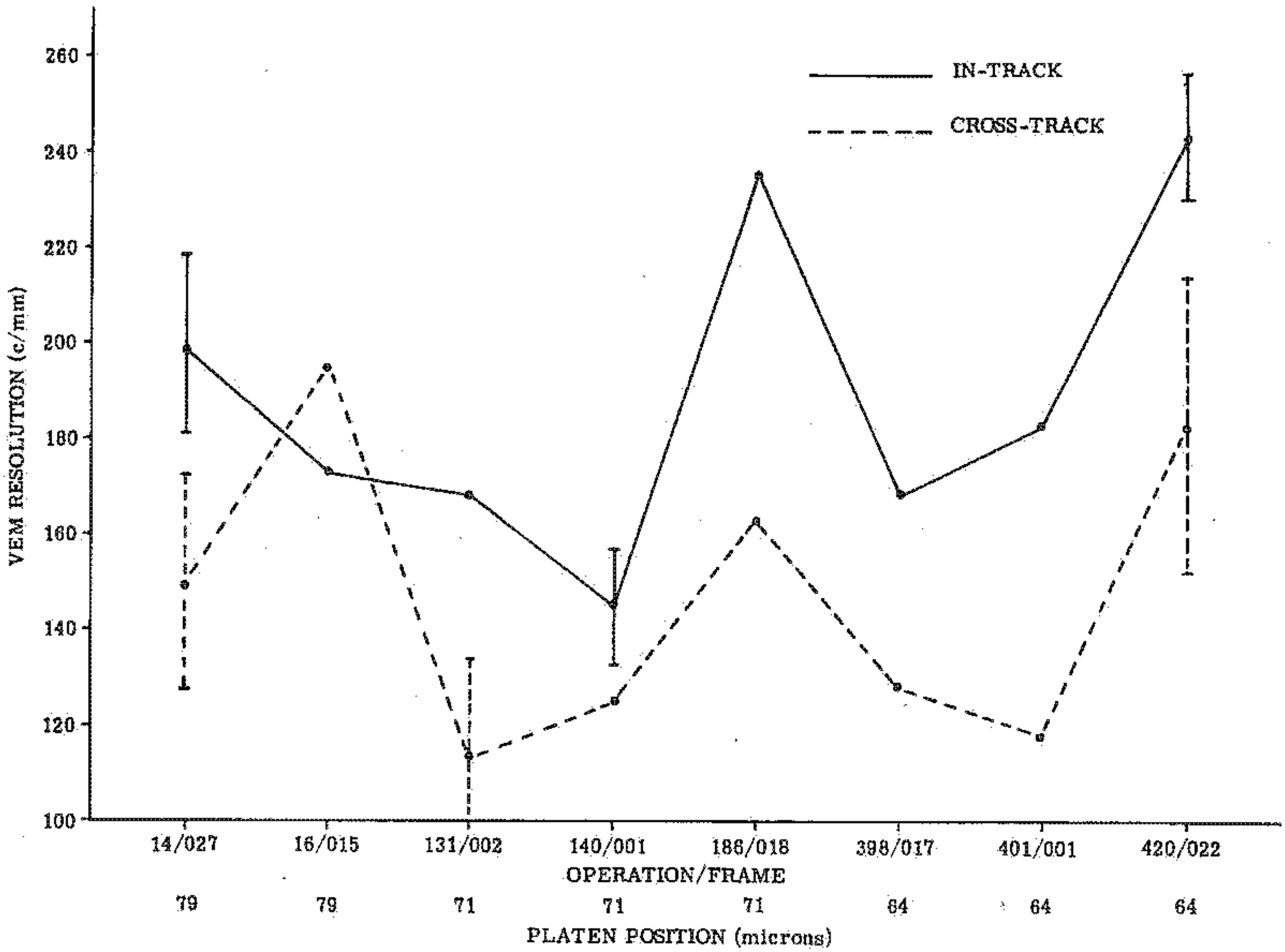

FIGURE 3-21

AFT CAMERA FRAME-TO-FRAME VARIABILITY
(Mean Resolution, 0° Field, 30° Scan Cell)

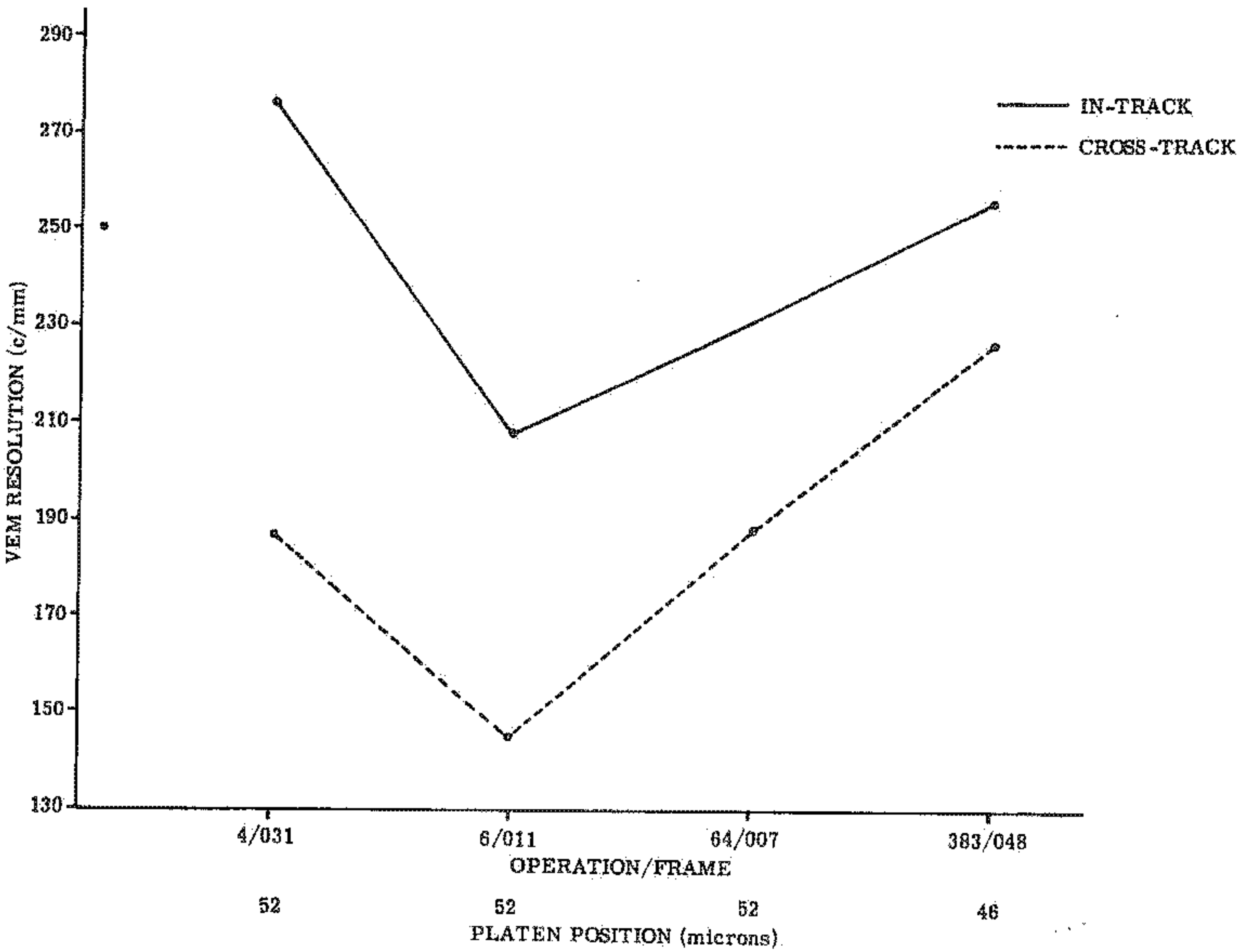

3.8.4 Conclusions

A. Utilizing the VEM measurement technique as discussed above, the KH-9 photography does exhibit a frame-to-frame variability.

B. Assessment of the VEM data cells by employing the "Student t" test fully supports the primarily subjective analyses performed during the PFA activity.

C. Frame-to-frame variability makes the analysis and evaluation of trends, such as appear on thru focus, across the film web, or film web plots difficult.

D. The operational variability inherent in the cameras themselves was no more severe than during laboratory operations.

## 3.9 TELEMETRY DATA ANALYSIS

### 3.9.1 Introduction

The data and analyses contained herein address the difficult question of electromechanical signals. Considerable effort has been expended in the past attempting to establish a valid base for correlating vacuum chamber acquired photography to specific electromechanical error signatures. The objective of these efforts was to develop and define a tool to assess on-orbit image quality based upon the telemetry error signals. Mission 1201 provided large amounts of both photographic and electromechanical data. The analysis techniques employed herein are varied in order to further establish a correlation between photography and error signals.

### 3.9.2 Comparison of Chamber A-2 and Orbital Metering Capstan Summed Error Data

Sequence M of the Chamber A-2 tests was chosen as the laboratory baseline, since it most closely simulated the overall orbital camera operating conditions. Table 3-30 shows a comparison of the ground test Sequence M parameters to the orbital conditions.

TABLE 3-30

COMPARISON OF GROUND TEST AND ON-ORBIT CONDITIONS

| Parameters | Seq M | Orbital |
|---|---|---|
| OB Temp | Forward 70° F | Forward 71° F |
| | Aft 71° F | Aft 67° F |
| Pressure | Vacuum | Vacuum |
| Vx/h | .044 | .038 to .042 |
| IMC | Enabled | Enabled |

Sequence M data clearly indicated a frame-to-frame variability in the average peak-to-peak value of the metering capstan summed error (MCSE) on both cameras. Laboratory testing resulted in an average maximum zero-to-peak (AC) velocity error for the Forward Camera of 0.06 inch/sec, an average minimum of 0.03 inch/sec, and the overall average over 147 frames of approximately 0.045 inch/sec. The orbital data for the Forward Camera indicated an average zero-to-peak maximum velocity error of 0.12 inch/sec, an average minimum value of 0.03 inch/sec, and an overall average of approximately 0.06 inch/sec. Similarly, for the Aft Camera, the laboratory test data indicated an average maximum of 0.07 inch/sec, an average minimum of 0.03 inch/sec, and an overall average was 0.05 inch/sec. The orbital data indicated an average maximum (AC) velocity error of 0.10 inch/sec, an average minimum of 0.05 inch/sec, and an overall average of 0.07 inch/sec.

The summary evaluation of the orbital performance as indicated by the metering capstan summed error measurement is as follows:

The AC velocity error varied frame-to-frame on both cameras throughout the mission. Capstan performance in general was the same at the end of the mission as at the beginning. The poorest performance of the Forward Camera is equal to the poorest of the Aft. The best performance of the Forward is better than the best of the Aft. The frame-to-frame variability on the Forward was more pronounced than on the Aft, as the maximum to minimum average AC velocity error varied by a factor of 4 to 1 on the Forward Camera and 2 to 1 on the Aft, see Figure 3-22. In addition, frame modulation, which was intermittently present on both cameras during Sequence M, is much more prevalent on the Aft Camera than the Forward, see Revs 14, 32, 48, 129, and 323 in Figure 3-22. This modulation is attributed to the fine tension sensors used during this mission. A new configuration which dynamically balances the fine tension sensors will be used on Mission 1202. In addition, the frequency of the disturbance on the MC summed error during test and on-orbit for both cameras was approximately the same, 90 to 95 Hz. This corresponds to a twice per rev MC disturbance or once per rev of a 1/2" diameter roller, such as the fine tension sensors. The summary of the "average" values of the summed error are as presented in Table 3-31.

TABLE 3-31

SUMMED ERROR AVERAGES

| | | Forward Camera | Aft Camera |
|---|---|---|---|
| On-Orbit | Maximum | 0.12 inch/sec | 0.10 inch/sec |
| | Minimum | 0.03 inch/sec | 0.05 inch/sec |
| | Overall | 0.06 inch/sec | 0.07 inch/sec |
| Seq M | Maximum | 0.06 inch/sec | 0.07 inch/sec |
| | Minimum | 0.03 inch/sec | 0.03 inch/sec |
| | Overall | 0.045 inch/sec | 0.05 inch/sec |

Important points of comparison can be made from image smear measurements made from line analysis. The Forward Camera imagery exhibits more smear variability than the Aft. This is commensurate with TM signal data which reveals more variability in MCSE for the Forward than the Aft Camera.

VARIABILITY OF METERING CAPSTAN SUMMED ERROR

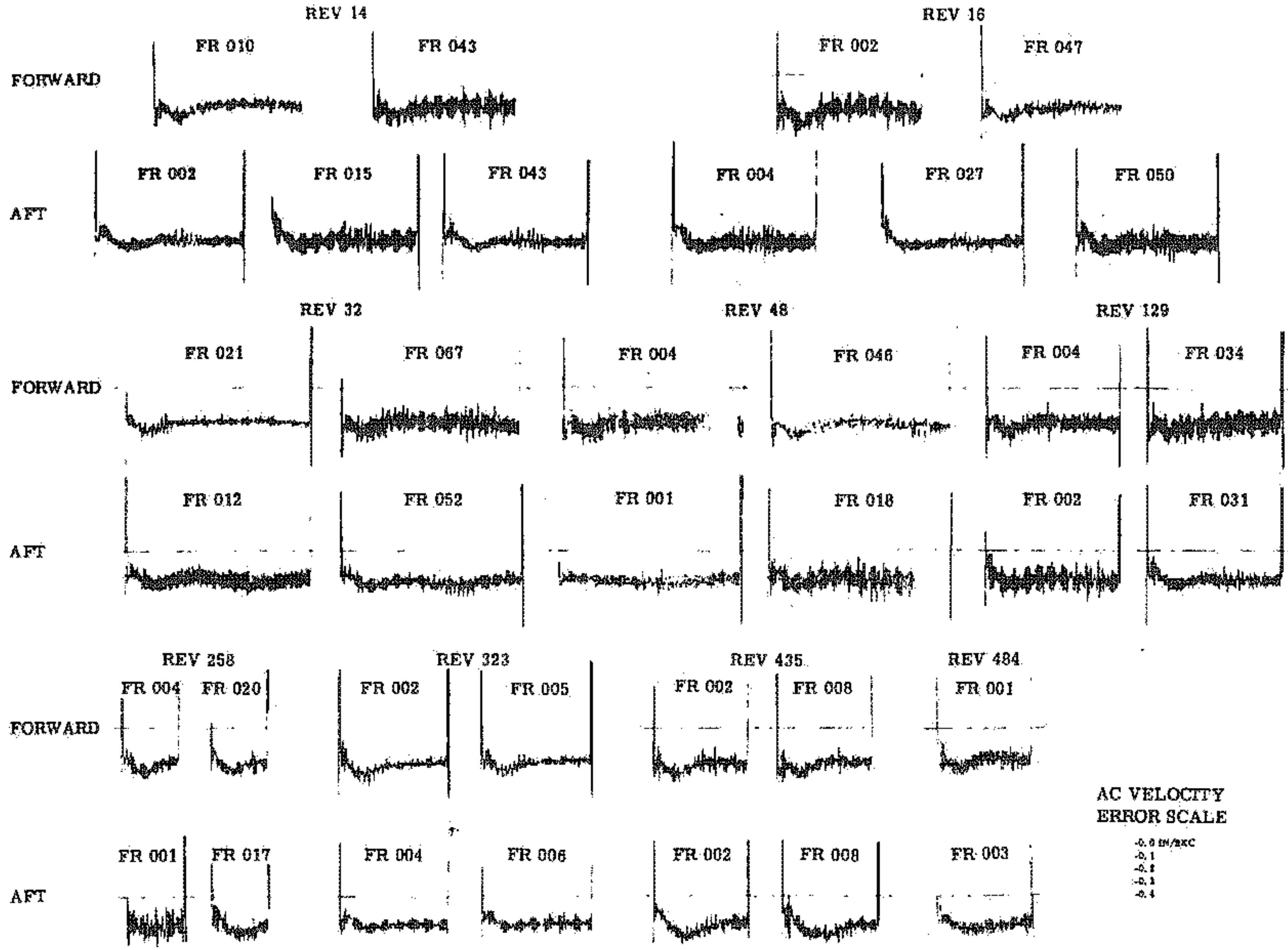


FIGURE 3-22

On the other hand, photo and TM indications disagree on the nature of the behavior throughout the mission. Whereas error signals indicate general consistency, the line analysis indicates a decreasing average level and variability with time. Cross-track photo smear was more severe and more variable on the Forward Camera (6±2.0μ) than on the Aft Camera (4±1.5μ). Once again, however, these comparisons can't be made directly because defocusing variations complicate the issue.

3.9.3 Results of Fourier Analysis of Capstan Summed Error Signals

A Fourier analysis of the capstan summed errors was performed to determine if there were any major components produced by resonances or roller irregularities. A Fourier component of significant magnitude was found to occur at a two peaks per rev frequency of the capstans. The two peaks per rev frequency is approximately 100 Hz for Mission 1201. Figures 3-23 thru 3-28 contain a plot of the two peaks per rev and the peak low frequency component ( > 0, < 5 Hz) for all the capstans on both cameras. The low frequency component was included to determine if there was only correlation between the size of the MC velocity modulation resonance value at the time the phase lock closed and the size of the settling transient. A large settling transient would have been evidenced by a large low frequency component. No particular correlation was noted. This analysis verifies the existence of the modulation effect discussed in the preceding paragraph regarding an unbalance of the fine tension sensor rollers.

3.9.3.1 Metering Capstan Error Signal Fourier Analysis

Figures 3-23 and 3-24 give the peak magnitudes of the high (≈100 Hz and 2/rev) and low frequency components of the Forward and Aft metering capstan summed errors. Note once again that the data points are taken in chronological order but are not necessarily equally spaced in time. Considering the high frequency (2/rev) peaks, it can be seen that for the Forward side there is a large increase during Take up 2 but no beginning-to-end trend. A dashed line is shown at the Aft Camera, Take up 4 data point in Figure 3-24 to indicate that the magnitude of the component may be larger than indicated by this analysis. This is the case because the Fourier analysis program indicated two relatively large components located close to each other for this data point. When this occurs neither magnitude may be representative; the program in effect has split the component present in the data between two neighboring harmonics because the frequency of the component does not coincide with an integer multiple of the fundamental harmonic. No exact means of combining the two neighboring harmonics is known at this time, therefore, it can only be stated that the Take up 4 peak 2/rev component has a value somewhat higher than that indicated by the Take up 4 data point. There does not appear to be any beginning-to-end increase in the 2/rev component on the Aft side. The low frequency peak components in Figures 3-23 and 3-24 seem to reflect, in some degree, the trends shown in the two peaks per rev components.

3.9.3.2 Input Drive Capstan Error Signal Fourier Analysis

The input drive capstan summed error peak components are shown in Figures 3-25 and 3-26

FORWARD CAMERA METERING CAPSTAN SUMMED ERROR

TWO PEAKS PER REV

(100 Hz Component)

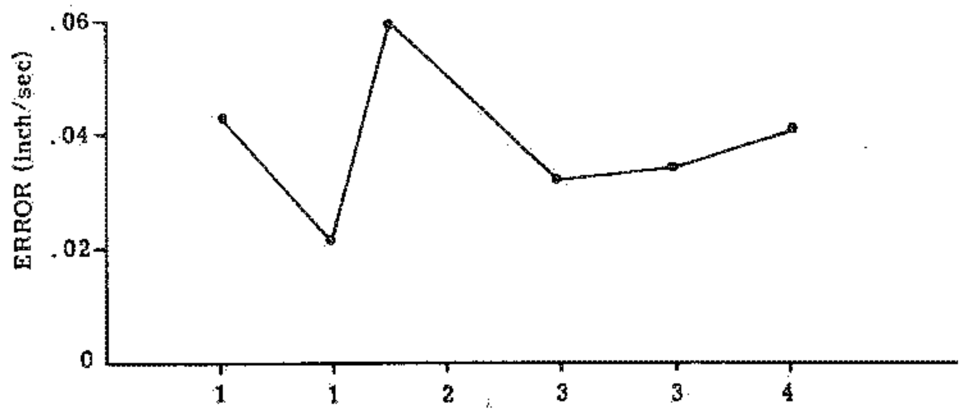


LOW FREQUENCY PEAKS

( >0, <5 Hz)

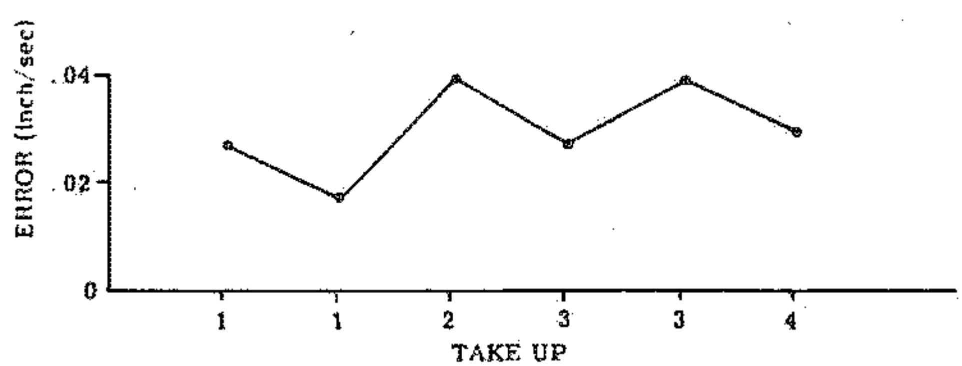


FIGURE 3-23

AFT CAMERA METERING CAPSTAN SUMMED ERROR

TWO PEAKS PER REV

(100 Hz Component)

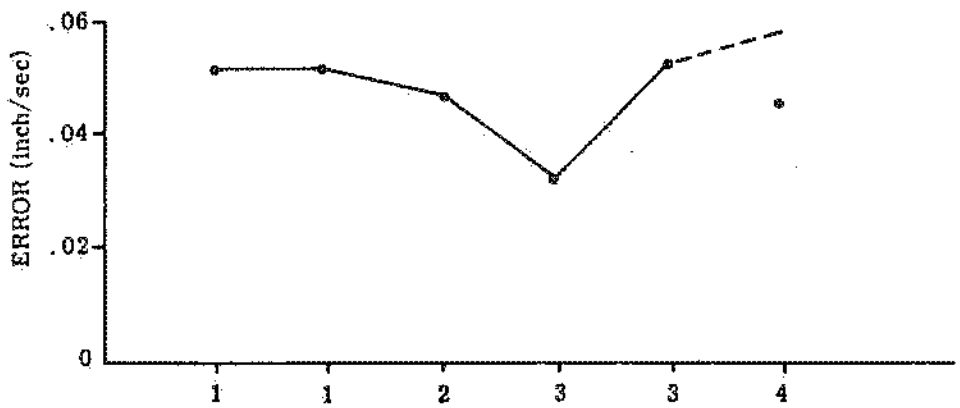


LOW FREQUENCY PEAKS

( >0, <5 Hz)

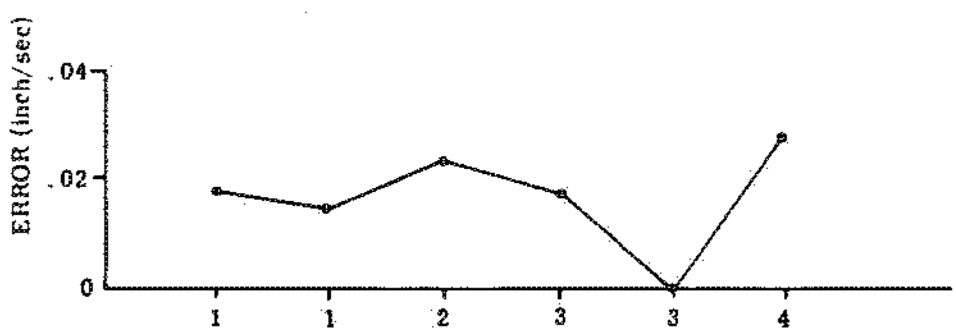


FIGURE 3-24

FORWARD CAMERA INPUT DRIVE CAPSTAN SUMMED ERROR

TWO PEAKS PER REV

(100 Hz Component)

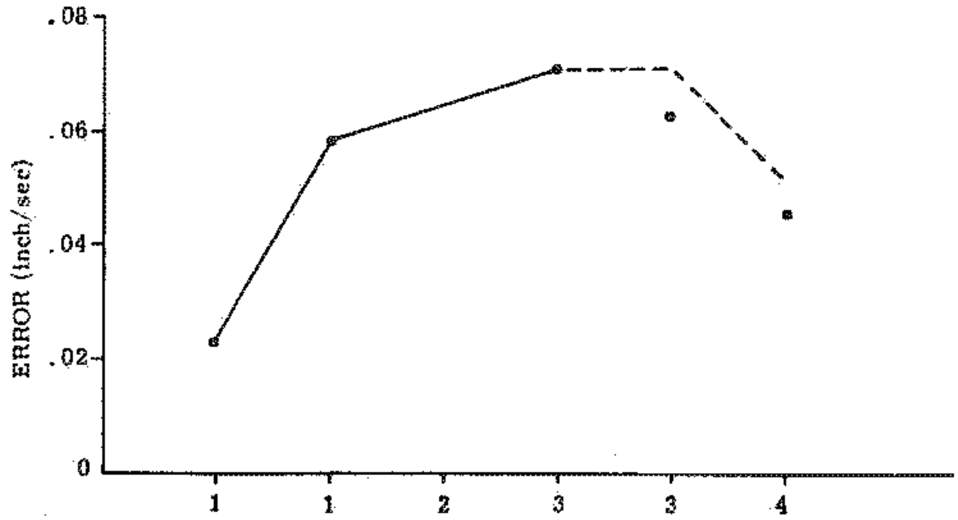


LOW FREQUENCY PEAKS

( >0, <5 Hz)

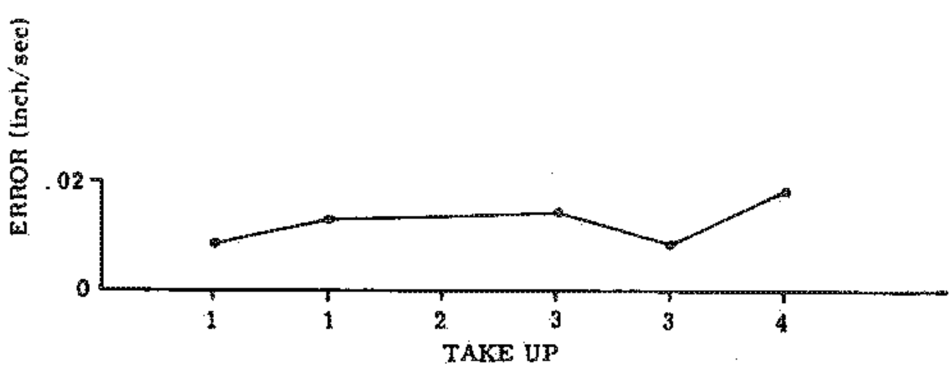


FIGURE 3-25

AFT CAMERA INPUT DRIVE CAPSTAN SUMMED ERROR

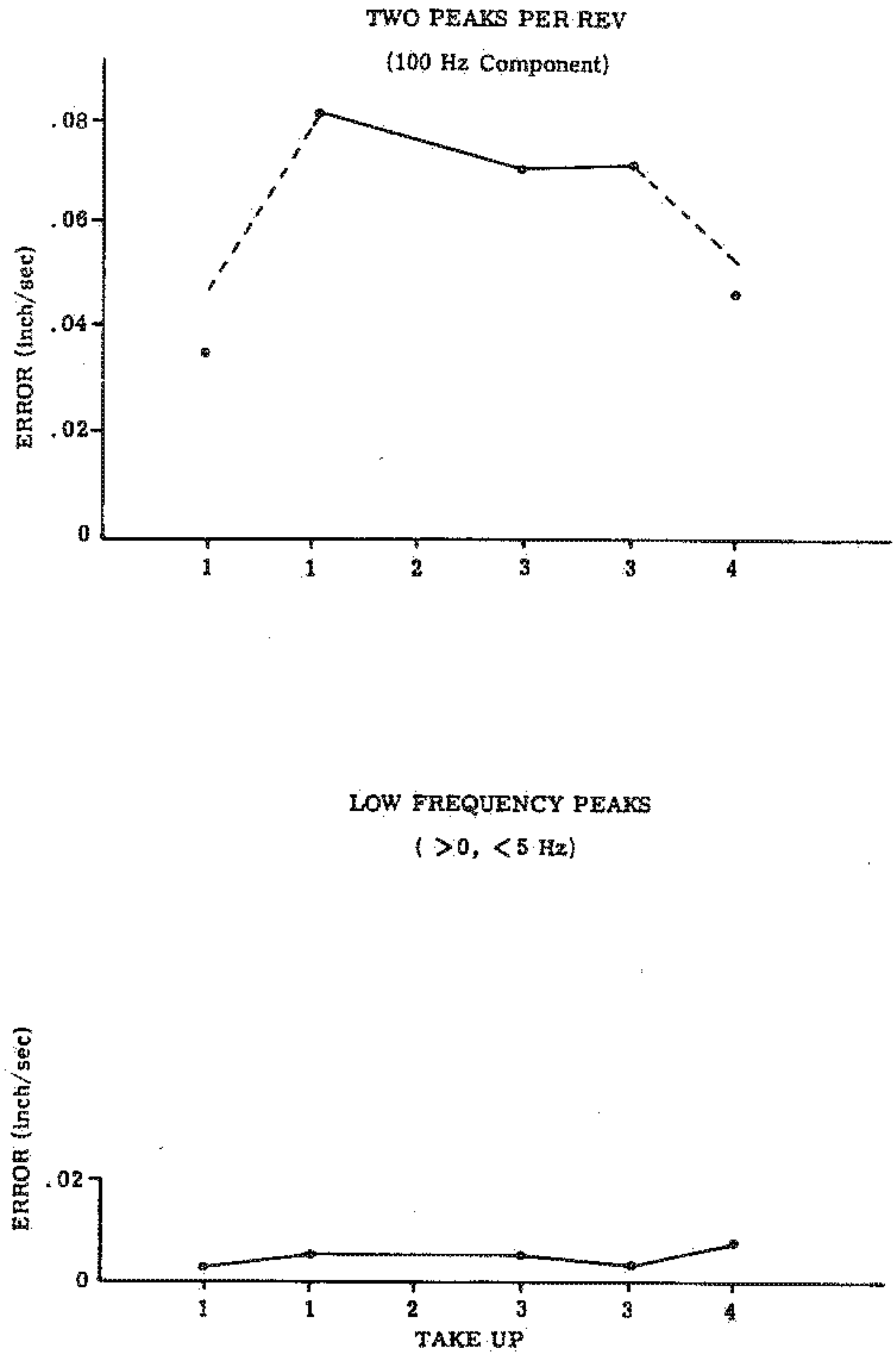


FIGURE 3-26

FORWARD CAMERA OUTPUT DRIVE SUMMED ERROR

TWO PEAKS PER REV

(100 Hz Component)

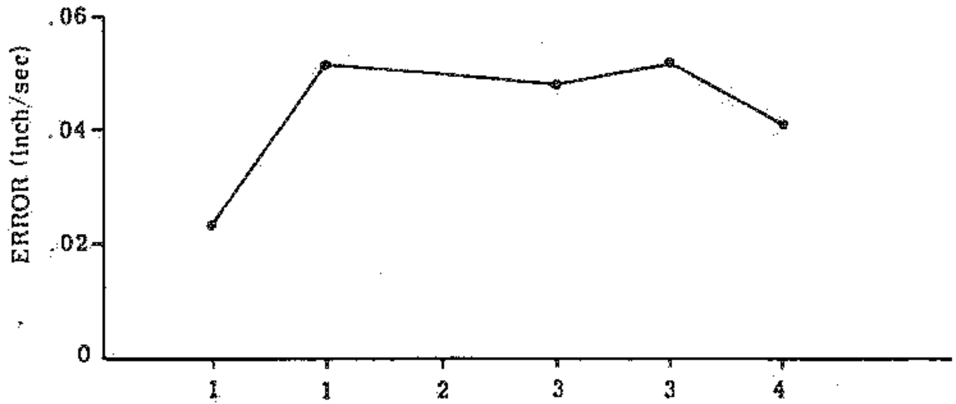


LOW FREQUENCY PEAKS

( >0, <5 Hz)

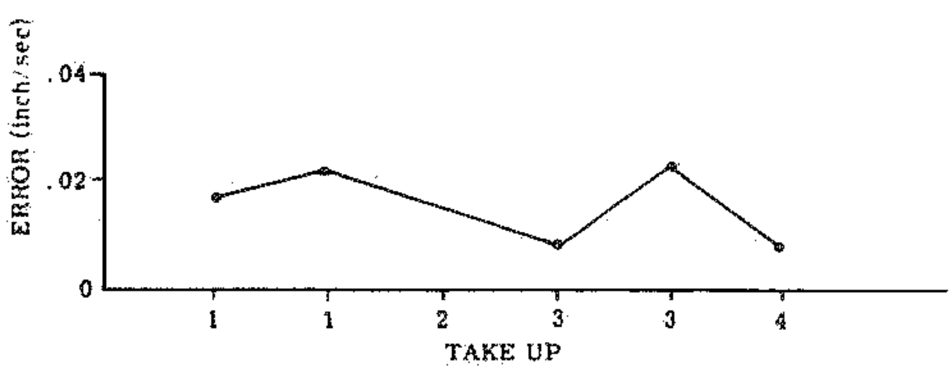


FIGURE 3-27

AFT CAMERA OUTPUT DRIVE CAPSTAN SUMMED ERROR

TWO PEAKS PER REV

(100 Hz Component)

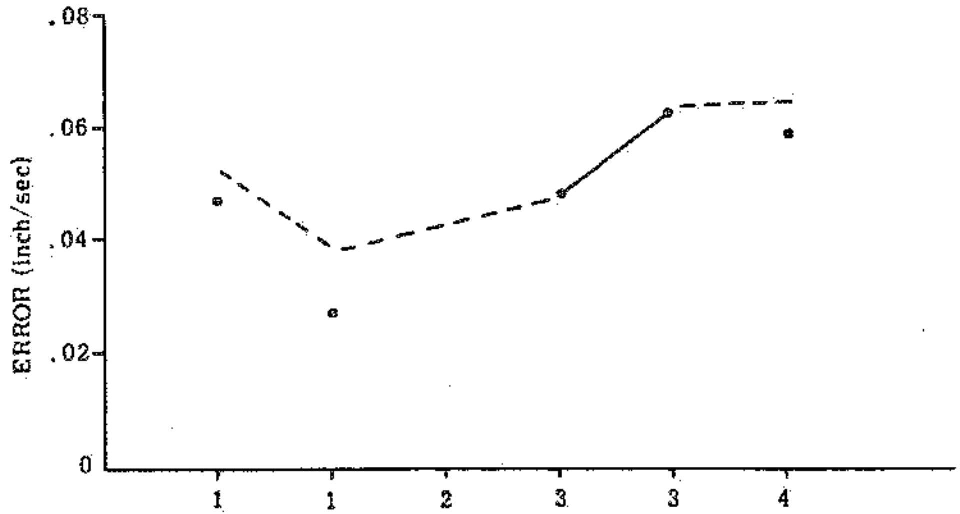


LOW FREQUENCY PEAKS

( >0, <5 Hz)

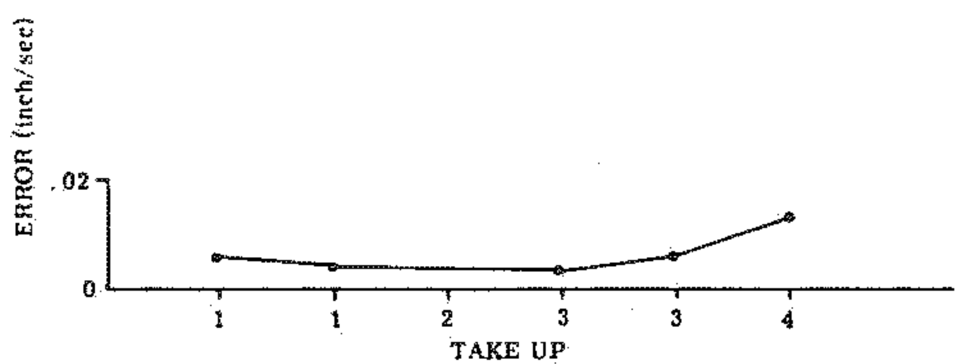


FIGURE 3-28

for the Forward and Aft Cameras respectively. The two peaks per rev components are generally higher than those for the metering capstan. There does not seem to be any trend of increases or decreases as the mission progresses, but the intermediate peaks are higher than those at either the beginning or end of the mission. There are no Take up 2 data points for the drive capstans due to the fact that only C mode telemetry data was available. The low frequency components for the input drive capstans are generally lower than the corresponding components in the MC and in addition show no discernible increasing or decreasing trend.

3.9.3.3 Output Drive Capstan Error Signal Fourier Analysis

Figures 3-27 and 3-28 present the peak high and low frequency Fourier components for the Forward and Aft output drive capstan summed errors. The Forward side two peaks per rev components, shown in Figure 3-27, are larger near the middle of the mission than at either the beginning or the end. The Aft peak 2/rev components in Figure 3-28 decrease for periods near the middle of the mission while displaying a rise of 25.2% from beginning-to-end. The low frequency peaks are greater for the Forward side than the Aft side. In addition there is no discernible trend in the low frequency peaks on the Forward Camera, whereas there is a slight increasing trend on the Aft.

3.9.4 Mean Value of Capstan Summed Error Signals

The trend of the mean of the MCSE for successive points in the utilization of the Take ups is shown in Figure 3-29. Each data point was taken in succession as the mission continued, however, note that the data was not taken at equally spaced periods of time. There was no beginning-to-end increase in the mean metering capstan error for the Forward Camera. There was, however, an increase during the period when Take up 2 was in use. Figure 3-29 shows that there was an upward trend in the Aft side mean error as the mission progressed. A more pronounced increase will be noted during the period in which Take up 2 was in use. The overall, beginning-to-end, increase in the Aft side mean metering capstan error was 37.2%. The cause of the increasing mean error on the Aft side is attributed to a slight increase of the friction level.

Figure 3-30 shows the trend for the mean summed error of both the Forward and Aft input drive capstans. For the Forward side there appears to be no rising trend in the mean summed error as the Take ups succeed each other. There is no beginning-to-end or intermediate increase in the mean, however, notice that no Take up 2 data has been included in this figure. The reason for the absence is that at the present time only C mode TM data is available during the period in which Take up 2 is in operation and in C mode the input and output drive summed errors are telemetered. There is a consistent beginning-to-end rise in the mean value of the Aft Camera input drive capstan summed error as is shown in Figure 3-30. Although the rise is consistent it is not drastic and amounts only to 12.7% from Take up 1 to Take up 4.

MEAN VALUE OF METERING CAPSTAN SUMMED ERROR

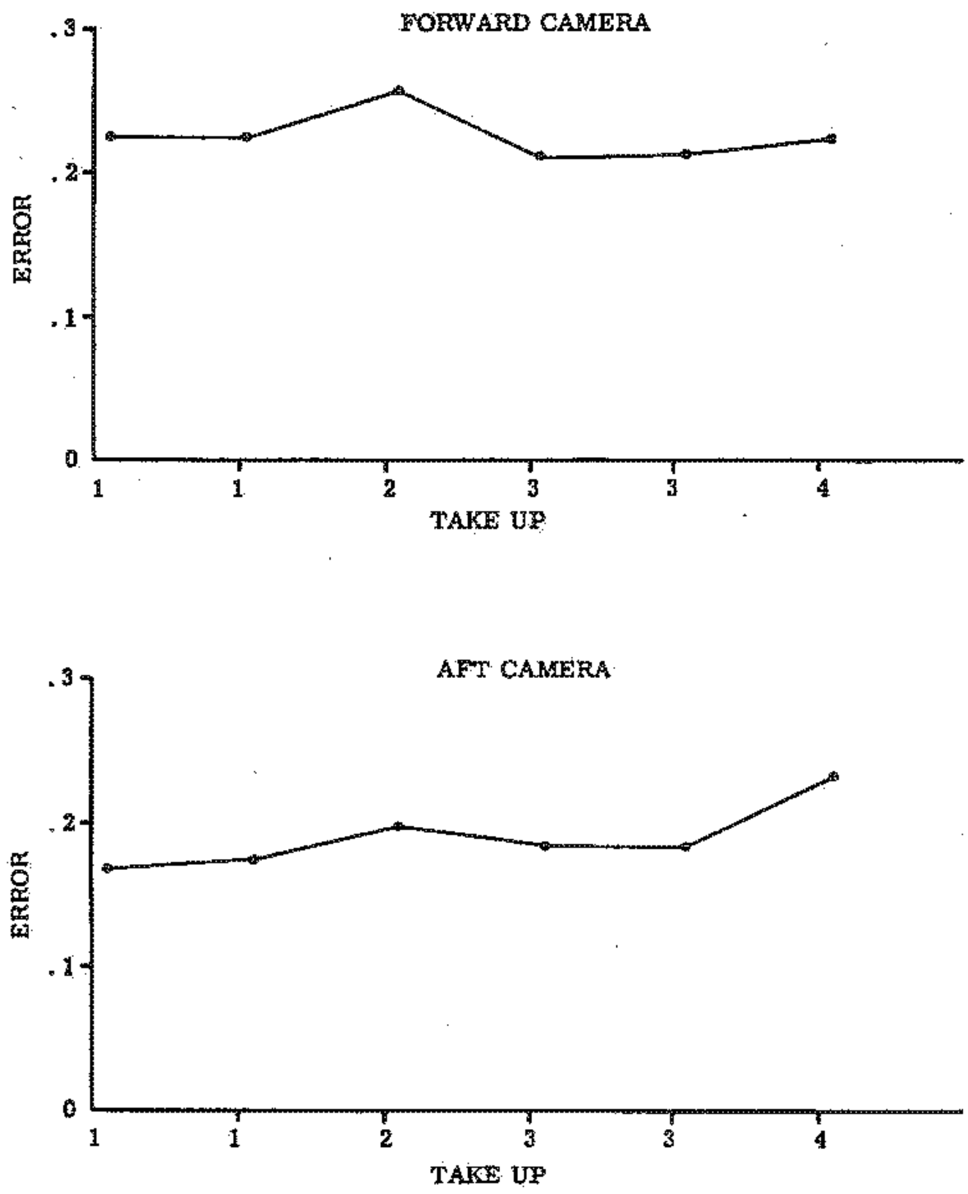


FIGURE 3-29

## MEAN VALUE OF INPUT DRIVE SUMMED ERROR

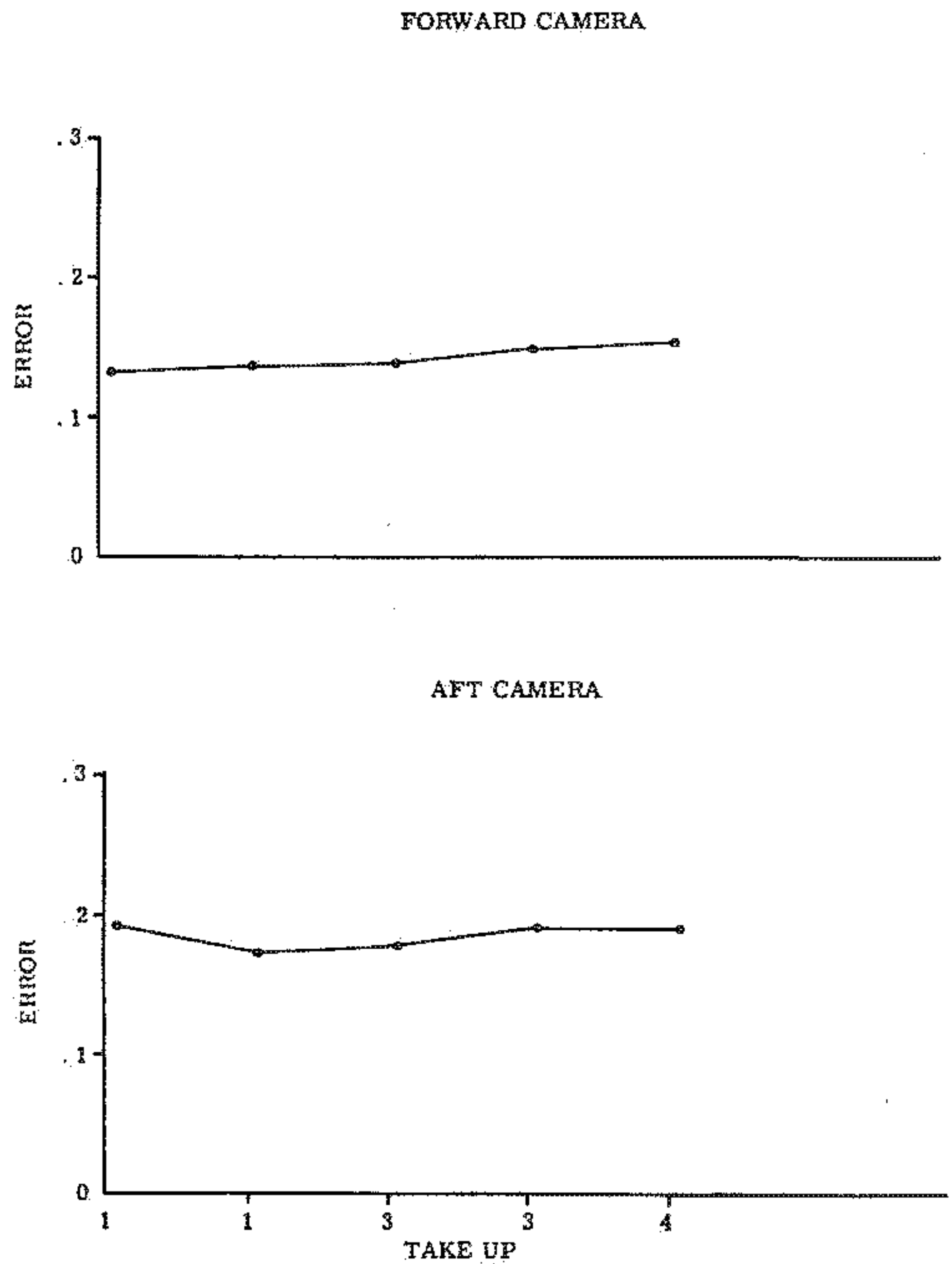


FIGURE 3-30

The subject of Figure 3-31 is the trend in the Forward and Aft output drive capstan mean summed error. The Forward side mean error increased only 9.9% from beginning-to-end, but the size of the error is higher than the mean summed error for the Forward side input drive capstan. The output drive capstan error has always been greater than input drive capstan error due to the lower gain of the output drive capstan Forward loop amplifier. Figure 3-31 shows a decrease of 10.5% from beginning-to-end in the mean output drive capstan summed error for the Aft Camera.

3.9.5 Correlation of Mobile CORN Target Resolution to the Metering Capstan Summed Error

Mobile CORN targets were selected, which exhibited high and low values of resolution in the scan direction, see Table 3-32. Computer plots were made of the MC summed error for the frames of interest at sufficient scale to accurately isolate the summed error characteristic at the time of target exposure. A window of several milliseconds either side of the predicted exposure interval was used to allow for any uncertainty and maximum AC velocity error that occurs during the time period that the window was recorded. The resolution values used were normalized for focus and 2:1 contrast.

TABLE 3-32

MOBILE CORN TARGET RESOLUTION VERSUS METERING CAPSTAN SUMMED ERROR

| | | | Cross-Track | | In-Track | |
|---|---|---|---|---|---|---|
| Camera | Rev/Frame | Scan Angle (degrees) | Normal Resolution (c/mm) | T Motion (microns) | MC Velocity Error | Normal Resolution (c/mm) |
| Forward | 16/048 | +19.5 | 121 | 3.4 | -.01 to -.01 | 163 |
| | 16/029 | -5.9 | 63 | 13.7 | -.01 to -.02 | 103 |
| | 32/008 | +6.7 | 83 | 9.3 | 0 to +.06 | 124 |
| | 32/055 | +5.3 | 135 | 3.5 | -.04 to +.07 | 196 |
| | 96/008 | -14.4 | 78 | 10.3 | -.04 to +.05 | 103 |
| | 129/025 | +53.0 | 98 | 7.5 | 0 to +.02 | 111 |
| | 145/012 | +10.3 | 182 | 0 | +.02 to -.04 | 192 |
| | 435/002 | -8.0 | 208 | 0 | 0 to -.02 | 250 |
| | 484/001 | -10.8 | 112 | 5.8 | -.08 to +.07 | 173 |
| | 484/001 | -8.2 | 98 | 7.5 | -.05 to -.01 | 133 |
| | 484/002 | -8.1 | 91 | 8.5 | +.08 to -.04 | 173 |
| Aft | 129/019 | +10.8 | 173 | 1.5 | -.02 to +.05 | 209 |
| | 129/027 | +53.4 | 157 | 2.2 | 0 to +.02 | 180 |
| | 145/012 | +11.1 | 173 | 0 | -.05 to +.08 | 171 |
| | 484/002 | -9.9 | 128 | 4.8 | -.01 to 0 | 241 |
| | 484/002 | -7.3 | 112 | 6.2 | -.12 to +.07 | 201 |

MEAN VALUE OF OUTPUT DRIVE SUMMED ERROR

FORWARD CAMERA

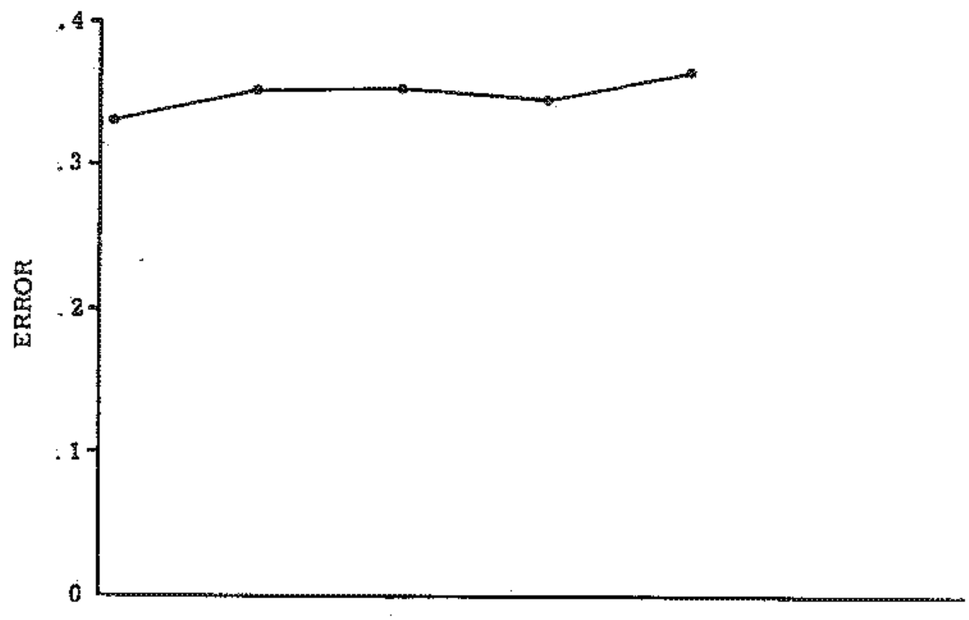


AFT CAMERA

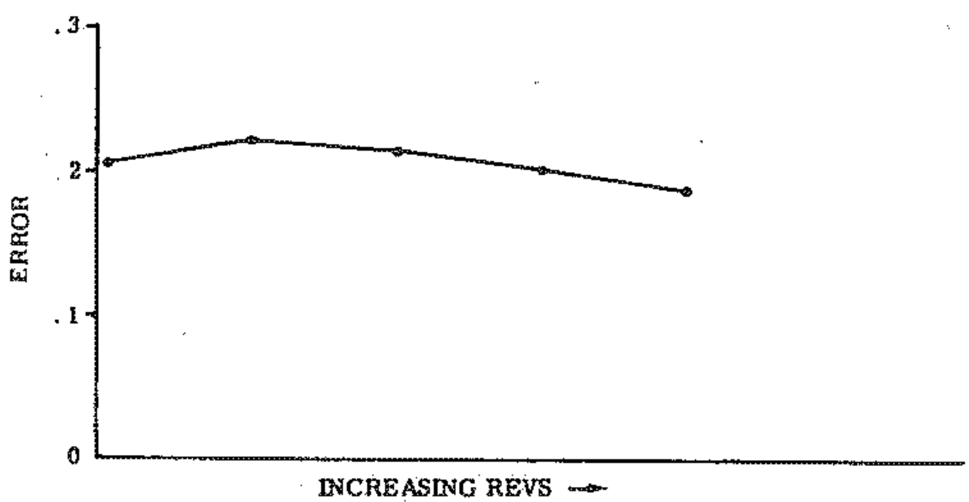


FIGURE 3-31

There is no correlation between cross-track resolution and velocity error as measured by the MC summed error measurement. For example, resolution measurements as high as 208 cycles/mm and as low as 63 cycles/mm are obtained when the worse case AC velocity error (as determined by the MC summed error) was 0.02 inch/sec. This remains true even when various DC velocity error biases are added to the capstan predicted errors. In addition the maximum AC velocity errors predicted during the windows are in the order of 0.10 inch/sec, which is equivalent to 2 1/2 microns of smear. However, the values of smear predicted analytically indicated values as high as 8 to 13 microns.

The resolution values on the Forward Camera, when comparing in-track to cross-track for the same target, has a correlation coefficient of 0.84. This means when the in-track is high, the cross-track is high and when the in-track is low, the cross-track is low. This also holds true for intermediate values of resolution. There is no such correlation on the Aft Camera.

In addition, Frame 026 on the Forward and Frame 027 on the Aft Camera of Rev 145 were selected to take in and cross-track VEM readings every 1/4 of an inch. These frames were over Los Angeles and exhibited continuous cultural detail for a span of 10° in the scan direction. The results are plotted in Figures 3-32 and 3-33 and in general (based on a limited number of samples) tend to substantiate the statements made above. In addition, the frequency of the variability in the cross-track direction does not correlate with the frequency of the MCSE measurement. Where the VEM data indicates a repetitious variability, it occurs at approximately twice the frequency seen on the summed error, in this case approximately 90 to 97 Hz.

### 3.9.6 Phase Lock Loop Anomalies

Phase lock loop error data taken from eight TM tapes were studied. The study included data taken during the use of each of the four Take ups. The intermittent performance of the Forward Camera phase lock loop, occurring in Rev 90, was discovered on all but two of the tapes. It was found that this error signal reset to some random value at the end of photography. At the start of the next period of photography the loop then closed with an offset or bias appearing on the error signal. However, the MC failed to respond to this bias in all cases and it is assumed that the anomaly must have occurred in the telemetry signal processor. The intermittent performance did not degrade the loop operation.

Except for the apparent offsets, computed theoretical variations in loop error due to IMC agreed with the actual TM signals. It was also noted that phase lock loop error transients occurring during loop closure were a good indication of the magnitude of the settling transients of the metering capstan.

A detailed discussion of the analysis of each of the eight data tapes is discussed in the following paragraphs.

#### 3.9.6.1 Rev 16 Engineering Pass, Mode B (0°/±90°), Tape MT-1811

This data tape contained 52 frames of photography for both cameras. The phase lock loop errors for both cameras were plotted for Forward Camera Frames 004, 017, 018, and 047-049. The Aft

FORWARD CAMERA RESOLUTION VERSUS SCAN ANGLE

REV 145, FRAME 026

IN-TRACK

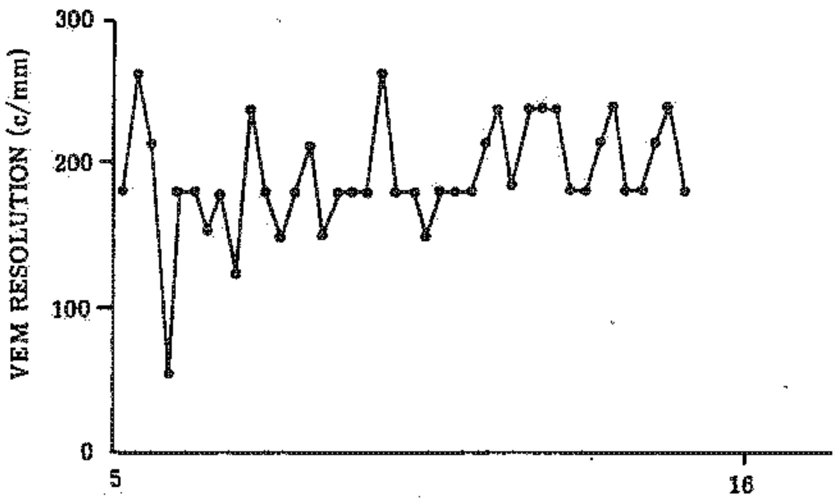


CROSS-TRACK

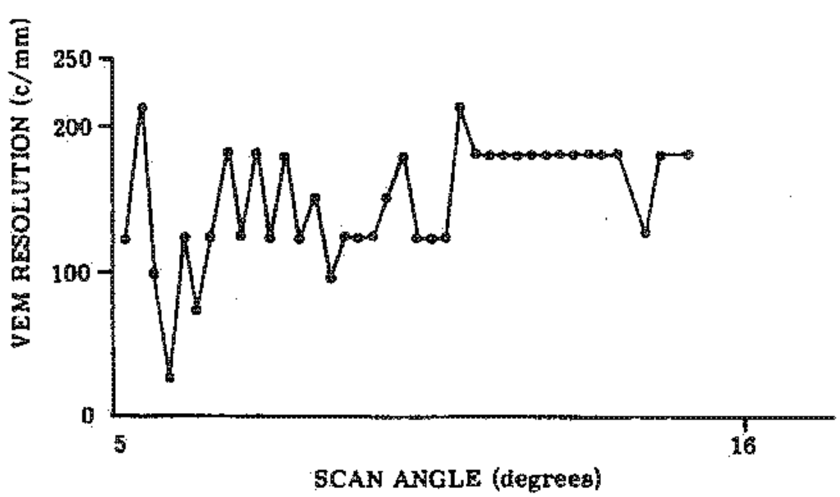


FIGURE 3-32

AFT CAMERA RESOLUTION VERSUS SCAN ANGLE

REV 145, FRAME 027

IN-TRACK

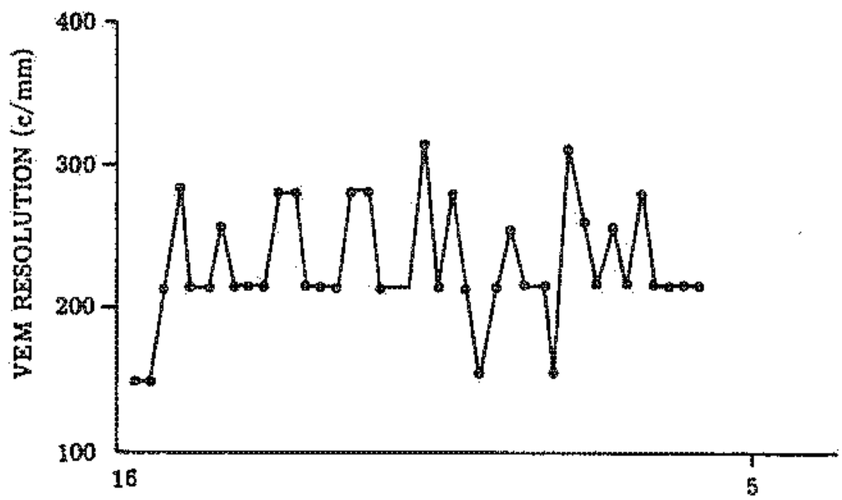


CROSS-TRACK

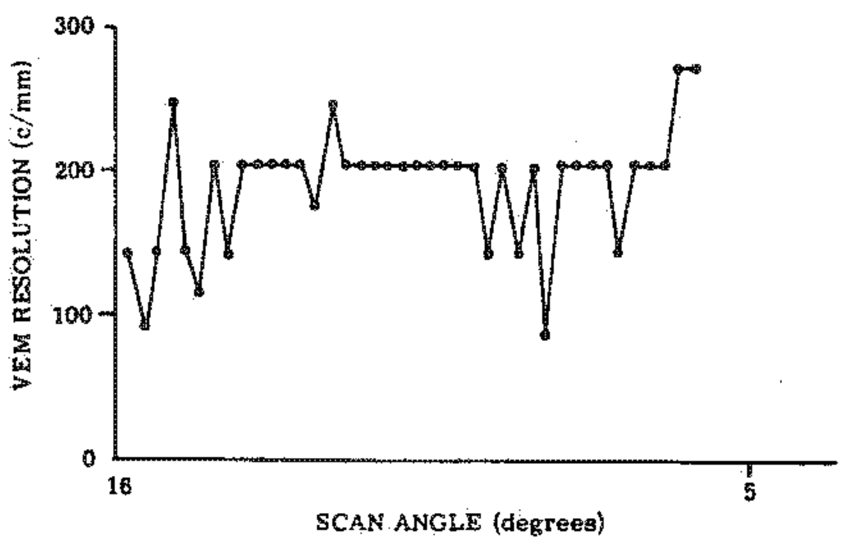


FIGURE 3-33

Camera always reset to the nominal value of zero. The Forward Camera, however, always reset to a constant offset of -120 millivolts (-0.077 inch). The theoretical phase lock loop errors due to IMC were computed for Frames 004, 017 and 049 and except for the constant offsets were in good agreement with the TM data.

3.9.6.2 Rev 90 Mission Op 80, Mode C (-30°/±30°), Tape MT-1267

This tape contained 22 frames of photography for both cameras. The phase lock loop errors were plotted for the first seven frames of the Forward and the first four frames of the Aft Camera. The Aft Camera profiles were normal and reset to zero. The Forward Camera offsets at reset were very large and not constant, varying from 490 to 510 millivolts (-0.319 ±0.007 inch). This operation represents the largest magnitude and the only non-constant offset.

3.9.6.3 Rev 152 Normal Mode C (-30°/±30±), Tape MT-1281

Of the 28 frames of photography the phase lock errors were plotted for Frames 019 and 020. The Aft Camera was normal while the Forward Camera had a constant reset offset of -40 millivolts (-0.0254 inch). The plots show abnormally large transient at the instant of phase lock loop closure. The corresponding MCSE plots also show very poor settling characteristics.

3.9.6.4 Rev 242 Engineering Pass, Mode B (15°/±30°), Tape MT-1188

Fifteen of the 25 frames on this tape were plotted and studied. Again the Aft side reset normally to zero while the Forward reset to a constant value of -60 millivolts (-0.0381 inch) near the end of the operation. During this engineering operation the value of Vy/h was step changed. The theoretical values were computed for each of three phases and were in agreement with actual values. The agreement during transition periods was not acceptable.

3.9.6.5 Rev Unknown Normal Mode C (-30°/±60°), Tape MT-1248

This tape represents an unknown rev in Take up 4 and was analyzed because of extremely poor MC settling characteristics. The phase lock loop plots appeared normal except that the Forward side reset offset of -60 millivolts (-0.0373 inch). The Forward Camera did show a larger than normal transient at closure which did not appear on the Aft side.

3.9.6.6 Rev 476 Engineering Pass, Mode B (0°/±60°), Tape MT-1289

This tape and the one for Rev 484 are the only ones investigated in which both phase lock loop errors reset normally to zero. The plots also show a correlation between the MC transient and the phase lock loop transient at closure.

3.9.6.7 Rev 484 Engineering Pass, Mode B (0°/±60°), Tape MT-1011

This tape contains 9 photographic frames for which the phase lock loop errors and reset appear normal.

3.9.6.8 Rev 493 Normal Mode C (0°/±120° and 15°/±60°), Tape MT-1128

Two frames from Op 1 and three frames from Op 3 were studied. The reset offset returned on the Forward Camera. In addition the offset was not constant for either operation.

3.9.7 Optical Bar Velocity Perturbations

The effect of OB velocity perturbations on system performance was evaluated by the following methods:

A. Use of the 0/179 Optical Bar Position pulses to determine velocity.

B. Use of the frozen SVT to determine velocity.

C. Application of Fourier analysis techniques to tachometer and summed error signals.

The first two methods produced only the average velocity over a rev and provided no information about the variations during any given rev. In addition, the accuracy of these techniques was questionable since the points used are quantized to 2 milliseconds and Fourier analysis of a large number of points tend to produce a more accurate mean or average.

Time plots of the tachometer output and servo summed error signals indicated a definite once per rev variation. Major frequency components of once and twice per rev have been verified by Fourier analysis. For example the Fourier analysis performed for Rev 484 at a Vx/h of 0.0413 gives the following speed and means in degrees per second:

| | | |
|---|---|---|
| Theoretical speeds | = | 148.564 |
| Forward Camera mean | = | 149.169 |
| Aft Camera mean | = | 148.403 |

Major cyclic components are:

| | | |
|---|---|---|
| Forward side | - | 0.122 degree/second at once per rev |
| Aft side | - | 0.288 degree/second at once per rev |
| Aft side | - | 0.306 degree/second at twice per rev |

The once per rev components are believed to result from the once per rev cyclic bearing and seal friction introduced through the platen motion. The generally higher frequency component appearing on the Aft Camera may result from the fact that the camera is phase locked to the Forward Camera which serves as the system clock. The phase relationships indicated that the scan is centered about the peak value of the sinusoidal variation which tends to minimize the effect of the variation. Consequently, it is concluded that variations of the optical bar velocity as the platen recycles has minimal effects upon camera performance.

3.9.8 Orbital Performance of the Lateral Separation Focus Sensor (LSFS)

LSFS performance data is summarized in Table 3-33. Sequence M of the second Chamber A-2 tests is chosen as the laboratory baseline for orbital performance, since it most closely approximates orbital camera operating conditions.

LSFS calibration as a function of temperature was established from Chamber A test data. The calibration showed that at photographically determined best focus, the LSFS, on both cameras, will

## TABLE 3-33

### SUMMARY OF LATERAL SEPARATION FOCUS SENSOR (LSFS) PERFORMANCE DATA

| | Forward Camera | | | | | | Aft Camera | | | | | |
|---|---|---|---|---|---|---|---|---|---|---|---|---|
| Rev | Platen Position (microns) | LSFS (counts) | Frames | FP Temp (°F) | Prim Temp (°F) | Corr Temp (°F) | Platen Position (microns) | LSFS (counts) | Frames | FP Temp (°F) | Prim Temp (°F) | Corr Temp (°F) |
| Seq M | 60.9 | 172 | 001-015 | 71.5 | 70.0 | 70.7 | 33.2 | 141 | | 70.3 | 71.2 | 71.3 |
| | 64.6 | 175 | 016-025 | | | | 38.8 | 143 | | | | |
| | 70.1 | 177 | 026-045 | | | | 46.2 | 145 | | | | |
| | 75.7 | 179 | 047-065 | | | | 49.8 | 147 | | | | |
| | 79.4 | 181 | 066-085 | | | | 53.5 | 149 | | | | |
| | 83.1 | 183 | 086-105 | | | | 57.2 | 151 | | | | |
| | 86.6 | 185 | 106-125 | | | | 60.9 | 152 | | | | |
| | 92.3 | 188 | 126-135 | | | | 67.4 | 155 | | | | |
| | 97.8 | 190/191 | 136-147 | | | | 73.8 | 158 | | | | |
| 14 | 79.4 | 185 | 40 | 69 | 69.2 | 69.8 | 51.7 | 157 | 40 | 63.0 | 66.2 | 65.3 |
| 16 | 79.4 | 185 | 40 | 69 | 69.2 | 69.8 | 51.7 | 157 | 40 | 63.0 | 66.2 | 65.3 |
| 31 | 79.4 | 184 | 001-013 | 71.0 | 69.6 | 71.5 | 51.7 | 156 | 001-010 | 65.0 | 66.0 | 66.5 |
| | 62.8 | 177 | 015-018 | | | | 35.1 | 149 | 012-016 | | | |
| | 70.1 | 180 | 020-024 | | | | 44.3 | 152 | 017-021 | | | |
| | 79.4 | 184 | 025-029 | | | | 51.7 | 156 | 022-026 | | | |
| | 86.8 | 188 | 030-034 | | | | 59.1 | 160 | 027-031 | | | |
| | 94.1 | 192 | 036-039 | | | | 67.4 | 164 | 033-036 | | | |
| | 79.4 | 184 | 041-080 | | | | 51.7 | 156 | 038-080 | | | |
| 48 | 79.4 | 184 | 001-025 | 72.0 | 70.8 | 71.5 | 51.7 | 156 | 001-022 | 65.0 | 66.2 | 66.8 |
| | 62.8 | 176 | 027-031 | | | | 35.1 | 149 | 024-028 | | | |
| | 70.1 | 179 | 033-036 | | | | 44.3 | 152 | 030-033 | | | |
| | 79.4 | 183 | 038-041 | | | | 51.7 | 156 | 035-038 | | | |
| | 86.6 | 187 | 043-047 | | | | 59.1 | 159 | 040-044 | | | |
| | [illegible] | [illegible] | [illegible] | | | | 67.4 | 163 | 046-049 | | | |

TABLE 3-33 (CONT'D)

SUMMARY OF LATERAL SEPARATION FOCUS SENSOR (LSFS) PERFORMANCE DATA

| | Forward Camera | | | | | | Aft Camera | | | | | |
|---|---|---|---|---|---|---|---|---|---|---|---|---|
| Rev | Platen Position (microns | LSFS (counts) | Frames | FP Temp (°F) | Prim Temp (°F) | Corr Temp (°F) | Platen Position (microns) | LSFS (counts) | Frames | FP Temp (°F) | Prim Temp (°F) | Corr Temp (°F) |
| | 79.4 | 184 | 054-072 | | | | 51.7 | 156 | 051-072 | | | |
| 63 | 79.4 | 183 | ALL | 72.0 | 70.8 | 71.5 | 51.7 | 155.5 | ALL | 65.0 | 66.2 | 66.8 |
| 96 | 79.4 | 183 | 001-012 | 73.0 | 71.2 | 71.8 | 51.7 | 155 | 001-009 | 66.0 | 66.6 | 67.3 |
| | 62.8 | 175 | 015-018 | | | | 35.1 | 148 | 012-015 | | | |
| | 70.1 | 179 | 020-024 | | | | 43.4 | 151 | 017-021 | | | |
| | 79.4 | 183 | 025-029 | | | | 51.7 | 155 | 022-026 | | | |
| | 86.8 | 186 | 031-034 | | | | 59.1 | 159 | 028-031 | | | |
| | 94.1 | 190 | 036-040 | | | | 67.4 | 163 | 033-037 | | | |
| | 79.4 | 183 | 042-046 | | | | 51.7 | 155 | 039-046 | | | |
| 119 | 79.4 | 183 | ALL | 72.0 | 71.4 | 72.5 | 51.7 | 155 | ALL | 65.0 | 67.8 | 67.8 |
| | 79.4 | 182 | ALL | | | | 51.7 | 155 | ALL | | | |
| | 79.4 | 182 | ALL | | | | 51.7 | 155 | ALL | | | |
| 129 | 72.0 | 179 | 001-008 | 73.0 | 71.8 | 71.8 | 46.2 | 152 | 001-005 | 67.0 | 67.4 | 68.0 |
| | 79.4 | 182 | 010-014 | | | | 53.5 | 156 | 007-012 | | | |
| | 72.0 | 179 | 016-026 | | | | 46.2 | 152 | 013-023 | | | |
| | 62.8 | 175 | 028-032 | | | | 36.9 | 149 | 025-030 | | | |
| | - | - | | | | | 46.2 | 152 | 031-033 | | | |
| 145 | 70.1 | 178 | 001-004 | | | | 46.2 | 152 | 001 | | | |
| | 62.8 | 175 | 006-011 | 72.0 | 72.2 | 72.5 | 37.3 | 148 | 003-008 | 65.0 | 68.4 | 67.8 |
| | 70.1 | 178 | 012-017 | | | | 46.2 | 152 | 009-014 | | | |
| | 79.4 | 182 | 016-023 | | | | 53.5 | 156 | 016-020 | | | |
| | 72.0 | 179 | 025-034 | | | | 46.2 | 152 | 022-034 | | | |
| 160 | 70.1 | 177 | 001-006 | | | | 46.2 | 152 | 001-003 | 65.0 | 68.0 | 67.7 |
| | 62.6 | 175 | 008-013 | | | | 38.7 | 148 | 005-009 | | | |

TABLE 3-33 (CONT'D)

SUMMARY OF LATERAL SEPARATION FOCUS SENSOR (LSFS) PERFORMANCE DATA

| | Forward Camera | | | | | | Aft Camera | | | | | |
|---|---|---|---|---|---|---|---|---|---|---|---|---|
| Rev | Platen Position (microns) | LSFS (counts) | Frames | FP Temp (°F) | Prim Temp (°F) | Corr Temp (°F) | Platen Position (microns) | LSFS (counts) | Frames | FP Temp (°F) | Prim Temp (°F) | Corr Temp (°F) |
| | 70.1 | 177 | 014-019 | 72.0 | 72.0 | 72.5 | 46.2 | 152 | 011-016 | | | |
| | 79.4 | 182 | 020-025 | | | | 53.4 | 155 | 017-022 | | | |
| | 70.1 | 179 | 027-029 | | | | 46.2 | 152 | 024-029 | | | |
| 209 | 72.0 | 179 | ALL | 72.0 | 71.8 | 71.8 | 46.2 | 152.5 | ALL | 65.0 | 67.4 | 67.3 |
| 258 | 73.8 | 180 | 002-008 | 73.0 | 71.6 | 72.5 | 46.2 | 152 | ALL | 66.0 | 67.4 | 67.7 |
| | 66.5 | 176 | 009-013 | | | | | | | | | |
| | 57.2 | 173 | 014-End | | | | | | | | | |
| 274 | 64.6 | 176 | ALL | 73.0 | 71.6 | 72.5 | 46.2 | 152 | ALL | 66.0 | 67.4 | 67.3 |
| 290 | 64.6 | 176 | ALL | 73.0 | 71.4 | 72.5 | 46.2 | 152 | ALL | 66.0 | 67.4 | 67.3 |
| 306 | 64.6 | 176 | ALL | 73.0 | 71.4 | 72.2 | 46.2 | 152 | ALL | 66.0 | 67.0 | 67.2 |
| 323 | 64.6 | 176 | ALL | 72.0 | 71.4 | 72.0 | 46.2 | 152 | ALL | 65.0 | 67.0 | 67.0 |
| 397 | - | 177 | ALL | 70.0 | 70.6 | 70.8 | 46.2 | 154 | ALL | 63.0 | 66.2 | 66.0 |
| 420 | 64.6 | 177 | ALL | 70.0 | 70.6 | 70.8 | 46.2 | 154 | ALL | 63.0 | 66.2 | 66.0 |
| 435 | 64.6 | 177 | ALL | 70.0 | 70.0 | 70.5 | 46.2 | 154 | ALL | 63.0 | 65.4 | 66.0 |
| 445 | 64.6 | - | ALL | 70.0 | 70.0 | 69.0 | 46.2 | 151 | ALL | 64.0 | 66.0 | 66.5 |
| 484 | 64.6 | 177 | ALL | 71.0 | 70.2 | 71.2 | 46.2 | 154 | ALL | 64.0 | 65.8 | 66.0 |

indicate a one TM count lower reading per 2.8° F increase in temperature over the 65° - 75° F range. This is attributed to the primary mirror optical surface characteristics at the mounting point, "bump/hole", that the LSFS looks at.

During Sequence M the Forward Camera's temperature was 70° F and the Aft, 71° F. This was measured on the primary mirror, the corrector plate, and at the focal plane. The LSFS read 181 and 148 TM counts on the Forward and Aft Cameras when the focal plane position diagnostics read 79.4 and 51.7 microns respectively. The initial orbital data on Revs 14 and 16 indicated at 79.4 and 51.7 microns for the Forward and Aft Cameras respectively, the LSFS read 185 and 157 TM counts. In addition, the orbital temperatures of the above indicated thermal sensors read an average of 69 and 65° F for the Forward and Aft Cameras respectively. Adjusting the data for temperature, would indicate that the Forward Camera should be advanced 6 microns and the Aft by 16 microns. The evaluation of the imagery eventually resulted in the Forward Camera being advanced by 16 microns and the Aft by 6 microns. The difference in the final setting of the focal plane based photography and that indicated by the LSFS was 8 microns for the Forward and 9 microns for the Aft. Since the LSFS is looking at the primary mirror mounting point deformation, part of the discrepancy may be attributable to a change in size and the distortion in a zero gravity (g) environment since the primary is weightless. Significant contour changes have been noted interferometrically at the mounting point by placing a primary mirror in both vertical and horizontal positions and measuring mounting point induced surface distortion.

The repeatability of both LSFS units as observed during thru focus runs on-orbit was excellent (62μ) and within the LSFS tolerance of ±6 microns. This repeatability also included predicted changes due to temperature.

### 3.9.9 First Frame In-Track Smear

Excessive in-track smear was noted by the PFA Team on RV-2 on the first Aft Frame of Op 80. This frame was photographed at a 30° scan with a center of -30°. Detailed analysis of TM data revealed that on Op 109, Rev 113, that the in-track IMC function (skew angle) was improperly generated on the first Forward frame, see Figure 3-34. Analysis revealed that the error is inherent in all flight models and occurs only on 30° and 60° off-center scans. The smear occurs on the first Forward frame only for positive scan centers and the first Aft frame only for negative scan centers. The improper generation of the skew angle modulation function is associated with the command sequencer logic.

The skew angle function is primarily a cosine function generated via a sinusoidal bit density track (encoder) on the optical bar. The bits are gated into a counter, whose count is made proportional to a voltage, which is used to modulate the platen position with respect to the OB position. The counter is enabled by ANDING the following events: (a) start of platen P mode for each frame; and (b) the first forward transition prior to the first shutter open on the camera in question. For 30° and 60° off-center scans, forward transition occurs after start of P mode. The degree of "lateness" in enabling the

~~TOP SECRET RUFF~~ Handle via ~~Talent-Keyhole~~ Controls Only


TELEMETRY DATA INDICATIVE OF FIRST FRAME IN-TRACK SMEAR

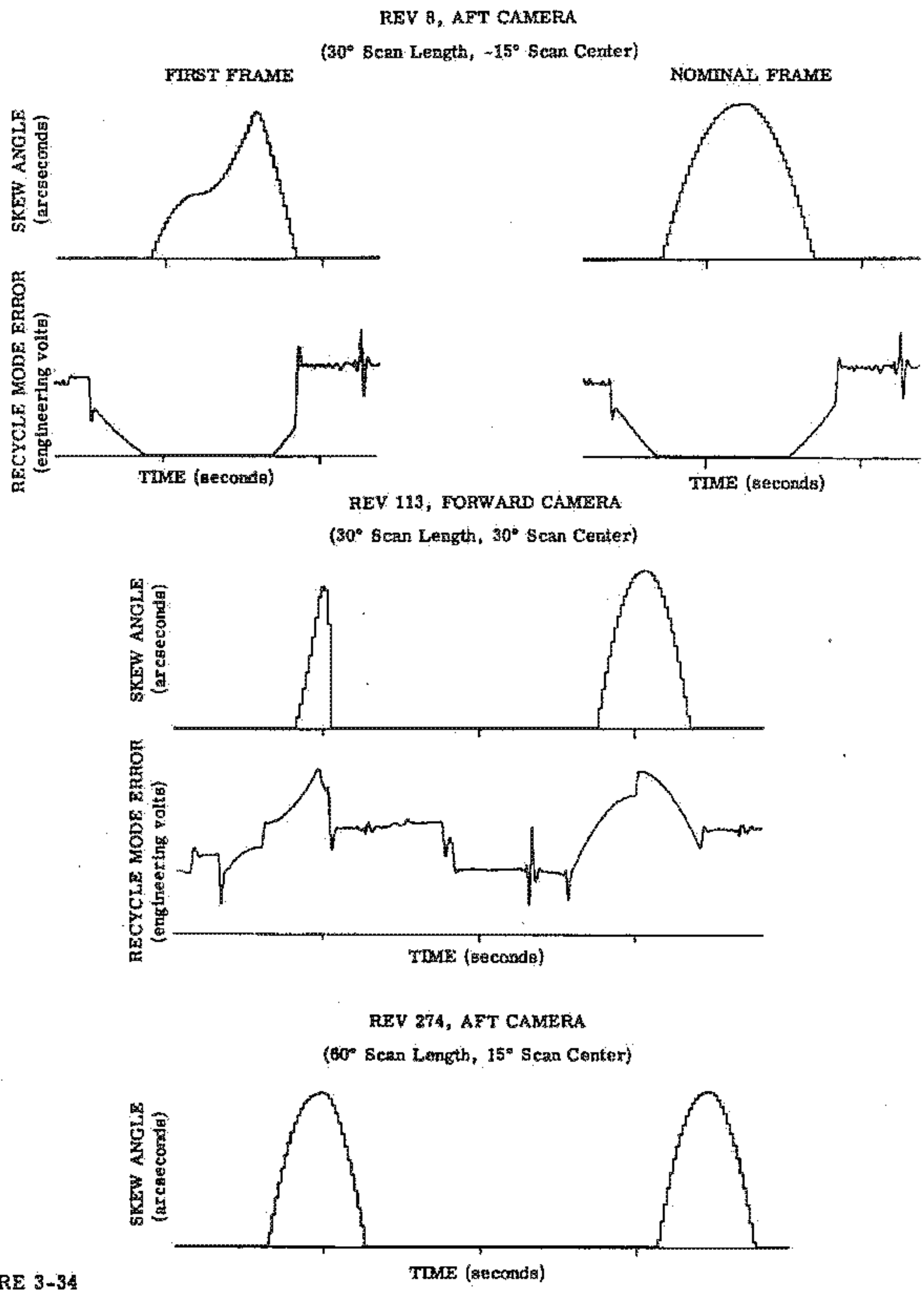


FIGURE 3-34

counter is a function of scan angle length and scan center angle. Thus, when the enable is late, bits are not counted which should have been and skew is improperly generated. Figure 3-35 is a plot of theoretical versus actual skew angle for the sectors mentioned. The worse case errors are associated with 30°/±45° sectors, with 30°/±30°, 60°/±30°, 30°/±15°, and 60°/±15° containing skew angle errors of decreasing magnitude. In addition, the associated in-track velocity error as a function of OB position is shown for a Vx/h = .040 rad/sec. Figure 3-34 contains plots of TM data indicative of the anomaly. Examination of Figure 3-35 indicates that velocity errors as great as 0.7 inch/sec in-track will occur on the first frame and associated camera of the sectors described. This is equivalent to 18 microns of smear for a 1 millisecond exposure time.

### 3.9.10 Conclusions

The following conclusions address, in general, the overall effectiveness of the telemetry data to indicate on-orbit photographic quality.

A. The overall average velocity error of the metering capstan summed error increased slightly while on-orbit as compared to the ground test data.

B. The degree of variability of the telemetry signals indicative of film synchronization remained consistent between the orbital and ground test data. However, as is the case with ground evaluations, the orbital TM data gave no indication of the mean smear errors in the in-track and cross-track directions.

C. A point-to-point correlation of mission photography to synchronization error levels was not possible.

D. It is desirable to define and correct the Command Sequence Logic error which causes high smear on the first frame of certain scan modes.

### 3.9.11 Summary

In summary, it must be stated that the TM does provide a tool for on-orbit diagnosis of camera malfunctions. This fact is fully substantiated on the basis of the diagnostic work that was accomplished during the series of emergency shutdowns that occurred on the Aft Camera during RV-4.

The assesement of imagery by the VEM technique has shown that the predicted variability of resolution in the laboratory was present on-orbit. This is also evident in the metering capstan summed error signal. This correlation although not on a point-to-point basis and not correlatable in terms of absolute magnitude is encouraging and worthy of further VEM investigation.

IN-TRACK VELOCITY ERROR AS A FUNCTION OF SCAN SECTOR AND OB POSITION

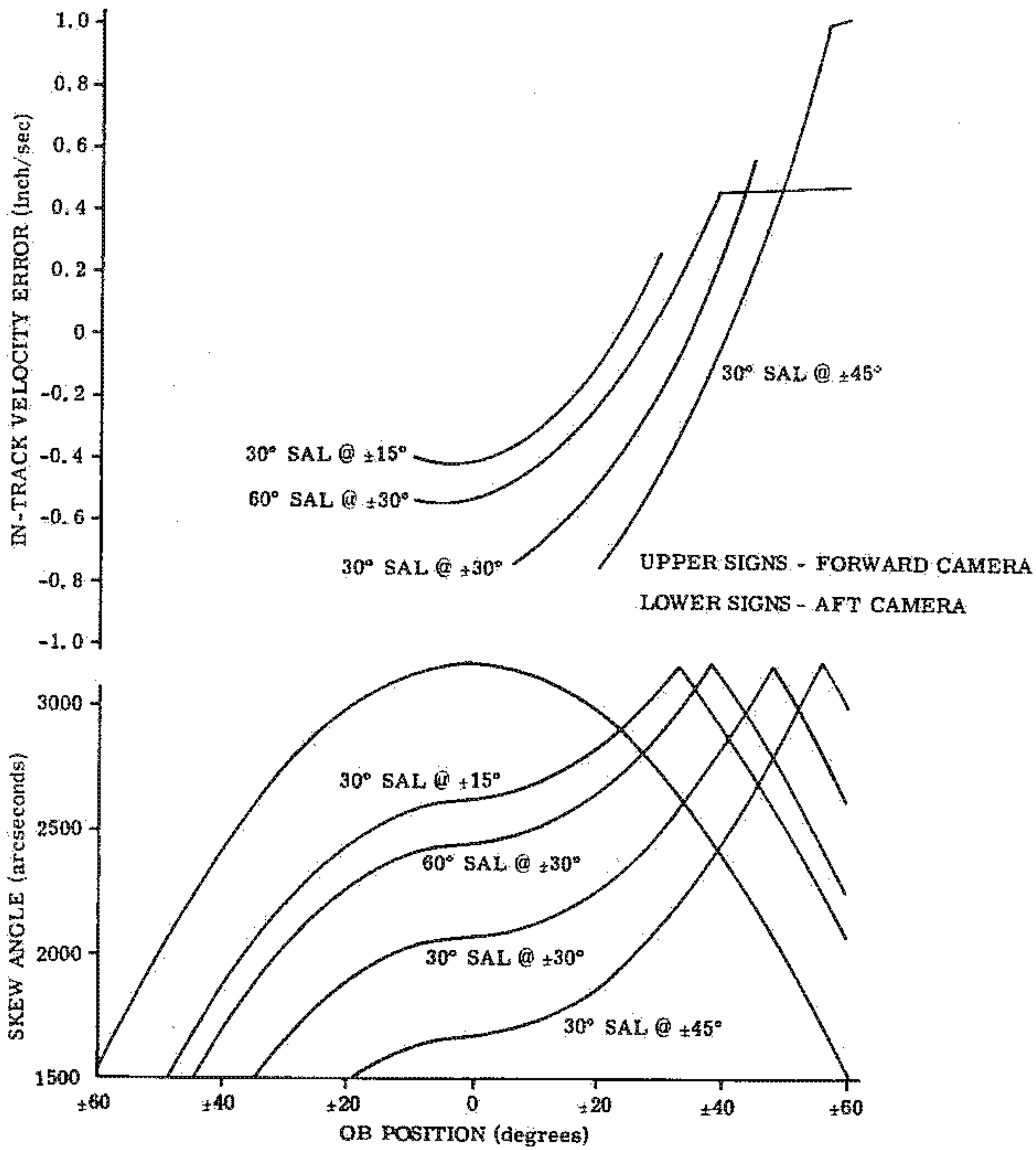


FIGURE 3-35

## 3.10 ANALYSIS OF CAMERA EXPOSURE

### 3.10.1 Introduction

A reduction in camera exposure of .06 log E, above a solar altitude of 10°, was indicated by objective and subjective analysis of RV-1 photography. The change was implemented during Operation 135 of RV-2, and verified as appropriate by analysis of material acquired subsequent to that operation. No gross camera exposure deficiencies were apparent.

### 3.10.2 Initial Camera Exposure Recommendation

The exposure times were computed using the KALEIDOSCOPE radiometric acquisition program. Additional checking with regard to exposure time/smear trade-off relationships was accomplished using the CRYSPER system model.

The underlying criteria for the initial recommendation were:

A. Above 15° solar altitude, advantage is taken of the consistency of the apparent mean scene radiance for cultured areas at a given solar altitude. The mean radiance is exposed at a point on the sensitometric curve where the sum of the products of the film resolution and the frequency of occurrence of radiances for an average scene is at a maximum. For Film Type 1414, the speed point for the process used was $\bar{1}.34$ log meter candle seconds.

B. Below 15° solar altitude, the exposure required is less than that required by the mean criteria, since considerable compression of the scene radiance range occurs due to increasing atmospheric effects. In this case, the mean object shadow radiance is exposed at the $\bar{1}.02$ log meter candle seconds point on the 1414 sensitometric curve. Figure 3-36 illustrates the initial recommendation.

### 3.10.3 Description of the Method of Camera Exposure Analysis

The frames to be analyzed were selected by the NPIC Tiger Team. The selection criteria included the following features:

A. The frames have as much cultural detail as possible.

B. The frames cover a wide range of solar altitudes.

C. Frames with apparent deficiencies in exposure, regardless of the amount of culture present.

After subjective analysis, the selected frames were then scanned with a microdensitometer collecting an average of 1,000 contiguous data points per scan. The data was processed to obtain both density and log radiance distributions. The mean points of the distributions are used to determine general exposure adequacy; however, the 5% and 95% frequency of occurrence levels are also examined to determine the position on the curve of shadow and highlight detail. With regard to the mean value, the expected accuracy of the determination for a single measurement of suitable culture is ±.10 log E from a predicted value.

INITIAL KH-9 EXPOSURE RECOMMENDATION

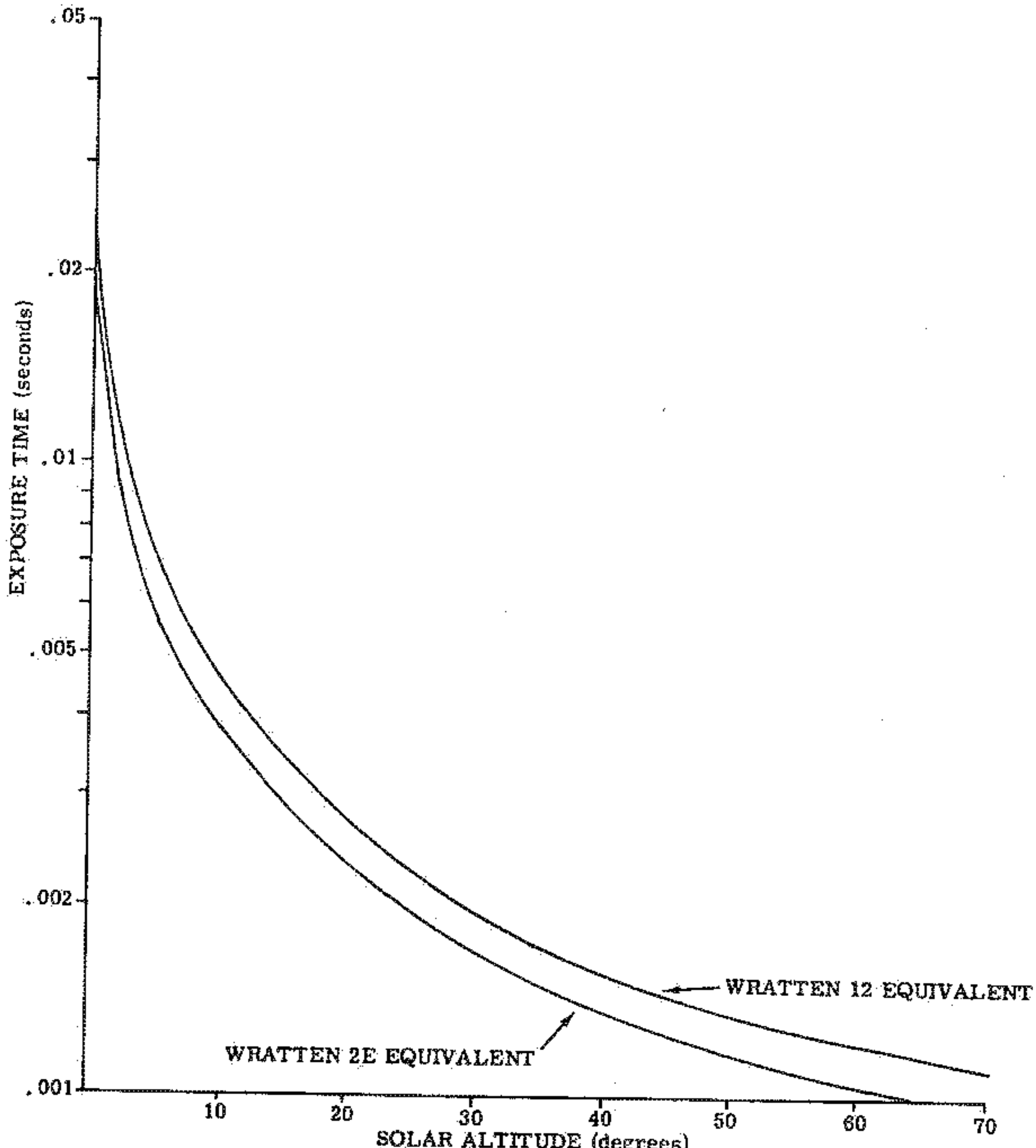


FIGURE 3-36

3.10.4 Comments on Apparent Exposure Deficiencies

The majority of frames which appeared grossly overexposed were from the Forward Camera and contained specular reflections. These reflections were either due to the material of construction, shape, and orientation of objects (aircraft in particular) for which little corrective action can be taken; or due to the specular component of reflectance of objects in general which is the more severe of the two effects. The position of occurrence of the later effect is predictable in relative severity, position in the frame, and latitude. This subject is dealt with in more detail in paragraph 5.8 of this report.

Apparent underexposure was typified by frames containing a scarsity of culture, generally those which were heavily forested. No cases of gross underexposure were found.

3.10.5 Exposure Experiment

Stepped exposure experiments were conducted during Ops 34 and 53. The exposure increments were .15 log E, extending to ±1 Stop on either side of nominal. This experiment also gives some appreciation of the precision and accuracy of the density distribution analysis. This data is presented in Figure 3-37.

Subjective examination of the material indicated a reduction in exposure would be possible, but not to the extent of 1/2 Stop, since it was felt the shadow record was beginning to suffer at that level. The average mean for the nominal exposure fell at a density of 1.16, the aim density being 1.00, this agreed with the subjective analysis recommendation that a slight exposure reduction was needed.

With regard to the precision of the microdensitometric analysis, Table 3-34 lists the $\Delta$ log E's relative to the nominal exposure for the programmed and average measured increments. It should be noted that the average for the largest departure of a single measured mean from its group mean is -.03.

TABLE 3-34

MEASURED DELTA LOG E'S RELATIVE TO NOMINAL EXPOSURE

| Programmed | Average Measured | Single Mean |
|---|---|---|
| -.30 | -.27 | -.15 |
| -.15 | -.09 | -.07 |
| 0.00 | 0.00 | +.18 |
| +.15 | +.15 | +.06 |
| +.30 | +.26 | -.05 |

In summary, the experiment suggested a slight exposure reduction would benefit the mission imagery. It also indicated that the precision of the analytical method and the combined accuracy of the predicted exposure recommendation is adequate. This is especially true when it was found that frames with "sufficient cultural detail for measurement," could not in all instances be located.

3.10.6 Camera Exposure Adequacy as a Function of Solar Altitude

A high percentage of the frames in RV-1 were taken above a solar altitude of 55°, thus it was

FIGURE 3-37

URBAN/INDUSTRIAL SCENE DENSITY DISTRIBUTIONS

EXPOSURE EXPERIMENT ON OPS 034 & 053

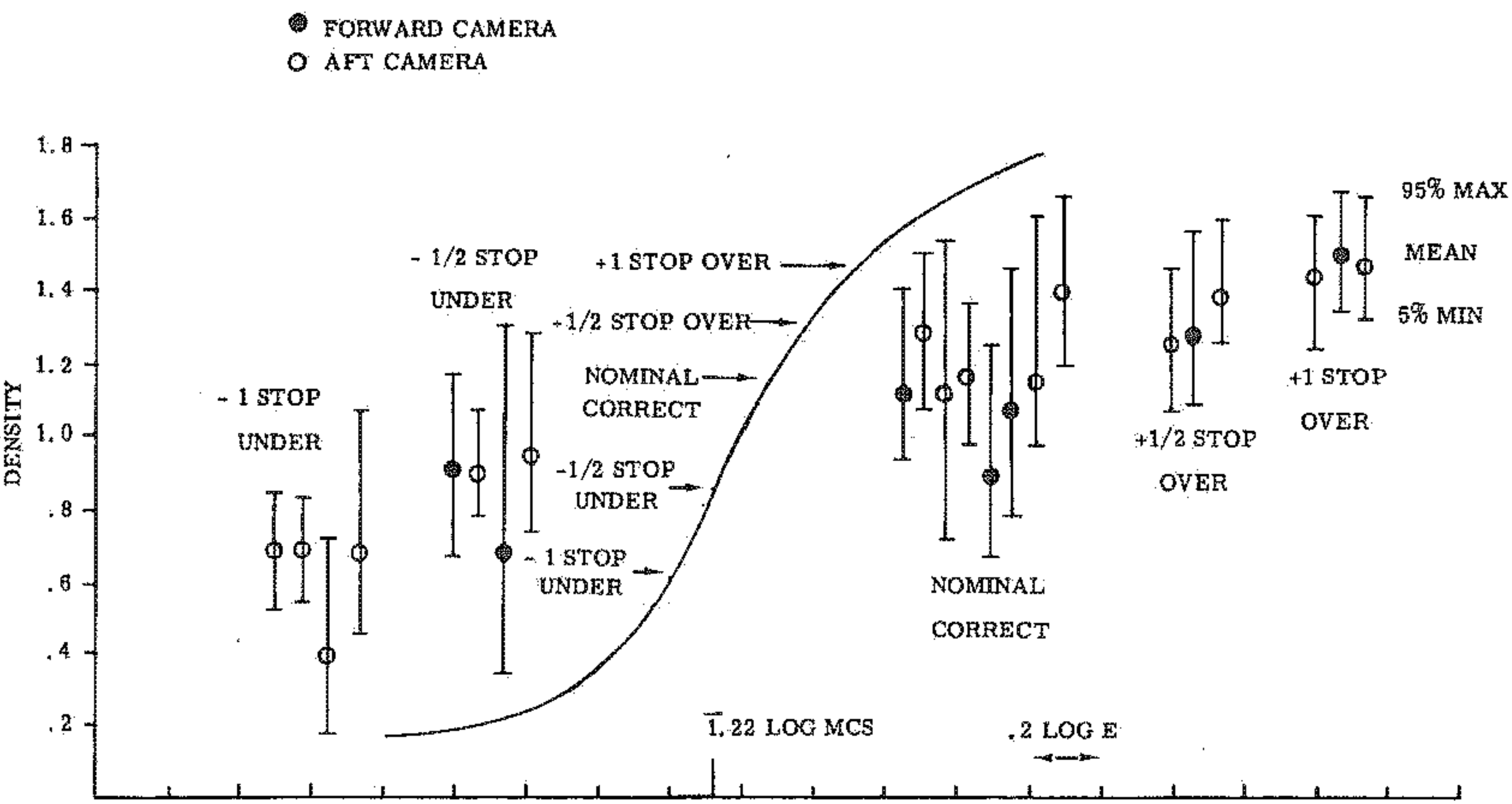


TOP SECRET RUFF

Handle via Talent-Keyhole Controls Only



Approved for Release: 2022/03/03 C05132845

difficult to locate suitable culture at the lower solar altitudes. This was compounded by the fact that the lower solar altitudes of a June mission are at very high latitudes where culture tends to be sparce. However, it was determined that reasonably good culture was located down to aprx 6° solar altitude. Figure 3-38 illustrates the results of the density frequency distribution analysis. The largest $\Delta$ log E between the mean of any one solar altitude group and that of the mean of another group, does not exceed .13 log meter candle seconds.

3.10.7 Exposure Adequacy as a Function of Scan Angle

Frame 023 of Op 165, on both cameras afforded an excellent opportunity to examine camera exposure as a function of scan angle. Both frames contained a series of small cities and towns across a right-looking 60° scan, -30° center relative to the flight direction. The results from the density distribution analysis are illustrated in Figure 3-39. For a particular unit, the $\Delta$ log E between any individual mean and the mean for the unit, does not exceed .06 log E. This agrees with previous data from panoramic-type camera systems, and suggests that a single camera exposure level gives essentially the same mean log exposure value throughout the frame.

3.10.8 Comparison of Exposure Between the Forward and Aft Camera Units

The mean scene density averaged for all frames analyzed in RV-1 resulted in .99 for the Forward and 1.17 for the Aft. This is a significant difference when comparing it to a standard deviation of the mean of .031; however, it is only a $\Delta$ log E of .09 in terms of exposure. The $\Delta$D between the 5% and 95% points was averaged over all scanned frames. The overall difference in density scene range between the Forward and Aft Cameras was .17; the Forward unit being greater. This indicates there is a significant difference when compared to a standard deviation of the mean $\Delta$'s of .031. This could be anticipated, as the Forward Camera looks into specular reflections and object shadows, which both tend to extend the scene range over that seen by the Aft Camera unit.

The fact that the Forward Camera looks into the shadows is also consistent with the observed slightly lower mean density, in that, shadows would tend to bias the mean downward.

3.10.9 Evaluation of Density Distribution Data

Analysis of the combined distribution data before the exposure change indicates the mean density was approximately 1.06, see Figure 3-40. Since the subjective analysis of the material also indicated a slight reduction in exposure was possible, the decision was made to reduce the exposure time by .2 Stop (.06 log E). The exception to this change was determined from subjective analysis of low solar altitude acquisitions. Presence of snow and ice complicates analysis by densitometric means. It was felt that a correction below 10° solar altitude might eliminate some shadow detail, therefore, the change was implemented above 10° solar altitude only.

FIGURE 3-38

URBAN/INDUSTRIAL SCENE DENSITY DISTRIBUTIONS
USING NOMINAL CORRECT EXPOSURE

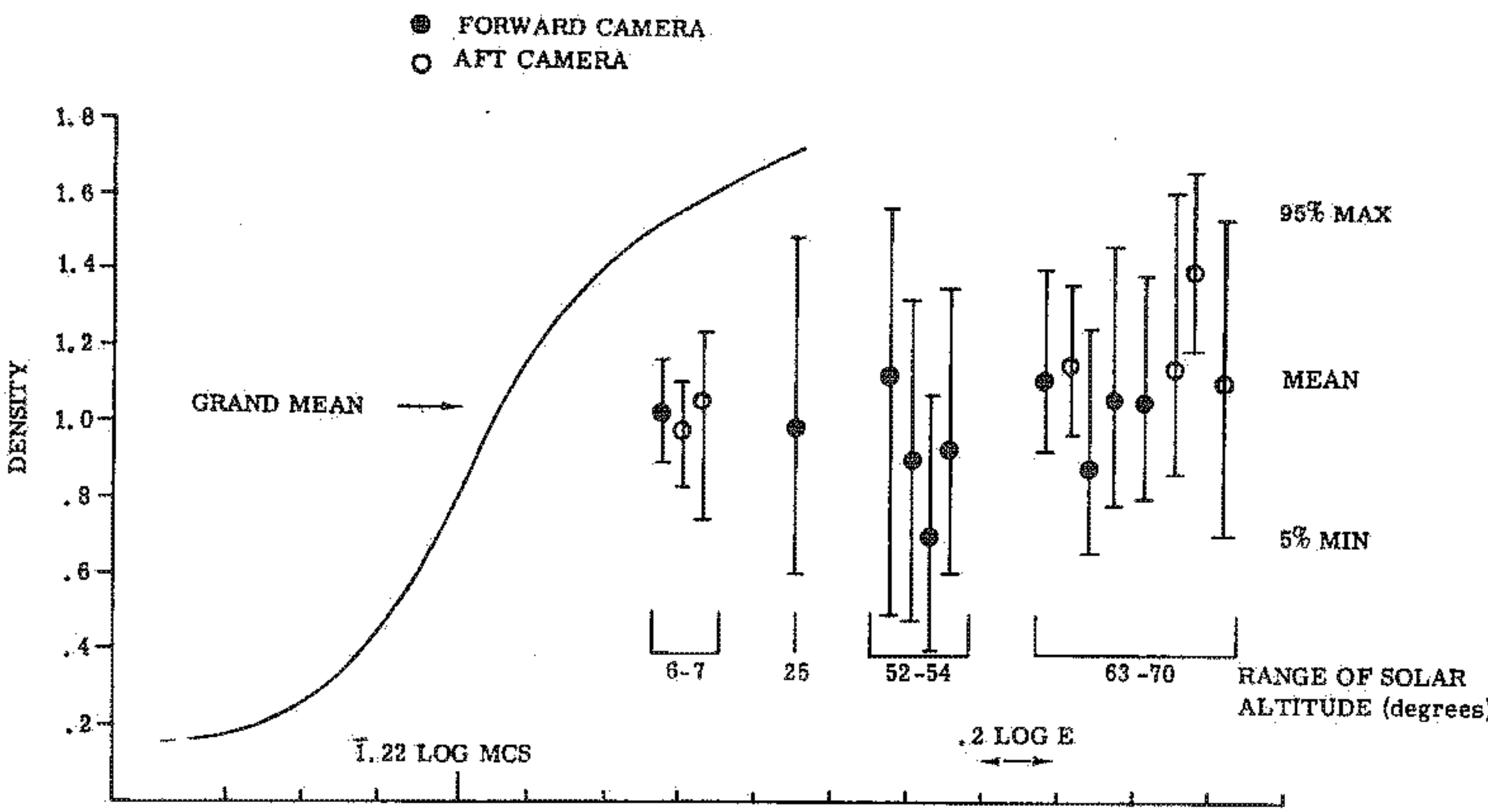


TOP SECRET RUFF

Handle via Talent Keyhole Controls Only



Approved for Release: 2022/03/03 C05132845

FIGURE 3-39

URBAN SCENE DENSITY DISTRIBUTIONS FOR
OP 165 FRAME 023 AS A FUNCTION OF SCAN ANGLE

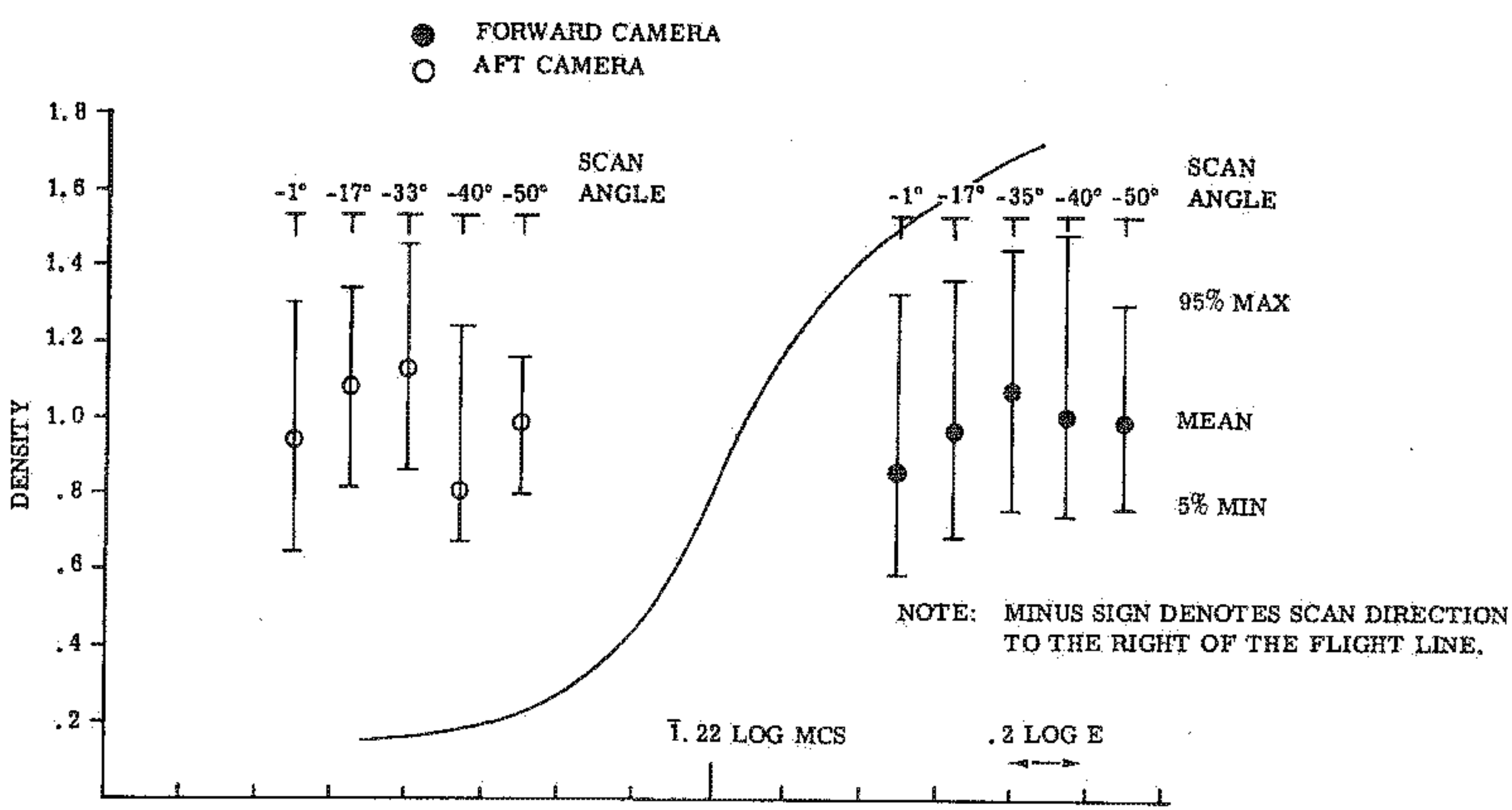

FIGURE 3-40

URBAN/INDUSTRIAL SCENE DENSITY DISTRIBUTIONS
BEFORE AND AFTER EXPOSURE CHANGE

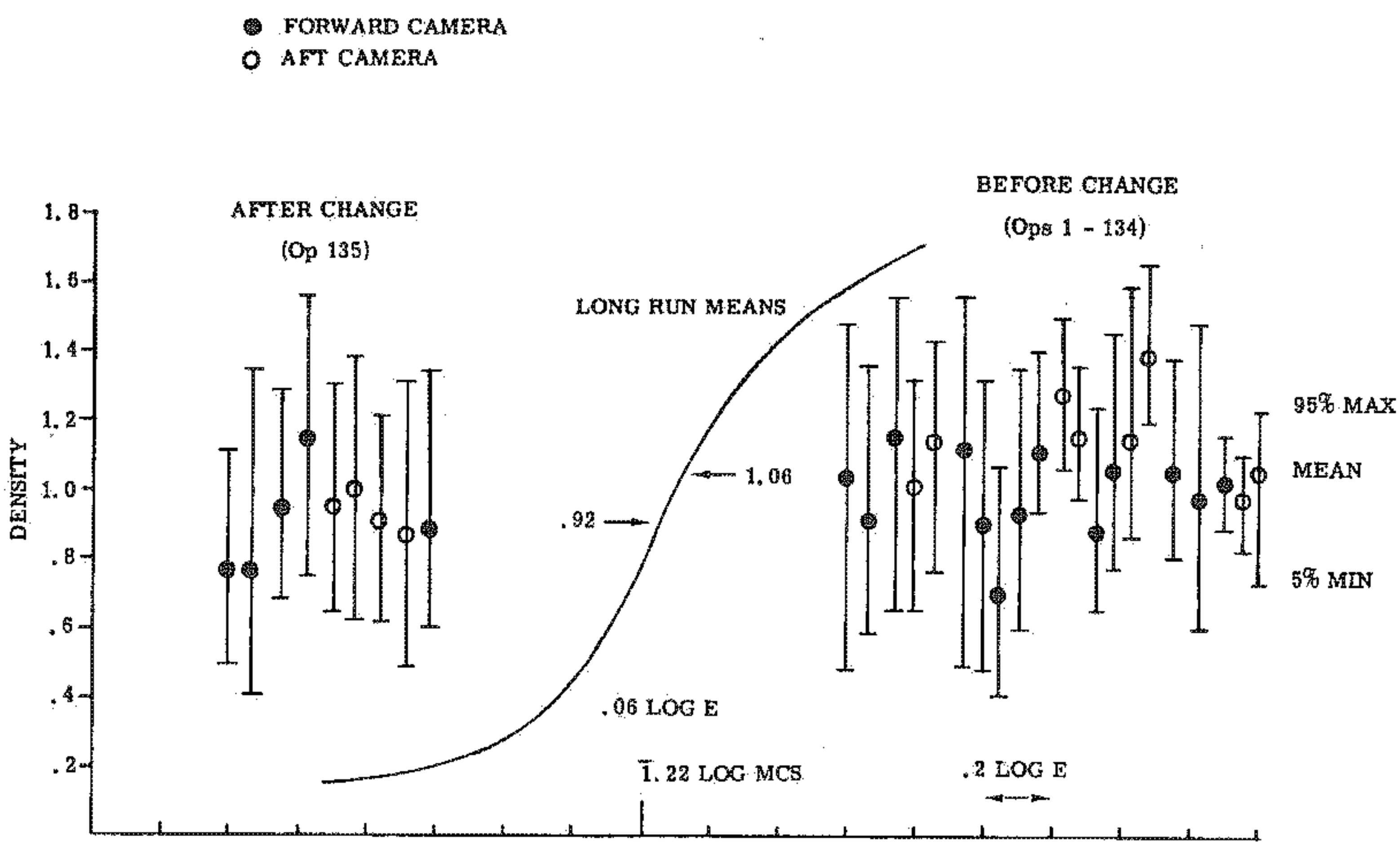


TOP SECRET RUFF

Handle via Talent-Keyhole Controls Only



Approved for Release: 2022/03/03 C05132845

3.10.10 Analysis of Post Exposure Change Acquisitions

Figure 3-40 illustrates the results of density frequency distribution analysis for photography accomplished subsequent to the exposure change. The mean density fell from 1.06 to .92 ($\Delta$ log E of .06), which is precisely the programmed change.

The 5% frequency of occurrence point did not fall below a density of .40 in any of the scenes measured after the exposure change. The mean 5% point for the group fell at a density of .59. Past experience has shown that the 5% frequency point for a total scene distribution is extremely close in density to the mean of a distribution measured entirely within object shadows. Radiances recorded below the mean shadow radiance generally do not contain much information, due to the extremely low contrast. A shadow distribution was measured in Frame 003, Op 109, prior to exposure change. The shadow mean density was .72. The average 5% value after the exposure change of .59 is entirely consistent with the programmed exposure change (.06 log E), since it amounts to a log E reduction of approximately .07.

3.10.11 Comments on the Shape of the Luminance Frequency Distributions

Preliminary examination of the scene radiance distributions suggested that the shapes of the distributions were somewhat unusual. However, examination of synthesized and actual radiance distributions, indicated only that the shape was normal for higher than average haze levels. Examination of the minimums of the radiance distributions gave a haze radiance value 1.3 times higher than the yearly average as measured in the U.S.A. From this, it was deduced that the transmittance of the atmosphere was probably 10% lower than the yearly average value for the U.S.A. Comparison of a distribution synthesized from this data, to actual distributions from the mission, indicated good agreement.

3.10.12 Conclusions

A. The camera exposure, as modified, was optimum for the mission even for frames acquired under very clear atmospheric conditions.

B. No cross-frame exposure anomalies were exhibited.

C. Most differences encountered were within the $\pm$.10 log E analysis/prediction error anticipated

D. It was determined that no exposure adjustment was required between the Forward and Aft Cameras.

E. The results from the exposure algorithm are consistent through the solar altitude range encountered on Mission 1201.

3.10.13 Recommendations

The lack of data at the lower solar altitudes, precluded a thorough analysis. A more complete analysis should be conducted.

## 3.11 MISSION 1201 FILTERS

### 3.11.1 Introduction

Mission 1201 was flown with a Wratten 2E Filter on the Forward and Wratten 12 Filter on the Aft Camera. The principal difference between these filters is that the Wratten 2E has a cut-off wavelength in the blue region of the spectrum approximately 80 nanometers lower than the cut-off wavelength of the Wratten 12.

The basic design of the KH-9 System filtration was determined on the basis of SO-380 Film and an atmospheric model contained in the Performance Specification (SP-621-001-C). The option of a selection of any specific filter was included in the design by means of a ground (preflight) interchangeable filter. Thus for Missions 1201-1206 the final selection of the flight filters is a preflight decision. The decision to change from a Wratten 12 to a Wratten 2E filter was based upon two considerations. They are:

A. Mission 1201 was flown with Film Type 1414 instead of SO-380 as originally planned. Since 1414 has less sensitivity in the wavelength region of 400 to 500 nanometers and an effectively faster film speed, a filter change appeared desirable. Another benefit of the change of film type is the decreased curvature in the focal plane.

B. Chamber A acceptance testing showed severe cross-track smear on the Forward Camera. The film and camera manufacturers conducted studies which dealt with atmospheric attenuation versus smear tradeoffs and concluded the Wratten 2E Filter would be more beneficial for overall performance. Subsequent testing in Chamber A-2 with the Wratten 2E filter was reported in the SN-003 Flight Readiness Report. This report concluded:

"In general the performance of the Forward Camera, particularly in the cross-track direction, has improved since the original Chamber A acceptance tests. This improvement in camera resolution is probably attributed to the use of a Wratten 2E Type Filter which allows use of shorter exposure times than the Wratten 12. It should be pointed out that servo electronic box changes were made in the field which also have been shown on subsequent flight models to improve the cross-track smear."

### 3.11.2 Camera Performance Analysis

The predicted camera performance is based upon optical performance, image motion, and dynamic focus. The optical performance is obtained by testing each optical bar interferometrically at a single wavelength and computing a polychromatic response. The spectral sensitivities for each filter/film combination are given in Figures 3-41 and 3-42. Based upon this computation the expected tribar resolution for each of the camera/filter combinations is obtained by intersecting the optical bar modulation function with an aerial image modulation (AIM) curve. The results of these computations are shown in Figures 3-43 and 3-44. These plots show tribar resolution as a function of focus position. They also present the resolution change as a function of target contrast at the entrance pupil of the camera. The interesting thing to note is the difference in performance with the different filters. It shows an expected

FIGURE 3-41

SPECTRAL SENSITVITY OF 1414 FILM PLUS WRATTEN 12 FILTER

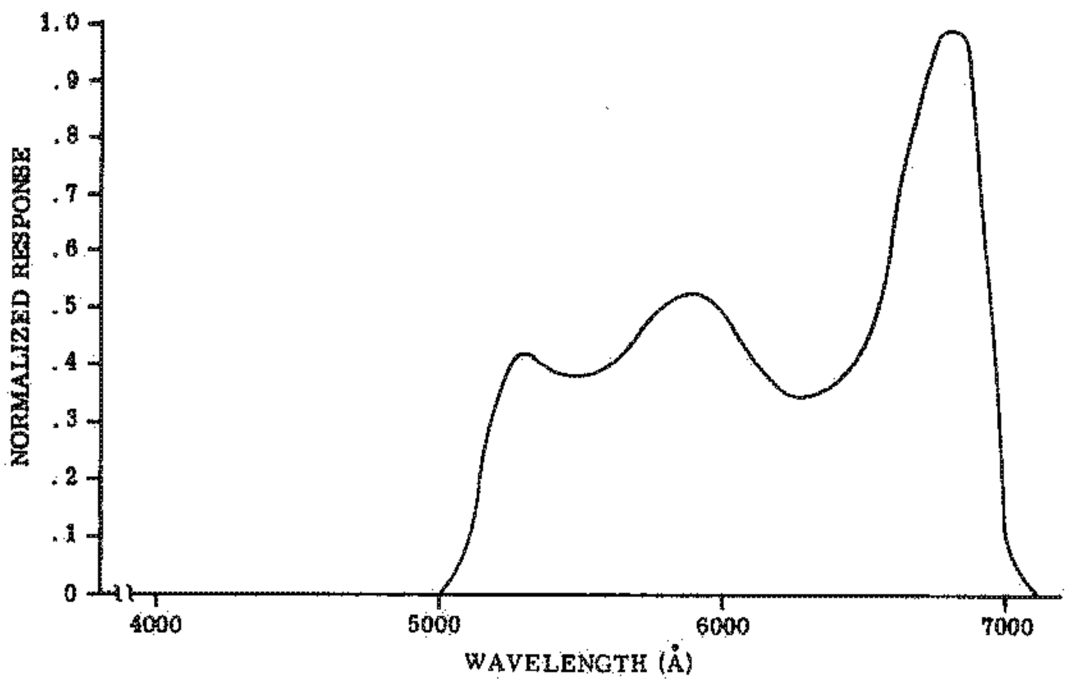


| λ | W (λ) |
|---|---|
| 5100 | .03 |
| 5300 | .08 |
| 5500 | .08 |
| 5700 | .09 |
| 5900 | .11 |
| 6100 | .09 |
| 6300 | .08 |
| 6500 | .10 |
| 6700 | .17 |
| 6900 | .16 |
| 7100 | .01 |

~~TOP SECRET RUFF~~
Handle via ~~Talent-Keyhole~~ Controls Only



Approved for Release: 2022/03/03 C05132845

FIGURE 3-42

SPECTRAL SENSITIVITY OF 1414 FILM PLUS WRATTEN 2E FILTER

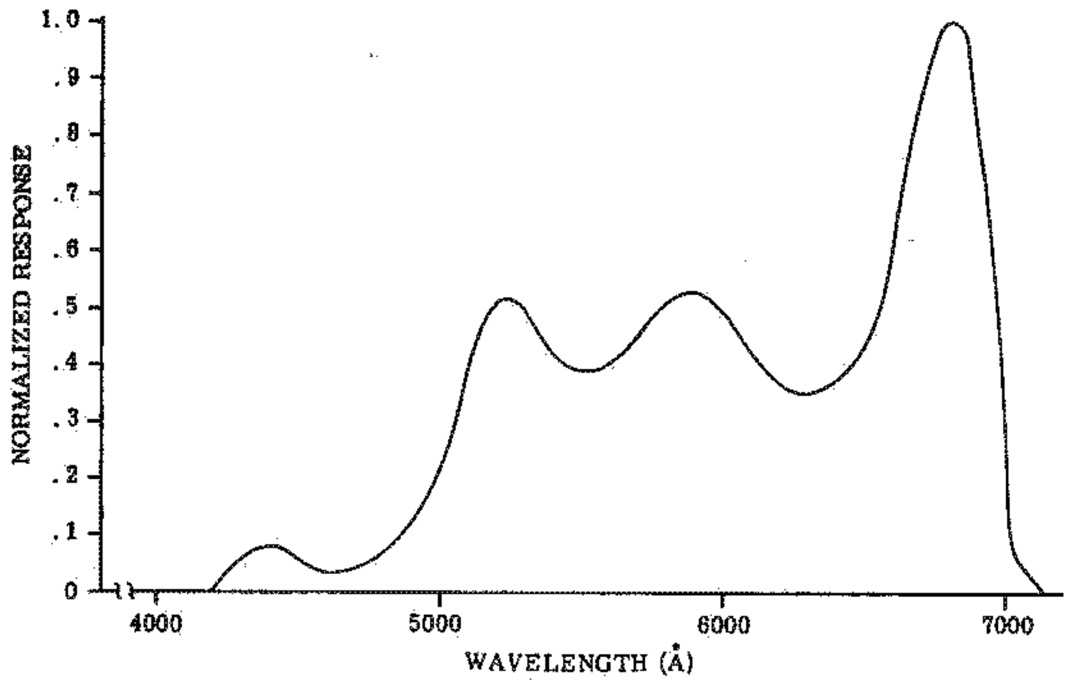


| λ | W (λ) |
|---|---|
| 4300 | .01 |
| 4500 | .01 |
| 4700 | .01 |
| 4900 | .03 |
| 5100 | .08 |
| 5300 | .09 |
| 5500 | .07 |
| 5700 | .08 |
| 5900 | .10 |
| 6100 | .08 |
| 6300 | .07 |
| 6500 | .09 |
| 6700 | .16 |
| 6910 | .13 |
| 7100 | .01 |

## FORWARD CAMERA STATIC RESOLUTION PREDICTIONS WITH WRATTEN 12 FILTER

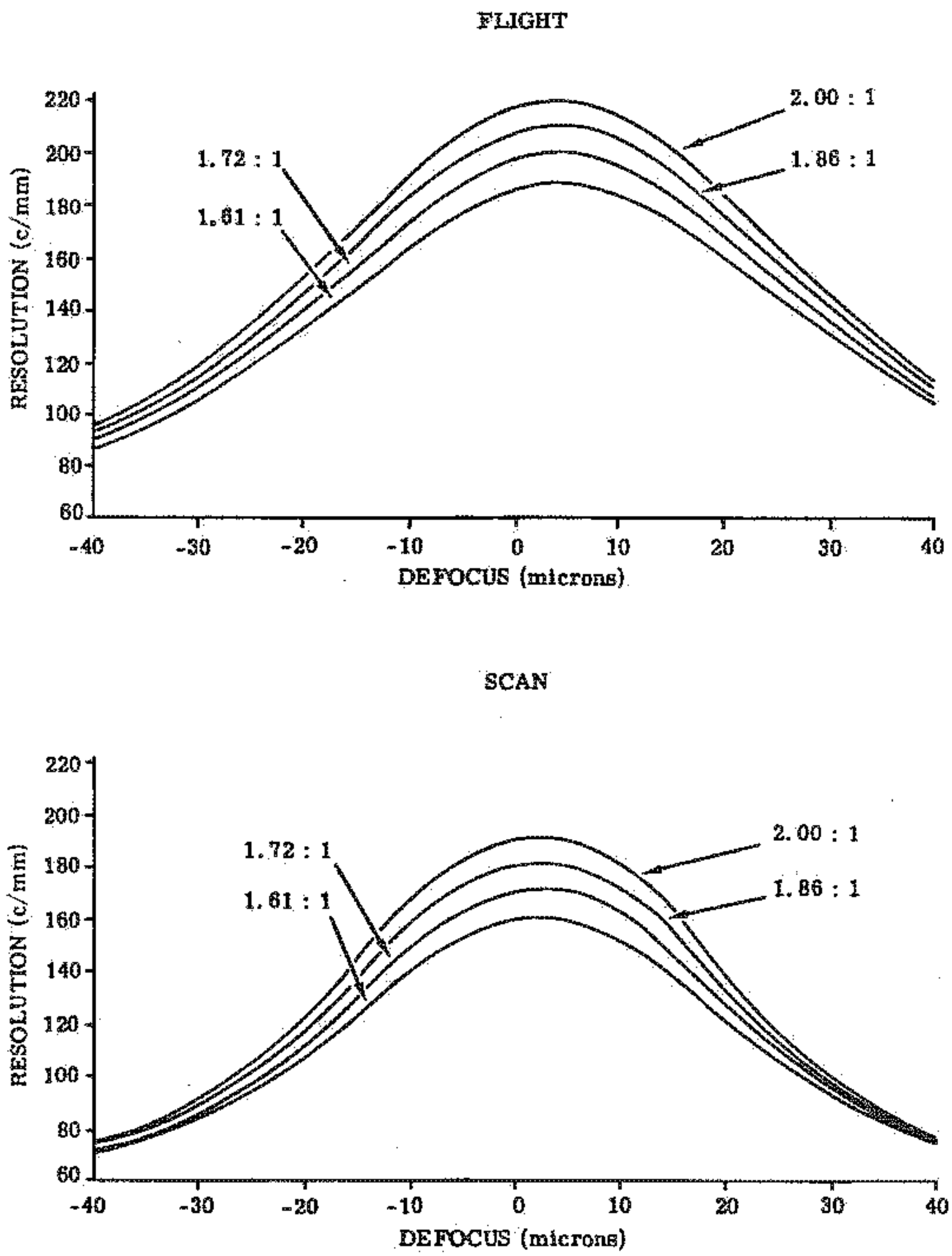


FIGURE 3-43

FORWARD CAMERA STATIC RESOLUTION PREDICTIONS

WITH WRATTEN 2E FILTER

FLIGHT

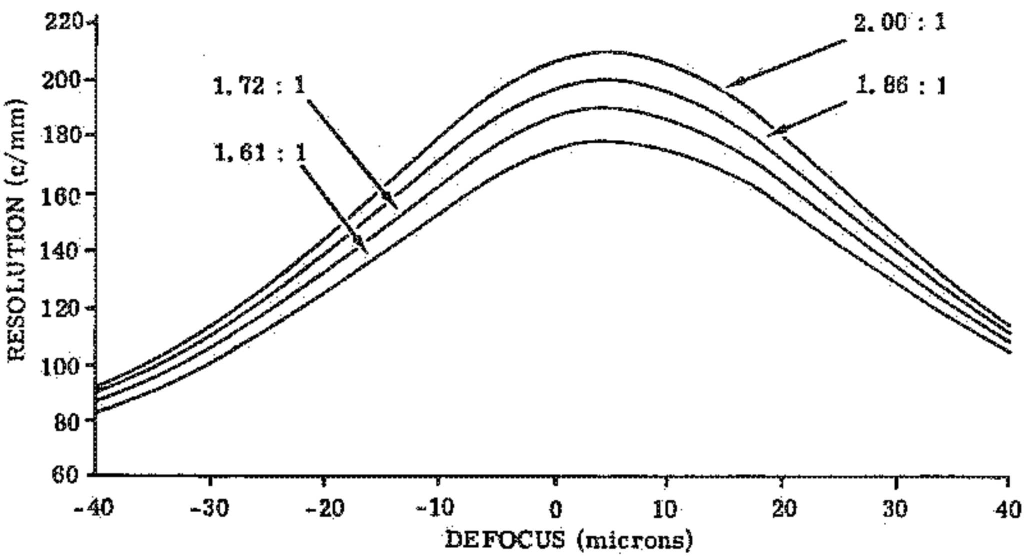


SCAN

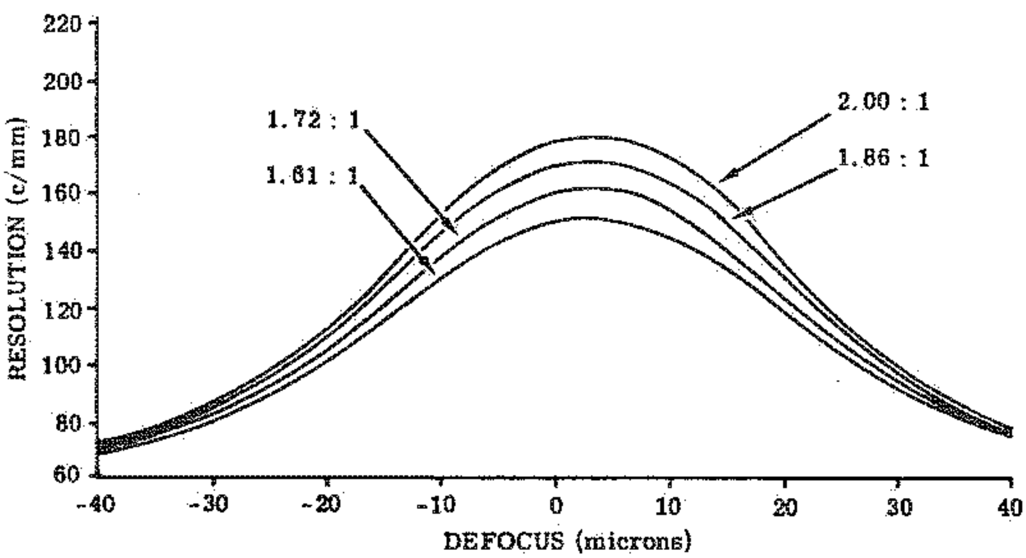


FIGURE 3-44

loss of 10 cycles/mm as one changes from a Wratten 12 Filter to a Wratten 2E for the same target contrast. This is true only at the position of best focus. The difference decreases with defocus. These plots contain no image motion. The effect of a fixed amount of image motion on camera performance is shown in Figure 3-45. Here the point to be noted is that as the amplitude of smear increases, the difference between performance decreases for the same target contrast. Finally the change from a Wratten 12 to a Wratten 2E Filter results in a decrease in exposure time or the amount of smear the camera would see during an exposure. Figure 3-46 shows the exposure recommendations implemented on RV-2.

If the contrast at the entrance pupil of the camera is essentially the same for each filter and the smear amplitude is large, then the Wratten 2E performance will be as good if not better than the Wratten 12 Filter.

### 3.11.3 Mission Flight Results

Several techniques were used to measure contrast. This data is reported in more detail in paragraph 3.4.8. Table 3-35 is an extract from the complete set of data. The purpose of showing this particular set is not to show the absolute magnitude of contrast but to show the difference between the contrasts obtained with the Wratten 12 and Wratten 2E filters. The conclusion is that the contrast resulting from both filters is virtually the same.

TABLE 3-35

TRIBAR CONTRAST FROM GRAY PANEL

| Rev | Operation | Frame Fwd/Aft | Contrast Wratten 2E | Contrast Wratten 12 |
|---|---|---|---|---|
| 16 | 5 | 029/029 | 1.65 | 1.51 |
| 16 | 5 | 048/049 | 1.66 | 1.75 |
| 32 | 17 | 008/009 | 1.93 | 2.13 |
| 32 | 17 | 055/056 | 1.48 | 1.48 |
| 129 | 120 | 018/019 | 1.87 | 1.79 |
| 129 | 120 | 025/026 | 1.78 | 1.73 |
| 129 | 120 | 026/027 | 1.69 | 1.70 |
| 145 | 145 | 012/012 | 1.67 | 1.63 |
| 435 | 384 | 002/003 | 1.62 | 1.53 |
| 484 | 409 | 001/002 | 1.73 | 1.57 |
| 484 | 409 | 001/002 | 1.61 | 1.71 |
| | | | 1.70 | 1.68 Averages |

FORWARD CAMERA OPTICAL BAR

(CONTRAST = 2.00:1)

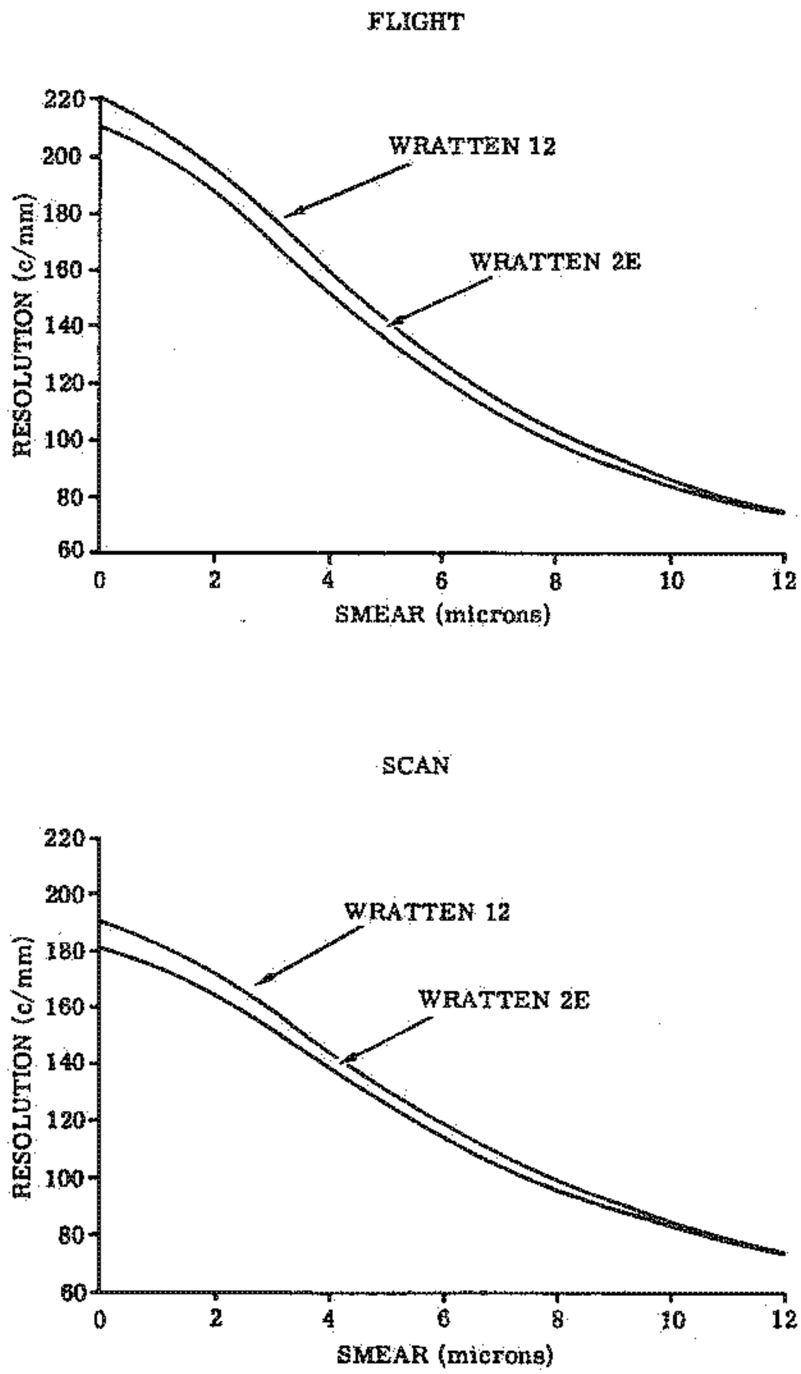


FIGURE 3-45

MISSION 1201-2 EXPOSURE CRITERIA

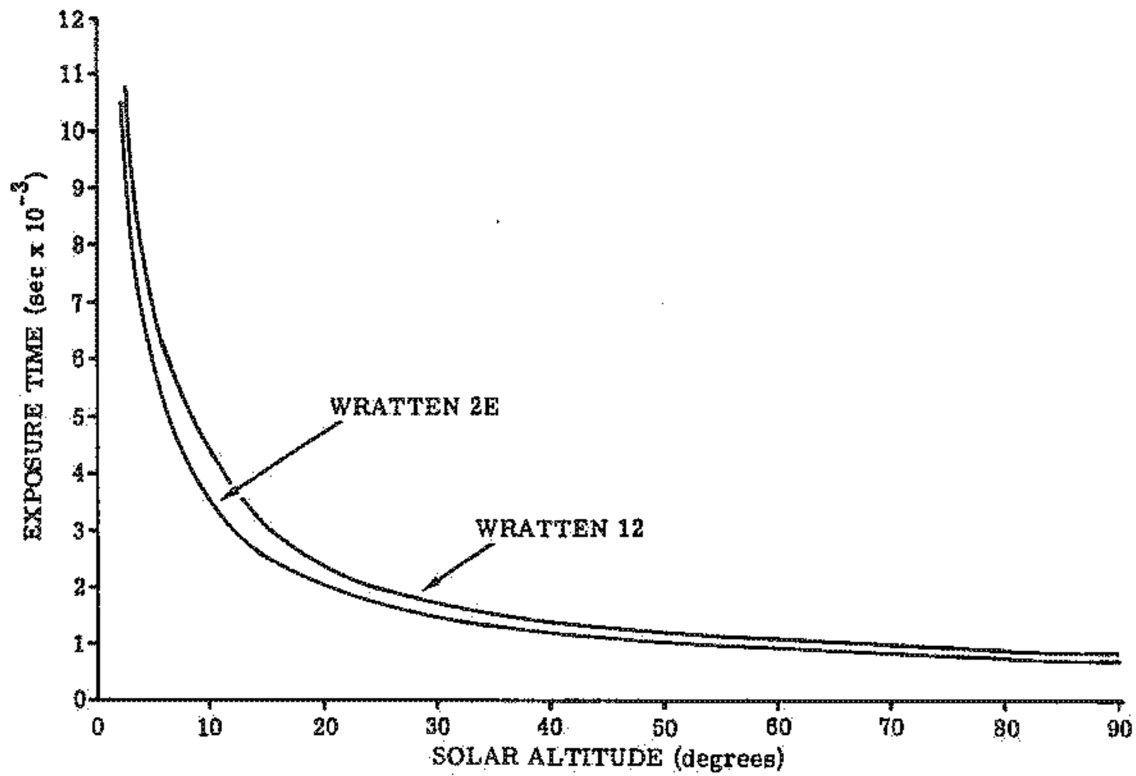


FIGURE 3-46

Paragraph 6-1 of this report contains an analysis of line targets from which the smear for Mission 1201 was determined. It is estimated that the Forward Camera average in-track and cross-track smear for the samples analyzed is approximately 4 microns and 6.5 microns respectively. Table 3-36 shows the predicted smear for a Wratten 12 Filter. This table also shows that there is better performance with the Wratten 2E Filter than with the Wratten 12 Filter.

TABLE 3-36

PREDICTED SMEAR

| Direction | Measured Smear Wratten 2E (microns) | Image Velocity (inch/sec) | Computed Smear Wratten 12 (microns) | Predicted Resolution Wratten 2E (c/mm) | Predicted Resolution Wratten 12 (c/mm) |
|---|---|---|---|---|---|
| In-Track | 4.0 | .17 | 4.6 | 151 | 149 |
| Cross-Track | 6.5 | .27 | 7.5 | 109 | 103 |

3.11.4 Subjective Analysis

In subjectively analyzing the dupe positive it was determined that the imagery appears to be essentially the same from the two different camera filters. There are local areas where one record seem to produce more contrast than the other, however, these are minor considerations when compared to the total mass of similar responses.

The one area of noticeable contrast difference is found in the recording of vegetation. Tree-to-background contrast is slightly higher for the Wratten 12 Filter. The cut-off for this filter is higher on the response curve for vegetation which resulted in a small increase in contrast.

Having broad band spectral coverage has decided advantages in reconnaissance photography, i.e. objects are rendered in a more natural tonal relationship. Inclusion of the blue and blue-green bands provides a bonus in recording vegetation and filling in shadows which normally are void of significant detail. There were no differences in the photographic resolution which could be directly attributed to either filter being used.

3.11.5 Conclusions

A. Estimates of smear obtained from line analysis indicate that the Forward Camera benefitted from the use of the Wratten 2E Filter.

B. There is very little if any contrast loss due to contrast attenuation by haze between the filters.

### 3.11.6 Recommendation

Mission 1201 demonstrated that use of a Wratten 2E Type Filter on the Forward Camera with narrow slit widths does not deteriorate operational photography. In fact, the real possibility exists that some performance improvement can be gained with shorter wavelength cutoff filtration, especially with wider slit widths. Mission 1201 is scheduled for flight in the winter with low solar altitudes requiring wide slit widths. In order to be certain that the baseline Wratten 12 Type Filter can be replaced by the 2E Type without loss to the operational image quality, it is recommended that for Mission 1201 the Forward Camera be fitted with a Wratten 12 and the Aft with a Wratten 2E Type Filter.

## 3.12 INTERFACE SPECIFICATION EVALUATION

### 3.12.1 Introduction

The conformance of the associate contractors to the Interface Control Document (ICD) requirements was evaluated. The limitations on diagnostic instrumentation and the loss of some flight TM data has restricted this effort to an evaluation of the more contentious areas of the past four years and has not permitted a point-to-point comparison of every ICD. In particular, the following group of ICDs were addressed:

| | | |
|---|---|---|
| A. | 1420304 | SBA/SS Electrical Power |
| | 1420355 | SS/RV Electrical |
| B. | 1420316 | SBA/SS Thermal |
| | 1420357 | SS/RV Thermal |
| C. | 1420314 | SBA/SS Structural Environments |
| | 1420361 | SS/RV Structural Environments |
| | 1420318 | SV Alignment |
| D. | 1420313 | SBA/SS Mass Properties |
| | 1420358 | SS/RV Mass Properties |
| | 1420317 | SBA/SS Attitude Disturbance & Control |

The purpose of this review was to determine if the ICD limitations had been exceeded, and to determine if the ICD requirements were unduly conservative and should be relaxed.

### 3.12.2 Electrical Power (ICDs 1420304, 1420355)

In order to determine the on-orbit electrical power consumption of the Sensor Subsystem (SS) during the mission, Satellite Basic Assembly (SBA) bus voltage and current data was retrieved and analyzed for 11 of the 19 available data tapes. In general, the data obtained from the tapes was exceptionally good during the photo mode but in most cases the start-up or shutdown sequence data was not on the tape. Since the start-up and shutdown data was not available, comparison of sensor power consumption with ICD values was not possible in all cases. The power requirements were determined by assuming that the SBA load remained constant during camera operation and was equal to that which appeared on the SBA electrical bus just prior to Measurement Filter Assembly (MFA) turn on. This value was then subtracted from the SBA bus load during SS operation. Some discrepancies occur in the reduced data. It is believed that the discrepancies are due primarily to the fact that the SBA loads are probably not constant during SS operation.

The primary variables affecting SS power requirements are scan angle and amount of film on the Supply Unit (SU) and Take up Unit (TU). Since data was not available for all possible combinations of the above parameters, the data shown in Table 3-37 was analyzed in an effort to obtain a representative cross section. The effects of SU and TU load were obtained by reviewing the 60° scan angle data from beginning-to-end of the mission. One run of each of the other 3 scan angles was analyzed to determine power consumption as a function of scan angle. The maximum allowable power consumption limits specified in the SS/SBA power ICD 1420304 is specified at a Vx/h of .052; therefore, the power consumptio in all cases is less than the maximum specified in the ICD.

TABLE 3-37

FILM/SCAN ANGLE COMBINATIONS

| Rev | Scan Angle (degrees) | Take Up Unit |
|---|---|---|
| 16 | 90 | 1 |
| 40 | 60 | 1 |
| 90 | 30 | 2 |
| 160 | 60 | 2 |
| 242 | 60 | 3 |
| 476 | 60 | 4 |
| 484 | 60 | 4 |
| 493 Op 1 | 120 | 4 |
| 493 Op 2 | 60 | 4 |
| 493 Op 3 | 60 | 4 |

Bus voltage maximum, minimum, SS ripple current, and SBA ripple voltage are given in Table 3-38. The peak and average power consumed by the SS for the various operating modes are given in Table 3-39.

TABLE 3-38

BUS VOLTAGE

| Parameter | Rev | Condition | Value | ICD |
|---|---|---|---|---|
| Voltage Maximum Observed | 484 | SBA Only | 30.81 | 33 |
| | | MFA On | 30.79 | 33 |
| | | OB Accel. | 30.11 | 33 |
| | | FT Accel. | 30.11 | 33 |
| | | P Mode | 30.06 | 33 |
| Voltage Minimum Observed | 493 | SBA Only | 30.5 | no req |
| | | FT Accel. | 29.4 | 24.0* |
| | | P Mode | 29.0 | 24.0 |
| Ripple Current Maximum | 16 | P Mode | 10.8 amps P-P | 25 amps P-P |
| Maximum Bus Ripple (SS Not Operating) | 484 | SBA Only | .05 V P-P | .250 P-P |
| | 476 | SBA Only | 3.5 Amp P-P | not specified |

*Including ripples.

TABLE 3-39

ON-ORBIT ELECTRICAL POWER REQUIREMENTS

| Condition/Status | Scan Angle (degrees) | Watts Peak Rev | Watts Peak Mission | Watts Peak ICD(max) | Watts Average Rev | Watts Average Mission | Watts Average ICD(max) |
|---|---|---|---|---|---|---|---|
| PNU, MFA Environments | - | 476 | 89 | 204 | 476 | 30 | 134 |
| Start | 30 | 90 | 786 | 1587 | - | - | 1300 |
| | 60 | 476 | 891 | 1634 | 40 | 648 | 1340 |
| | 90 | 16 | 975 | 1664 | - | - | 1380 |
| | 120 | 493 | 836 | 1770 | - | - | 1440 |
| Operate | 30 | 258 | 973 | 1638 | 258 | 801 | 1380 |
| | 60 | 476 | 904 | 1713 | 476 | 787 | 1440 |
| | 90 | 16 | 1076 | 1729 | 16 | 917 | 1460 |
| | 120 | 493 | 905 | 1820 | 493 | 776 | 1551 |

TABLE 3-39 (CONT'D)

ON-ORBIT ELECTRICAL POWER REQUIREMENTS

| Condition/Status | Scan Angle (degrees) | Rev | Watts Peak Mission | Watts Peak ICD(max) | Rev | Watts Average Mission | Watts Average ICD(max) |
|---|---|---|---|---|---|---|---|
| Stop | 30 | 258 | 873 | 1889 | - | - | 1542 |
| | 60 | 40 | 1031 | 1889 | - | 710 | 1547 |
| | 90 | 16 | 1115 | 1889 | 16 | 887 | 1564 |
| | 120 | 493 | 891 | 1943 | - | - | 1589 |
| Standby | - | 493 | 706 | 1135 | - | NA | NA |

Since available data was not sufficient to compute peak and average power for both beginning and end of mission, available numbers are compared with the maximum ICD values only. All measured values are within the ICD and therefore no violations of the ICD at maximum values of Vx/h occurred.

### 3.12.3 Interface Specifications (ICDs 1420316, 1420357)

A check of telemetry temperature data in regards to compliance with the thermal interface specifications was conducted at several selected points in the mission.

Table 3-40 compares flight data results and interface temperature requirements for a typical day during the mission. The table shows most of the temperature requirements are being satisfied with margins considered more than adequate. The spatial variations of temperatures in the Two Camera Assembly (TCA) Forward bulkhead and SU zones 1 and 5 were close to and in some cases exceed the ICD values. These slight violations of the ICD are not considered to be significant.

Figure 3-47 plots significant Mid-section temperatures occurring during a 30 day period. The thermal environment provided by the SBA to the SS was very close to a mean temperature of 70-F, the nominal value, throughout the mission.

### 3.12.4 Structural Environments (ICDs 1420314 and 1420361)

The evaluation of the structural load resulting from the ascent environment, pyro shock at shroud separation, and take up separation and recovery was severely curtailed by the lack of useful TM data. As a result, only a qualitative assessment of the questionable areas could be accomplished.

The absence of any film path problems which could have had any connection with film path alignment, and the lack of pressure or light leaks is substantial evidence that the structure was not over-stressed.

The supply and supply steerer performed properly throughout the mission.

The survival of the Take up Beryllium shafts through both air and water recovery has alleviated the concern whether or not the shafts would stand the recovery stress.

TABLE 3-40

THERMAL INTERFACE COMPLIANCE

REV 189.9

| | Item | Zone | Interface Requirement (°F) | Flight | Margin (°F) |
|---|---|---|---|---|---|
| | $\bar{\bar{T}}_{TCA} - \bar{\bar{T}}_{SU}$ | | ±6 | 2.0 | 4.0 |
| | $\bar{\bar{T}}_{TCA} - \bar{\bar{T}}_{FS}$ | | ±20 | 2.5 | 17.5 |
| TCA | $\bar{\bar{T}}_{TCA}$ | | 70 ± 21 | 72.1 | 18.9 |
| TCA | Variation of Mean Temp Between Zones | 1-4 | 9 | 4.9 | 4.1 |
| | | 2-3 | 6 | 4.6 | 1.4 |
| | | 1-2, 3-4 | 4 | 2.2, 2.5 | 1.8, 1.5 |
| | | Blk'd to Blk'd | 6 | 2.8 | 3.2 |
| TCA | Variation of Average Temp Within a Zone | 1,4 | 11 | 7.9, 4.1 | 3.1, 6.9 |
| | | 2,3 | 9 | 5.4, 5.3 | 3.6, 3.7 |
| | | Fwd Blk'd | 5 | 4.4 | 0.6 |
| | | Mid Blk'd | 17 | 12.9 | 4.1 |
| TCA | Peak to Valley Time Temp Variation Within a Zone | 1,4 | 46 | 12.0, 15.0 | 34.0, 31.0 |
| | | 2,3 | 20 | 2.0, 2.0 | 18.0, 18.0 |
| | | Fwd Blk'd | 26 | 4.0 | 22.0 |
| | | Mid Blk'd | 57 | 17.0 | 40.0 |
| SU | $\bar{\bar{T}}_{SU}$ | | 70 ± 23 | 74.1 | 18.9 |
| SU | Variation of Mean Temp Between Zones | 1-4 | 57 | 33.7 | 23.3 |
| | | 2-3 | 30 | 19.5 | 10.5 |
| | | 1-2, 3-4 | 16 | 5.8, 8.4 | 9.2, 7.6 |
| | | Blk'd to Blk'd | 4 | 1.2 | 2.8 |
| | | 2-5, 3-5 | 16 | 9.8, 9.7 | 6.2, 6.3 |
| SU | Variation of Average Temp Within a Zone | 1,4 | 19 | 20.5, 2.5 | -1.5, 16.5 |
| | | 2,3 | 11 | 6.1, 2.1 | 4.9, 8.9 |
| | | 5 | 1 | 0.2 | 0.8 |
| | | Aft Blk'd | 35 | 22.1 | 12.9 |
| SU | Peak to Valley Time Temp Variation Within a Zone | 1,4 | 128 | 44.0, 64.0 | 84.0, 64.0 |
| | | 2,3 | 47 | 3.0, 8.0 | 44.0, 39.0 |
| | | 5 | 16 | 1.0 | 15.0 |
| | | Aft Blk'd | 53 | 13.0 | 40.0 |
| FS | $\bar{\bar{T}}_{FS}$ | | 70 ± 23 | 74.6 | 18.4 |
| FS | Max Variation of Mean Temp. Between RV Zones | 4-3(RV-4) | 50 | 9.4 | 40.6 |
| | Max. Path ΔT | | 12 | 0.2 | 11.8 |

FIGURE 3-47

MISSION 1201 THERMAL PERFORMANCE

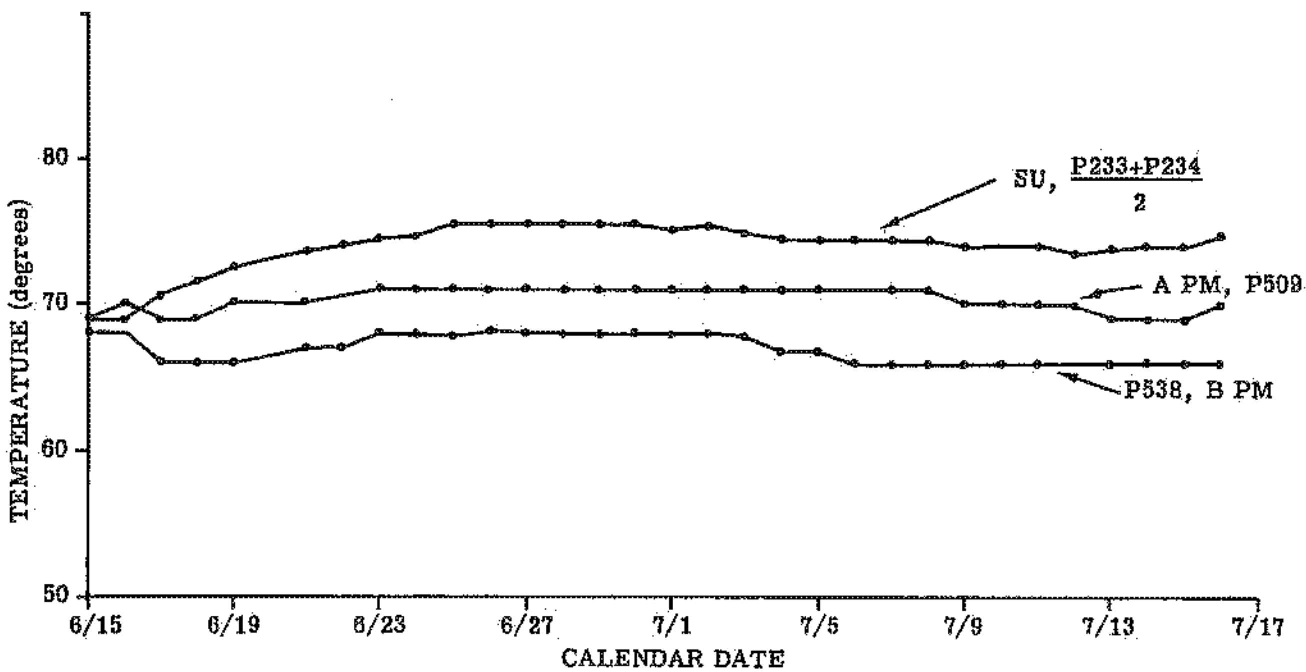

3.12.5 Mass Properties and Attitude Disturbances (ICDs 1420313, 1420317, 1420358)

The flight diagnostic data allows an evaluation of three areas of concern under the general topic of mass properties and attitude disturbance. These areas are the Take up film load, sensor generated disturbances, and SV attitude control. The details of the analyses are contained in the following sections with the result that all performance is well within the ICD requirements.

3.12.5.1 Take Up Film Load Accuracy

The amount of film on each Take up was predicted prior to recovery both by monitoring the Take up radius measurement, and by integrating the footage moved by the metering capstan. The predictions were compared with the film footage and weight removed from the Take up after recovery. The values are given in Table 3-41 which shows that the ICD value of ±4.3 pounds was not met in one case. The "as measured" weight is suspect as several individual weighings are required to determine the film weight. Further a procedural error is suspected for RV-2.

3.12.5.2 Sensor Generated Disturbance

The objective of this analysis is to compare the performance criteria specified in the disturbance ICD for mechanically induced disturbances, with equivalent disturbance calculations made using TM performance data. Specifically the disturbance criteria checked out in the ICD include the mechanical disturbance characteristics that can be checked out using TM records over the limited time range of the test sample. The calculated disturbances are assumed to be caused by the five largest momentum producing system components and are categorized for ICD comparison purposes as follows:

A. SU disturbances

B. TU disturbances

C. TCA disturbances (Optical Bar, Platen, and Looper)

These disturbances are calculated using assumed mass property characteristics for each component, and real time TM data on the velocity history of each component during the test sample. This is done using the Vehicle Disturbance Program (VDP) which calculates for each component and the sum for the Forward and Aft Cameras, periodic force and torque, acceleration torque, and torque about the Center of Gravity (CG) caused by the periodic force. From these calculations of the ICD specified criteria for steady operation, i.e., unbalanced momentum fluctuations, periodic torque and momentum fluctuations for start/stop operation.

3.12.5.3 Selected Performance Tapes

The data selected for analysis is listed in Table 3-42.

TABLE 3-41

TAKE UP FILM LOAD ACCURACY

| Take up Camera | TM Data Radius Measurement (inches) | Radius Pred Weight (pounds) | Measured Weight (pounds) | Error (pounds) | MC TM Data Length of Film (feet) | MC Pred Weight (pounds) | Error (pounds) |
|---|---|---|---|---|---|---|---|
| RV-1/Fwd | 15.16 | 160.0 | 161.0 | -1.0 | 20,469 | 160.4 | -0.6 |
| RV-1 Aft | 14.99 | 155.6 | 158.0 | -2.4 | 20,033 | 156.2 | -1.8 |
| RV-2 Fwd | 16.60 | 206.4 | 207.0 | -0.6 | 26,094 | 204.5 | -2.5 |
| RV-2 Aft | 16.56 | 205.0 | 211.0 | +6.0 | 26,164 | 204.0 | -7.0* |
| RV-4 Fwd | 12.88 | 99.5 | 104.0* | -4.8 | 13,044 | 102.2 | -2.1 |
| RV-4 Aft | 12.89 | 99.5 | 100.0 | -0.3 | 12,753 | 99.5 | -0.3 |

*Measurement procedures are suspect.

TABLE 3-42

DATA CYCLES FOR DISTURBANCE ANALYSIS

| Tape | Rev | Take up | Cycles | Description |
|---|---|---|---|---|
| MT1181 | 16 | 1 | 1-30 | Stereoscopic start-up with photographic mode. |
| 0399 | 497 | 4 | 275-292 | Monoscopic shutdown. |

The disturbance data obtained from these runs is compared with the ICD specification for mono and stereo performance shown in Tables 3-43 and 3-44.

TABLE 3-43

ICD REQUIREMENTS FOR STEREOSCOPIC OPERATION

| Mode | Description (Units) | ICD Paragraph | ICD Requirements Roll | Pitch | Yaw |
|---|---|---|---|---|---|
| STEADY | Unbalance Momentum (ft lbs sec) | 3.2.2 | 6 | 32 | 20 |
| | Momentum Flux (ft lbs sec) | 3.2.3 | 1.4 | 16.5 | 22 |
| | Periodic Force SU (lb) | 3.2.4 | - | - | 2.06 |
| | Periodic Force TU (lb) | 3.2.4 | 0.96 | - | - |
| | Periodic Force TCA (lb) | 3.2.4 | 2.50 | - | 0.42 |
| | Periodic Torque SU (lb ft) | 3.2.5 | 1.44 | 8.67 | - |
| | Periodic Torque TCA (lb ft) | 3.2.5 | 3.85 | 0.80 | - |
| | Low Frequency Torque (lb ft) | 3.2.8 | 0.02 | 0.12 | 0.02 |
| START | Total Torque (lb ft) | 3.2.6 | 0.5 | 2.5 | 1.6 |
| | Torque SU (lb ft) | 3.2.6 | - | 2.5 | - |
| | Torque TU (lb ft) | 3.2.6 | - | 0.3 | - |
| | Torque TCA (lb ft) | 3.2.6 | 0.5 | - | 1.6 |
| STOP | Total Torque (lb ft) | 3.2.6 | 16.8 | 2.5 | 4.1 |
| | Torque SU (lb ft) | 3.2.6 | - | 2.5 | - |
| | Torque TU (lb ft) | 3.2.6 | - | 0.3 | - |
| | Torque TCA (lb ft) | 3.2.6 | 16.8 | - | 4.1 |
| START/STOP | Momentum Flux SU (ft lbs sec) | 3.2.6 | - | 7.3 | - |
| | Momentum Flux TU (ft lbs sec) | 3.2.6 | - | 6.6 | - |
| | Momentum Flux TCA (ft lbs sec) | 3.2.6 | 1.2 | - | 0.2 |

NOTE: All start/stop mode values are specified within a 0.6 second interval.

TABLE 3-44

ICD REQUIREMENTS FOR STEREOSCOPIC OPERATION

| Mode | Description (Units) | ICD Paragraph | ICD Requirements Roll | Pitch | Yaw |
|---|---|---|---|---|---|
| STEADY | Unbalance Momentum (ft lbs sec) | 3.2.2 | 55 | 280 | 10 |
| | Momentum Flux (ft lbs sec) | 3.2.3 | 1.6 | 8.2 | 1.1 |
| | Periodic Force SU (lb) | 3.2.4 | | - | 1.03 |
| | Periodic Force TU (lb) | 3.2.4 | 0.48 | - | - |
| | Periodic Force TCA (lb) | 3.2.4 | 1.25 | - | 0.21 |
| | Periodic Torque SU (lb ft) | 3.2.5 | 0.72 | 7.16 | - |
| | Periodic Torque TCA (lb ft) | 3.2.5 | 3.15 | 0.40 | - |
| | Low Frequency Torque (lb ft) | 3.2.8 | 0.03 | 0.10 | 0.12 |
| START | Total Torque (lb ft) | 3.2.6 | 5.0 | 20.0 | 1.0 |
| | Torque SU (lb ft) | 3.2.6 | - | 20.0 | - |
| | Torque TU (lb ft) | 3.2.6 | - | 2.5 | - |
| | Torque TCA (lb ft) | 3.2.6 | 5.0 | - | 1.0 |
| STOP | Total Torque (lb ft) | 3.2.6 | 16.8 | 20 | 3.0 |
| | Torque SU (lb ft) | 3.2.6 | - | 20 | - |
| | Torque TU (lb ft) | 3.2.6 | - | 2.5 | - |
| | Torque TCA (lb ft) | 3.2.6 | 16.8 | - | 3.0 |
| START/ STOP | Momentum Flux SU (ft lbs sec) | 3.2.6 | - | 7.3 | - |
| | Momentum Flux TU (ft lbs sec) | 3.2.6 | - | 6.0 | - |
| | Momentum Flux TCA (ft lbs sec) | 3.2.6 | 0.6 | - | 0.1 |

NOTE: All start/stop mode values are specified within a 0.6 second interval.

### 3.12.5.4 Mass Property Characteristics

Table 3-45 lists the assumed mass property and alignment characteristics. Path characteristics for both cameras are assumed identical with the spin axis misalignment for the Forward and Aft having opposite signs. Table 3-46 lists the vehicle CG and TU location where TU-1 and TU-4 are used in the test.

TABLE 3-45

ASSUMED FORWARD AND AFT CAMERA MASS PROPERTY CHARACTERISTICS

| Description (units) | Component | | | | |
|---|---|---|---|---|---|
| | Supply Unit | Take Up Unit | Optical Bar | Platen | Looper |
| Mass (lb $sec^2$/ft) | 1.5 | 0.8 | 17.18 | 0.758 | 0.077 |
| Inertia Principle (ft lb $sec^2$) | 2.05 | 0.35 | 16.77 | 0.08 | - |
| Product (ft lb $sec^2$) | 0.002 | 0.01 | 0.018 | 0 | 0 |
| Mass Offset Radial (inch) | 0.025 | 0.025 | 0.006 | 0.0015 | - |
| Offset Axial (inches) (Reference Axis) | 3.3 | 3.3 | 1.0 | 0.01 | 0.5 |
| Spin Axis Misalignment (radians) | ±0.0043 | ±0.0043 | ±0.00174 | ±0.00147 | ±0.003 |
| Orothogonal to Spin Axis (radians) | ±0.0029 | ±0.0029 | ±0.174 | ±0.174 | ±0.003 |

TABLE 3-46

CENTER OF GRAVITY AND TAKE UP

REFERENCE AXIS POSITIONS

| Description | Vehicle Axis Positions X | Y | Z | Test Rev |
|---|---|---|---|---|
| Vehicle CG Posn (TU-1) | 1993 | -0.2 | 2.9 | 16 |
| TU-1 Location A | 1676 | -4.55 | 24.9 | 16 |
| TU-1 Location B | 1676 | +4.55 | 24.9 | 16 |
| Vehicle CG Posn (TU-4) | 2024 | -0.4 | 1.4 | 497 |
| TU-4 Location A | 1871 | -4.55 | 24.9 | 497 |
| TU-4 Location B | 1871 | +4.55 | 24.9 | 497 |

#### 3.12.5.5 Analysis Result

The analysis results for the stereoscopic and monoscopic cases referenced in Table 3-42 are presented in Tables 3-47 and 3-48. The tables show the test results and are keyed to the ICD requirements shown in Tables 3-43 and 3-44. The test cycle column shows the beginning and end of the analyzed section of data.

A. Stereoscopic Start-up

Because the model has assumed equal Forward and Aft Camera inertias, the disturbance properties in general are lower than the requirements as shown by Table 3-47. The values noted by an asterisk designate those properties which calculated as lower, e.g., the total torque for roll and pitch during start-up is lower, and reflects the product of inertia effect on start-up. The total yaw torque, however, is dominated by the rate of change of the unbalanced OB yaw momentum vector. This value is near the ICD stated value.

B. P Mode

With reference to Table 3-47 the P mode terms show essentially the same results. The acceleration torques SU, TU, and OB are reduced small values, and the disturbance torque contributions are caused chiefly by the product of inertia and mass unbalance forces acting about the center of gravity.

TABLE 3-47

REV 16 TEST RESULTS OF SENSOR START-UP AND STANDBY OPERATIONS

| Mode | Description (units) | ICD Paragraph | ICD Requirements | | | Test Cycles | |
|---|---|---|---|---|---|---|---|
| | | | Roll | Pitch | Yaw | Begin | End |
| STEADY | Unbalance Momentum (ft lbs sec) | 3.2.2 | .30 | 6.12 | 14.5 | 14 | 18 |
| | Momentum Flux (ft lbs sec) | 3.2.3 | .08 | 2.01 | .14 | 14 | 18 |
| | Periodic Force SU (lb) | 3.2.4 | - | - | .15 | 14 | 18 |
| | Periodic Force TU (lb) | 3.2.4 | .051* | - | - | 14 | 18 |
| | Periodic Force TCA (lb) | 3.2.4 | .02 | - | .10 | 14 | 18 |
| | Periodic Torque SU (lb ft) | 3.2.5 | .06 | .80* | - | 14 | 18 |
| | Periodic Torque TCA (lb ft) | 3.2.5 | .10* | .30 | - | 14 | 18 |
| | Low Frequency Torque (lb ft) | 3.2.8 | 0 | 0 | 0 | 14 | 18 |
| START | Momentum Flux SU (ft lbs sec) | 3.2.6 | - | .02* | - | 8 | 12 |
| | Momentum Flux TU (ft lbs sec) | 3.2.6 | - | .46 | - | 8 | 12 |
| | Momentum Flux TCA (ft lbs sec) | 3.2.6 | .42 | - | 1.2 | 2 | 4 |
| | Total Torque | 3.2.6 | .06 | .9 | - | 8 | 12 |
| | Total Torque | 3.2.6 | - | - | 1.6 | 2 | 4 |
| | Torque SU (lb ft) | 3.2.6 | - | .62 | - | 8 | 12 |
| | Torque TU (lb ft) | 3.2.6 | - | .36 | - | 8 | 12 |
| | Torque TCA (lb ft) | 3.2.6 | .30 | - | .92 | 2 | 4 |

C. Monoscopic Shutdown

The monoscopic cases shown are shutdown with the Aft Camera operational while the Forward Camera is shutdown, see Table 3-48. These cases show 10% to 20% higher total pitch torque contributions than the specification allows. This conclusion is the result of calculations and not direct inflight measurement and is known to have been within the capability of the Attitude Control System (ACS) to accomodate. The momentum fluctuation terms in this case were difficult to access because of the large absolute value, and represent the best estimate away from the nominal shutdown transient value. In general, the vehicle disturbances caused by mono operation were much lower than expected.

TABLE 3-48

REV 497 SENSOR SHUTDOWN

| Mode | Description (units) | ICD Paragraph | ICD Requirements Roll | Pitch | Yaw | Test Cycles Begin | End |
|---|---|---|---|---|---|---|---|
| STEADY | Unbalance Momentum (ft lbs sec) | 3.2.2 | 32 | 22.4 | 6.0 | 270 | 270 |
| | Momentum Flux SU (ft lbs sec) | 3.2.6 | - | 3.0* | - | 278 | 282 |
| STOP | Momentum Flux TU (ft lbs sec) | 3.2.6 | - | .8* | - | 278 | 282 |
| | Momentum Flux TCA (ft lbs sec) | 3.2.6 | 1.3* | - | 1.0* | 278 | 282 |
| | Total Torque (lb ft) | 3.2.6 | 8.9 | 29.4 | 1.6 | 278 | 282 |
| | Torque SU (lb ft) | 3.2.6 | - | 29.4 | - | 278 | 282 |
| | Torque TU (lb ft) | 3.2.6 | - | 2.1 | - | 278 | 282 |
| | Torque TCA (lb ft) | 3.2.6 | 8.9 | - | 1.6 | 278 | 282 |

3.12.6 Satellite Vehicle Attitude Control

The ability of the ACS to maintain the vehicle attitude within the required bounds was evaluated for both monoscopic and stereoscopic operation. The ICD values and the largest errors of the orbits evaluated are given in Table 3-49. All measurements are well within the ICD constraints.

TABLE 3-49

SATELLITE VEHICLE ATTITUDE CONTROL

Fine Attitude Control

| Attitude Error | Spec Values (degrees) | Monoscopic Rev | Monoscopic Measured Value | Stereoscopic Rev | Stereoscopic Measured Value |
|---|---|---|---|---|---|
| Roll | ±0.70 | 497 | 0.118 | 493 (Op 2) | 0.125 |
| Pitch | ±0.70 | - | Horizon Sensor Out | 484 | 0.166 |
| Yaw | ±0.69 | 497 | 0.135 | 484 | 0.118 |

TABLE 3-49 (CONT'D)

SATELLITE VEHICLE ATTITUDE CONTROL

Satellite Vehicle Rates

| Attitude Error | Spec Values (degrees/sec) | Monoscopic | | Stereoscopic | |
|---|---|---|---|---|---|
| | | Rev | Measured Value | Rev | Measured Value |
| Roll | 0.021 | 497 | 0.009 | 16 | 0.0077 |
| Pitch | 0.014 | 497 | 0.009 | 493 (Op 3) | 0.0056 |
| Yaw | 0.014 | 497 | Date Days Out | 484 | 0.0112 |

The stereo rates were evaluated for 4 operations (Revs 16, 484, and 493-Ops 2 and 3).

3.12.7 Conclusions

A. Although some insignificant violations of requirements were observed specifically in the thermal area, the general result was that the ICD requirements are conservative.

B. With few minor exceptions, the data indicated that all SS thermal interface requirements were met.

3.12.8 Recommendations

A. It is recommended that the film load weighing technique be monitored and modified if necessary to improve accuracy of deriving the measured weight of the film load.

B. Although it was determined that the ICD requirements were conservative, no change to the ICDs is recommended because future flights may experience more severe environments than those encountered on Mission 1201.

C. It is recommended that a detailed analysis be undertaken to evaluate the Attitude Control System data to determine: (1) If the ICD limits are too stringent; and (2) What the mission duration would be if there were requirements to run the system for extended periods in the mono mode.

# Processing and Reproduction

# SECTION IV

# PROCESSING AND REPRODUCTION

## 4.1 INTRODUCTION

This section, prepared by the BRIDGEHEAD Processing Facility and AFSPPF, discusses defilming, processing/optical titling, and reproduction of the Mission 1201 original negatives. Defilming, processing/optical titling, and all Priority 1 and 2 reproduction requirements, except those for Target Complexes, were accomplished at BRIDGEHEAD. AFSPPF accomplished all Priority 3 requirements as well as the Priority 1 and 2 Target Complex requirements.

## 4.2 RECEIPT AND DEFILMING

### 4.2.1 Mission 1201-1

The shipping container and RV/TU arrived at the processing site in good condition on 21 June 1971. The back end of the RV showed the effect of some heating, but the ablative heat shield maintained the canister temperature at less than 100°F. One of the flapper doors was not latched and allowed some hot gas to leak around it. The second flapper door catches were pulled loose from the RV. Two loose RV shims were found in the canister. There was some salt water in the recesses in the base of the RV and mortar canister, but the film was dry.

The TU hub electronics were not damaged and the film stack was very good, allowing a rapid defilming operation. Minor anomalies were noted during defilming. A bump was present in the Forward roll about 8,400 feet from the tail, but it disappeared in a few feet. At the end of the Forward roll defilming operation, the film was pulled loose from the takeup core and the core pin engaged. A small, triangular-shaped piece of film was missing from the tail cut of the Aft roll. No static was noted during the defilming of either roll.

The Forward-looking Camera Record weighed 161 lbs. and the Aft-looking Camera Record weighed 158 lbs. Predicted weights from TM data were 160.8 lbs. for the Forward and 155.5 lbs. for the Aft.

### 4.2.2 Mission 1201-2

The shipping container and RV/TU arrived at the processing site in good condition on 27 June 1971. One of the flapper door latches had been removed. The TU hub electronics were undamaged and the film stack was very good. Static discharges occurred frequently throughout the Forward roll, necessitating a slower than normal defilming rate. No static was observed while defilming the Aft roll. A gritty substance was felt on the base side of both rolls. This occurred at approximately 9,600 feet from the tail of the Forward roll and at approximately 15,000, 20,000 and 22,000 feet from the tail of the Aft roll. Similar to 1201-1, there was a small triangular-shaped piece of film missing from the tail cut of the Aft roll.

The Forward-looking Camera Record weighed 207 lbs. and the Aft-looking Camera Record weighed 211 lbs. These weights may be incorrect because of a suspected error in the weighing operatio for RV-2. Predicted weights from TM were 204.6 lbs. for the Forward and 204.1 lbs. for the Aft.

4.2.3 Mission 1201-3

Not recovered.

4.2.4 Mission 1201-4

The shipping container and RV/TU arrived at the processing site in good condition, with only a small dent in the shipping container, on 17 July 1971. It was necessary to clean foreign material from the holes for one of the guide pins on the A side, -X axis. Three small pieces of film were found in the cutter seals, and scored and torn film was encountered at the tail cuts of each roll. The Aft roll tears were similar to those on the Aft roll of 1201-2. The core-locking pin on the Aft side would not lock out a the jamming nut on the core-locking tool was used to hold the pin. Both film stacks were good with only few wraps sticking out slightly from each roll. No static was noted during the defilming of either roll.

The Forward-looking Camera Record weighed 104 lbs. and the Aft-looking Camera Record weighed 100 lbs. Predicted weights from TM were 101.8 lbs. for the Forward and 98.9 lbs. for the Aft.

4.3 PROCESSING/OPTICAL TITLING

4.3.1 Mission 1201-1

4.3.1.1 Processing Data

Irregular tears and emulsion pickoffs occurred on Op 64, Frames 004 and 005 of the Forwa Camera Record as the film was being despooled from the transport dolly into the processor. Two convo tions of film were stuck together as a result of contact with moisture during defilming. The moisture apparently originated from external recesses of the RV at the start of the defilming operation. All other processing was accomplished without incident.

TABLE 4-1

PROCESSING DATA, RV-1

| | Forward | Aft |
|---|---|---|
| Processor | Yardleigh 5 | Yardleigh 6 |
| Developer | Dual Gamma(16DN) | Dual Gamma(16DN) |
| Operational Frames | | |
| 30° Scan | 12 | 12 |
| 60° Scan | 602 | 601 |
| 90° Scan | 1,085 | 1,085 |
| 120° Scan | 346 | 346 |
| Totals | 2,045 | 2,044 |

TABLE 4-1 (CONT'D)

PROCESSING DATA, RV-1

| | Forward | Aft |
|---|---|---|
| Footage | | |
| Thread-up | 0 | 0 |
| Preflight | 1,730 | 1,295 |
| Operational | 18,584 | 18,602 |
| Manufacturing Splices | 12 | 15 |

4.3.1.2 Optical Titling

The Optical Titling System operated successfully on both records and over 99% of the frame were titled completely. Some spurious and early frame marks were encountered but they did not interfer with optical titling.

The reinforcing tape that is added to manufacturing splices during the defilming operation caused titles to be partially obscured on one frame and inhibited on another. In each case, the titling wa corrected manually.

4.3.2 Mission 1201-2

4.3.2.1 Processing Data

A processor-induced emulsion scratch occurred on the Aft Camera Record, beginning with ( 64, Frame 012 and ending, after corrective action was taken, on Op 67, Frame 057. No other difficultie were encountered during processing.

TABLE 4-2

PROCESSING DATA, RV-2

| | Forward | Aft |
|---|---|---|
| Processor | Yardleigh 5 | Yardleigh 6 |
| Developer | Dual Gamma(16DN) | Dual Gamma(16DN) |
| Operational Frames | | |
| 30° Scan | 979 | 979 |
| 60° Scan | 739 | 739 |
| 90° Scan | 1,751 | 1,751 |
| 120° Scan | 94 | 94 |
| Totals | 3,563 | 3,564 |
| Footage | | |
| Thread-up | 0 | 0 |
| Preflight | 0 | 0 |
| Operational | 25,930 | 25,978 |
| Manufacturing Splices | 20 | 17 |

4.3.2.2 Optical Titling

The Optical Titling System operated successfully on both records and over 99% of the frames were titled completely. Spurious and early frame marks were encountered, however, and affected titling in several instances. On one frame of the Forward Record and six frames of the Aft, early frame marks occurred during the first five frames of an op. Titling was inhibited for one frame in five of these instances because the full capability of the software to ignore spurious and early frame marks is not established until after the first five frames of each op. The other two early frame marks occurred in consecutive frames and caused the titling of the second frame to be misplaced. Whenever titling was inhibited or misplaced, the appropriate title was added manually. The other instances of spurious and early frame marks did not affect optical titling.

The first frame of the Forward Record was Frame 009 of Op 64 rather than Frame 008 as expected. Consequently, all nine frames of Op 64 received incorrect frame numbers which had to be erased and manually added. A similar discrepancy was anticipated on the Aft Record, so the frame numbers were inhibited during optical titling and added manually later.

The reinforcing tape added to manufacturing splices caused titles to be inhibited or partially obscured on eight frames. In each case, the titling was corrected.

4.3.3 Mission 1201-3

Not recovered.

4.3.4 Mission 1201-4

4.3.4.1 Processing Data

Processing of both camera records was accomplished without incident.

TABLE 4-3

PROCESSING DATA, RV-4

| | Forward | Aft |
|---|---|---|
| Processor | Yardleigh 5 | Yardleigh 6 |
| Developer | Dual Gamma(16DN) | Dual Gamma(16DN) |
| Operational Frames | | |
| 30° Scan | 24 | 24 |
| 60° Scan | 409 | 403 |
| 90° Scan | 510 | 424 |
| 120° Scan | 401 | 459 |
| Totals | 1,344 | 1,310 |
| Footage | | |
| Thread-up | 0 | 0 |
| Preflight | 0 | 0 |

TABLE 4-3 (CONT'D)

PROCESSING DATA, RV-4

| | Forward | Aft |
|---|---|---|
| Footage (Cont'd) | | |
| Operational | 12,945 | 12,697 |
| Manufacturing Splices | 8 | 7 |

4.3.4.2 Optical Titling

The Optical Titling System operated successfully on both records and 99% of the frames were titled completely. Spurious and early frame marks were encountered, but only a spurious frame mark at the start of Op 384 (Forward) affected optical titling. Titling was inhibited on three frames and later adde manually. One frame was incorrectly titled because an op not called for in the roadmap was present. It was corrected manually. Several frames of the Aft Record were either not titled or only partially titled as synchronization was reestablished in the portion affected by the ESD. Again, the titles involved were completed manually.

The reinforcing tape caused titles to be inhibited or partially obscured on five frames. In each case, corrections were made. On seven frames of the Forward Record, the binary data block is missing from the title because of a hardware problem. These binary blocks were not added manually.

4.3.5 Sensitometry

Sensitometric exposures are used to establish and maintain process control. In the case of the original camera films, flight roll film samples are evaluated prior to mission arrival so that process conditions can be adjusted, if necessary. This technique is followed to obtain the optimum photographic speed with reasonable fog for the particular batch of flight film involved. The mission records are then processed under these adjusted conditions with additional flight roll sensitometric strips attached. Sensitometric curves from these strips are shown in Figures 4-1 thru 4-6 for each RV and are most representative of the sensitometry of the flight film.

## 4.4 REPRODUCTION AT BRIDGEHEAD

### 4.4.1 Breakdown

After processing, the original negative was "broken down" according to the Geographic Area covered. For Mission 1201 there were 18 Geographic Areas designated in the world and the coverage (ops frames) for each area was spliced together to form composite rolls (aprx 450 feet long). Duplicate copies for each customer were then prepared according to their requirements for each Geographic Area.

### 4.4.2 Regular Duplication

4.4.2.1 Duplicate Positives

All of the regular duplicate positive copies of complete composite rolls for customers in

TCS 354016-71

POST FLIGHT ANALYSIS REPORT
1201

## 1201-1 FORWARD CAMERA SENSITOMETRIC CURVE FROM MISSION MATERIAL

### FILM TYPE 1414-8-19

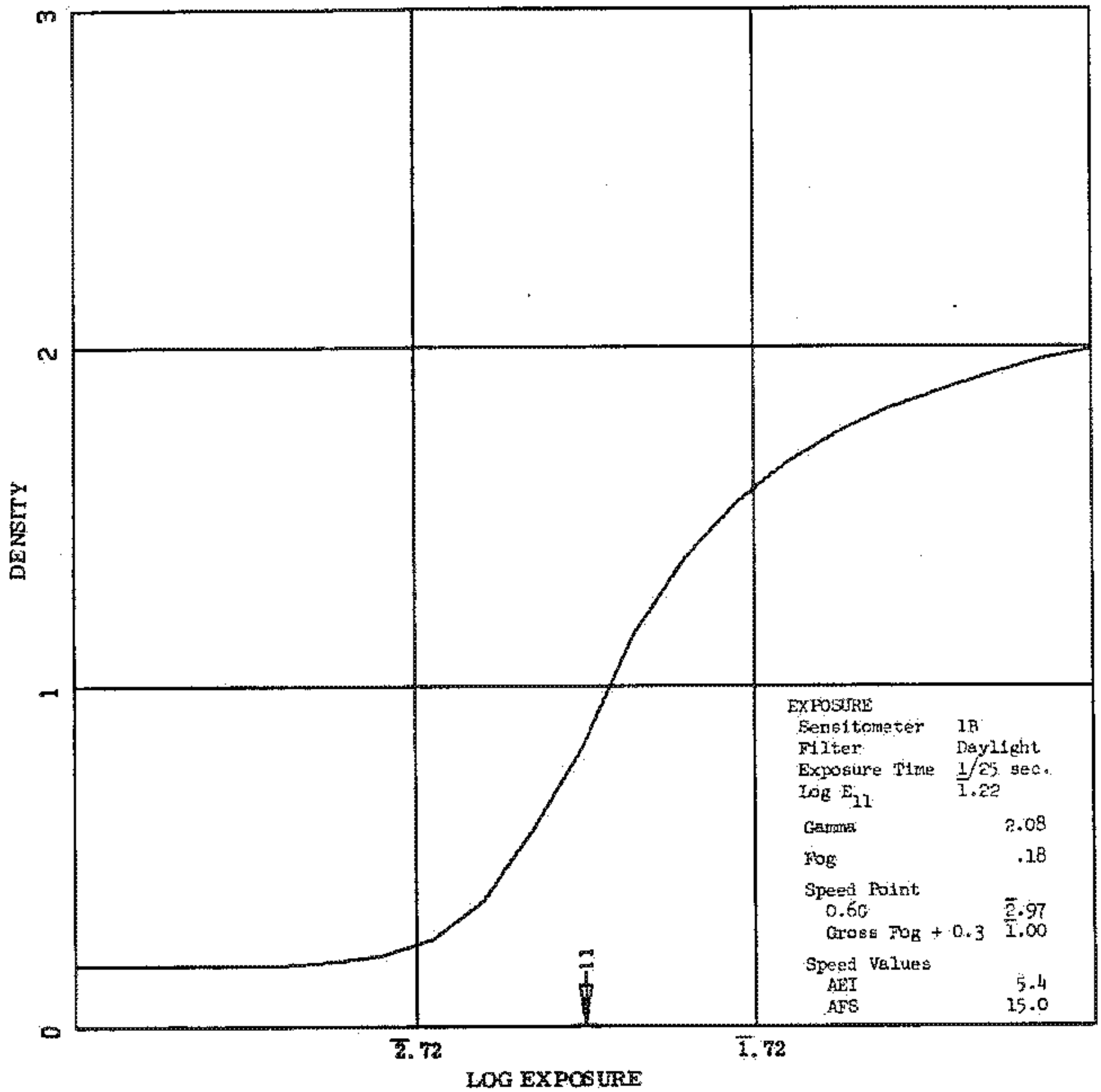


FIGURE 4-1

TCS 354016-71

POST FLIGHT ANALYSIS REPORT
1201

## 1201-1 AFT CAMERA SENSITOMETRIC CURVE FROM MISSION MATERIAL

FILM TYPE 1414-8-3

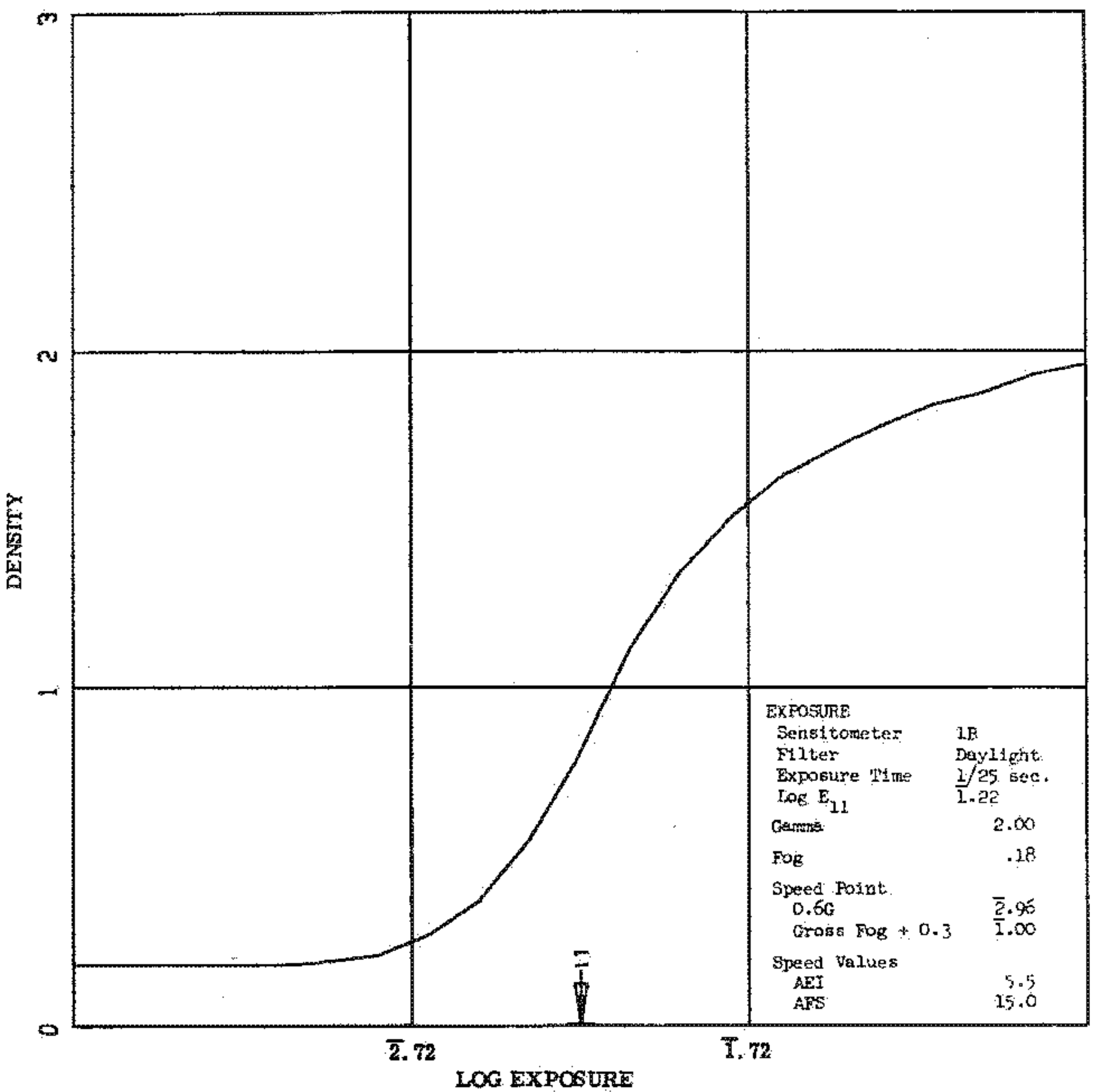


FIGURE 4-2

1201-2 FORWARD CAMERA SENSITOMETRIC CURVE FROM MISSION MATERIAL

FILM TYPE 1414-8-19

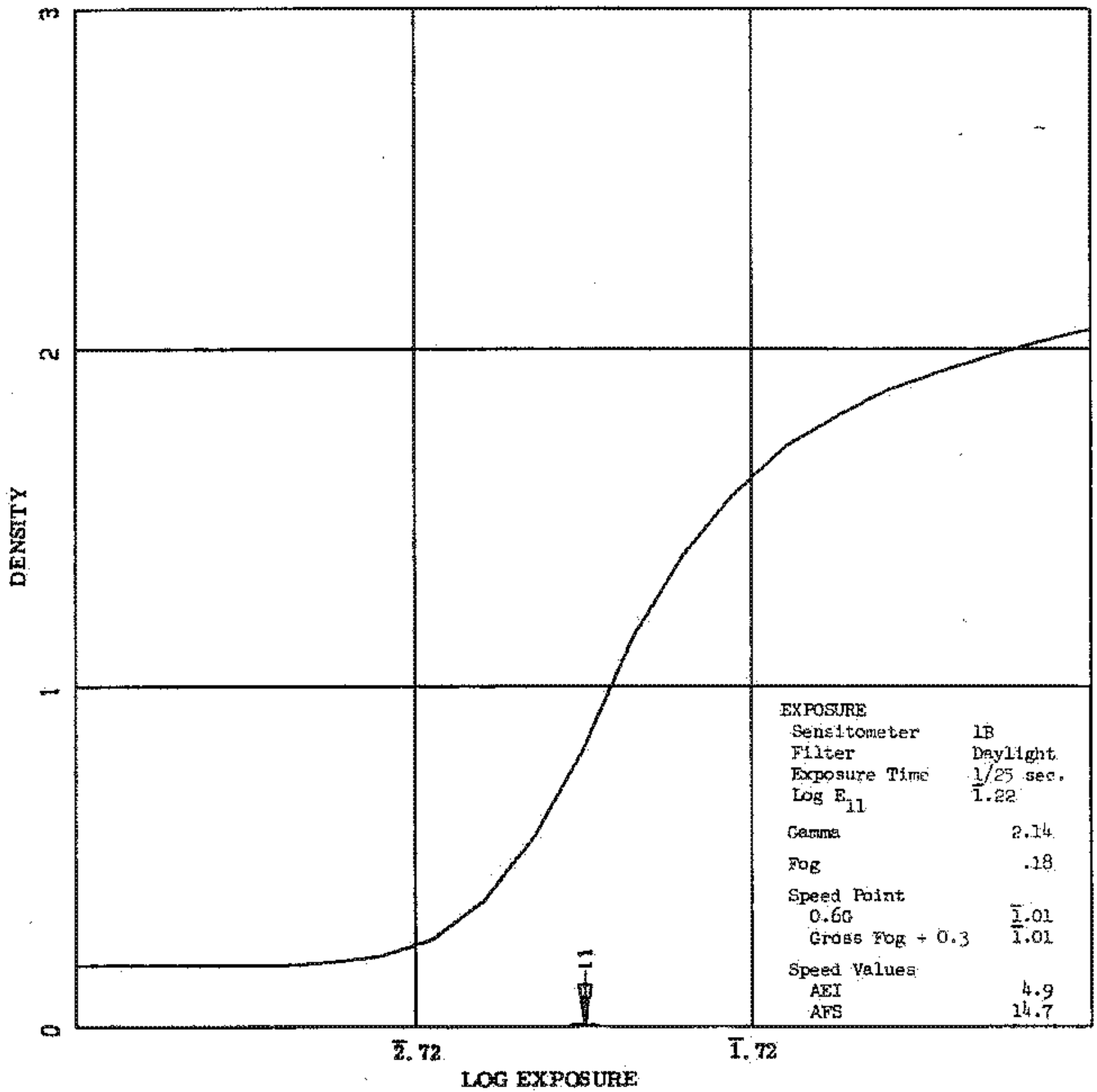


FIGURE 4-3

## 1201-2 AFT CAMERA SENSITOMETRIC CURVE FROM MISSION MATERIAL

### FILM TYPE 1414-8-3

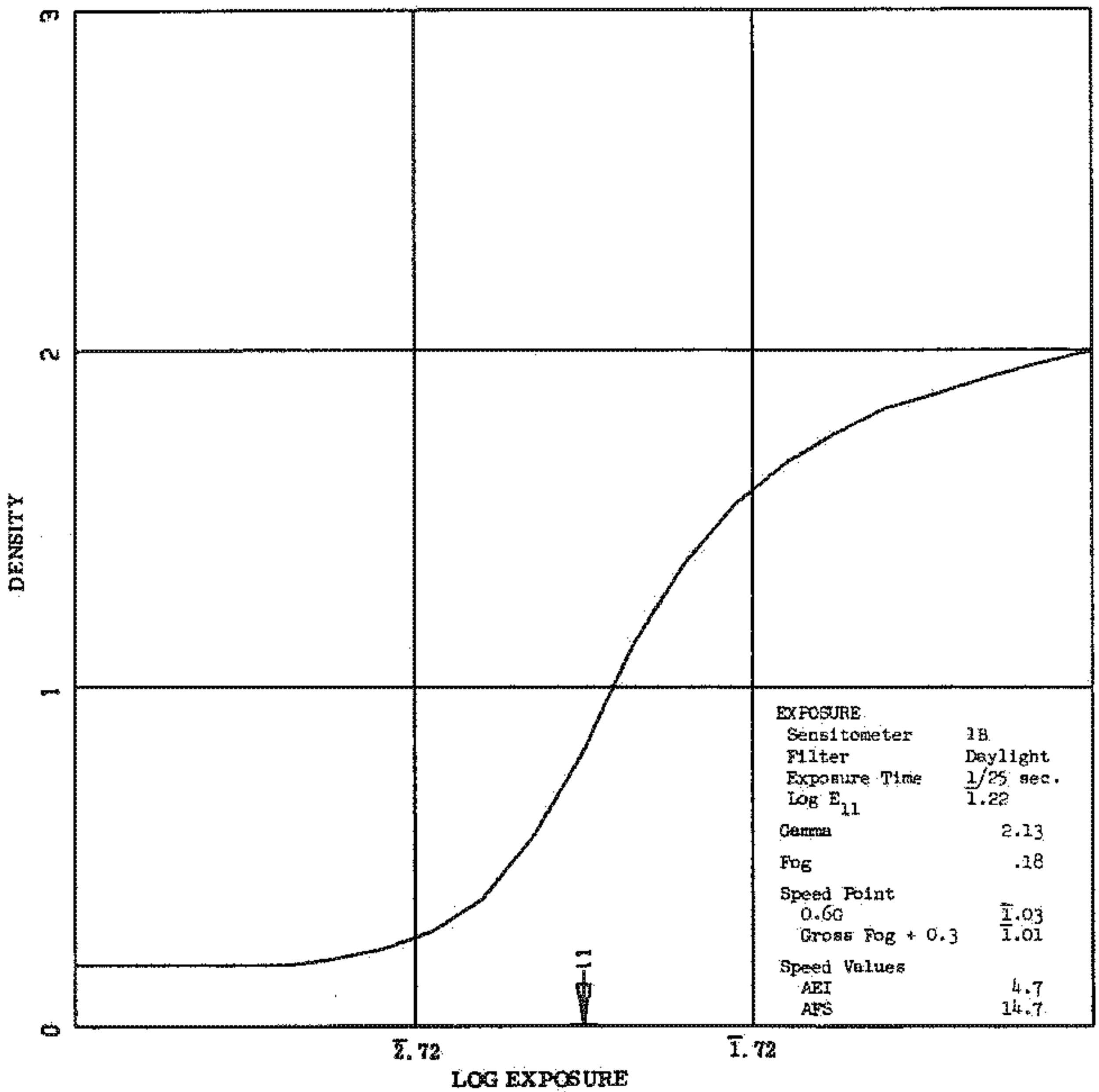


FIGURE 4-4

### 1201-4 FORWARD CAMERA SENSITOMETRIC CURVE FROM MISSION MATERIAL

### FILM TYPE 1414-8-19

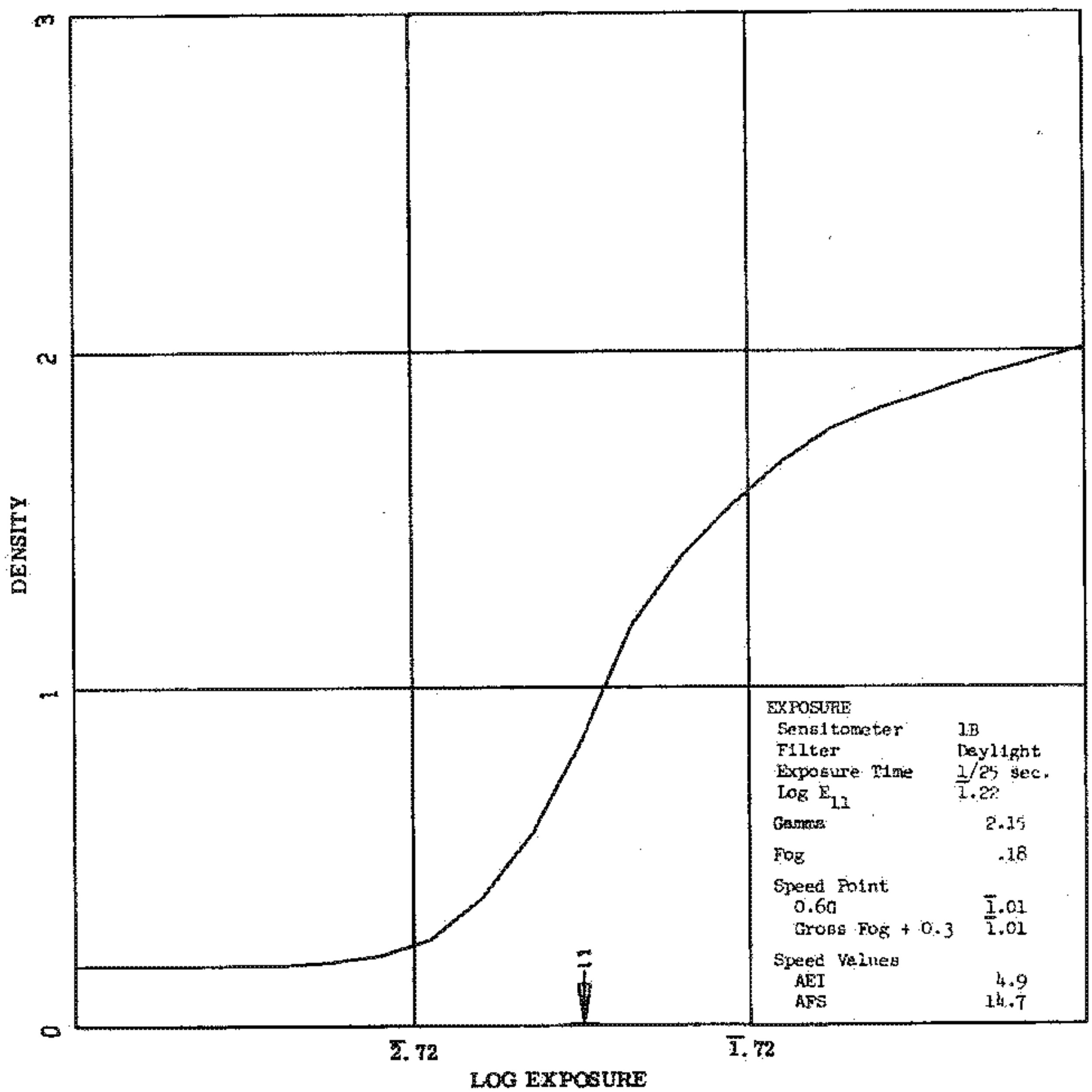


FIGURE 4-5

TCS 354016-71

POST FLIGHT ANALYSIS REPORT
1201

## 1201-4 AFT CAMERA SENSITOMETRIC CURVE FROM MISSION MATERIAL

### FILM TYPE 1414-8-3

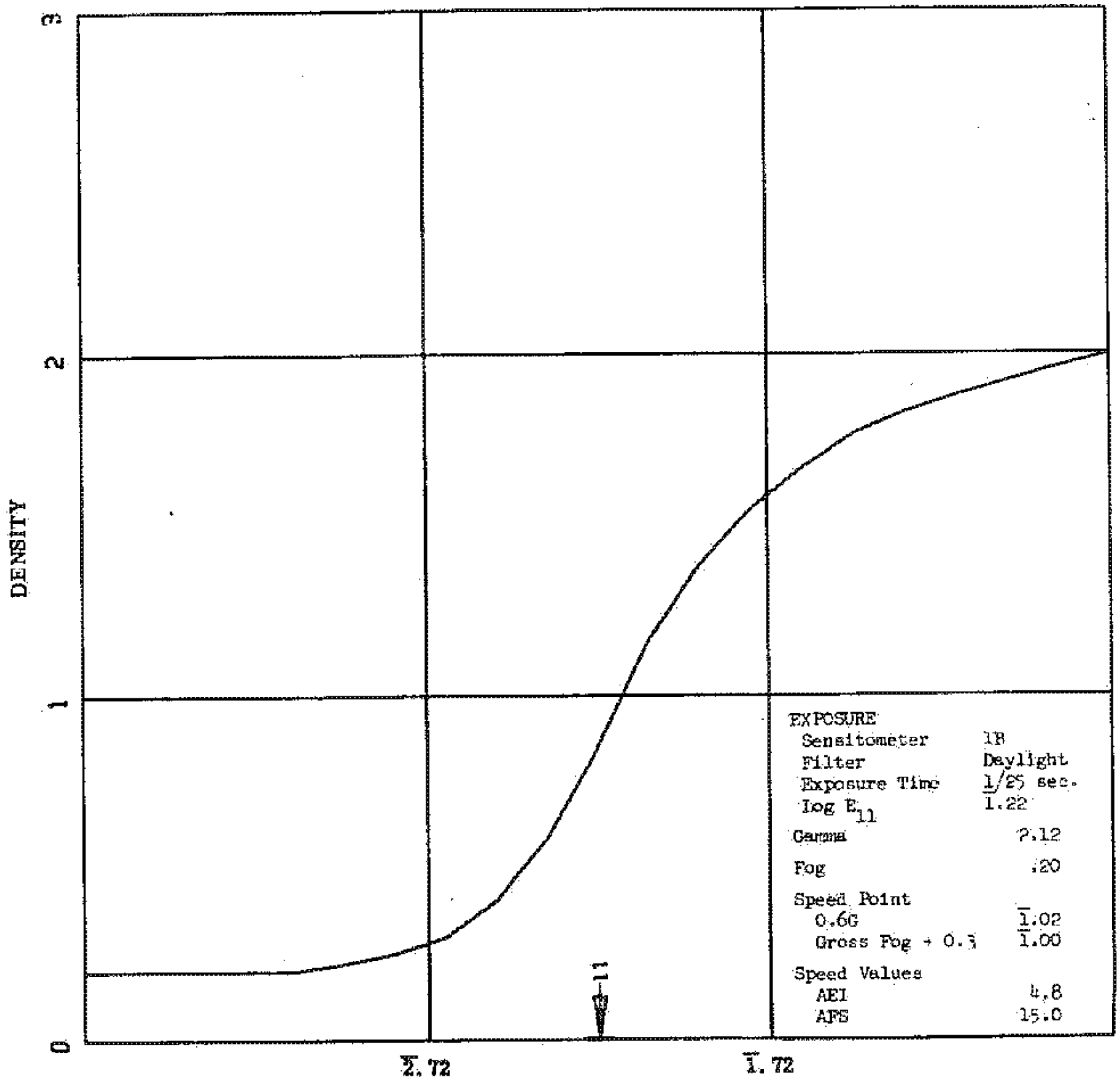


FIGURE 4-6

Priorities 1 and 2 (NPIC, DIA, CIA/IAS and SAC) were prepared using Kodak High Resolution Aerial Duplicating Film (Estar Base) SO-192. This film was processed to a low contrast in the viscous mode to provide a system sensitometry suitable for reproducing entire composite rolls, see Figure 4-7. Niagara Printer settings were selected to return the original negative densities of each op/area part between 0.40 and 1.75. When the input density range was too great to be returned between the desired limits on a singl "medium" print, two or three levels were utilized, generating "multiple prints" ("light", "medium", and/ or "dark" copies). Multiple prints were required as follows:

| Mission | Percentage of Parts* Multiple Printed |
|---|---|
| 1201-1 | 1.2 |
| 1201-2 | 3.0 |
| 1201-4 | 0.0 |

NOTE: These percentages are lower than expected because of the generally narrow density range encountered on the 1201 original negatives.

4.4.2.2 Duplicate Negatives

All duplicate negative copies of the mission records were prepared using Kodak Direct Duplicating Aerial Film (Estar Base) SO-239, processed in the spray mode, see Figure 4-8. Niagara Printer settings were selected to return the adjusted minimum density (average of three lowest Dmins for each op/area part) to 0.40. If the Dmax for the part then exceeded 1.70, a second "light" print was provided to reduce the density in areas of heavy exposure. Light prints were required as follows:

| Mission | Percentage of Parts* Printed Light |
|---|---|
| 1201-1 | 2.5 |
| 1201-2 | 9.5 |
| 1201-4 | 0.0 |

*Excluding Area 5A (Noforn) material which is not multiple printed.

4.4.3 Single Light Duplicates

To provide duplicate positives for PFA and NPIC Team evaluations as quickly as possible, "sing light" copies were provided. These copies are printed before each "machine-cut" of approximately 1,30 feet is broken down into Geographic Area parts. Each entire machine-cut was printed onto SO-192 at a single printer setting, see Figure 4-7; thus, the terminology of "single light". After the PFA and NPIC Teams were finished with these copies, they were shipped to NPIC and TOPOCOM, respectively.

4.4.4 Specialized Duplication

Specialized duplication techniques were employed for selected low contrast target areas of particular interest as identified by the NPIC "Tiger" Team. Two films, providing different contrast levels for expanding the original negative density range, were used; Kodak Minicard Film 6451 and Koda High Resolution Aerial Duplicating Film SO-192 (spray processed to high contrast). The system sensi-

TONE REPRODUCTION CURVES

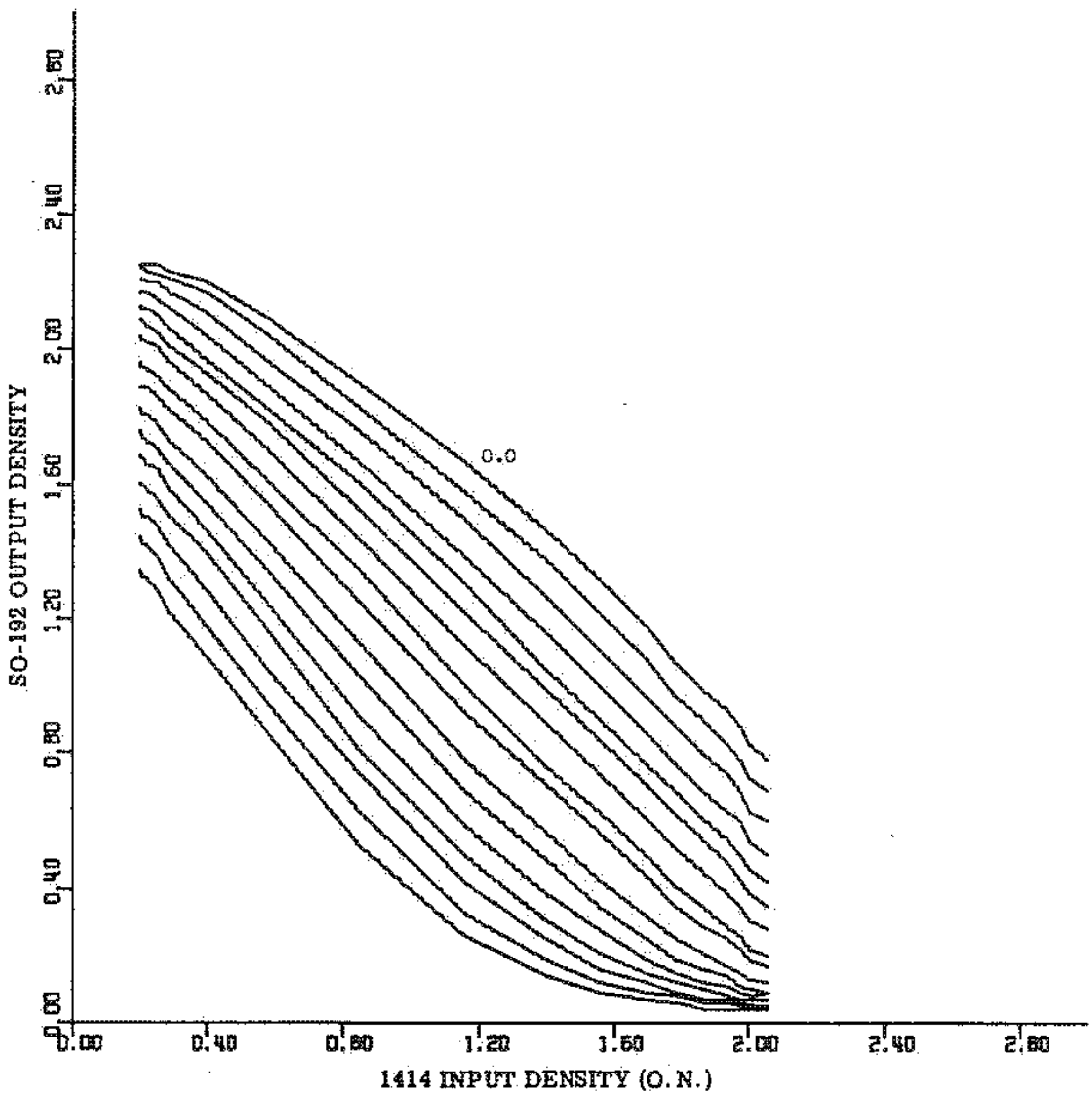


NOTES:

1. Niagara Printer settings 0.0 to 1.5.
2. Input data Film Type 1414.
3. Output data Film Type SO-192 (viscous processed, low contrast).

FIGURE 4-7

TONE REPRODUCTION CURVES

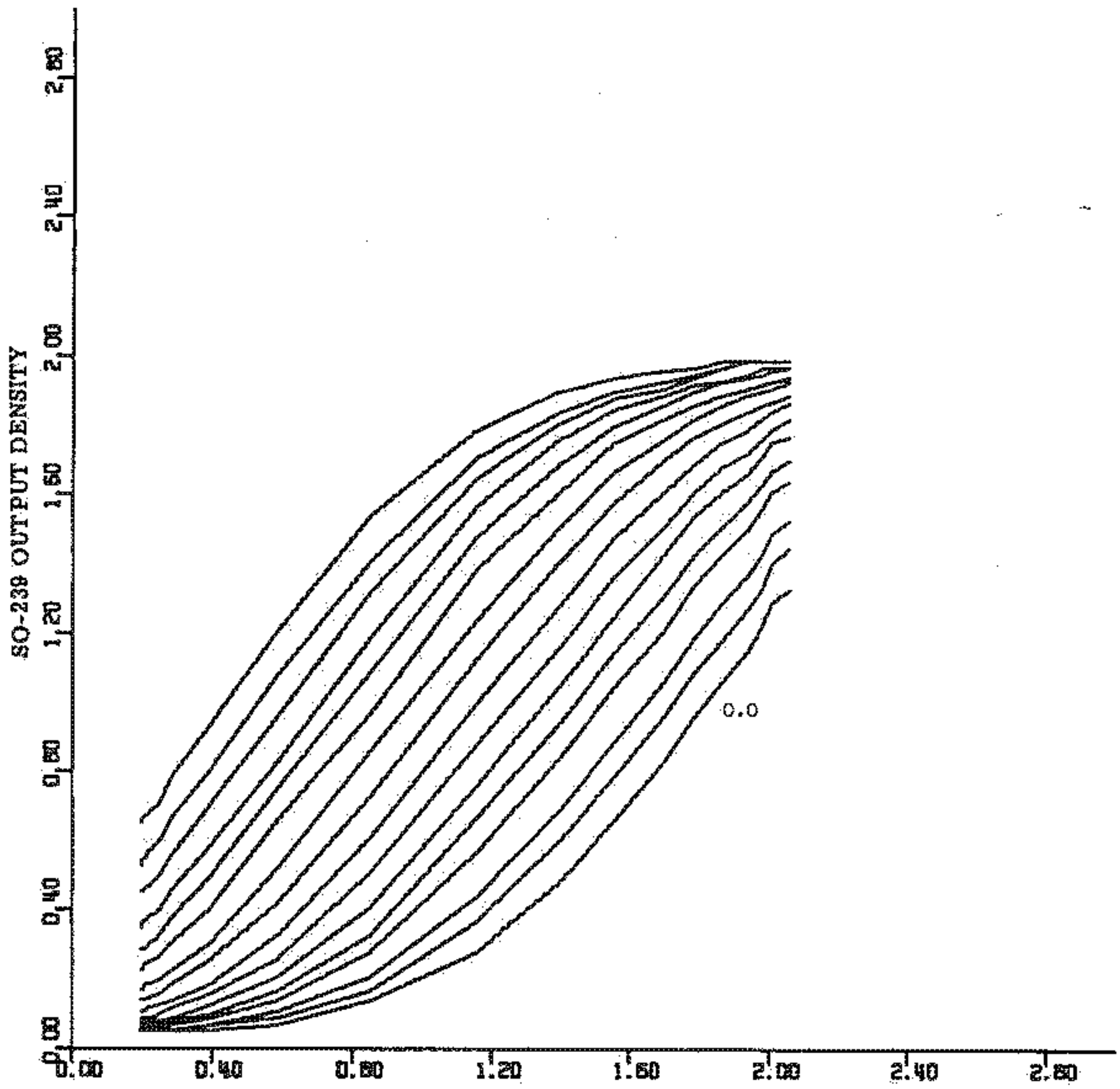


NOTES:

1. Niagara Printer settings 0.0 to 1.5.
2. Input data Film Type 1414.
3. Output data Film Type SO-239.

FIGURE 4-8

tometry for this application is shown in Figures 4-9 and 4-10.

Most of the specialized duplicate copies are shipped to customers in 6.6" x 12" clear sleeves, although some requestors required the entire op/area parts. Table 4-4 summarizes the amount of specialized duplication done on Mission 1201.

TABLE 4-4

UNITS OF SPECIALIZED DUPLICATION

| | 1201-1 | 1201-2 | 1201-4 |
|---|---|---|---|
| Single Prints (6.6" x 12") | | | |
| 6451 | 3 | 4 | 0 |
| SO-192 (High contrast) | 20 | 72 | 20 |
| Complete Op/Area Parts | | | |
| SO-192 (High Contrast) | 2 | 32 | 6 |

A copy of each single print and each part were shipped to NPIC, DIA and CIA/IAS. In addition, one each of 6 single prints on 1201-4 were shipped to the ARMY.

#### 4.4.5 Total Footages

The total duplicate footages shipped from BRIDGEHEAD were as follows:

| Mission | Regular and Single Lights | Specialized Duplication |
|---|---|---|
| 1201-1 | 536,592 | 459 |
| 1201-2 | 758,640 | 19,749 |
| 1201-4 | 415,925 | 2,476 |
| Totals | 1,711,157 ft. | 22,684 ft. |

### 4.5 REPRODUCTION AT AFSPPF

#### 4.5.1 General

Reproduction at AFSPPF consisted of duplicating both Target Complexes and Geographic Areas. Target Complexes are smaller areas of major interest within the Geographic Areas. Select frames from operations over these complexes were identified by the Exploitation Subcommittee of COMIREX (EXSUBCOM) and reproduced by complex number. BRIDGEHEAD prepared three inter-negatives on SO-239 at different density levels for all coverage over each complex. These inter-negatives were forwarded to AFSPPF for reproduction on the established priority system. After Priority 1 and 2 reproduction requirements were completed at BRIDGEHEAD, the original negative was sent to AFSPPF for completion of the Priority 3 Geographic Area requirements.

TONE REPRODUCTION CURVES

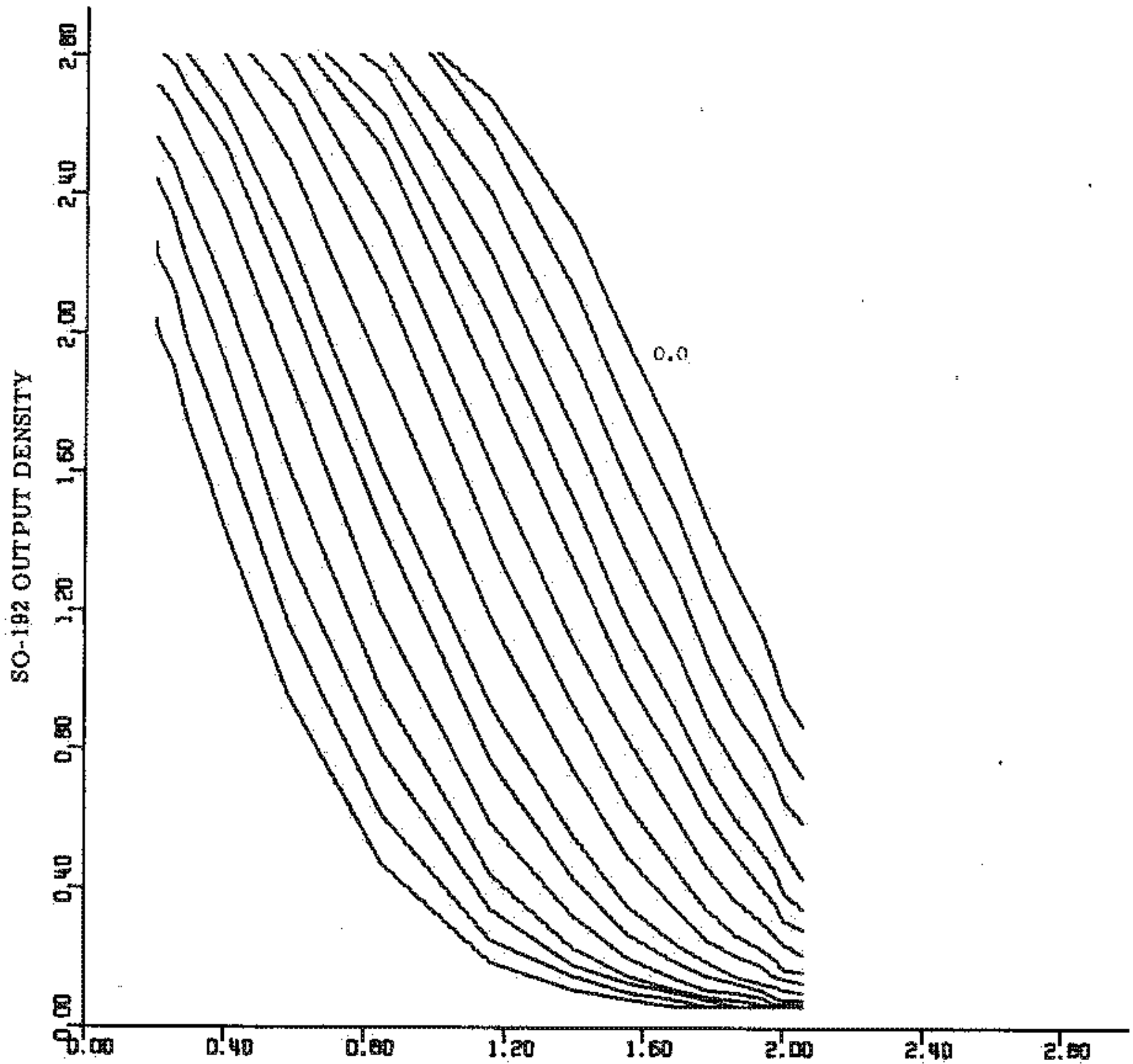


NOTES:

1. Niagara Printer settings 0.0 to 1.5.
2. Input data Film Type 1414.
3. Output data Film Type SO-192 (spray processed, high contrast).

FIGURE 4-9

TONE REPRODUCTION CURVES

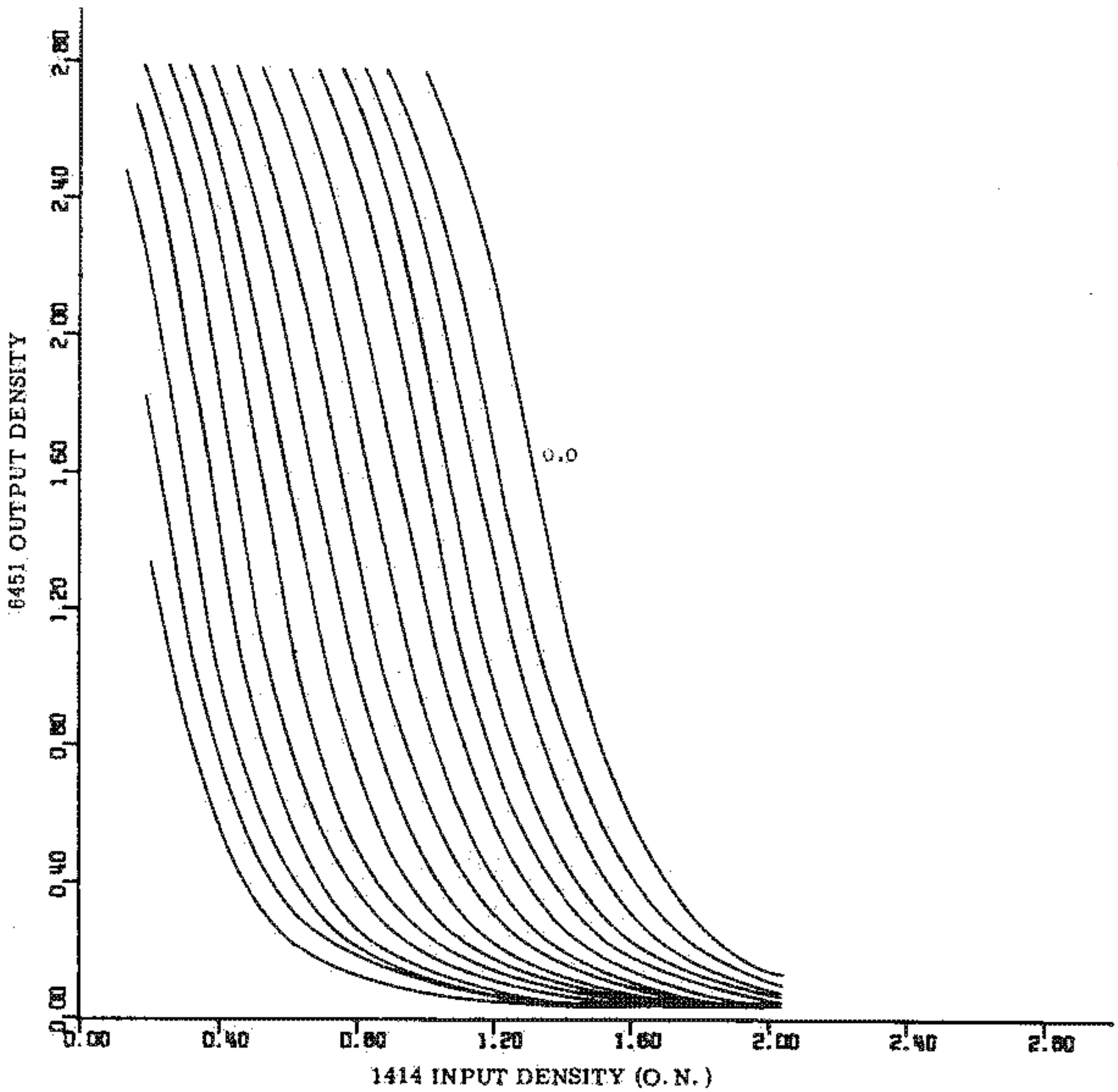


NOTES:

1. Niagara Printer settings 0.0 to 1.5.
2. Input data Film Type 1414.
3. Output data Film Type 6451.

FIGURE 4-10

4.5.2 Target Complex Duplication

AFSPPF evaluated the three density printings produced by BRIDGEHEAD and selected the best for subsequent reproduction. Operations over the same target complex were assembled together in composite rolls up to a maximum of 150 feet. Each composite roll contains only one numbered target complex. Customer copies were reproduced as third generation duplicate positives on Kodak Fine Grain Aerial Duplicating Film (Estar Base) 2430. Special SO-239 to 2430 reproduction system sensitometry (Figure 4-11) was used and the 2430 was spray processed to the normal standard.

4.5.3 Regular Duplication

4.5.3.1 Duplicate Positives

Geographic Area duplicate positives for all Priority 3 customers were prepared using 2430 and processed in the spray mode to provide the system sensitometry shown in Figure 4-12. Niagara Printer settings were selected to return the original negative densities of each op/area part between 0.40 and 1.80 with appropriate tolerances for system variability. No multiple printing was required.

4.5.3.2 Duplicate Negatives

All duplicate negative copies for Priority 3 customers were prepared using Kodak Direct Duplicating Aerial Film (Estar Base) SO-239, processed in the spray mode to provide the system sensitometry shown in Figure 4-13. Niagara Printer settings were selected to return the original negative densities of each op/area part between 0.30 and 1.80.

4.5.4 Total Footages

The total duplicate footages shipped from AFSPPF were as follows:

| Mission | Target Complex | Area Coverage |
|---|---|---|
| 1201-1 | 57,016 | 334,140 |
| 1201-2 | 95,402 | 531,124 |
| 1201-4 | 64,855 | 252,474 |
| Totals | 217,273 | 1,117,738 ft. |

4.5.5 Customers

The following is a listing of customers for 1201 material divided into those who required Area coverage and those who just needed Target Complex coverage.

4.5.5.1 Area Coverage

| | |
|---|---|
| ARMY/SPAD | ARMY/MID |
| NRTSC | 548TH (PACAF) |
| FICPAC | 497TH (USAFE) |
| FICEUR | FICLANT |
| U. K. | AUST. |
| ACIC | CONTIC |
| 480TH (TAC) | SSC (Domestics only) |

## TONE REPRODUCTION CURVES

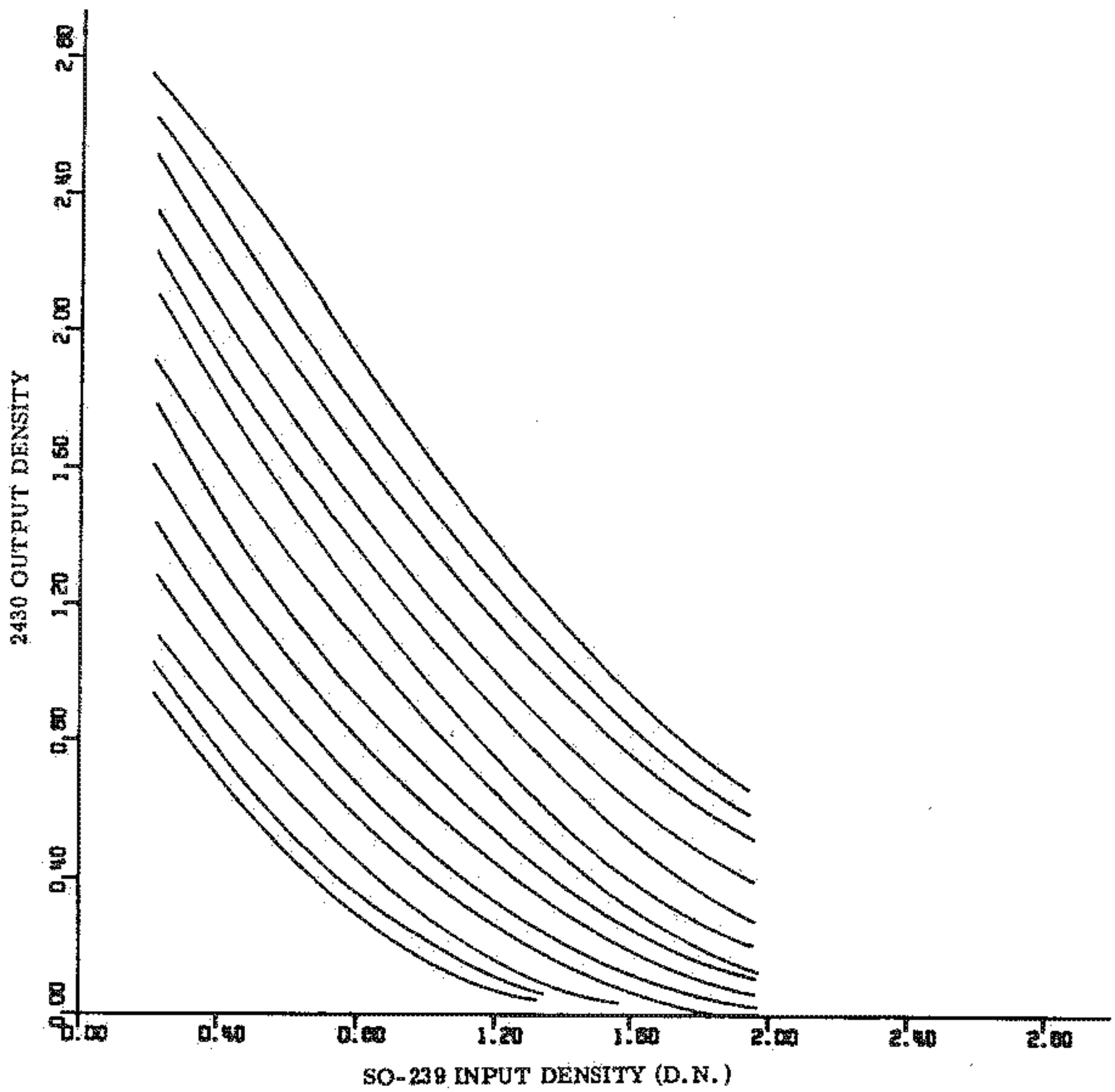


NOTES:

1. Niagara Printer settings 0.0 to 1.30.
2. Input data Film Type SO-239.
3. Output data Film Type 2430 (spray processed).

FIGURE 4-11

## TONE REPRODUCTION CURVES

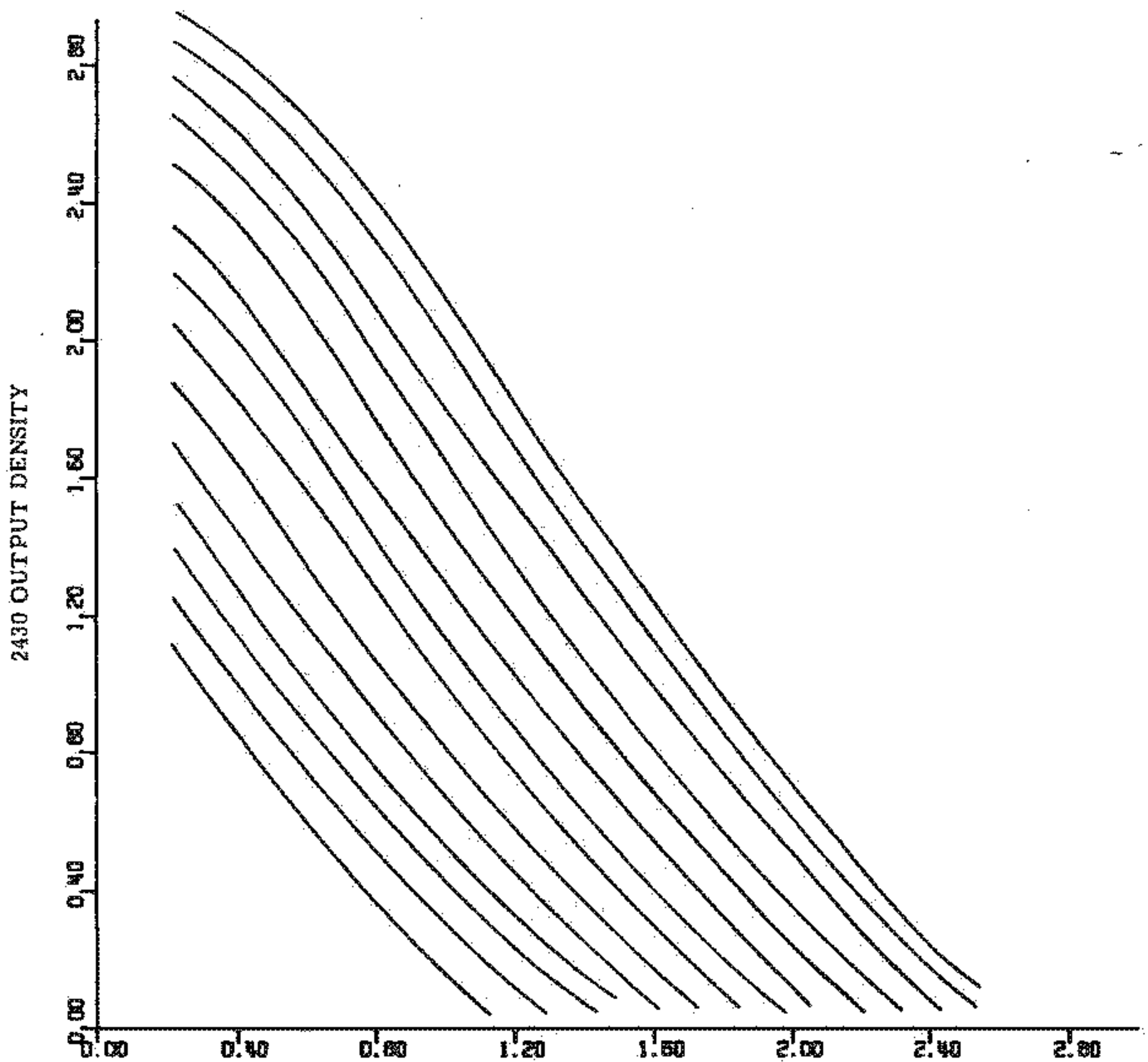


NOTES:

1. Niagara Printer settings 0.0 to 1.50.
2. Input data Film Type 1414.
3. Output data Film Type 2430 (spray processed).

FIGURE 4-12

TONE REPRODUCTION CURVES

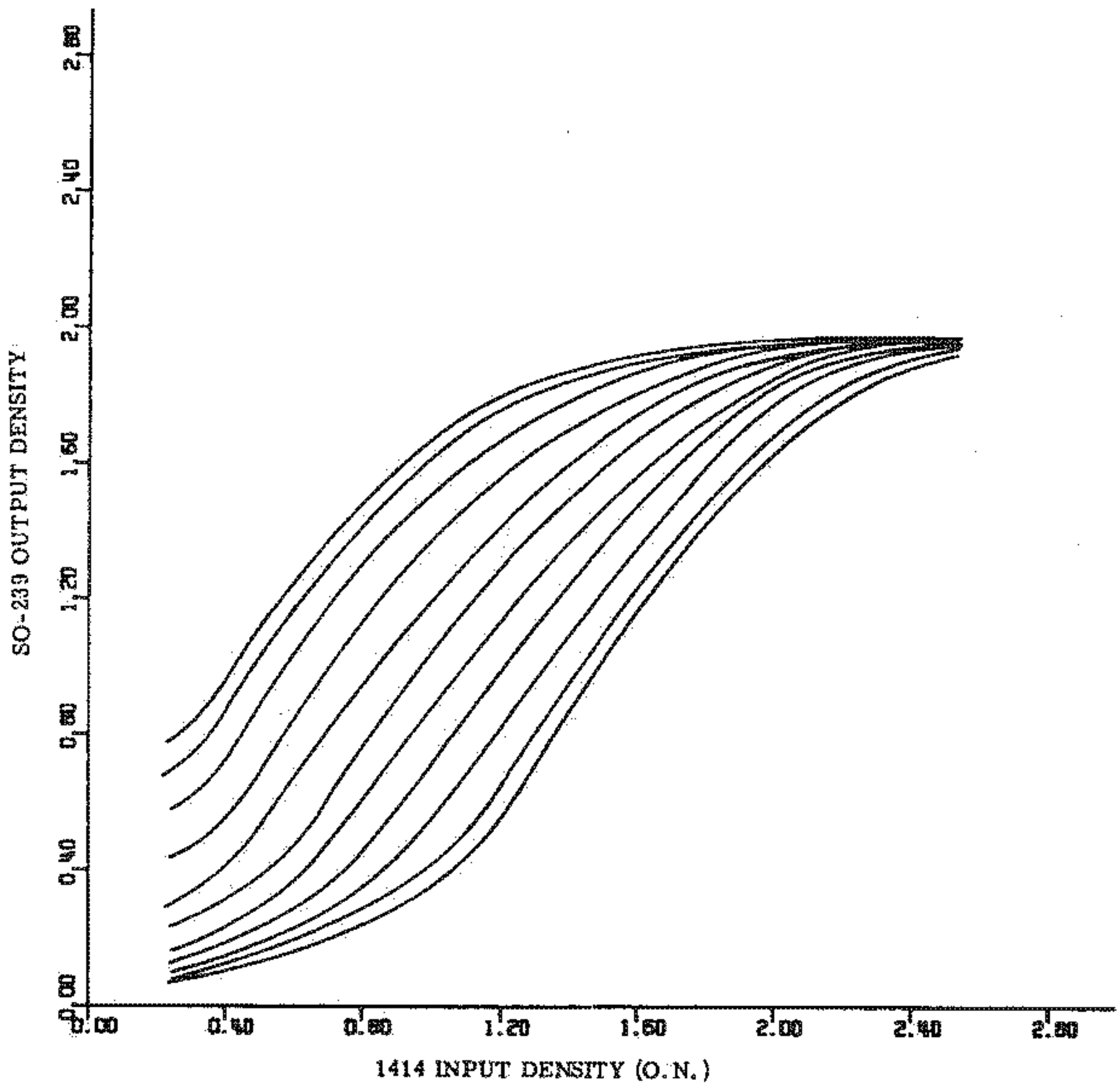


NOTES:

1. Niagara Printer settings 0.0 to 1.20.
2. Input data Film Type 1414.
3. Output data Film Type SO-239 (spray processed).

FIGURE 4-13

4.5.5.2 Target Complex Coverage

NPIC

CIA

DIA

SAC

NRTSC

PAC/KOREA

FICLANT

480TH (TAC)

CONTIC

CANADA

AF/FTD

# Exploitation Suitability

# SECTION V

# EXPLOITATION SUITABILITY

## 5.1 INTRODUCTION

This section, prepared by the National Photographic Interpretation Center (NPIC), reviews Mission 1201 as exploited by the Center. This exploitation takes the form of subjective (interpretation) and objective (mensuration) readouts to satisfy specific Intelligence Community requirements.

The complexity of analyzing Mission 1201 from a user's viewpoint has prompted the use of several techniques. At this time, the validity and meaning of these can only be estimated. As subsequent missions are reviewed, many of these will change or be modified.

## 5.2 INTERPRETABILITY

Although the interpretability of a mission's imagery is the best measure of a total system's performance, it is also the least objective technique. Many factors affect the interpretability of a photographi image. These range from resolving power to local weather conditions, from the position of an object within its surround, to such subtle differences as the degree of target activity at the time of photographic acquisition. The experience of the individual interpreter also affects the suitability rating of a particular image.

### 5.2.1 Terminology

In order to clarify the meaning of the subjective terms used to describe mission interpretability, readout techniques, and readout requirements, the pertinent terms are defined in the Glossary, Appendix A. Although some may conflict with previously conceived definitions, these are the ones used by the NPIC interpreters.

### 5.2.2 Readout Analysis

The majority of the data presented and analyzed within this section is drawn from first phase readouts. The specific targets read out for the OAK, from which this data has been extracted, change from mission to mission. Therefore, data from different buckets and/or missions does not in the majority of cases pertain to the same targets.

#### 5.2.2.1 Interpretation Suitability Summary

Since the interpreters give a quality rating that is in most cases based upon stereo viewing, quality ratings cannot be examined by camera. Table 5-1 summarized the percent interpretability ratings for the three recovered buckets of Mission 1201. A total of 591 targets was read out. After considering the conditions under which each bucket's imagery was acquired (focus, weather, etc.) no correlation appears to exist between the known image quality changes (i.e., focus adjusts) and the suitability rating given the three buckets.

TABLE 5-1

SUMMARY OF QUALITY RATINGS

(percent)

| Ratings | RV-1 | RV-2 | RV-4 | Msn Avg |
|---|---|---|---|---|
| Excellent | 0.8 | 1.6 | 0.5 | 1.0 |
| Good | 29.8 | 27.6 | 10.4 | 22.4 |
| Fair | 47.8 | 45.6 | 50.5 | 47.7 |
| Poor | 21.6 | 25.5 | 38.6 | 28.9 |

As for overall mission quality, an answer cannot be obtained directly from suitability ratings, since no equation relating excellents, goods, fairs, poors, and photographic quality exists. An attempt to give the reader some indication of the interpreters subjective impression of the interpretability of Mission 1201 imagery is presented in paragraph 5.2.2.3.

5.2.2.2 Interpretation Ratings Within Format

Several factors affect image quality differences within a frame's format. If the geographic area covered is considered and if targets were randomly distributed around the world, then twice as many targets would be imaged at the ±60° scan area as compared with 0° scan. However, since these conditions do not exist, and since some effort is made to place targets near zero scan, the interpretability versus scan angle and field position question is not easily answered. It can be said that if the image quality decreases, information is lost and in general interpretability decreases. A more complete study of PI suitability ratings as related to its location within a frame format can be found in paragraph 5.8.

5.2.2.3 Interpretability of Mission 1201 Imagery

Many attempts have been made to assess the quality of a particular missions' imagery by examining the information extracted by the interpreters. Experiments have been conducted comparing photographic quality (resolving power, tone reproduction, etc.) with the information contained within an image. However, these experiments presuppose that intelligence is present within the image. The real world of photographic interpretation does not have the exact location of information established prior to its extraction. Neither does the interpreter have the option of using only imagery of optimum quality. The majority of the interpreters surveyed were satisfied with the interpretability of the Mission 1201 imagery. Most of the requirements for first phase readout were satisfied. The larger scale of the imagery aided the interpreters in most cases. The increased quantity of film was significant in that it not only gave many interpreters multiple coverage of their target areas, but provided coverage of areas not previously available at ground resolution of better than five or six feet. The 10° convergence angle and 50 percent stereo overlap, although different than that of previous systems, presented no problems to the interpreters. First and second phase readouts concentrated on order of battle. Although the first missio of this series did cover many different targets, only one set of acquisition conditions was sampled. Other seasonal conditions of weather and lighting will have to be sampled before a definitive answer as to order of battle and the KH-9 can be given. The order of battle readout was satisfactorily accomplished relative to premission predictions. Some difficulties existed with the determination of ground order of battle, particularly armored vehicles. This situation is easily understood when one realizes that these types of questions are answered with criteria such as the type and length of the gun barrel. Some camera operations permitted the entire air order of battle for a particular country to be read out. This is a major source of intelligence to those who must estimate the military posture of a particular country. Perhaps the greatest disappointment of the mission was the loss of RV-3. It contained a large quantity of needed coverage.

## 5.3 MISSION INFORMATION POTENTIAL (MIP) RATINGS

### 5.3.1 Mission 1201 Ratings

The MIP ratings for Mission 1201 are presented in Table 5-2.

TABLE 5-2

MISSION 1201 MIP RATINGS

| Mission | Camera | Ratings |
|---|---|---|
| 1201-1 | Forward-looking | 125 |
| | Aft-looking | 140 |
| 1201-2 | Forward-looking | 135 |
| | Aft-looking | 135 |
| 1201-4 | Forward-looking | 145 |
| | Aft-looking | 140 |

A comparison of the six MIP chips indicates that they are ranked properly by their MIP values. There is a greater difference in image quality between the 125/135 chips than between the 135/140 and 140/145 chips. The comparison of the two 135 and the two 140 chips indicates that the image quality of these identically rated chips is approximately equal.

A comparison of the MIP ratings with resolution data from PFA CORN target readings shows very little or no correlation between the two. For comparison purposes the best in-track and cross-track readings and their respective means are listed for each mission and camera in Table 5-3.

TABLE 5-3

COMPARISON OF MIP RATINGS AND CORN RESOLUTION

| Mission/Camera | Best In-Track | Mean In-Track | Best Cross-Track | Mean Cross-Track | Geometric Mean All Targets | MIP Ratings |
|---|---|---|---|---|---|---|
| 1201-1 Fwd | 2.2 | 2.9 | 3.2 | 4.4 | 3.6 | 125 |
| Aft | 2.5 | 2.8 | 3.1 | 3.9 | 3.3 | 140 |
| 1201-2 Fwd | 2.4 | 3.3 | 3.4 | 4.3 | 3.8 | 135 |
| Aft | 2.3 | 2.8 | 2.8 | 3.3 | 3.0 | 135 |
| 1201-4 Fwd | 2.0 | 2.6 | 2.6 | 3.9 | 3.2 | 145 |
| Aft | 2.1 | 2.4 | 3.3 | 3.6 | 2.9 | 140 |

Since the standard MIP chips will eventually be replaced with KH-9 imagery, NPIC has evaluated the 1201 chips to determine if they might meet these requirements. Of the six chips, four are being considered; however, NPIC feels that one or two more missions are needed to adequately fulfill this requirement. Illustrations of the 1201 MIP Areas are shown in Figures 5-1 thru 5-6.

## 5.4 MENSURATION ANALYSIS

An error analysis investigation of Mission 1201 was conducted to determine empirical accuracy statements for mensuration. The analysis consisted of measuring distances, heights, geodetic positions, and azimuths in seven domestic and five foreign ground truth areas. The mensuration sample included data measured from a variety of scan angles and from each of the three buckets. The accuracy statements given are valid only for Mission 1201 and are not the final KH-9 System accuracies. Future mensuration of KH-9 missions may or may not fall within these stated accuracies. NPIC will provide mensuration statistics on future missions to either validate or change the present KH-9 accuracy statements.

The results from Mission 1201 are as follows:

A. KH-9 monoscopic mensuration at a two sigma (95%) confidence interval.

(1) Horizontal distances - ±1.3m (average) for all scan angles
±1.4m cross-track
±1.2m in-track

NOTE: The monoscopic horizontal distance errors appear to be uniform from -60° to +60° from nadir. No systematic error has been determined for Mission 1201, as it generally requires a detailed study of data from several missions before a statistical determination can be made.

(2) Vertical distances - The error is determined by propagating the horizontal distance erro This could vary with the method used to measure the height, the location of the measurement on the film relative to nadir, and the sun elevation.

SALT LAKE CITY INTERNATIONAL AIRPORT, UTAH

MIP = 125

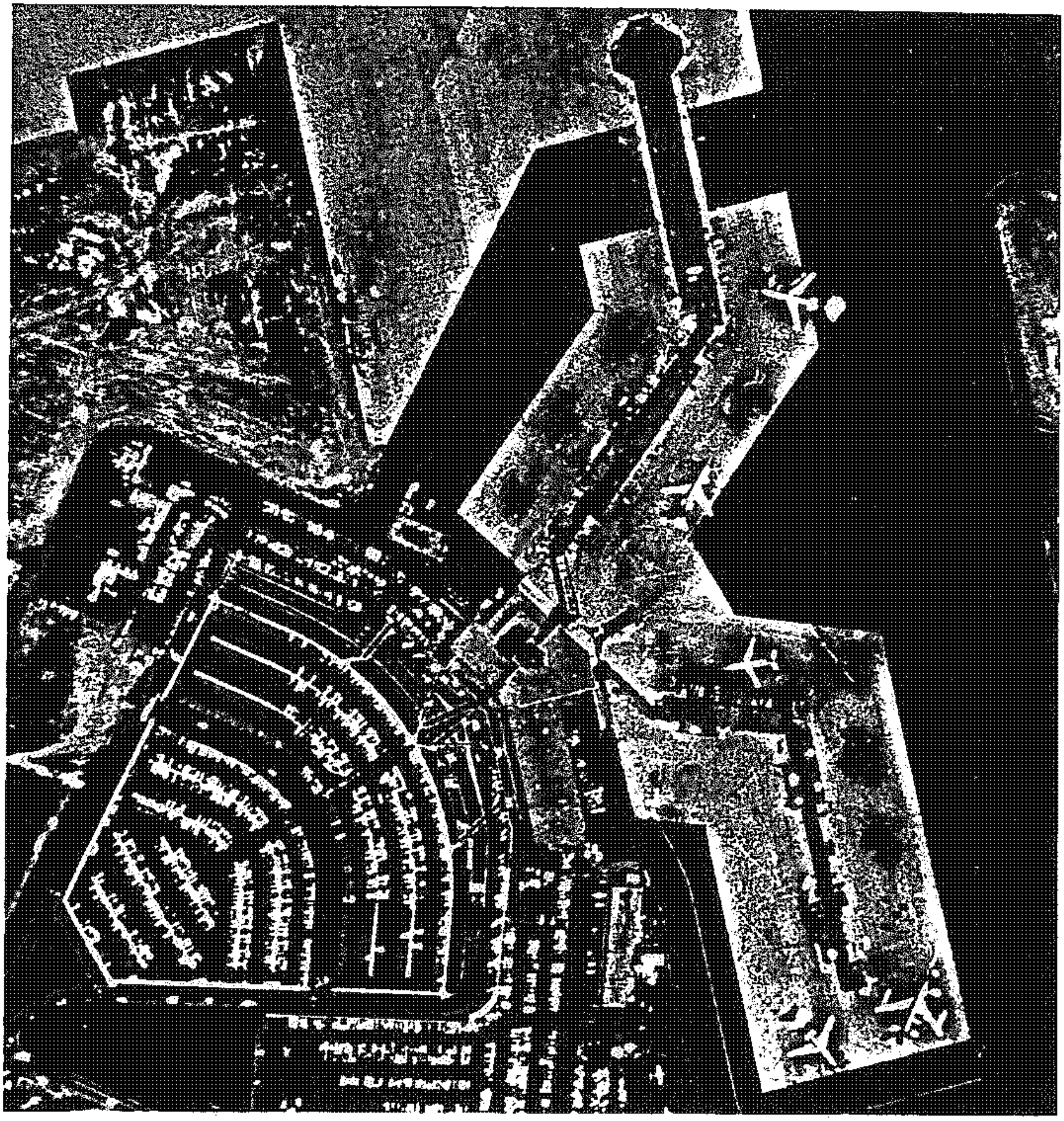

MISSION 1201-1 FWD CAMERA OP 35 FRAME 013 40X ENLARGEMENT

FIGURE 5-1

SALT LAKE CITY INTERNATIONAL AIRPORT, UTAH

MIP = 140

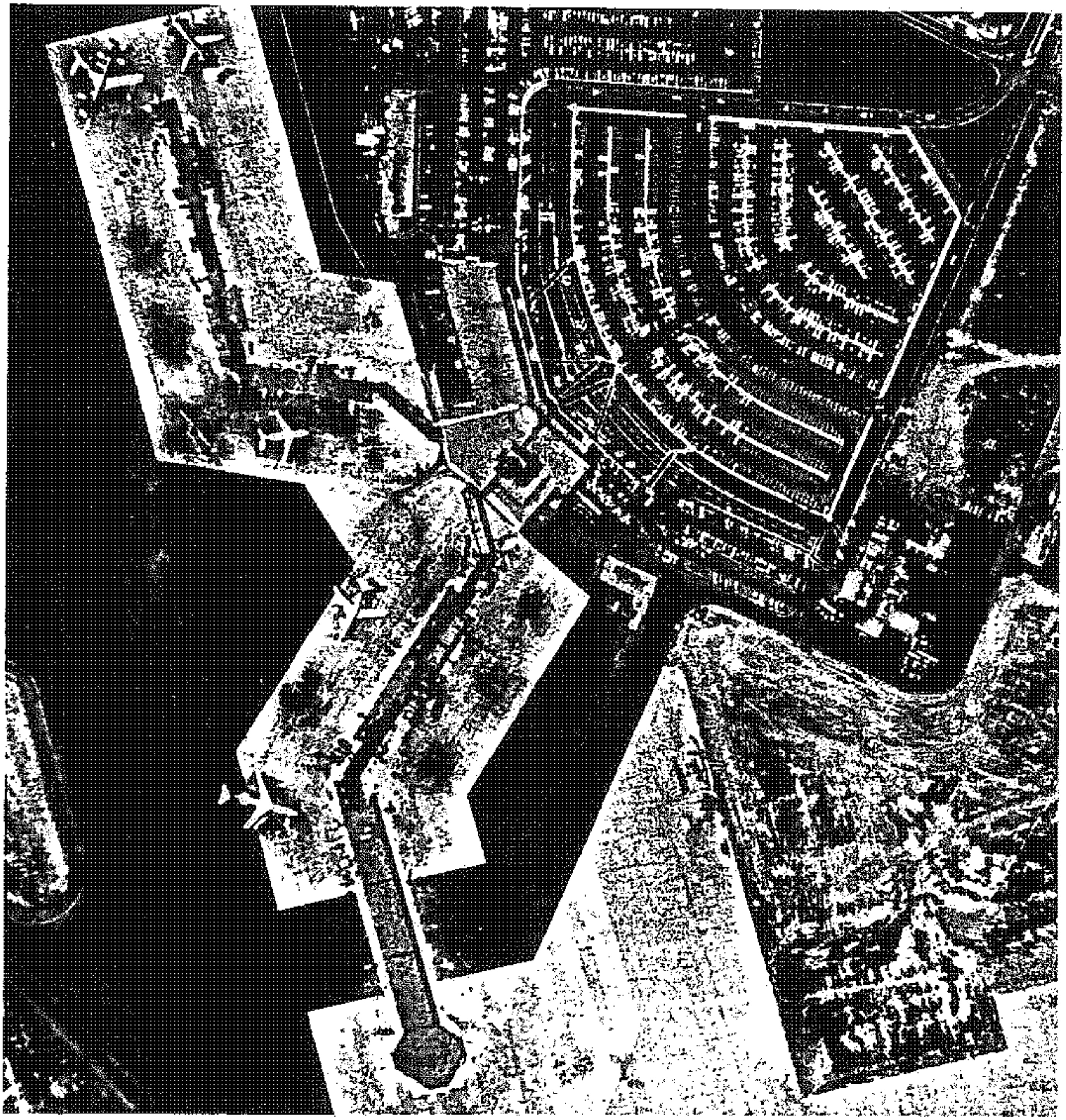

MISSION 1201-1 AFT CAMERA OP 35 FRAME 014 40X ENLARGEMENT

FIGURE 5-2

3.3(b)(1)

3.3(b)(1)

TRAVIS AFB, CALIFORNIA

MIP = 145

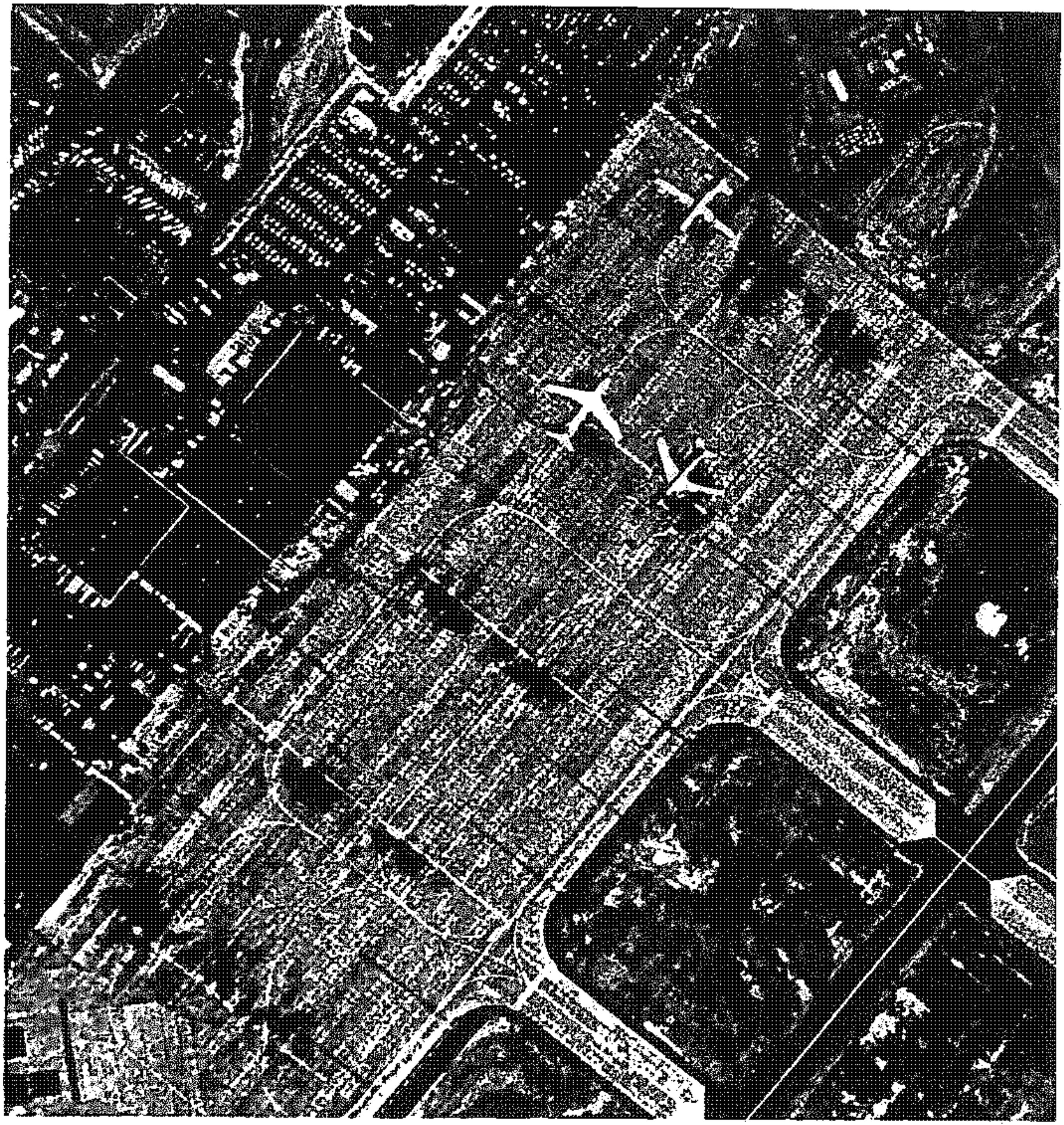

MISSION 1201-4 FWD CAMERA OP 409 FRAME 004 40X ENLARGEMENT

FIGURE 5-5

McCLELLAN AFB, CALIFORNIA

MIP = 140

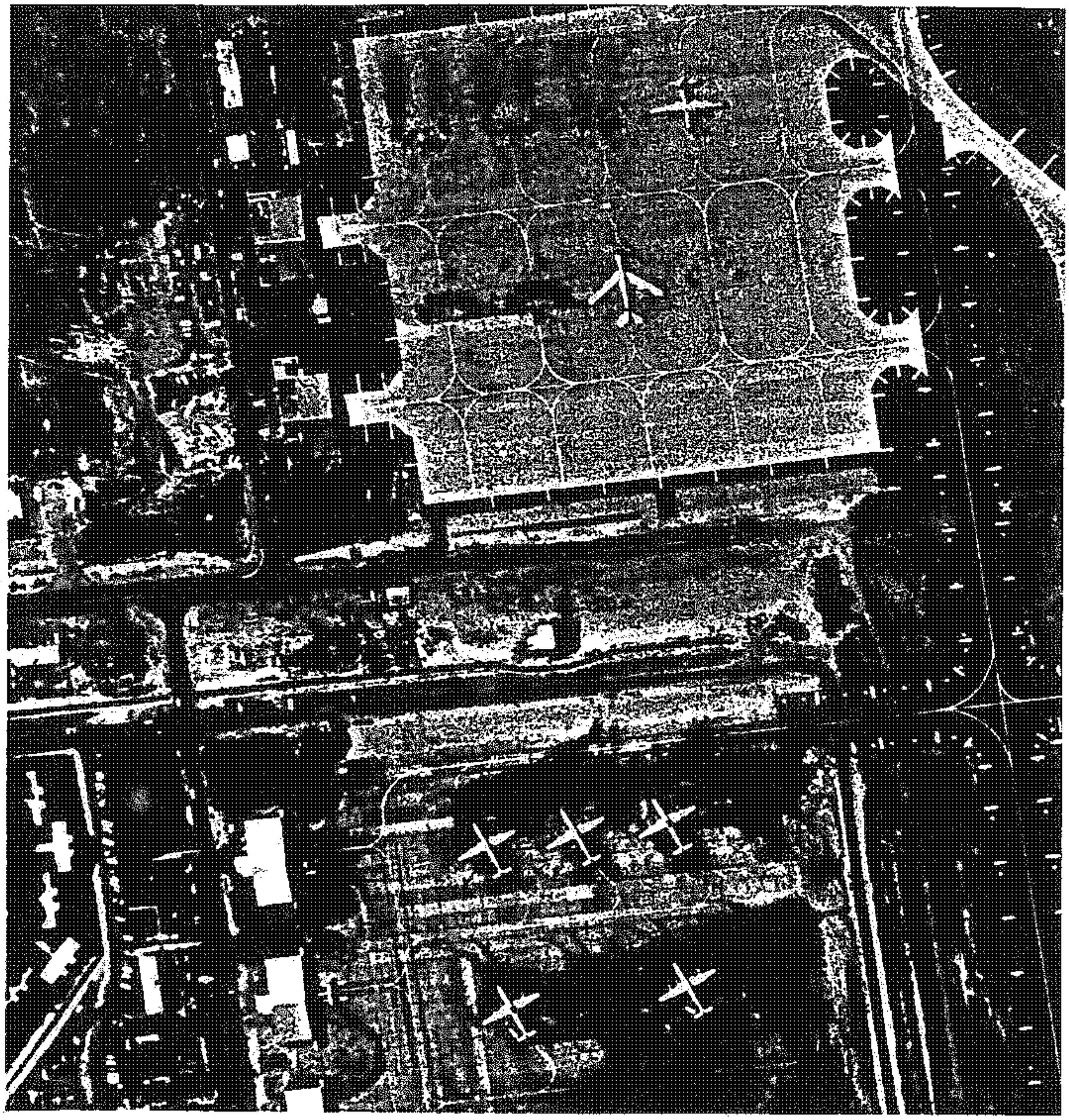

MISSION 1201-4 AFT CAMERA OP 409 FRAME 002 40X ENLARGEMENT

FIGURE 5-6

(3) Azimuth - The error is computed by the formula $\pm \left(\frac{105.3}{MD} + 0.05\right)$ degrees where MD is the measured distance in meters between the two end points.

(4) Geodetic coordinates - The error varies as a function of scan angle. The 90% circular error can be determined from the graph presented as Figure 5-7. Figure 5-7 shows that the computed latitude and longitude for a target imaged on the format between -36° and +60° of scan will be within 900 meters on the ground from the actual target 90% of the time. This is a preliminary assessment based on a limited sample. NPIC is reviewing their data reduction programs and this figure may change reflecting program modifications and more test analysis.

B. KH-9 stereoscopic mensuration two sigma (95%) confidence interval.

(1) Horizontal distances - The error varies as a function of scan angle and can be determined from the graph presented as Figure 5-8.

(2) Vertical distances - The error varies as a function of scan angle and can be determined from the graph presented as Figure 5-8.

(3) Azimuth - It is determined from mono only.

(4) Geodetic coordinates - It is determined from mono only.

Comparisons showing the KH-9 accuracy statements with KH-7 and KH-8 are shown in Tables 5-4 and 5-5.

The NPIC did not experience any major problems in the mensuration of Mission 1201. No differences were found between RV-1, RV-2 or RV-4. There were no individual frames which gave erroneous mensuration results. The out-of-focus imagery at the beginning of the mission was noticeable in that it affected the ability to point edges and corners, however, it did not effect the final mensuration results. Using the mensuration comparators set at the best magnification for the given imagery, KH-8 corners and edges are sharper than KH-9 corners and edges.

The scan angle marks on the titled side of the frame were out-of-focus and not circular. This had no discernable effect on mensuration. The missing time words did not effect mensuration because all of these frames were titled. If the frames are not titled, and the time word cannot be read, NPIC would be unable to associate the vehicle parameters with the frames. The instrumentation used at NPIC for KH-9

MISSION 1201 ACCURACY STATEMENT - GEODETIC POSITIONING

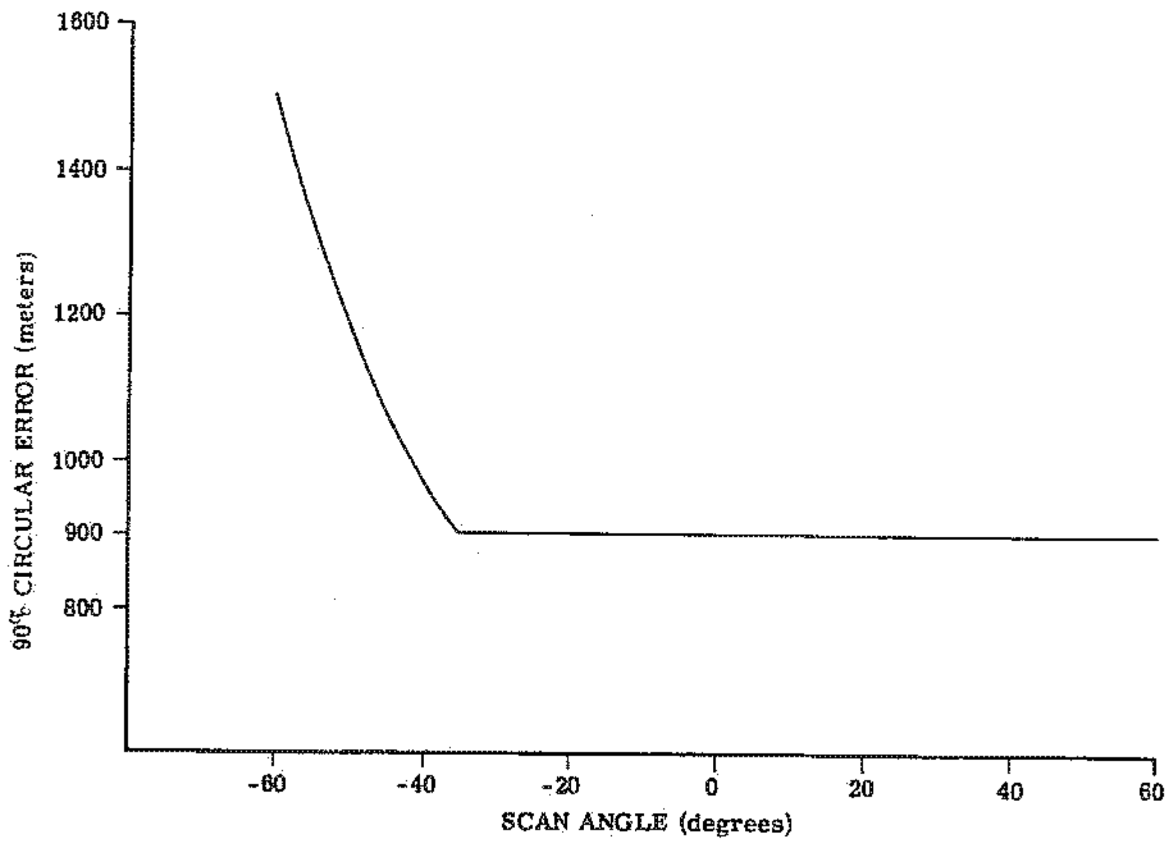


FIGURE 5-7

KH-9, STEREO ACCURACY (95% CONFIDENCE LEVEL)

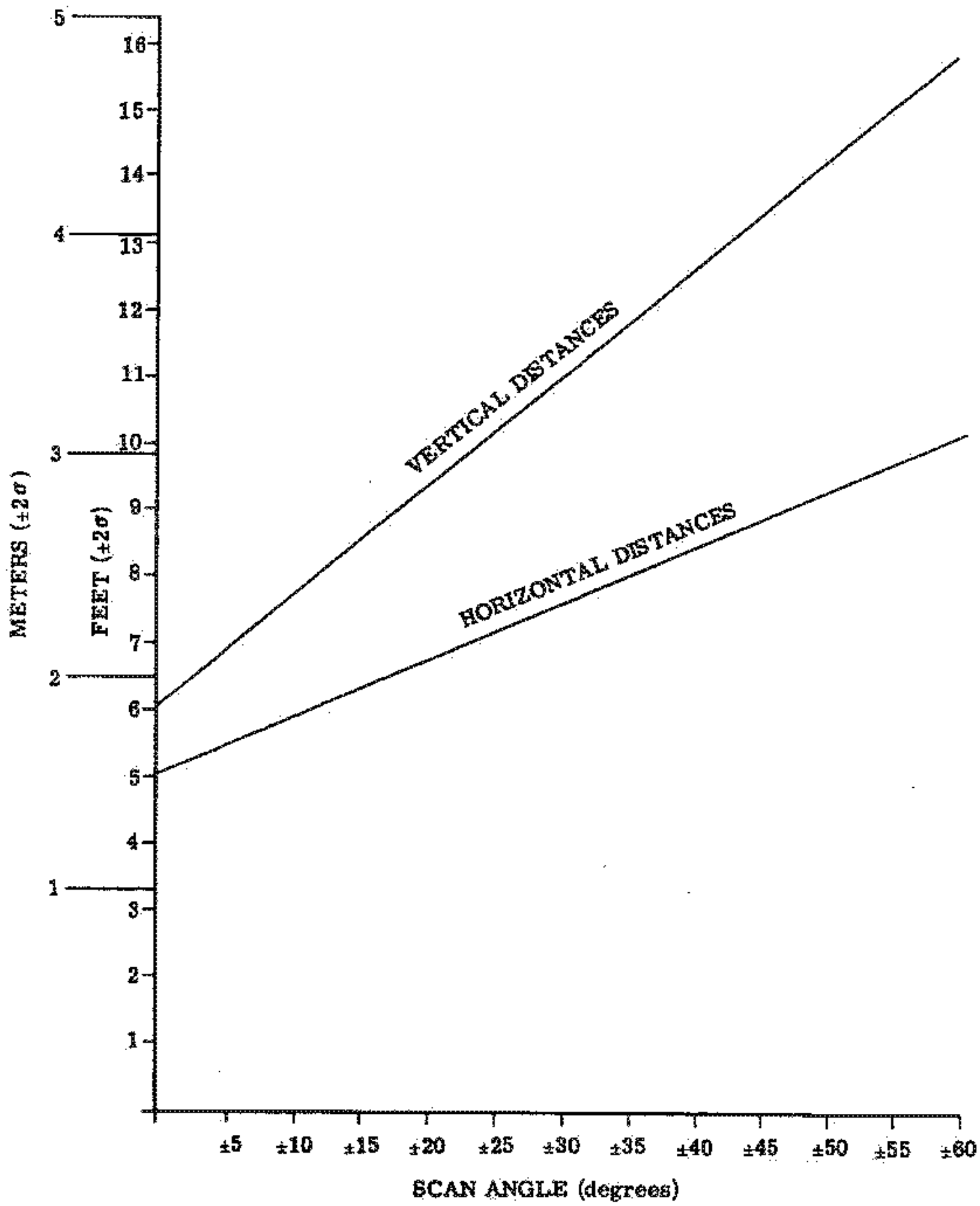


FIGURE 5-8

mensuration is:

Mann 621 Mono Comparator

Mann 1210 Mono Comparator

Mann 880 Mono Comparator

Optomechanism Point Transfer Device Stereocomparator

TABLE 5-4

COMPARISON OF MENSURATION ERRORS FOR KH SYSTEMS IN MONOSCOPIC MODE

| System | KH-9 (1201) | KH-8 | KH-7 |
|---|---|---|---|
| Horizontal Distances | ±1.3m (average) for all scan angles) | ±(0.8m + 1% MD) where MD > 5m | ±(1.6m + 1% MD) |
| Vertical Distances | error determined by mathematically propagating horizontal distance error (varies with method) | error is propagated same as KH-9 | error is propagated same as KH-9 |
| Azimuth | error in degrees is: $\pm(\frac{105.3}{MD} + 0.05)$ | error in degrees is: $\pm(\frac{46}{MD} + 0.57)$ | ±3° (±2° having stellar reduced vehicle attitude) |
| Geodetic Coordinates | error is a function of scan angle | not determined for this system | not determined for this system |

TABLE 5-5

COMPARISON OF MENSURATION ERRORS FOR KH SYSTEMS IN STEREOSCOPIC MODE

| System | KH-9 (1201) | KH-8 | KH-7 |
|---|---|---|---|
| Horizontal Distances | is a function of scan angle, see Figure 5-8 | ±(0.8m + 1% MD) where MD > 5m. | not determined for this system |
| Vertical Distances | is a function of scan angle, see Figure 5-8 | ±(1.0m + 1% MD) | not determined for this system |
| Azimuth | determined from mono only | error in degrees is: $\pm(\frac{46}{MD} + 0.57)$ | not determined for this system |
| Geodetic Coordinates | determined from mono only | not determined for this system | not determined for this system |

NOTE: All mensuration errors given at a two sigma (95%) confidence level.

## 5.5 VISUAL EDGE MATCHING (VEM) CORRELATION WITH PI SUITABILITY RATINGS

This study was conducted to determine whether a correlation exists between the photointerpreter's suitability ratings and a VEM analysis of selected targets of Mission 1201.

### 5.5.1 Correlation Procedures

Approximately 200 targets were selected from the OAK reports. The selection was limited to those targets available in stereo coverage, since the PI suitability ratings would be based upon a stereo readout to minimize any camera differences. These targets were examined for appropriate edges and weather restrictions. The following targets were rejected from the analysis:

A. Those with erroneous coordinates.

B. Those for which no suitable edges were available.

C. Those completely obscured by clouds.

D. Those partially off the format.

Edges of the selected targets were then matched against the VEM matrix. The analysis was made in both the flight and scan directions. An effort was made to include a representative sampling of target types (i.e., missile sites, airfields, naval bases, etc.) and the Good, Fair, and Poor ratings.

### 5.5.2 Analysis

Table 5-6 illustrates the number of targets used for each bucket, and their respective suitability ratings:

TABLE 5-6

NUMBER OF ANALYZED TARGETS BY SUITABILITY RATING

| Ratings | RV-1 | RV-2 | RV-4 |
|---|---|---|---|
| Excellent | 0 | 0 | 0 |
| Good | 25 | 31 | 14 |
| Fair | 35 | 24 | 35 |
| Poor | 4 | 8 | 8 |
| Total | 64 | 63 | 57 |

The percentages of these figures are shown graphically in Figures 5-9 thru 5-12 plotted against the VEM Dupe Matrix #3. No obvious correlations are evident from the graphs. This result is not entirely surprising since by definition the fundamental criteria for assigning a PI suitability rating may be reduced to (a) the scope of the photographic coverage, and (b) the degree to which a PI may extract useful and reliable information from the material, an obviously different rating technique from visually matching edges. This difference can be seen more clearly in the case of four targets found to be common to all three buckets. The targets are labeled A, B, C, and D. For Target A, the suitability rating was Fair for each bucket. However, the VEM Team read progressively better edge sharpness for each successive bucket in both the flight (in-track) and scan (cross-track) directions. For Target B, the suitability rating again was Fair for

MISSION SEGMENT 1201-1 CORRELATION HISTOGRAMS

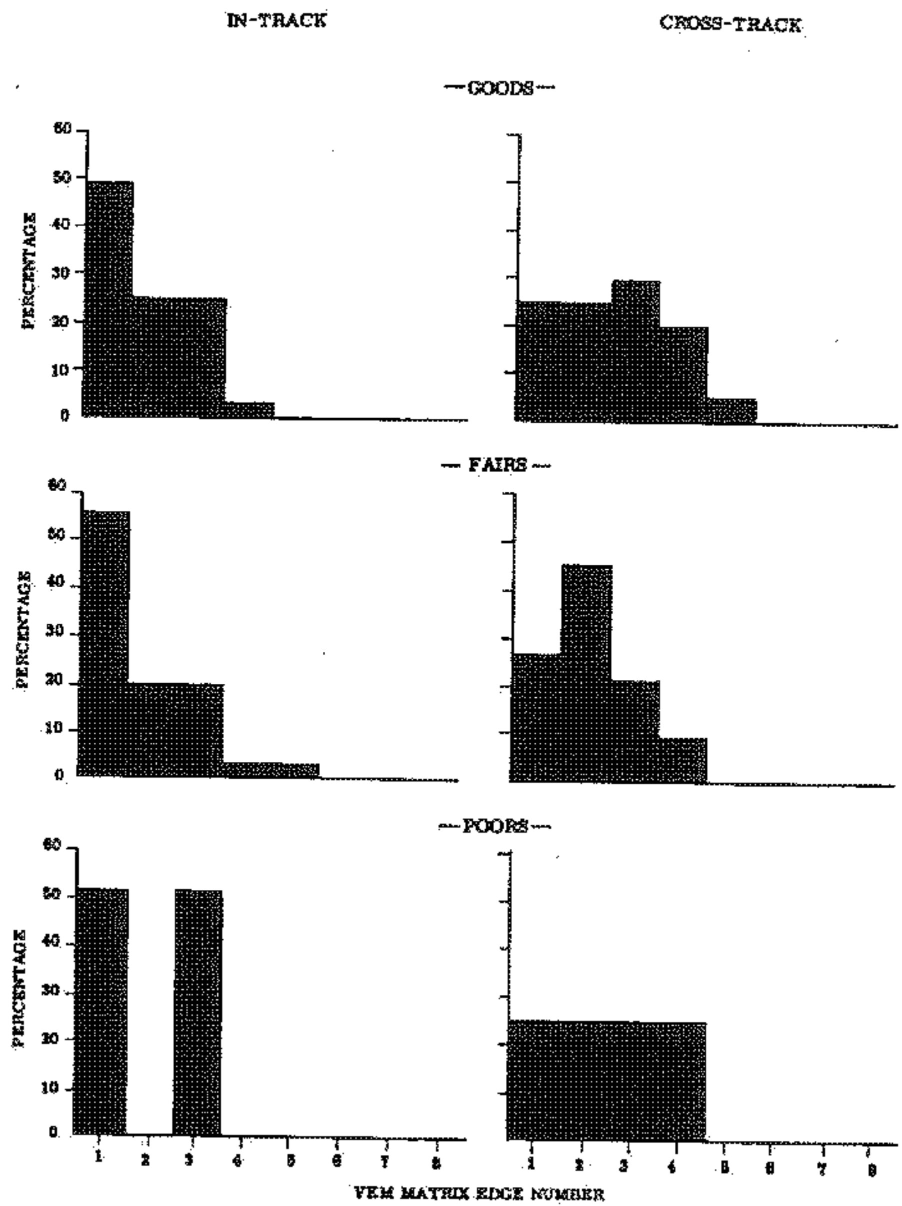


FIGURE 5-9

MISSION SEGMENT 1201-2 CORRELATION HISTOGRAMS

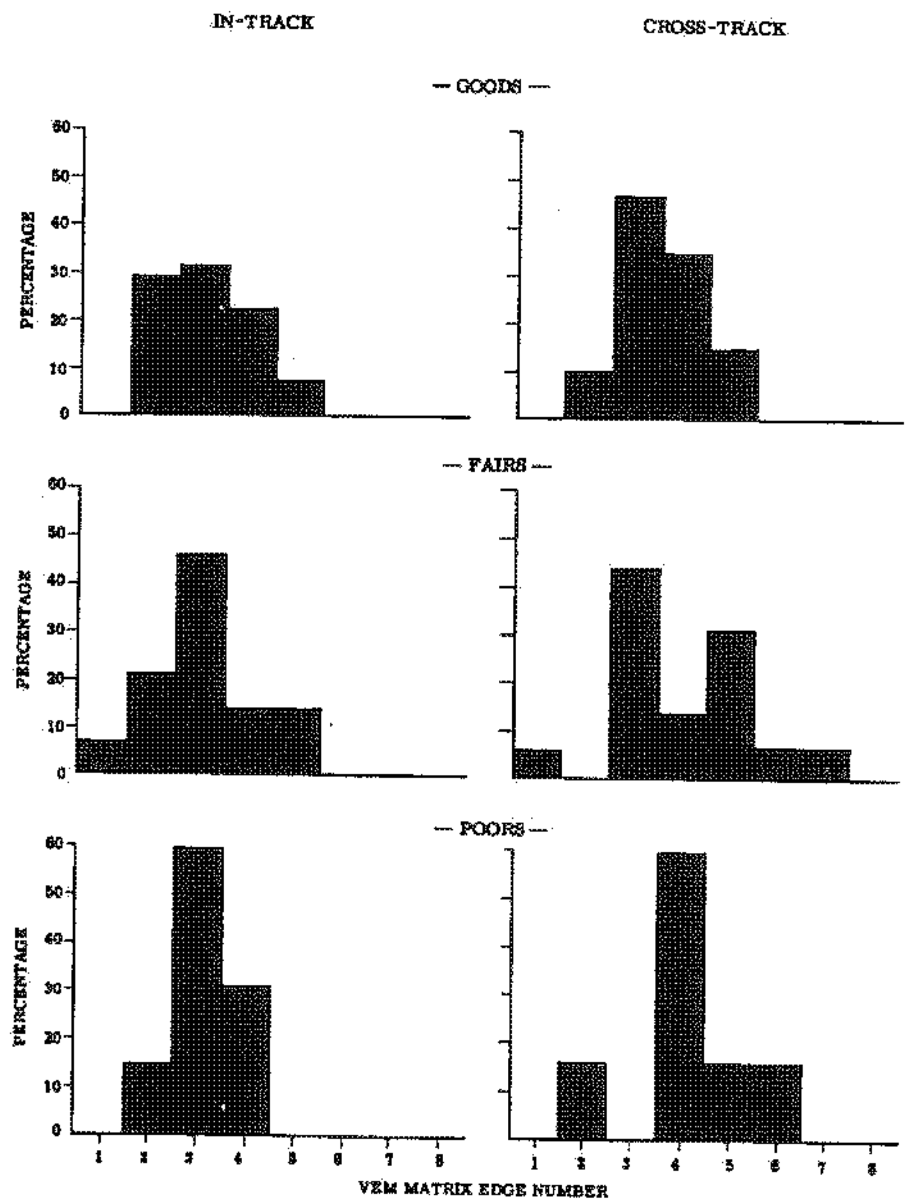


FIGURE 5-10

MISSION SEGMENT 1201-4 CORRELATION HISTOGRAMS

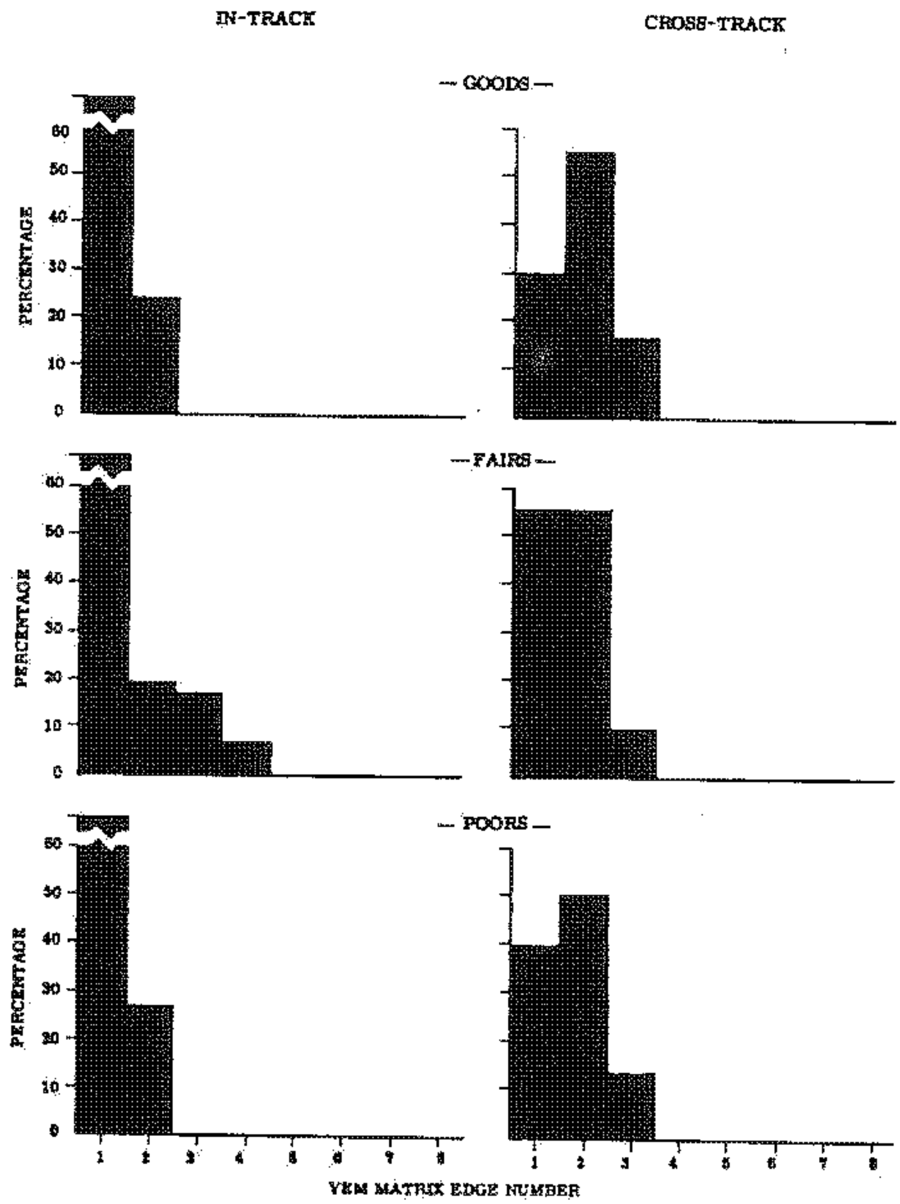


FIGURE 5-11

MISSION 1201-1, 2, 4 CORRELATION HISTOGRAMS

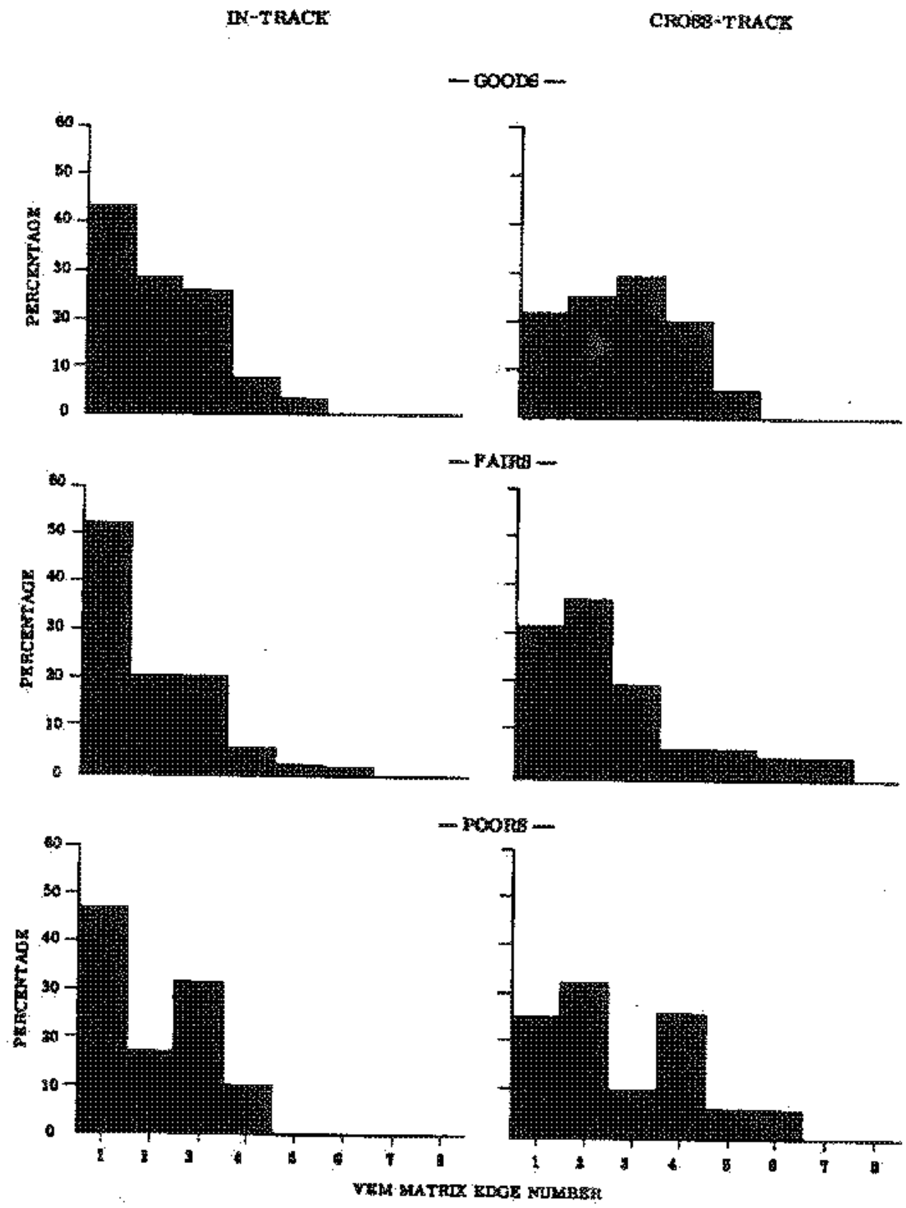


FIGURE 5-12

each bucket. The VEM Team now read the same edge sharpness for RV's -1 and 4, and better for RV-2. For Target C, the suitability ratings were Fair, Poor, Poor, for RV's -1, 2, and 4 respectively. The VEM readings improved, however, for each successive bucket. For Target D, the suitability ratings were Poor, Fair, Fair, for RV's -1, 2, and 4 respectively. In this case, the VEM readings indicated a decrease in edge sharpness for each successive bucket.

#### 5.5.3 PI Suitability Ratings Versus GRD (VEM)

A small sample of targets (168) was selected to investigate the possibility of correlation between VEM analysis converted to GRD and the PI suitability rating. The GRD values were obtained by conversion of the VEM edge values to lines per millimeter as defined by a system calibrated VEM matrix. These values were then converted to their corresponding GRDs.

#### 5.5.4 Conclusions

A. There is no obvious correlation between the PI suitability ratings and direct VEM readings.

B. A correlation was indicated for all targets between Good and Poor PI ratings when VEM edge values were converted to GRD.

#### 5.5.5 Summary

The PI is more concerned with a quantity readout, while the VEM is concerned primarily with edge sharpness; neither of which is a complete indication of image quality. The PI suitability ratings could possibly be expanded to be more indicative of image quality, and still satisfy the basic readout requirements. The VEM could be improved mechanically, and a broader range of calibrated edges would help. A more extensive study of the VEM is currently being done. It has, however, been apparent in this study that edge sharpness is not a complete indicator of image quality.

### 5.6 ASSESSMENT OF SPECIALIZED DUPLICATES

#### 5.6.1 Introduction

Several studies have been conducted to investigate the contrast of target images from reconnaissance camera system film. Although a search system will acquire some targets that need this special printing, specialized duplication is most beneficial to images acquired from a target orientated system.

It has been demonstrated that the two factors that most affect image contrast are exposure and scene weather conditions. Additionally, some unique environmental conditions, i.e., sand, snow, etc., also affect image contrast. In an attempt to recover the scene contrast lost by these effects, special prints are made on high contrast duplicating materials. Films SO-192, processed to a gamma of 2.5, and 6451, processed to a gamma of 6.0, are used to produce these duplicates.

#### 5.6.2 Image Selection

As a standard procedure, interpreters nominate to the NPIC "Tiger Team", targets they feel could benefit from special printing. The Team inspects the original negative for areas that they feel require special duplication, and eliminates some due to repetitive coverage or especially clear or poor weather conditions.

The photointerpreters submitted a total of 129 targets as candidates for specialized duplication. Eighty-six of these targets were acquired on Mission 1201. Of these, sixty-two were special printed.

#### 5.6.3 Observations

The interpreters rated most of the special prints superior to their standard reproductions. High contrast reproductions of 20 camera operations over low contrast terrain in the Middle East did aid the interpreters over that area. Generally, however, they felt that the standard reproductions were satisfactory for first phase readout. The unique best case acquisition conditions of Mission 1201 did provide a set of images very uniform in density and contrast. This condition makes it extremely difficult to define the role of high contrast reproductions with KH-9 exploitation. It will require numerous samples from several missions to definitively answer the question as to the value of special printing of KH-9 imagery.

### 5.7 ORIGINAL NEGATIVE (ON) VERSUS DUPLICATE POSITIVE (DP) IMAGE QUALITY

#### 5.7.1 Introduction

As more sophisticated and higher quality photographic reconnaissance systems are designed and flown, there is a need for a corresponding increase in quality of the reproduction process. It is of utmost importance that the information content of the original acquisition material, which the photointerpreter does not have the opportunity to evaluate, be transferred to the duplicate positive.

A study has been conducted to determine if a loss of information is apparent between the original negative and the second generation duplicate positive of Mission 1201. Both subjective and objective evaluation techniques were used. Subjectively the materials were evaluated by reading the mobile CORN target displays and comparing information content in the highlight and shadow areas of the two materials. The objective evaluation techniques consisted of an analysis of the acutance and granularity for the reproduction system by the use of microdensitometry.

An analysis of tone reproduction was planned as part of this study. Due to circumstances beyond the immediate control of NPIC, this study could not be accomplished.

The duplicate positives used for analysis were those prepared by the prime processing contracto

#### 5.7.2 Resolution

Resolution is not a complete measure of image quality, but when used with other evaluation techniques, it can be a useful tool. Resolution is an attractive measure since it correlates with those properties of an image which permit the distinction between small, similar, closely-spaced objects. Ground order of battle, an important portion of photographic interpretation, strains the resolution capability of a photographic system. Rows of vehicles, equipment, and supplies must be counted and identifie

The best resolution possible is often needed for this difficult task.

It must be recognized that the ability to distinguish pairs of small objects is not necessarily related to the photographic quality of single, isolated objects. Sharpness and resolution are not always related. The resolution of the ON and DP has been compared and analyzed.

5.7.2.1 Evaluation Parameters

All resolution readings analyzed are from 51/51 tribar mobile CORN displays. Both the ON and DP were read at 100X magnification using Wild microscopes.

Experienced readers were used, with the same observers reading both the original negative and the duplicate positive. Both the individual readers and the number of readers changed between buckets with a total of nine individual readers participating.

RV-1 contained seven cloud free CORN displays, the second bucket six, and the fourth bucket three. The targets were read in both the flight and scan directions on both cameras making a total sample size of 66 images for evaluation.

5.7.2.2 Evaluation Variables

Readings of resolution are subject to several sources of variability. The reliability of the results can be improved by minimizing the effects of these sources. Several procedures were used in this study to eliminate some of the variability.

Differences in scale due to slant height were corrected by converting ground resolution to lines/mm. Variability between readers of the same target was reduced by calculating a mean resolution for each target for the original negative and the duplicate positive. The difference between intervals over the 14 bar group range of the mission was equalized by determining the percent of change between the ON and DP. The mean and standard deviation were calculated for the percent change of all the targets. The following line graph shows a comparison of relative percentage change and resolution differences (lines/mm) between bar groups:

| | | | | | | | | | | |
|---|---|---|---|---|---|---|---|---|---|---|
| 9.9 | 10.5 | 12 | 14 | 16 | 17 | 20 | 22 | 25 | 28 | (lines/mm) |
| 12.3 | 12.7 | 11.8 | 12.3 | 12.5 | 11.8 | 12.4 | 12.2 | 12.2 | 12.3 | (%) |

For a sixth root of two target, the average change between bar groups is approximately 12 percent.

By treating the mean percent of change for the mission as the average difference between the ON and DP pair for each target, a "Student t" Test was performed to determine if the change in resolution from ON to DP is significant. Assuming that the distribution of resolution readings from the ON is normal, the "t" test will determine, with a certain level of confidence, if the difference between the means of the ON and DP readings is enough to indicate that they came from two separate populations.

The mean percent change in resolution between the ON and the DP for the mission is -0.7 percent (- denotes a loss) with a standard deviation of 9.5 percent. This change is not statistically significant with a 0.05 alpha risk (i.e., a five percent risk of saying the two means are from different populations when they are not). Therefore, with 95% confidence, it can be stated that there is no significant gain or loss in resolution for the DP from this mission. See Figure 5-13 for distribution of percent lost or gained for targets from this mission. The relatively small number of samples (16 frames out of a total of 6,883) prevented any meaningful comparison between buckets.

The range of percent change for all targets is from -18.6 percent to +25.1 percent throughout the mission. Figure 5-14 shows the mean percent change for each bucket and for the total mission within plus or minus two standard deviations of the mean.

For some targets the resolution reported by five readers varied by four bar groups (a change of 48 percent). Within some targets, the readers differed as to whether the resolution increased or decreased. For one target, one reader indicated a gain of 41.4 percent while another indicated a loss of 12.6 percent. Figure 5-15 shows the mean percent change between the ON and the DP for each bucket, for the entire mission, and plus or minus two standard deviations of that mean.

In this study, compensation was not made for possible variance introduced by the dupe emulsion batch, printers, or processing. Some forms of image degradations may lend themselves to enhancement by the duplication process more than others. Indications are that the greatest source of variability in resolution seems to be from differences in criteria between individual readers, since the range of percent change in resolution between targets is 43.7 percent, while the range between readers is 54 percent. These differences reduce the reliability of the resolution evaluation process and the ability to detect small changes.

### 5.7.3 Acutance

Acutance is an objective measure of sharpness, and is determined from the average slope of the microdensitometer trace of the edge. It indicates how well an edge has been reproduced in the image.

Ten sample edges were selected from the three buckets of Mission 1201. The samples consisted of roof tops and roof edges with an adjacent shadow area. The resulting change in density is 0.4 or greater. The regions on either side of the edge were examined for any changes in density level. The edges were traced on the Mann Trichromatic 1032T Microdensitometer with a 1 X 80 micron slit. The acutance was calculated using the normalized mean square slope formula with increments of 2.08 microns. For each edge, the difference of ON and DP acutance was found and a mean and standard deviation of the differences calculated. A statistical "t" test was performed to determine if a significant change in the mean difference between ON and DP had taken place.

The mean acutance for the ON is 0.0074. For the DP the mean is 0.0106. The mean difference between ON and DP is 0.0032 with a standard deviation of 0.0026. This difference is statistically significant and corresponds to an increase in DP acutance of 59 percent.

FREQUENCY DISTRIBUTION OF CORN TARGET

DERIVED DP RESOLUTION

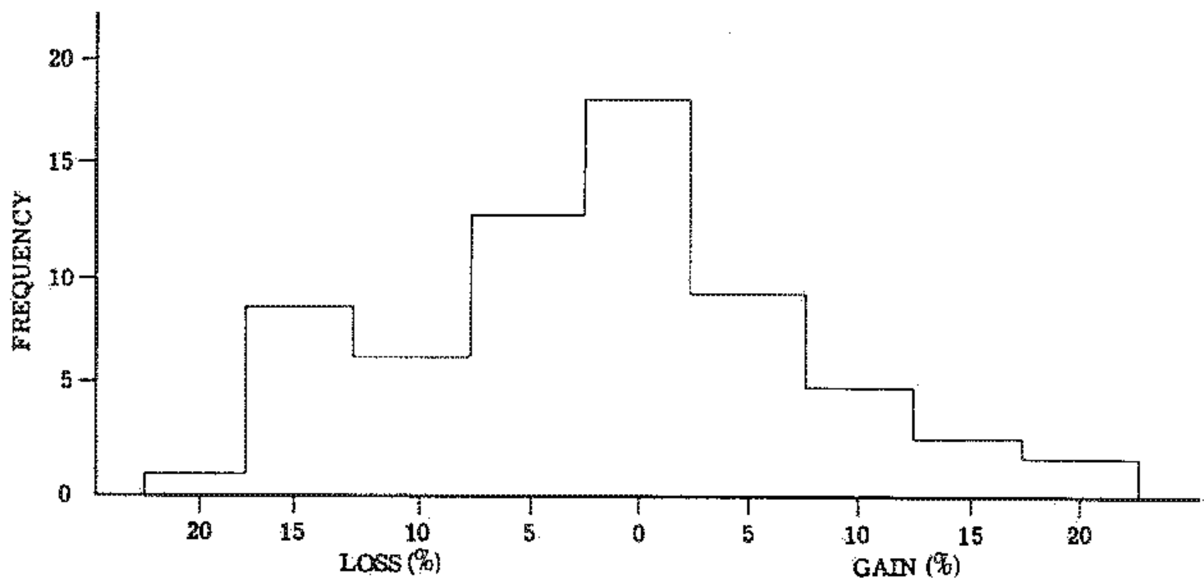


FIGURE 5-13

COMPARISON OF MEAN DIFFERENCE
BETWEEN ON AND DP

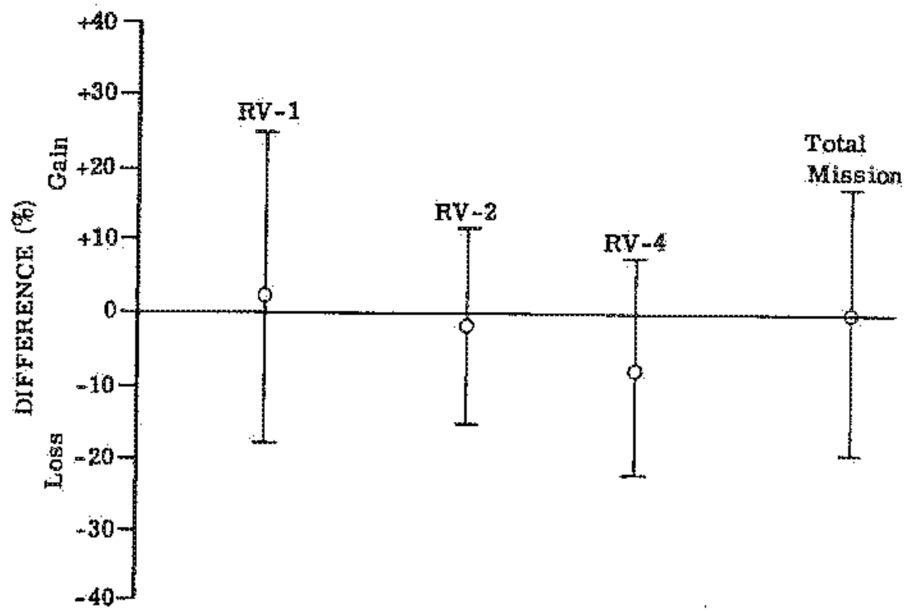


FIGURE 5-14

COMPARISON OF MEAN RESOLUTIONS

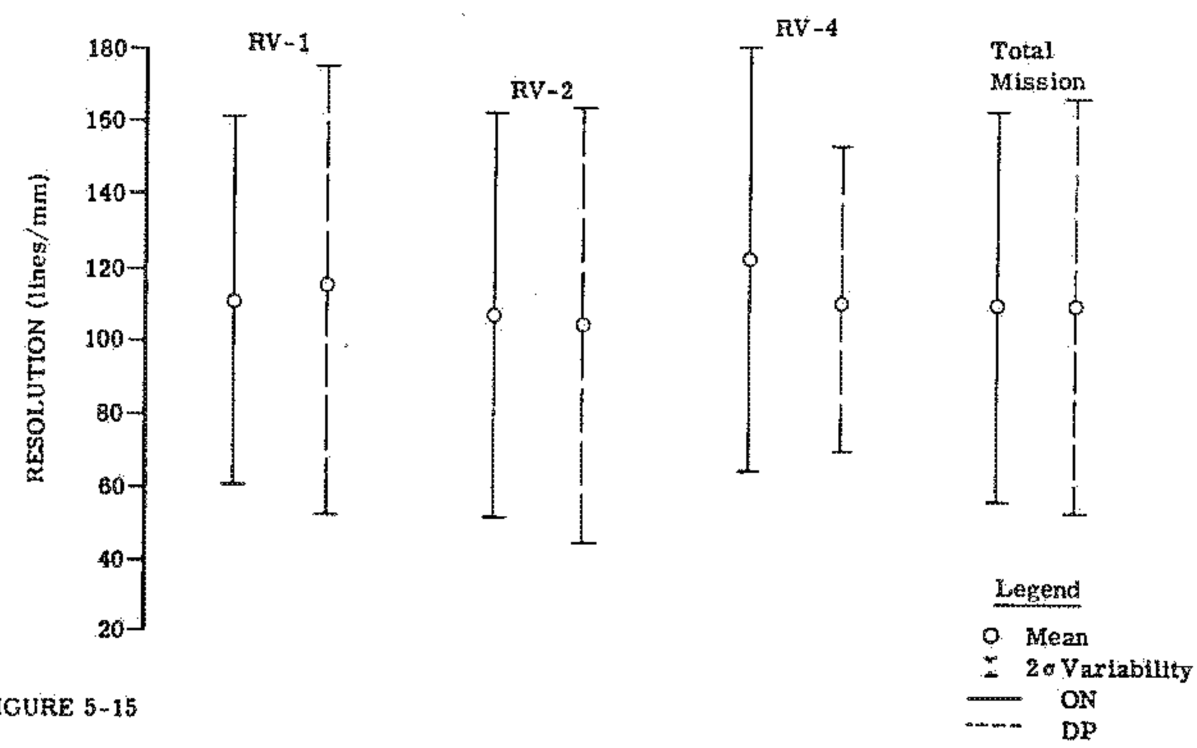


FIGURE 5-15

As a point of comparison, a special study was performed on Mission 1102 (TCS-20021/69) which indicated an average increase in acutance of 20 percent. It was determined that the increase in sharpness on the 1201 material was directly due to the edge-enhancement in processing.

5.7.4 Granularity

Granularity is the objective quality of an image associated with the non-uniformity of a uniformly exposed and processed area. Granularity limits the magnification to which an image can be viewed without serious effect on the appearance of the image. In a sense, granularity sets a limit to the detectability of a signal. Any additional granularity of the duplicate positive over that of the original negative may lower the signal-to-noise ratio of the image and in some cases could be responsible for a loss in information content.

Sixteen areas of apparently consistent density were chosen from operational imagery for a granularity analysis. These areas were building tops, airfield runways, and bodies of water. An attempt was made to choose areas with a range of mean density values. Both the ON and DP were traced using a Mann Trichromatic 1032T Microdensitometer with an effective aperture of 10 microns in diameter. The data was computer analyzed using an ensemble averaging technique. This technique was used with a sub-sample of 5 over approximately 300 samples and an alpha risk of $1.0 \times 10^{-5}$.

Figure 5-16 is a plot of the relative root mean square (RMS) granularity values for the two materials versus gross density of the materials. Due to the fact that the areas traced were not uniformly flashed areas, the absolute values of the RMS granularity may not be valid. The plot for SO-192 represents the combined granularity of the two materials. A direct comparison of difference in granularit of the two films at a given density cannot be easily determined due to the same subject on the ground having a different density on the DP than on the ON. An area of high density on the SO-192 has the granularity characteristics of the SO-192 at that density plus the low density granularity from the 1414 original negative.

5.7.5 Conclusions

A. On the basis of the sixteen targets evaluated, there is no significant change in resolution as a result of the duplication process.

B. There is an indication based on the ten sample edges that there is a significant increase (59%) in acutance in the DP.

C. The 16 samples selected for granularity analysis indicate an increase in granularity in the duplicate. An area of 0.9 density on both materials shows a noticeable increase in graininess on the duplicate positive.

D. Based on the overall evaluation of the photo quality measures, it has been determined that the PI received Mission 1201 DPs which are similar in image quality to that of the original negative.

GRANULARITY COMPARISON BETWEEN SO-192 AND 1414

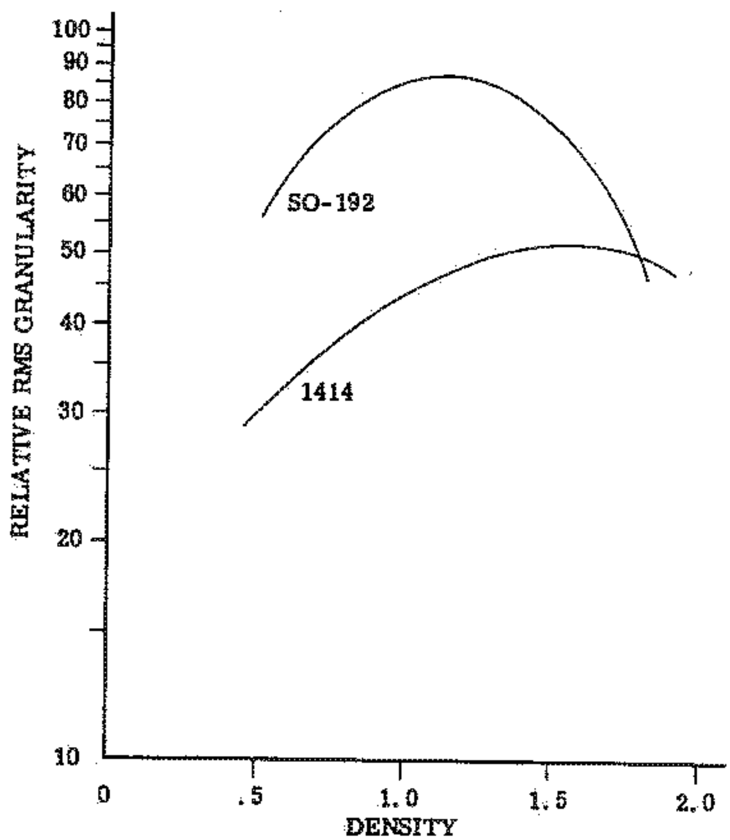


FIGURE 5-16

## 5.8 INTERPRETATION SUITABILITY VERSUS SCAN ANGLE

### 5.8.1 Introduction

The objective of this study is to determine the variability of interpretation suitability along the format of the 120 degree scan mode imagery in eight 15 degree scan angle sectors. Scan sectors 1-8 in a 120° scan mode are defined as follows:

| -60° | -45° | -30° | -15° | 0° | +15° | +30° | +45° | +60° |
|---|---|---|---|---|---|---|---|---|
| 1 | 2 | 3 | 4 | 5 | 6 | 7 | 8 | |

Special attention is directed toward the first (-60 to -45 degrees) and the last (+45 to +60 degrees) 15 degree scan sectors. As this is the first KH-9 mission, it should be noted that this first look analysis of the problem is based on a limited amount of data.

### 5.8.2 Procedures

To determine the PI suitability ratings versus scan angle of Mission 1201, all data in the OAK and OAK Supplements through Supplement 19, was obtained for the 120 degree scan mode operations. This resulted in 272 targets which were then divided into three main sets; OAK and OAK Supplements, Order of Battle, and Weather. Table 5-7 presents how these targets fell proportionately across the eight scan sectors.

TABLE 5-7

PERCENTAGE OF TARGETS BY SCAN SECTOR

| Scan Sectors | Percent |
|---|---|
| 1 | 11.0 |
| 2 | 12.5 |
| 3 | 11.0 |
| 4 | 9.1 |
| 5 | 11.8 |
| 6 | 15.2 |
| 7 | 16.4 |
| 8 | 16.0 |

As illustrated, each of the eight scan sectors contain approximately the same percentage of target ratings. The following discusses how the eight scan angle sectors vary in interpretability by OAK and OAK Supplement readouts, Order of Battle, and Weather.

#### 5.8.2.1 OAK and OAK Supplements

The OAK Report presents the results of first phase exploitation of satellite imagery, while the OAK Supplements contain second phase exploitation results. Both reports contain the basic information needed to examine interpretation suitability versus scan angle. Each target studied and its related data were extracted from the data base and tabulated into one of the eight scan sectors from -60 to +60 degrees The Weather rating was used to segregate clear targets from those obscured in any way by weather. Once the targets were segregated by weather, they were further separated by their quality ratings. Of the 899 frames acquired, 93 containing 272 targets were reported in the OAK and OAK Supplements. Of these 272 targets, 113 were in some way obscured by weather, leaving 159 clear targets. Table 5-8 presents the 272 targets divided by PI suitability ratings, and totals and percentages of total clear and obscured targets.

TABLE 5-8

SUMMARY OF TARGETS BY WEATHER CATEGORY

| PI Ratings | Clear | Percent of Total | Obscured by Weather | Percent of Total |
|---|---|---|---|---|
| Excellent | 0 | 0 | 0 | 0 |
| Good | 63 | 40 | 3 | 5 |
| Fair | 81 | 50 | 57 | 50 |
| Poor | 15 | 10 | 53 | 45 |

It should be noted that no Excellent ratings were given for clear photography, however, Good and Fair ratings outnumber Poor ratings 9:1, see Figures 5-17 and 5-18. The sixth scan sector contains the greatest number of Good ratings with the first sector containing the least. The Poors, in the eighth scan sector outnumber the Goods by 20 percent. When PI suitability is observed for other than clear weather, nearly the opposite is noted, see Figures 5-19 and 5-20. Approximately three percent of the total number of targets were reported to be Good. This compares to nearly 46 percent reported as being Poor. There were many more Poors reported in the first and eighth scan sectors than Goods. By comparing PI suitability with weather conditions for each scan sector, the results suggest that weather is a major factor in determining the interpretability of target imagery. This conclusion is further supported by comparing the Poor ratings at scan sectors one and eight for all weather conditions with the ratings for only clear weather conditions, see Figures 5-18 and 5-20.

5.8.2.2 Order of Battle (OB) Interpretability Ratings Versus Scan Angle

The Order of Battle for Mission 1201 was divided into three separate categories, Air, Ground, and Naval. The Air OB was further divided into aircraft and missile, because of the large number of targets sampled. In an attempt to show a relationship between interpretation suitability of a particular target type with its location in the format, the OB targets along with their suitability ratings are tabulated by frequency of occurrence in their corresponding one thru eight scan angle sectors, see Figure 5-21. Examining OB in terms of quantity, we find that scan angles to the right of nadir contain the

OAK TARGET SUITABILITY RATINGS FOR

CLEAR WEATHER CONDITIONS

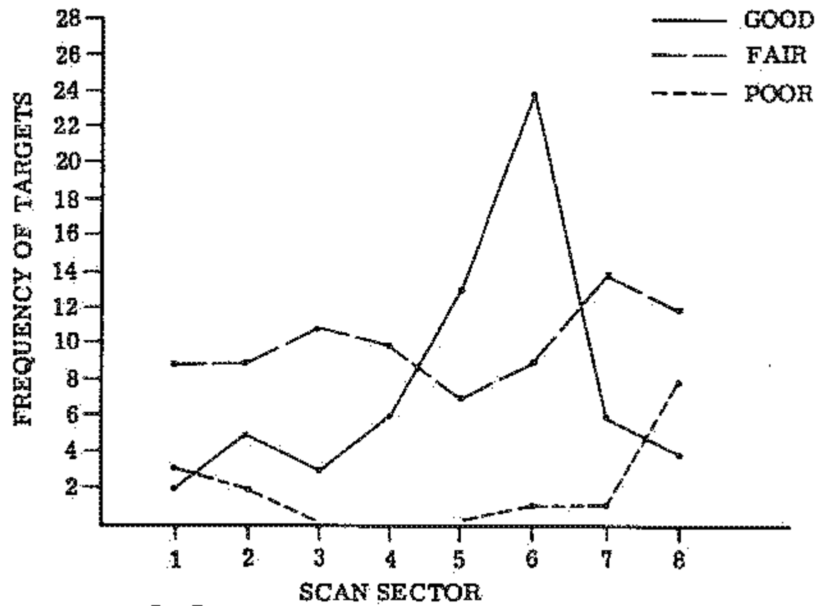


FIGURE 5-17

% OF OAK TARGET QUALITY RATINGS

FOR CLEAR WEATHER CONDITIONS

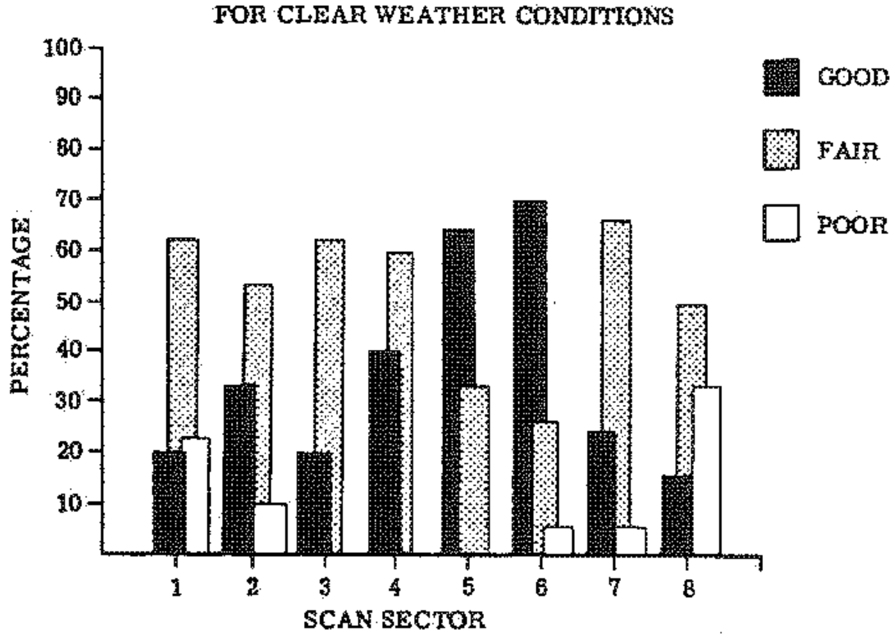


FIGURE 5-18

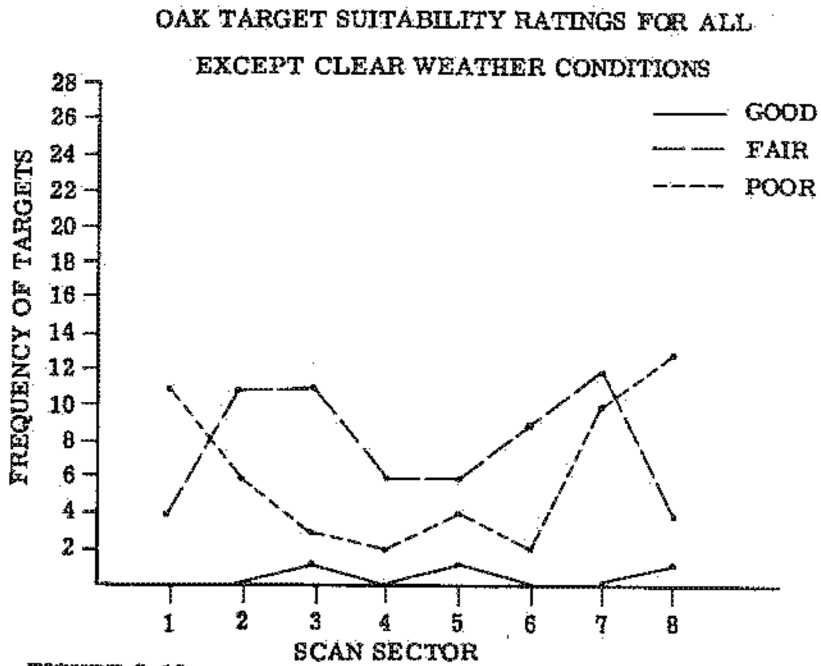


FIGURE 5-19

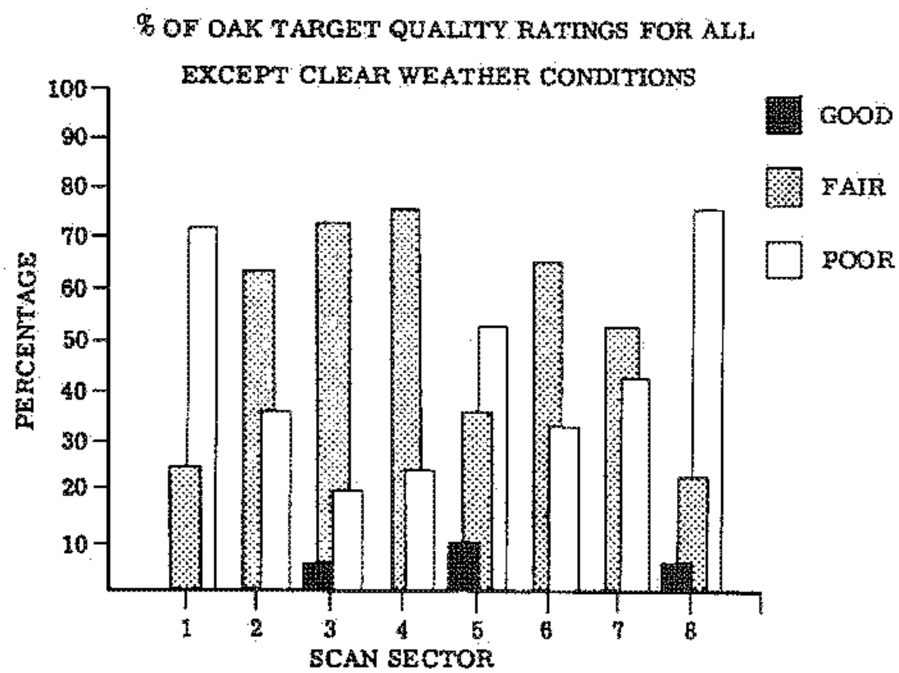


FIGURE 5-20

FIGURE 5-21

SCAN ANGLE VERSUS FREQUENCY OF ORDER OF BATTLE TARGETS FOR CLEAR WEATHER CONDITIONS

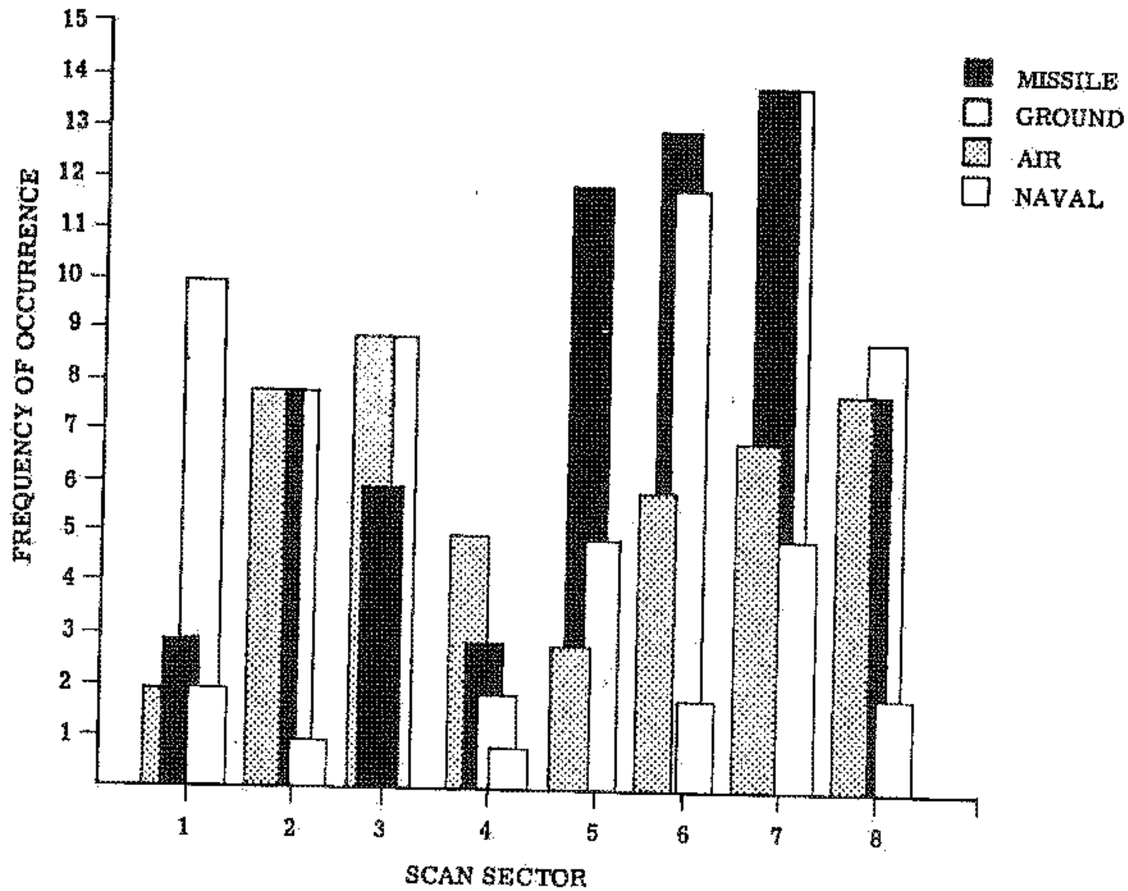

most targets. Missile OB has the highest total with naval OB the lowest. Turning attention to suitability, it is found that aircraft OB has the highest percentage of Goods in the sixth scan sector but very few are found in other scan sectors, see Figures 5-22 and 5-23. Most of the eight scan sectors produced targets of fair interpretability with the first and eighth scan sectors containing the most Poor ratings. Looking at missile OB we find most Good ratings in the fifth and sixth scan sectors with the most Poor ratings falling in the seventh and eighth scan sectors, see Figures 5-24 and 5-25. As with aircraft and Missile OB, ground OB has more Good ratings in the sixth scan sector, see Figures 5-26 and 5-27. Poor ratings are generally confined to the outer scan sectors. The naval OB category contained so few targets that no study of these targets was possible. Reviewing Order of Battle in its entirety, some general observations can be made:

A. Few targets were recorded at 0° scan.

B. Most targets were recorded at the outer scan angles with 23 percent of the total targets recorded falling in scan sectors one and eight.

C. The greatest number of targets were recorded in the sixth and seventh scan sectors.

D. The highest percentage of Good ratings fell in the sixth scan sector with very few in the seventh scan sector.

E. The highest percentage of Poor ratings fell in the outer scan sectors, notably the eighth.

5.8.2.3 Weather

A comparison of the weather readout conducted by the NPIC "Tiger" Team with the data collected to study target interpretability by scan sector supports the suspected effect that weather has on target interpretability. This observation is consistent with the resolution as a function of scan angle analysis reported in Section III.

Scan sectors that contained a high percentage of Good suitability ratings were the clearest while sectors with high levels of cloud cover received Poor suitability ratings.

5.8.3 Conclusions

A. Table 5-9 represents a ranking by interpretability of the eight scan sectors of the 120 degree scan mode.

TABLE 5-9

INTERPRETABILITY RANKING BY SCAN SECTION

| Interpretability | Scan Sector |
|---|---|
| Best | 6 |
| | 5 |
| | 4 & 7 |
| | 3 |
| | 2 & 8 |
| Poorest | 1 |

SCAN SECTOR VERSUS FREQUENCY OF AIR OB
FOR CLEAR PHOTOGRAPHY

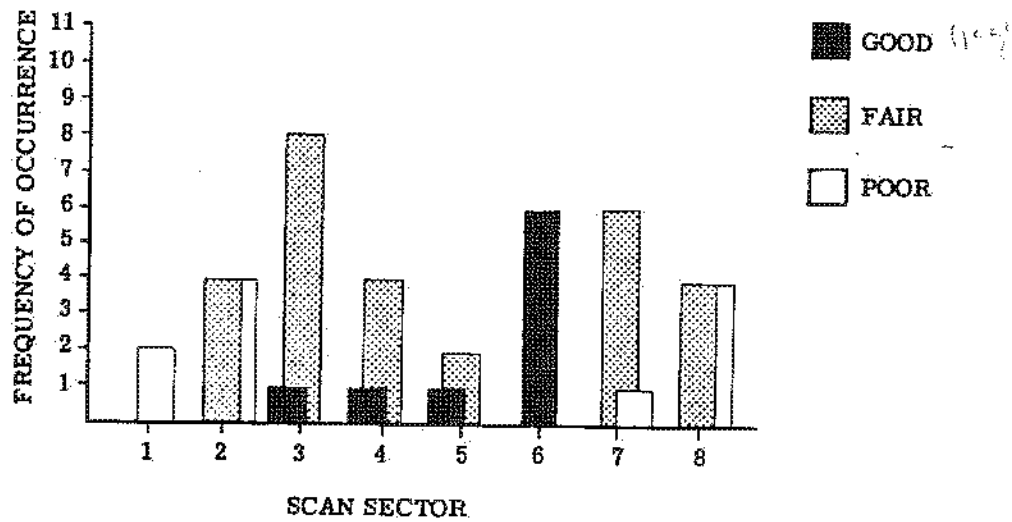


FIGURE 22

SCAN SECTOR VERSUS % OF TARGET
SUITABILITY RATINGS FOR AIR OB

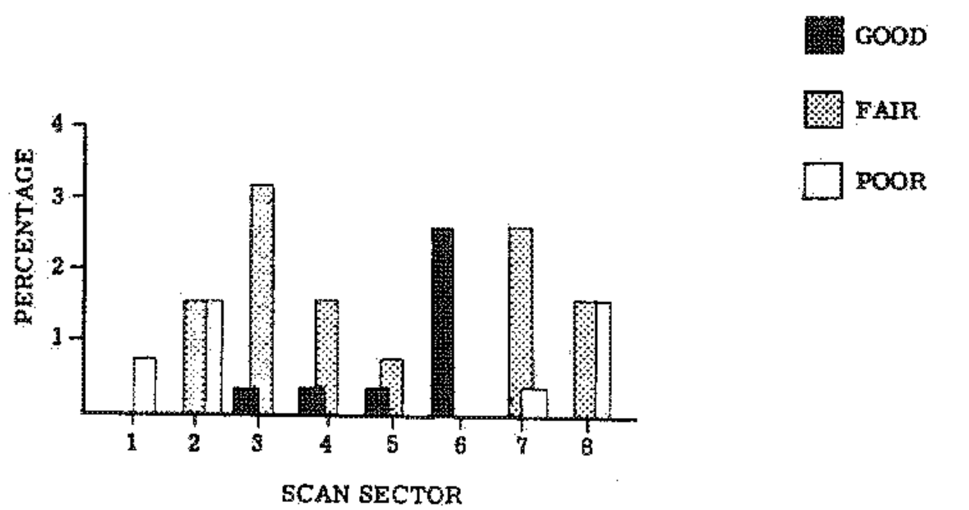


FIGURE 23

SCAN SECTOR VERSUS FREQUENCY OF MISSILE
OB FOR CLEAR PHOTOGRAPHY

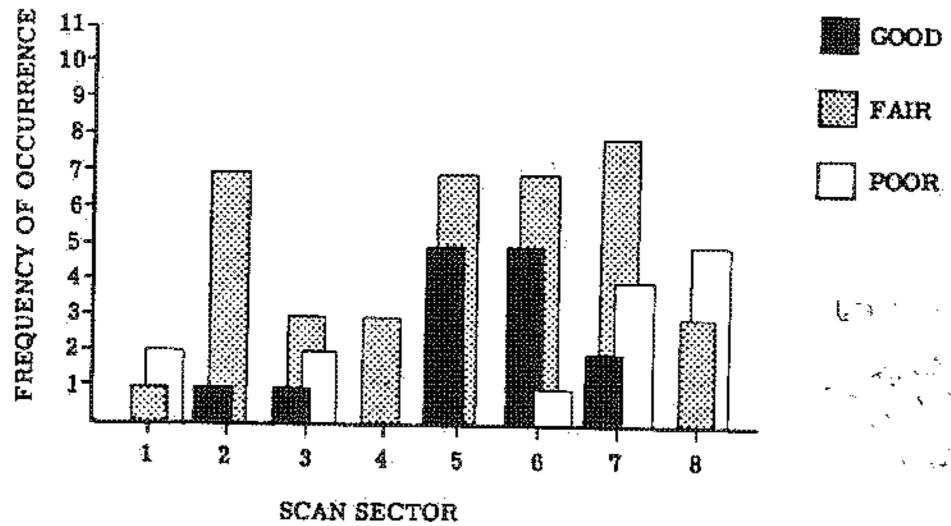


FIGURE 5-24

SCAN SECTOR VERSUS % OF TARGET SUITABILITY
RATINGS FOR MISSILE OB

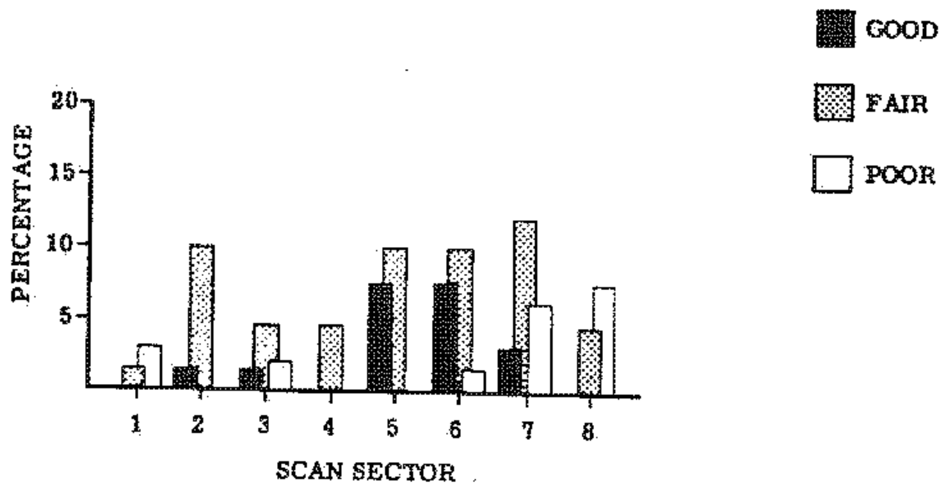


FIGURE 5-25

SCAN SECTOR VERSUS FREQUENCY OF GROUND OB FOR CLEAR PHOTOGRAPHY

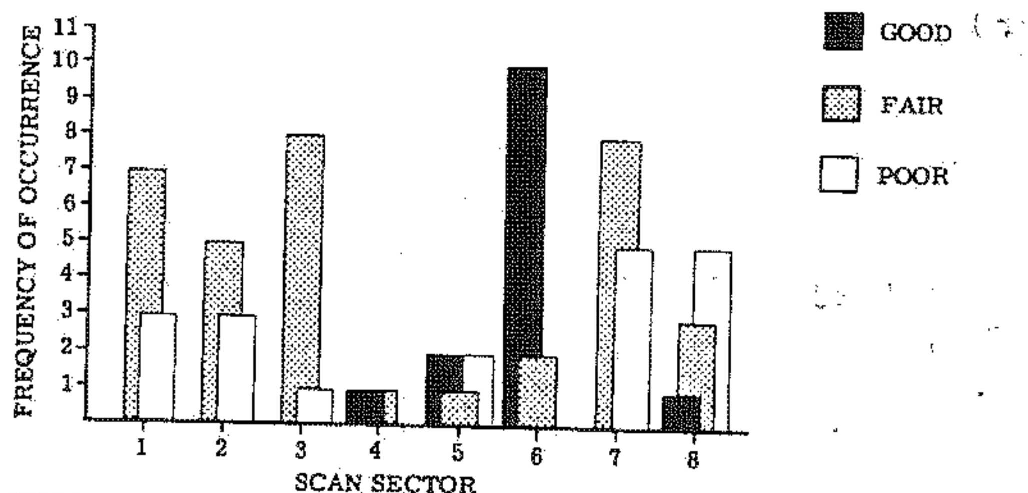


FIGURE 5-26

SCAN SECTOR VERSUS % OF TARGET SUITABILITY RATINGS FOR GROUND OB

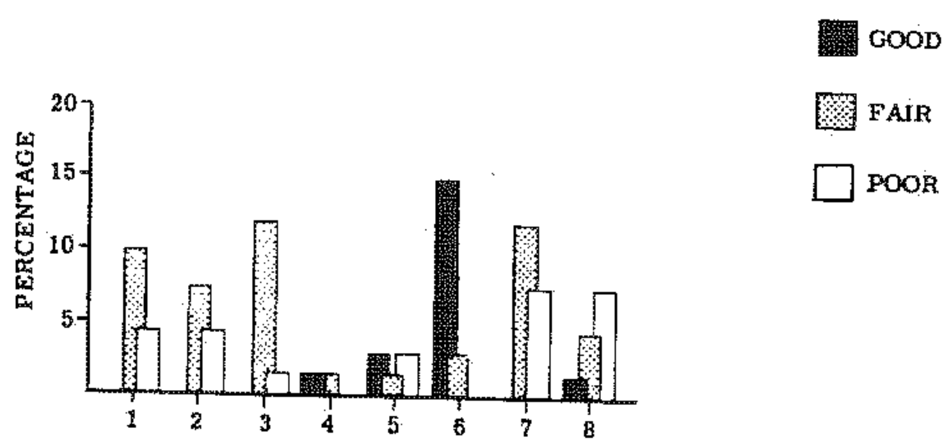


FIGURE 5-27

The following, in order of significance, are some of the interrelated factors that contributed to the ranking of these targets at the 120 degree scan mode:

(1) The greatest effect upon the interpretation suitability of a target is weather. Forty-five percent of all photography obscured in some way by weather was rated as Poor, while only nine percent of clear targets were rated as Poor. Conversely, only three percent of all targets obscured in some way by weather were rated as Good.

(2) Scan sector six has the largest number of clear targets and contains the most targets rated Good. This is also the sector that contains, according to the VEM analysis, the highest overall resolution on the Forward-looking Camera.

(3) 0° scan imagery contained the least number of read out targets.

(4) The outer scan angles contain the highest number of Poors, due mainly to weather.

(5) Very few naval OB targets were acquired.

(6) Twenty-three percent of all OB targets are located within the first and eighth scan sectors.

(7) Thirty-eight percent of the total targets acquired on the mission in the 120° scan mode were located in scan sectors one thru four. Ten percent of these targets were rated Good and three percent Poor. Sixty-two percent of the total targets were located in scan sectors five thru eight. Thirty percent were rated as Good and six percent as Poor.

B. This represents the first attempt to answer the interpretability versus scan angle question. The results thus far are based on one mission under near ideal acquisition conditions. A much more representative sample will have to be taken on subsequent missions to more definitively answer the question. Factors such as solar elevation, weather conditions, and lower altitudes (larger average scales) will no doubt affect the average mission's interpretation suitability versus scan sector profile.

C. Mission 1201 imagery from the high scan angles did provide useful information to the photointerpreters. Although the imagery did not contain the detail of that acquired near zero scan, interpretation tasks related to area search could be performed.

D. Some OB targets could be read out at the outer scan angles, however, not to the completeness of imagery toward the center of format.

E. Figures 5-28 thru 5-35 represent examples of PI suitability ratings of selected frames located at specific angular positions (center and two extremes) across the format of the 120° scan mode. All imagery was selected from the Forward Camera of Mission 1201 and the photographs enlarged 20 times (20X).

3.3(b)(1)

3.3(b)(1)

[redacted]

3.3(b)(1)

3.3(b)(1)

3.3(b)(1)

3.3(b)(1)

3.3(b)(1)

3.3(b)(1)

## 5.9 SPECULAR REFLECTIONS

### 5.9.1 Introduction

Specular reflections (halation) occur when highly reflective objects are photographed with the solar and ground azimuth aligned and the solar elevation is equal to the angle of view. These conditions cause the worse case of occurrence. Visually, the effect obscures objects in close proximity to the reflection, produces unsharp edges, and bloomed objects, thereby reducing the detectability of edges.

### 5.9.2 Evaluation

The occurrence of many specular reflections on this mission indicated the possibility of an occurrence pattern. Preliminary investigation of CRYSTAL BALL data indicated the worse case of occurrence would be in the area of +20° scan on the Forward-looking Camera. CRYSTAL BALL is a photometric orbital acquisition model which includes computations of most geometric quantities of interest. Data also indicated that the worse case should occur at approximately 38° latitude. This is illustrated in Figures 5-36 and 5-37 of Worden, Illinois, and Figures 5-38 [redacted] Both are in the area of predicted worse case at aprx 39° latitude and +20° scan on the Forward-looking Camera. The increased severity of the specular reflections at these two locations as compared to that experienced at [redacted] scan on the Forward-looking Camera is clearly evident, see Figures 5-40 and 5-41. This type of subjective data shows the reliability of CRYSTAL BALL as a means of predicting occurrence. A measure of the severity may be possible by relating four parameters as output from CRYSTAL BALL using the following equation:

3.3(b)(1)

$$\text{Cos BIDEC} = \text{Cos}\,|\text{AOR-SA}|\ {*}\text{Cos}\,|\text{LHEAD-AZ}|$$

Where BIDEC is the angle of interest, as it becomes smaller the severity increases.

AOR is angle of reflectance.

SA is solar altitude.

LHEAD is look heading.

AZ is ground azimuth.

A CRYSTAL BALL run was made for 15 frames from Op 115 of Mission 1201. A comparison of the severity of the reflections and the prediction of severity using the BIDEC angle seems to indicate agreement. The BIDEC angle is minimum on Op 115 at aprx 38° N latitude; however, a definite statement cannot be made about the area of worse case. That is because no reflections were evident as the ground image consisted primarily of forest lands which are not of a highly reflective nature. Figures 5-36 and 5-40 show the severity at 38° N latitude and are in agreement with the BIDEC angle predictions.

Reflections imaged from the Aft-looking Camera seem to occur much less frequently and with much less intensity than the reflections on the Forward-looking Camera imagery.

Because specular reflections were not associated with any particular type of target but with scan angle position and latitude, all statements relating to the effect on interpretability are of a general nature.

SPECULAR REFLECTIONS AT WORDEN, ILLINOIS

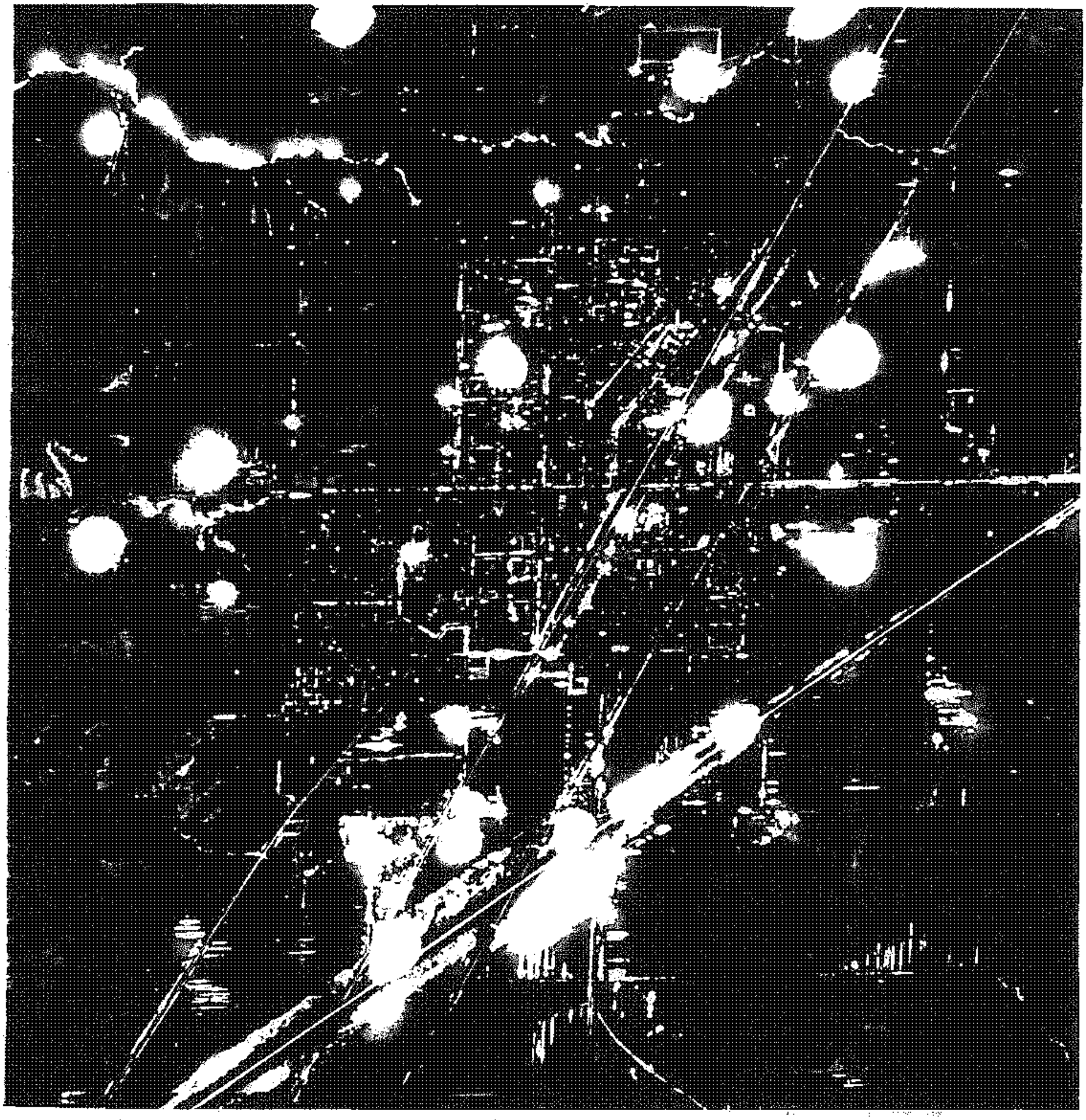

MISSION 1201-1 FWD CAMERA OP 034 FRAME 027 10X ENLARGEMENT

FIGURE 5-38

WORDEN, ILLINOIS

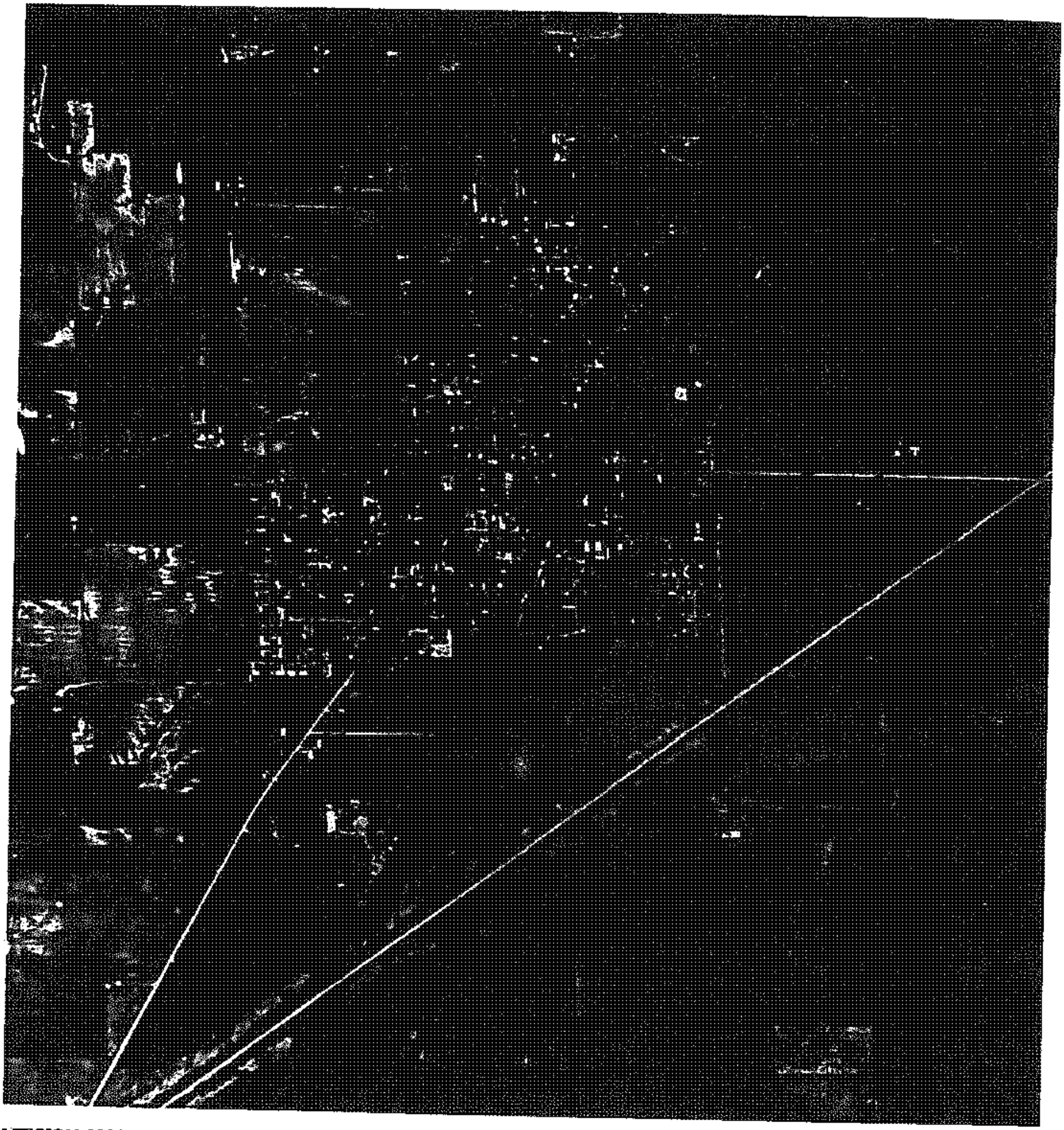

MISSION 1201-1 AFT CAMERA OP 034 FRAME 028 10X ENLARGEMENT

FIGURE 5-37

3.3(b)(1)

[redacted]

3.3(b)(1)



Approved for Release: 2022/03/03 C05132845

3.3(b)(1)

3.3(b)(1)

[redacted]

Isolated instances occur where specular reflections are a problem but the total complaints are few.

Specular reflections on stereoscopic coverage are not as serious a problem to the interpreter as those on monoscopic coverage. Stereo coverage gives two different looks at a target with the degradation being more severe on the Forward coverage. The readout of Forward monoscopic coverage near plus 20° of scan would be severely affected by specular reflections.

As a result of the sun synchronous orbit and the launch time for Mission 1201, there is a predominance of specular reflections at 35° to 40° N latitude on the Forward-looking Camera at plus 20° scan. The severity decreases with higher Northern latitudes.

A CRYSTAL BALL run based on a two hour earlier launch time indicates that in the area of worse case on Mission 1201, specular reflections would be much less severe than those experienced. Some occurrence of reflections might be expected in the area of 40 to 45° N latitude at +40° scan, but the severity would probably be less than that experienced on Mission 1201.

As shown on the target complex map, Figure 5-42, there is a heavy belt of targets from 35 to 40° N latitude which encompasses the area of worse case. If difficulties become evident due to specular reflections, a change in launch time would change the position of worse case but this would be possible only during the summer months. If a change in launch time is considered, some thought should be given to shifting the worse case area to fall in the region between 40° and 45° N latitude. Occurrence in this area would probably affect fewer targets than at its present location.

3.3(b)(1)



Approved for Release: 2022/03/03 C05132845

 ~~CRET RUFF~~

Handle via ~~Talent-Keyhole~~
Controls Only

# Special Studies

Handle via ~~Talent-Keyhole~~
Controls Only

~~TOP SECRET RUFF~~

# SECTION VI

# SPECIAL STUDIES

## 6.1 LINE TARGET ANALYSIS TECHNIQUE

### 6.1.1 Background

Experience gained with the line focus/motion analysis for KH-9 acceptance testing indicated that the same type of image motion analysis would be useful for analysis of the operational photography. The technique employed for Mission 1201 was to use special line targets included in some mobile CORN deployments. These lines are effectively narrower than the camera optical spread function on the ground and constitute an effective line impulse energy distribution. The line paints a signature of the one-dimensional system spread function when scanned by the camera slit. This image is traced with a microdensitometer and processed mathematically to yield both an estimate of the system transfer function and a plot of the image motion during the exposure.

### 6.1.2 Target Description

The Line Target designed for KH-9 analysis consists of a 150 ft x 50 ft nylon panel coated to a reflectance of approximately 4%, and a 150 ft long, 12" wide white strip with a reflectance of approximately 90% which is laid over the black panel. The contrast of this target is approximately 18.5:1. The line width was chosen to provide enough image-forming energy for an adequate signal-to-noise ratio in the developed image. Figure 6-1 shows a typical CORN display.

### 6.1.3 Random Lines

In an effort to expand the line data base, a search was made of the 1201 NOFORN material for runway centerlines which might be of adequate quality for tracing. Lines chosen were of high apparent contrast, usually on large airports where the middle of the runway would contain minimum tire marks. Other lines were chosen on small airports with black asphalt runways. Line widths were assumed to be one foot for basic runway markings, and three feet for instrument and all-weather runway markings. Figure 6-2 shows a representative all-weather runway.

### 6.1.4 Data Acquisition and Handling

#### 6.1.4.1 Microdensitometry

Tracing was accomplished on two Mann-Data Micro-Analyzers, one at BRIDGEHEAD and one at AFSPPF. The optical configuration of the BRIDGEHEAD machine uses a micro-slit attachment where the scanning aperture is projected on the film, and light is collected by a condensing system below. The AFSPPF machine uses the standard configuration of an illuminating preslit which overfills the collecting aperture, and a scanning slit in front of the photomultiplier which generates the scanning aperture on the collecting side. All tracing was done using a 1 x 80 micron slit with .5 micron sample spacing. Both organizations corrected the specular density outputs of their machines to equivalent diffuse densities by

TYPICAL CORN TARGET DISPLAY

MISSION 1201-4 FWD CAMERA OP 384 FRAME 002 40X ENLARGEMENT

FIGURE 6-1



Approved for Release: 2022/03/03 C05132845

3.3(b)(1)



Approved for Release: 2022/03/03 C05132845

calibrating against a mission process control step wedge which had been read on a diffuse densitometer.

6.1.4.2 Data Handling

The PFA Team identified those CORN line targets which were traced from each mission segment. The BRIDGEHEAD personnel performed the microdensitometry, processed the data through a program which calibrated the microdensitometer values and performed a preliminary edit, and prepared header cards. The data deck was then sent to AFSPPF via data link and processed on an IBM 360/40. A printer-image output tape was returned to the PFA via data link for analysis. Upon receipt of the ON, AFSPPF traced all CORN and selected and traced the random lines from the entire mission.

6.1.5 Line Analysis Program Theory

6.1.5.1 General

The line motion analysis program (PFALINES) represents the latest in an evolutionary series of line analysis programs. It consists of two major functional divisions and a number of smaller logical sections. The first division converts the data to effective exposure, edits for bad traces, and generates the system MTF. The second division performs the motion analysis on the MTF data.

6.1.5.2 Sensitometric Conversion

Since the primary objective of this program is to analyze the camera performance, the effects of the recording film must be removed. This is done by converting the density data to "effective exposure" by projecting density values through the process D log E curve. However, due to the dual gamma process, an additional computation is necessary in order to obtain a more reasonable conversion. Due to adjacency effects, the effective contrast of images increases with decreasing image size, finally approximating the Trenton-Full characteristic for images less than 10 microns wide. In an attempt to compensate for non-linear behavior, the program modifies the density-exposure conversion table by finding the maximum gamma point on the process D log E curve and extends this slope as a straight line from that point.

6.1.5.3 Data Editing

To suppress the effects of noise, multiple non-overlapping traces are made. Due to microdensitometer alignment difficulties, each line may not be in the same place in the data block. The program performs a cross-correlation between individual traces, based on the method of least squares, to determine optimal alignment. In addition, this technique allows individual traces to be tested against the others for relative error, and allows those traces which exceed a preset error to be rejected. After the proper alignment is achieved and bad traces are rejected, the effective exposure data traces are averaged. To further reduce noise and improve accuracy, several additional edit steps are taken, including removal of the density pedestal upon which the line sits, and a weighted smoothing of the line background data to suppress high frequency grain noise.

6.1.5.4 Fourier Analysis

The Fourier Transform of the edited exposure data is calculated using Fast Fourier Transform techniques, and further smoothing is accomplished on the resultant data. This data represents the MTF of the system combined with the film response and effects of the target. The program now divides out a film MTF. The film MTF in use at this time was derived from line-trace data during KH-9 acceptance testing. It represents the most reasonable estimate to date of the film-process-microdensitometer response for narrow lines.

6.1.5.5 Line Target Removal

The technique which permits the calculation of the MTF of an optical system is based on the system response to an impulse, which can be represented in one-dimension as an infinitely narrow line. Since the line target has a finite width, the transform of this line must be removed from the composite MTF. This transform takes the form of a "sinc" function, or $\sin(\pi wf)/\pi wf$. The known line width is combined with the apparent scale factor to give the line width on the film. The sinc function is calculated from this value. Dividing by a sinc function can cause problems because of the periodic zero values, so a variable width averaging technique is employed to avoid these zero values. This method tends to suppress output variations in the region of the zero values, but such effects usually appear only at the higher spatial frequencies where such loss is not critical.

6.1.5.6 Image Motion Analysis

The resultant MTF of the camera system consists of two major components: (a) The response of the optics, and (b) degradations due to image motion (smear). If the MTF of the optics is known for a given focal position, field angle, and orientation, it may be removed from the system MTF by division, leaving the transfer function of the residual image motion. This motion may have constant velocity (linear smear), in which case its transfer function is a sinc function. It may also change its velocity with time in a non-linear fashion, which gives a complex transfer function. The program, therefore, divides out the lens MTF for a given platen setting, field angle, and orientation (in or cross-track). The resulting transfer function is compared to a large "lookup" table which contains transfer functions which would be generated by varying amounts of linear and non-linear image motion. The best fit between the two is found by the least squares method. The results are presented as the amount of apparent smear in microns and a time history plot of the image motion that could have occurred during the exposure.

6.1.5.7 Smear Model

The present program assumes a non-linear image motion model of the form $s(t) = a_1 t + a_2 t^2$. This model contains a linear term with coefficient $a_1$, and a non-linear term with coefficient $a_2$. The range of values of the coefficients determine the relative linearity of the motion described, e.g., if $a_1$ were zero and $a_2$ some value, the motion would be entirely non-linear, whereas if $a_2$ were zero and $a_1$ some value, the motion would be entirely linear. This model describes motions of a quadratic nature. Other types of motion might occur, however, and not be described by this model. The types of smear seen on the KH-9 System have ranged from purely linear to random vibration. Linear smear is defined as a constant difference in speed between the film and the image. Random image motion (vibration) occurs when the relative velocity of film and image changes suddenly several times during the exposure.

6.1.5.8 Smear Presentation

The original method was to calculate the position of the image at the end of the exposure time, using the motion from the best fit case, and record the difference between the initial position and the final position as smear. It was chosen to attempt a correlation with other smear measures used during acceptance testing. This method was suspected of being unsatisfactory because it ignored the instantaneous motion of the image during the exposure interval. The current method assumes that the visual effect of various non-linear image motions may be characterized by a function which moves smoothly away from zero relative motion at some time during the exposure. This model appears to be more satisfactory than the previous method, but research and testing are continuing. Figure 6-3 shows examples of the smear presentation for both the old and new smear models.

6.1.6 Smear Data Analysis

6.1.6.1 General

For the sake of comparison, and to incorporate program improvements, all CORN line trace data were processed several times. The various conditions are presented in Table 6-1.

TABLE 6-1

CORN LINE DATA PROCESSING SPECIFICATIONS

| Case | Data | Motion Solution | Film MTF | AIM Curve |
|---|---|---|---|---|
| 1 | BRIDGEHEAD | Old | Acceptance | Spec |
| 2 | BRIDGEHEAD | New | Acceptance | Spec |
| 3 | AFSPPF | New | Acceptance | Spec |

The old and new motion solutions are discussed in paragraph 6.1.5.8. The random line data was processed the same as Case 3 above. Due to uncertainties in the data and processing technique, all the above cases are considered to be estimates.

6.1.6.2 Smear Characteristics

The Forward-looking Camera exhibited the greater variability of smear during the mission. This fact was expected from results of the acceptance testing. The smear in the scan direction showed great variability, being very evenly spread from values of 1 to greater than 10 microns in essentially random order. The flight smear was more normally distributed, with an average value of aprx 3.5

## SMEAR MODEL PRESENTATIONS

### OLD MODEL

SMEAR = 0.0 MICRONS

COEFFICIENTS ARE -14.66 AND 14376.61

RMS FIT ERROR = 0.0603

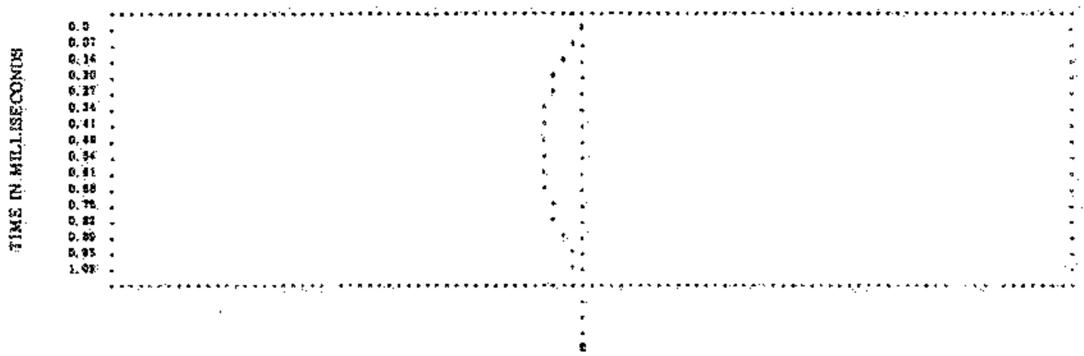


PLOT OF IMAGE DISPLACEMENT VERSUS TIME IN MILLISECONDS. MOTION IS IN MICRONS AND DESIGNATED +

### NEW MODEL

SMEAR = 3.300 MICRONS

COEFFICIENTS ARE 0.98 AND 2398.10

RMS FIT ERROR = 0.0591

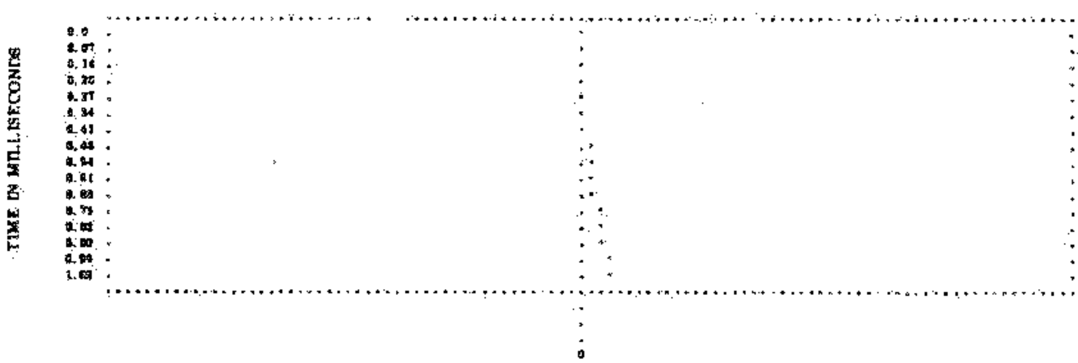


PLOT OF IMAGE DISPLACEMENT VERSUS TIME IN MILLISECONDS. MOTION IS IN MICRONS AND DESIGNATED +

FIGURE 6-3

microns. The Aft-looking Camera was better behaved throughout the flight, with both flight and scan smear approximately normally distributed. Mission average CORN smear data is presented in Table 6-2.

TABLE 6-2

LINE SMEAR DATA

| Camera | Direction | $\overline{X}$ | s | Worst |
|---|---|---|---|---|
| Fwd | Flight | 3.5μ | 2μ | 6μ |
| Fwd | Scan | 6μ | 3μ | 9μ |
| Aft | Flight | 2.5μ | 1.5μ | 4μ |
| Aft | Scan | 3.5μ | 2μ | 6μ |

NOTES:

1. $\overline{X}$ = Average of absolute value of smear estimates.
2. s = Standard deviation using small sample.

Figure 6-4 shows the smear frequency distributions for Case 2. The other two cases showed similar distributions, although not exactly of the same shape. The reported smear values are averages of the estimates from all three cases. One should also remember that the smear values were measured over a one millisecond exposure time, creating uncertainties in the data due to a short sampling period.

6.1.6.3 Smear Data Trends

Figures 6-5 thru 6-7 show a chronological plot of smear values by camera operation taken from random line data. Vertical dashed lines indicate where changes in operational focus were made. The apparent trend in both cameras at both orientations is one of decreasing average smear and variability as the mission progressed. There are at least three possible explanations for this:

A. Camera smear performance improved throughout the mission.

B. There is an uncertainty in optical MTF application.

C. The possibility that the current method of modeling smear does not account for all motion combinations.

6.1.6.4 Smear Correlation with CORN Tribar Resolution

Figures 6-8 and 6-9 show Case 1 smear estimates versus CORN tribar resolution uncorrected for apparent contrast. Smear values were determined from line targets in the same display from which tribar targets were read. The correlation is generally good, with the data spreading somewhat at low smear high resolution values. This spread is expected because as smear decreases to small values (approximately 1-4 microns), other degradations and variations in camera performance cause more significant effects on image quality. Figures 6-10 and 6-11 show a similar plot for Case 2, which employed the new motion description, see paragraph 6.1.5.8. The correlation and pattern are similar, with the major difference being that the new model does not predict very low smear values at moderate

FIGURE 6-4

SMEAR FREQUENCY DISTRIBUTIONS

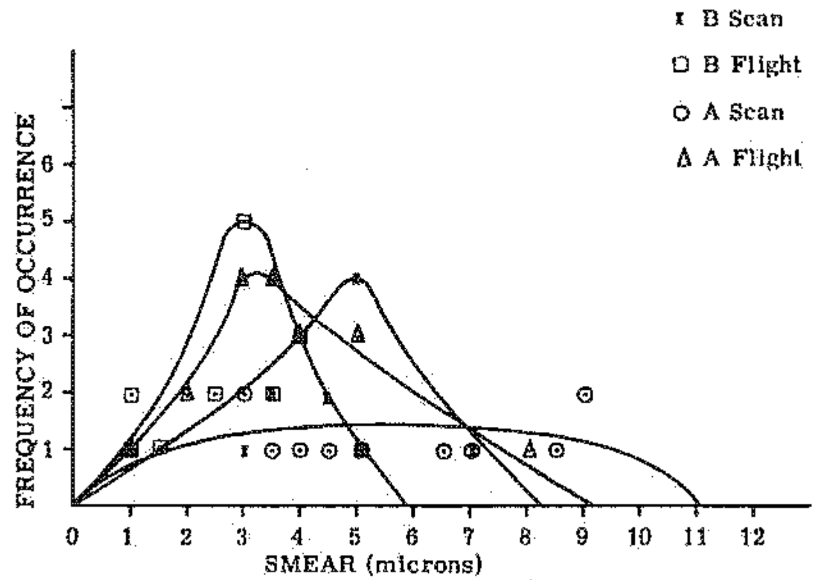

FIGURE 6-5

FORWARD CAMERA RANDOM LINE SMEAR IN BOTH DIRECTIONS

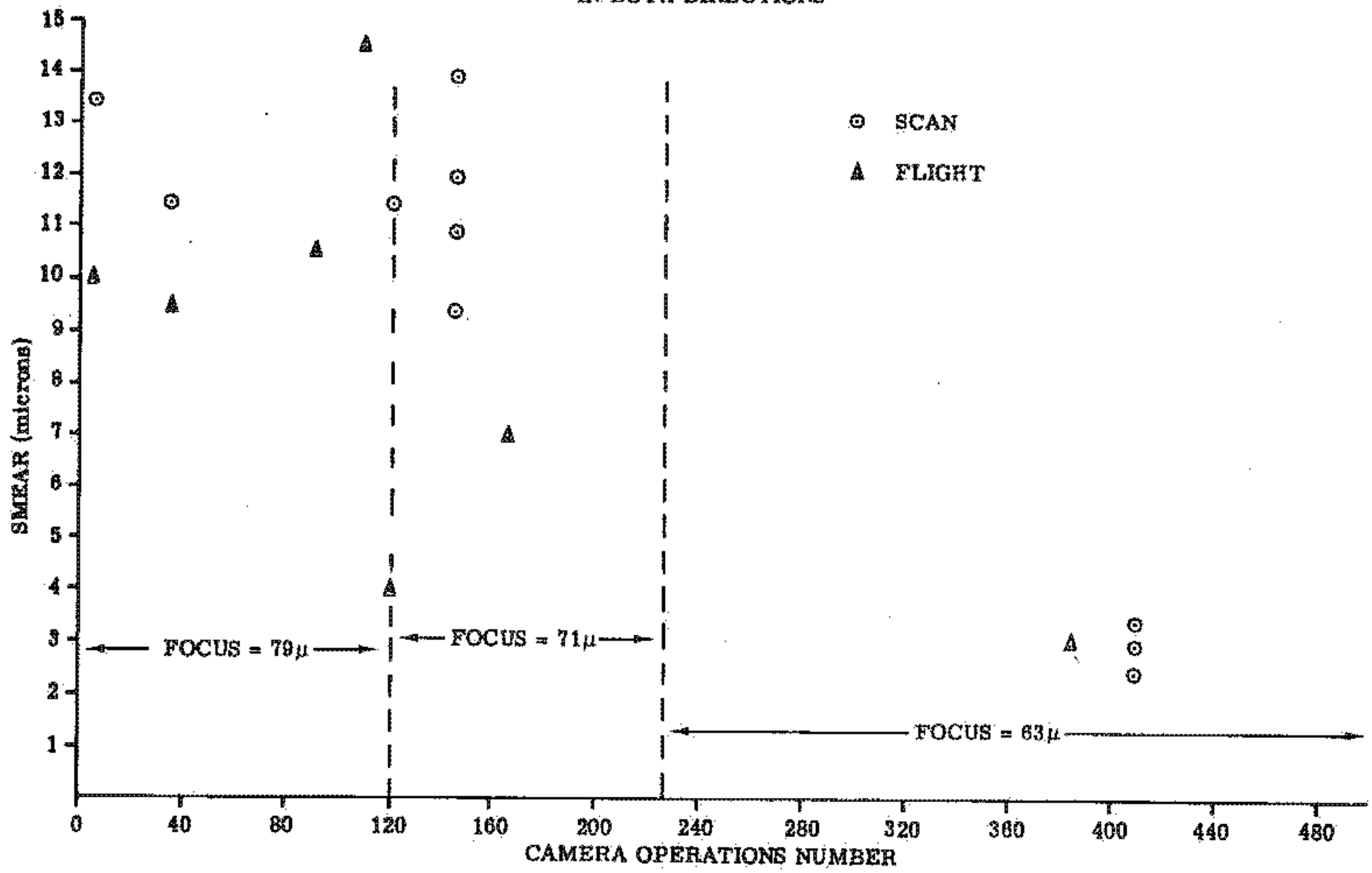


TOP SECRET RUFF

Handle via Talent-Keyhole Controls Only



Approved for Release: 2022/03/03 C05132845

FIGURE 6-6

AFT CAMERA RANDOM LINE SMEAR
IN SCAN DIRECTION

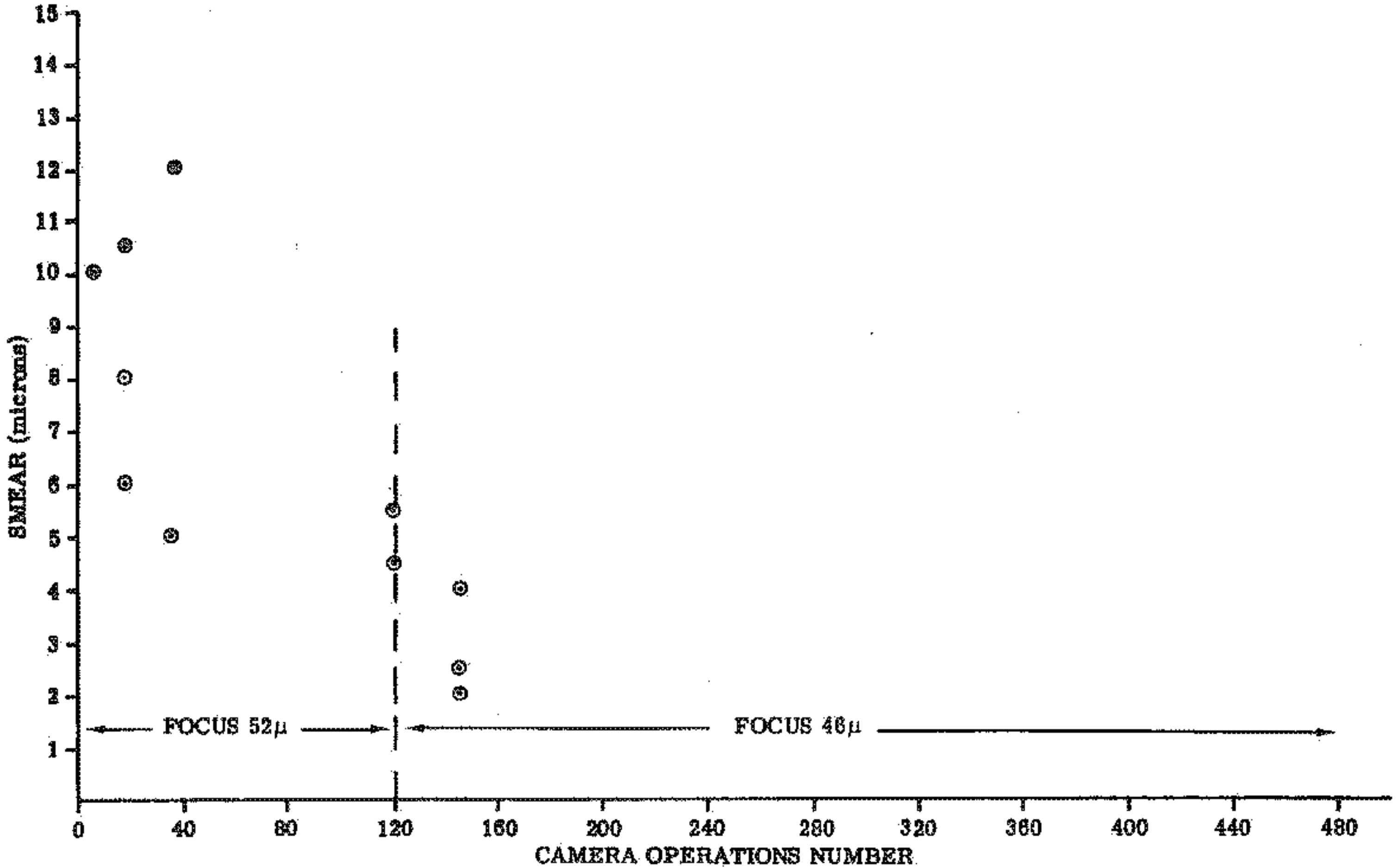

FIGURE 6-7

AFT CAMERA RANDOM LINE SMEAR
IN FLIGHT DIRECTION

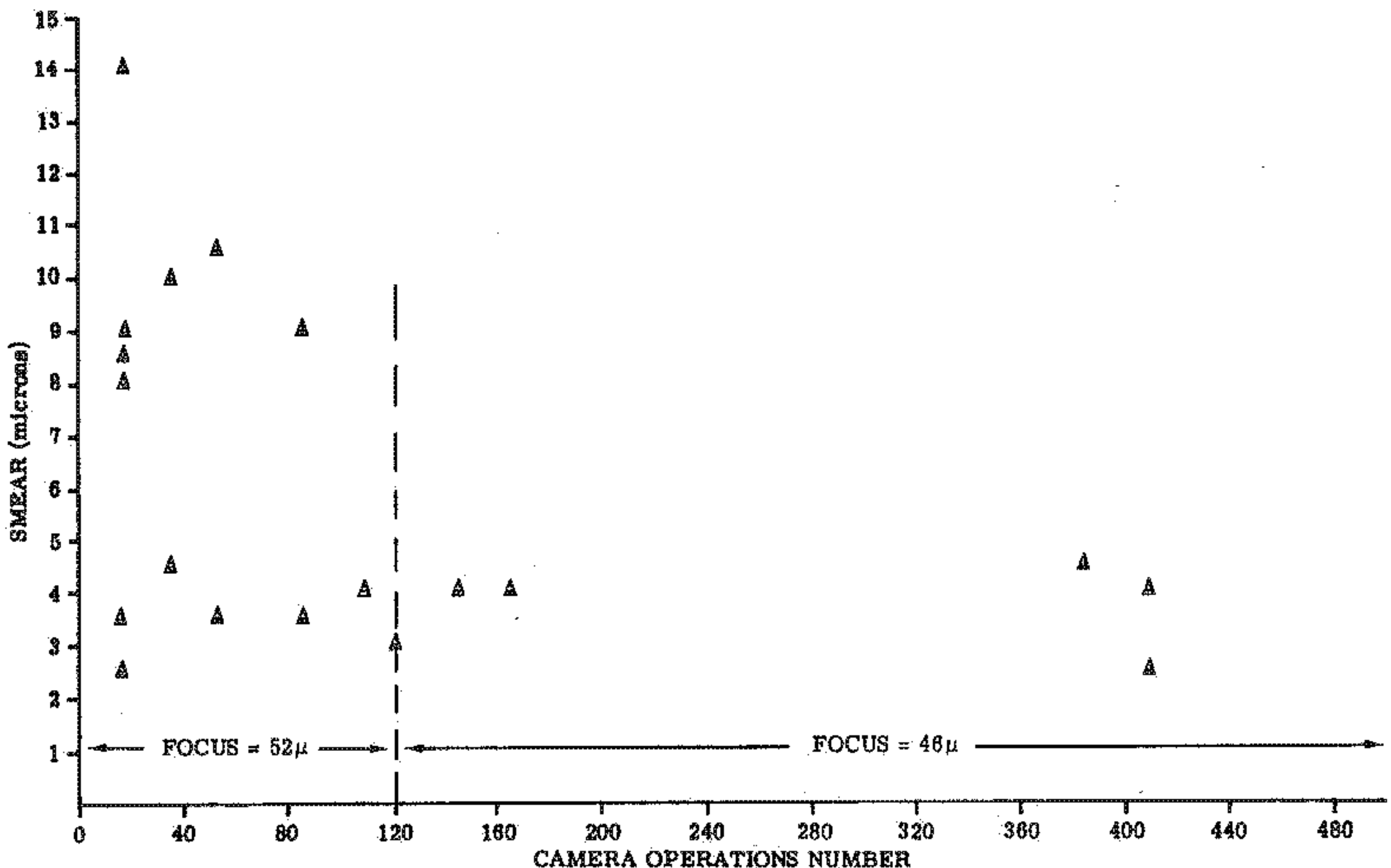

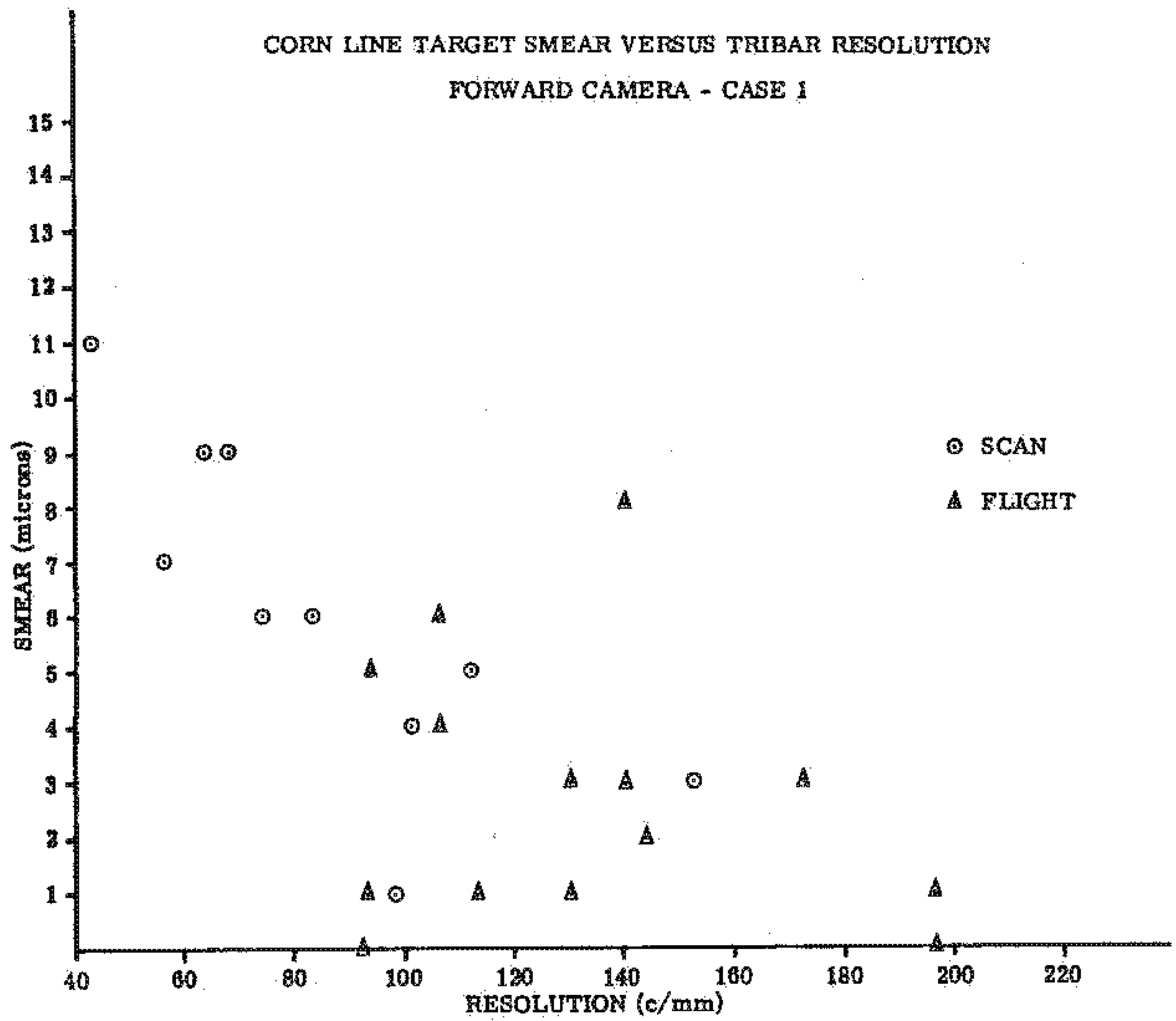


FIGURE 6-8

TOP SECRET RUFF

Handle via Talent-Keyhole Controls Only



Approved for Release: 2022/03/03 C05132845

FIGURE 6-9

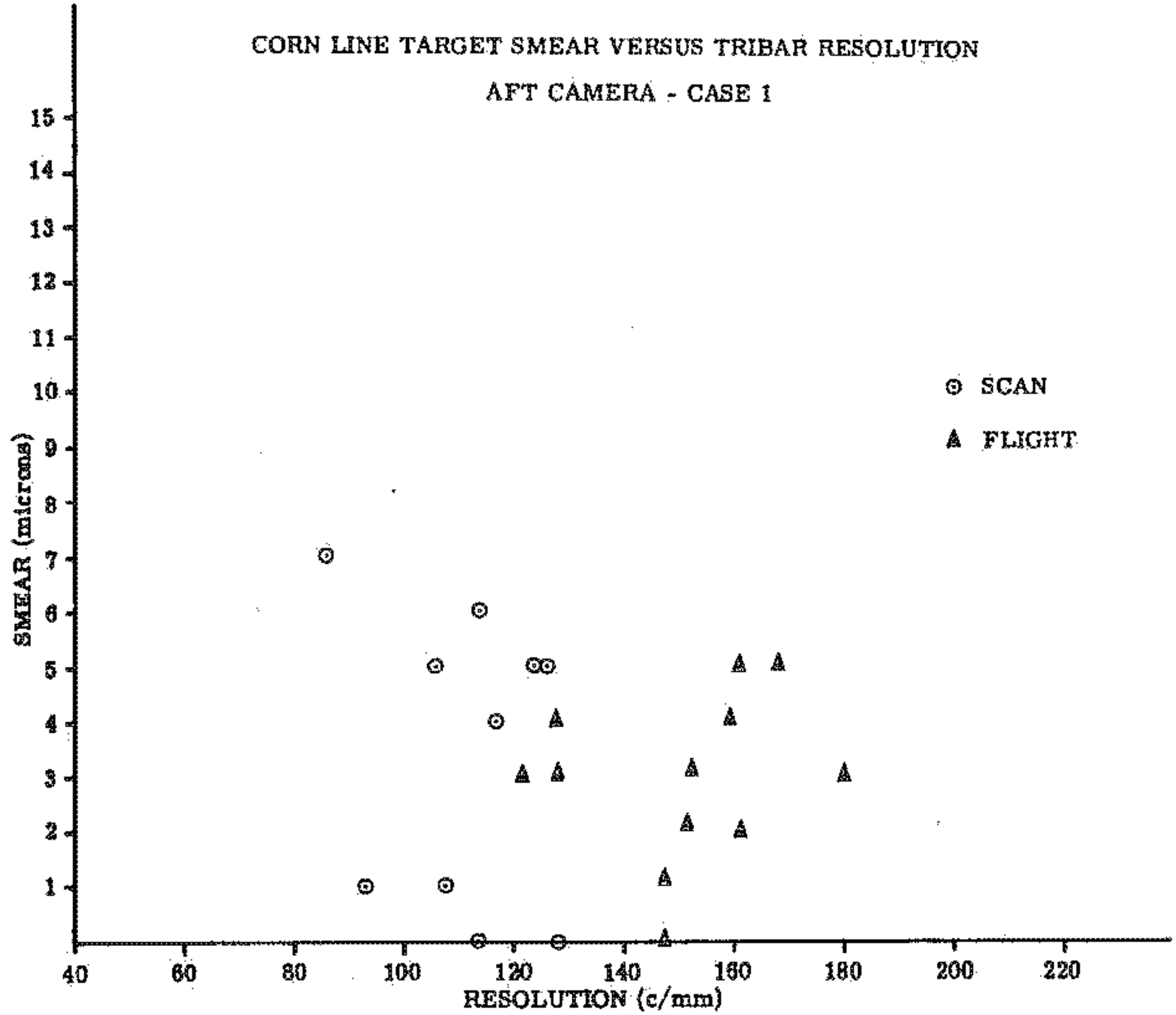
CORN LINE TARGET SMEAR VERSUS TRIBAR RESOLUTION
AFT CAMERA - CASE 1
SCAN
FLIGHT
SMEAR (microns)
15
14
13
12
11
10
9
8
7
6
5
4
3
2
1
40
60
80
100
120
140
160
180
200
220
RESOLUTION (c/mm)

FIGURE 6-10

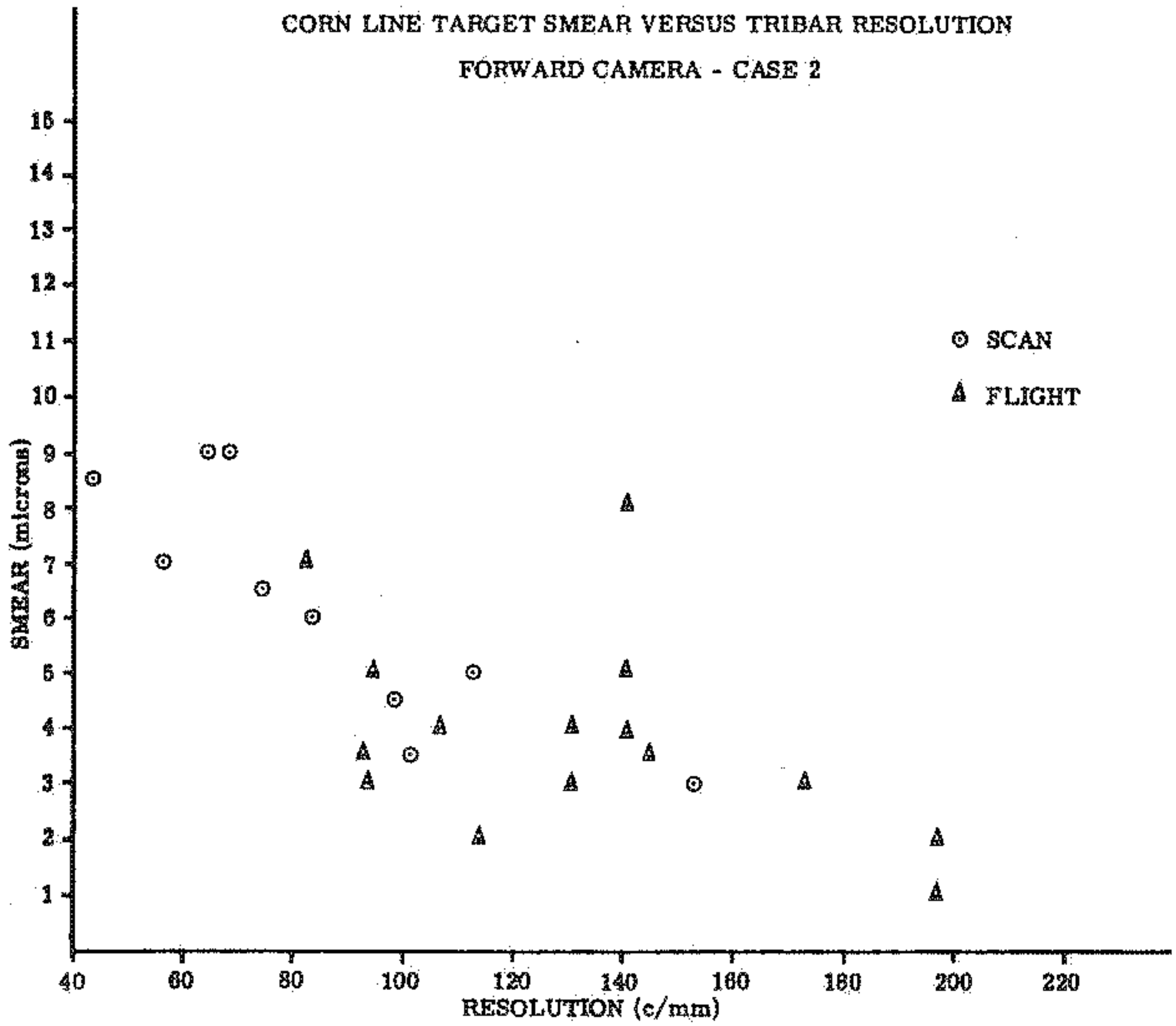


Handle via Talent-Keyhole Controls Only

TOP SECRET RUFF

TOP SECRET RUFF

Handle via Talent-Keyhole Controls Only

FIGURE 6-11

CORN LINE TARGET SMEAR VERSUS TRIBAR RESOLUTION

AFT CAMERA - CASE 2

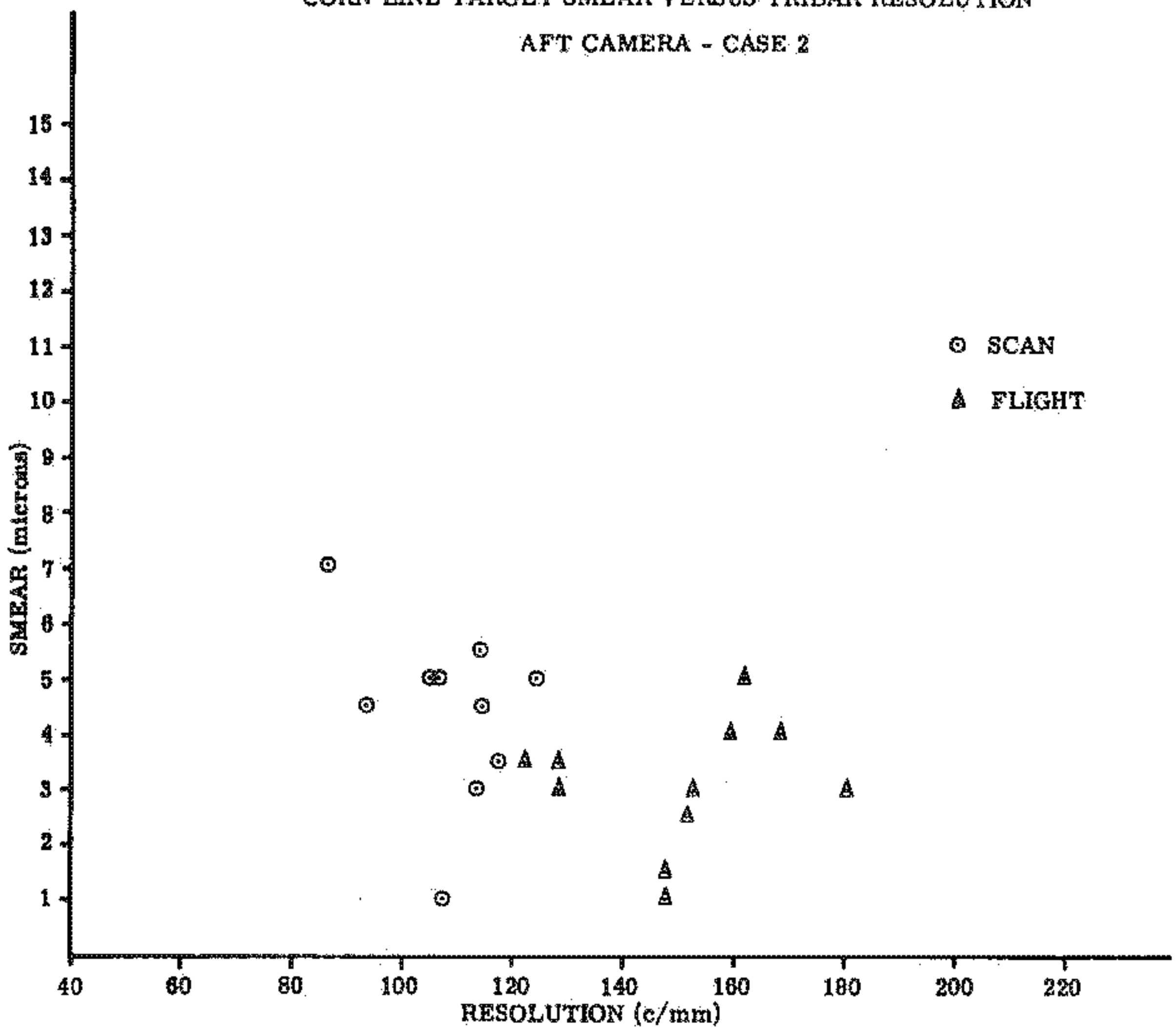

resolutions. Figure 6-3 shows a typical case wherein the old motion solution allowed the time history plot to double back, causing the reported smear to be small, even though the model indicated that the image had moved much farther. One may conclude that the smear model is at least approximately correct for the majority of cases observed on this mission.

6.1.6.5 AIM Intercept Correlation

Figure 6-12 shows the correlation between the uncorrected read CORN resolution values and the resolution predicted by the PFALINES MTF/AIM intercept for Cases 1 and 2. The dashed lines represent ± one bar group resolution. The correlation is good with two exceptions: (a) it shows a slight tendency for the program to predict high; and (b) the data is very noisy at high spatial frequencies. The first problem indicates that the film MTF used is not accurate enough. The second is a result of the noise present on the calculated MTF at high spatial frequencies, where it intersects the AIM curve at a very small angle. This will cause a large variation of predicted resolution for small changes in MTF value. The Case 3 data traced at AFSPPF shows the same slope and scatter characteristics, but indicates that the AFSPPF data tends to predict even higher than the Cases 1 and 2 data. This is most likely due to differences in microdensitometer optical performance, which is partly compensated for in the film MTF. One may therefore conclude that the line target technique will be useful for accurate performance analysis when refinements are made in the curve which compensate for the film and microdensitometer responses.

6.1.7 Data Anomalies

6.1.7.1 Microdensitometry

There were two significant problems apparent from tracing the same data on two different microdensitometers. The most obvious contributor to the disparities is the difference in optical configuration. This would yield very different microdensitometer MTF's, and to date neither machine has been characterized with sufficient accuracy to allow compensation in the analysis program. The second major difference was that the BRIDGEHEAD machine produced peak line densities on the average of .2 to .3 density units less than the AFSPPF machine. As a further test, AFSPPF traced several lines on a machine which has optical characteristics known to be different from the Mann-Data instrument. After conversion to equivalent diffuse density, the other machine produced values within ±.03 density units of the AFSPPF Mann-Data machine. One must therefore conclude that there is a fundamental difference in the calibration techniques used by the two organizations.

6.1.7.2 Film MTF

One of the key input parameters is the film MTF. The current method for determining the film MTF combines effects of the microdensitometer and the film. The film MTF is only valid when applied to data gathered by the same microdensitometers that was used to derive it. For future improvements in precision during post flight analysis either one machine must be used for all tracing, or

FIGURE 6-12

CORN TRIBAR RESOLUTION VERSUS PFALINES

MTF/AIM INTERCEPT

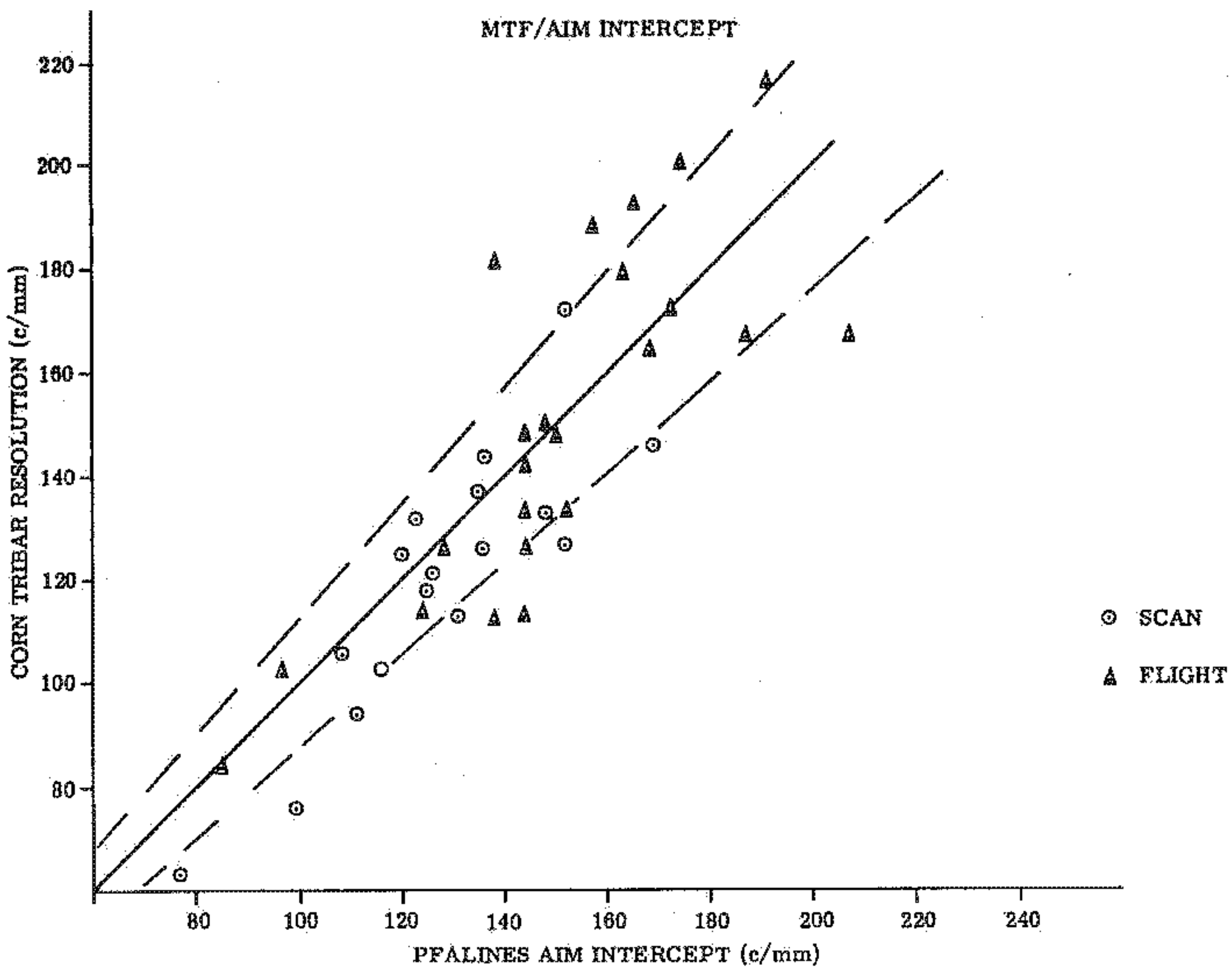

separate film-machine response characteristics must be found for each machine.

6.1.7.3 Random Lines

The attempt to use random lines has shown that the technique has great promise as a diagnostic aid. However, target line width has been shown to be a very significant factor in the accuracy of the output. To successfully employ this technique in the future, a catalogue of accurately-known lines must be assembled for areas of frequent use in engineering operations.

6.1.8 Conclusions and Recommendations

A. The line trace analysis method shows a good deal of potential for generating useful system diagnostic data. However, further refinements are required before the technique may be considered operational.

B. Recommend the following tasks be accomplished before the Mission 1201 evaluation:

(1) Improve the film MTF estimate.

(2) Standardize and measure the optical configurations of the microdensitometers.

(3) Refine and improve the present smear model.

(4) Investigate improvements in the use of camera lens MTFs for conditions of large defocus.

(5) Select and document a catalogue of random lines.

6.2 CRYSPER PERFORMANCE PREDICTIONS

6.2.1 Introduction

Preflight and postflight performance predictions were made for each mission segment using the CRYSPER computer program. CRYSPER simulates the on-orbit performance of the camera system in its predicted operating environment. The predictions are two sigma low estimates of resolution in both cycles per millimeter (c/mm) at the camera and ground resolved distance (GRD) in feet of the image. There is also a capability to compute the mean resolution that is used occasionally for special test evaluations. The program has the following three basic sections, each describing a major aspect of the final system resolution:

A. An orbital model which uses as input data the orbital elements for the mission and specific characteristics of the targets. The output of this section of the program is ordered by target access and consists of the solar ephemeris as well as the geometry of each access.

B. An atmospheric model which uses the data generated in the previous section and computes the apparent contrast of each target accessed. It uses an extensive data bank of atmospheric measurements which has been collected over the past five years. This data bank enables this section of the program to estimate the haze levels on a geographic and seasonal basis.

C. A camera performance model which is a mathematical description of the performance characteristics of the camera system and flight vehicle. This section uses the output from the previous sections as well as the film characteristics and camera smear/optical performance data under the various operating conditions. The calculation of resolution is obtained by intersecting the optical system modulation transfer function (MTF) with an aerial image modulation (AIM) curve that describes the film characteristics under the exposure/contrast conditions prevalent during exposure.

CRYSPER has three primary outputs:

A. A target listing which provides the predicted resolution (GRD and c/mm) for both cameras for each target accessed. This data is listed in sequential order and also contains the revolution, date, time, obliquity, altitude, slant range, solar elevation, and assumed target reflectances. This output is useful for correlation of system performance with other estimates of mission performance where a point-for-point comparison is desired.

B. An estimate of resolution (GRD and c/mm) sampled over the entire format. It is in the form of a table covering a 120° scan angle format in 10° scan angle increments and computed for a range in solar altitudes from 5° to 50° increments. Although it is computed for the specific conditions for a single access (i.e., altitude, Vx/h, target reflectances, etc.) the representation across the format for a range of solar altitudes makes it a very useful table relative to generalizing camera performance during the mission.

C. The third output is a plot of the cumulative frequency of GRD predictions for a given set of targets. This is necessary for correlation in a general sense where one must rely upon a large data base to find a pattern. It is particularly useful for postflight predictions where an actually acquired target deck can be employed.

CRYSPER has been used for estimating mission performance for the KH-9 System for the last two years. During this time most of the components of the program have been tested as individual units. The basic camera equations, for example, have been successfully related to the camera operations during chamber testings. The atmosphere section has been verified on numerous aircraft tests as well as with KH-8 missions. The orbital mathematics and targeting acquisition modes have been tested on KH-4 missions. Finally, the important film characteristics have been empirically determined during KH-9 acceptance testing. Until Mission 1201, however, there has been no opportunity to test the entire CRYSPER package as a single unit.

In an effort to carry out a correlation between actual mission results and the CRYSPER predictions, two different types of comparisons were made. The two measures of performance used for correlation to CRYSPER were: (a) photointerpreter suitability ratings, and (b) CORN tribar readings. These measures provide a completely different estimate of the mission's performance. Each measure has certain characteristics that provide for a useful correlation, however, each is also lacking some of the characteristics necessary for a complete correlation to CRYSPER.

### 6.2.2 PI Suitability Correlations

The most useful correlation, from a practical point of view, is one that involves the ultimate user, the photointerpreter. In order to carry out this correlation, the PI quality ratings for all targets were used. The ratings were made on the following four level scale: Excellent, Good, Fair, and Poor. The correlation addressed with this measure of mission performance was intended to ascertain whether or not CRYSPER worked in a general sense. That is, do the targets considered Good by the photointerpreters have better predicted GRD's than those considered Poor? Further, do the CRYSPER predictions for the targets rated as Fair fall between the predictions for the Goods and Poors?

There are certain characteristics of the acquisitions that have a significant influence on the PI rating that are external to the camera system, and therefore are not programmed in CRYSPER, i.e., a target partially obscured by clouds will probably evoke a Poor rating regardless of how well the camera performed. The photointerpreters indicate, on a target by target basis, some of these influencing characteristics. However, there are still conditions that, while having an influence on the rating, are not recorded in any way. An example of this is the poor quality photograph taken at a low solar altitude that contains excessive smear from long exposure time. The target, though, could be rated as Good because the PI may have discovered the shadow of a newly constructed radar antenna against a background of snow. It was for these kinds of reasons that a substantial amount of scatter in the data was anticipated.

In order to make a fair comparison of CRYSPER to PI suitability, steps were taken to avoid data influenced predominantly by the chance occurrence of various circumstances, rather than actual system operating performance. The target ratings were sorted by PI comment and not used in subsequent analysis unless the photointerpreter considered them to be in one of the following three general categories: (a) clear, (b) hazy, or (c) poor obliquity.

The remaining targets were then sorted by target category and then further separated by their suitability rating. At this point, there were only three target categories with a sufficient number of samples for a comparison, see Table 6-3.

TABLE 6-3

TARGET SUITABILITY RATINGS BY CATEGORY

| Complex No. | Target Category | Number of Targets Good | Fair | Poor |
|---|---|---|---|---|
| 1A | Missiles | 489 | 362 | 112 |
| 2C | Airfields | 255 | 273 | 38 |
| 7A | Military Complexes | 459 | 788 | 115 |
| | All Categories | 1,686 | 1,976 | 360 |

### 6.2.3 Data Handling/Program Operation

The normal mode of operating CRYSPER is to input a target deck consisting of the geographic coordinates of each target to be accessed and an estimate of the target's ground reflectance. The program arranges these targets in a time order of access and then computes the scan angle at which the target will be acquired and its apparent contrast. It then computes the ground resolved distance that should be attained for that particular position in the format. CRYSPER presently does not have the capability to compute the field angle of acquisition because there is no way of inputting camera on/off data before flight. Therefore, for correlation to PI suitability it was assumed that the targets, on the average, fell within the center of the field. Since the correlation intended was general, it was felt that this was a minor source of error. For a specific one-to-one correlation this error would have been a significant variable. For this study the reflectance chosen to represent intelligence targets was 10 to 20 percent. This is quite unlike the CORN targets used for engineering purposes where the reflectance ranges from 7 to 33 percent. Unfortunately, each target category, as well as individual elements within targets themselves, will vary markedly from the nominal in an unknown fashion. Therefore, for this correlation, the nominal 10/20 percent reflectance was assigned to every target.

The target deck used to drive CRYSPER for this correlation consisted of the acquisition falling into one of twelve groups (3 ratings times 4 target categories). The cumulative frequency graphs for these sets of data are shown in Figures 6-13 thru 6-16. These figures show that an excellent correlation exists between PI ratings in the Good and Poor categories and the GRD values computed by CRYSPER. There is a clear differentiation between the cumulative frequency distribution between the target rated Good and Poor up to the 85% level. Beyond that level the ratings appear to be uncorrelatable with GRD.

The Fair choices, in general, are grouped with the Good category, with the exception of the ICBM ratings which correlate with Good ratings at small GRDs (less than 6 feet), and the Poor category at larger GRDs. In fact, the Fair quality rating in this case exceeds the Poor rating in terms of GRD and in most cases occurs at smaller GRDs than the Good ratings. These observations do not necessarily suggest that the Fair category is poorly related to the predicted GRDs, but perhaps that the task given to the PIs of assigning a three-level rating is not a reasonable subjective task. This is particularly true when considering that paired comparisons were not made.

Table 6-4 lists the zero frequency, 50% frequency GRDs, as well as the ratios between the 50% values.

TABLE 6-4

STATISTICAL COMPARISON OF GRD BY CATEGORY

| Target Category | GRD at 50% Cumulative Frequency Point | | Ratio Between Good & Poor at 50% | Threshold GRD at 0% Frequency | |
|---|---|---|---|---|---|
| | Good | Poor | | Good | Poor |
| ICBM Deployments | 4.8 | 10.4 | 2.16 | 2.0 | 6.2 |
| Airfields | 5.6 | 9.4 | 1.68 | 2.8 | 2.8 |
| Military Installations | 6.0 | 7.3 | 1.22 | 2.4 | 3.2 |
| All Categories | 5.2 | 9.6 | 1.85 | 2.8 | 2.8 |

CUMULATIVE FREQUENCY DISTRIBUTION OF CRYSPER

PREDICTED GRD FOR ICBM DEPLOYMENTS

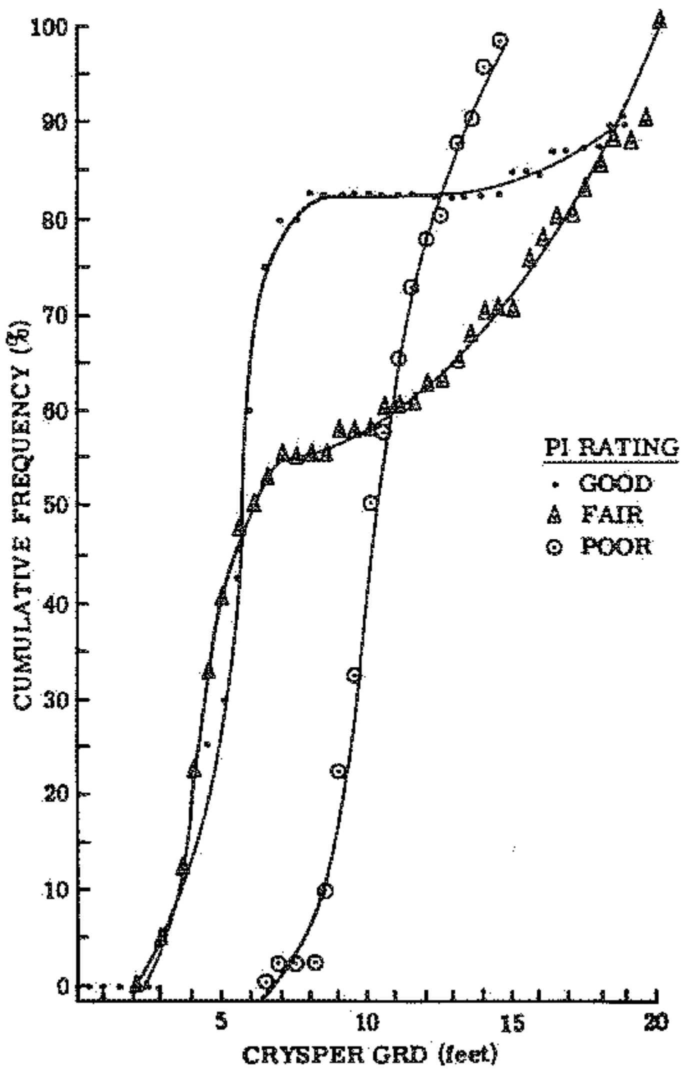


FIGURE 6-13

CUMULATIVE FREQUENCY DISTRIBUTION OF CRYSPER PREDICTED GRD FOR AIRCRAFT INSTALLATIONS

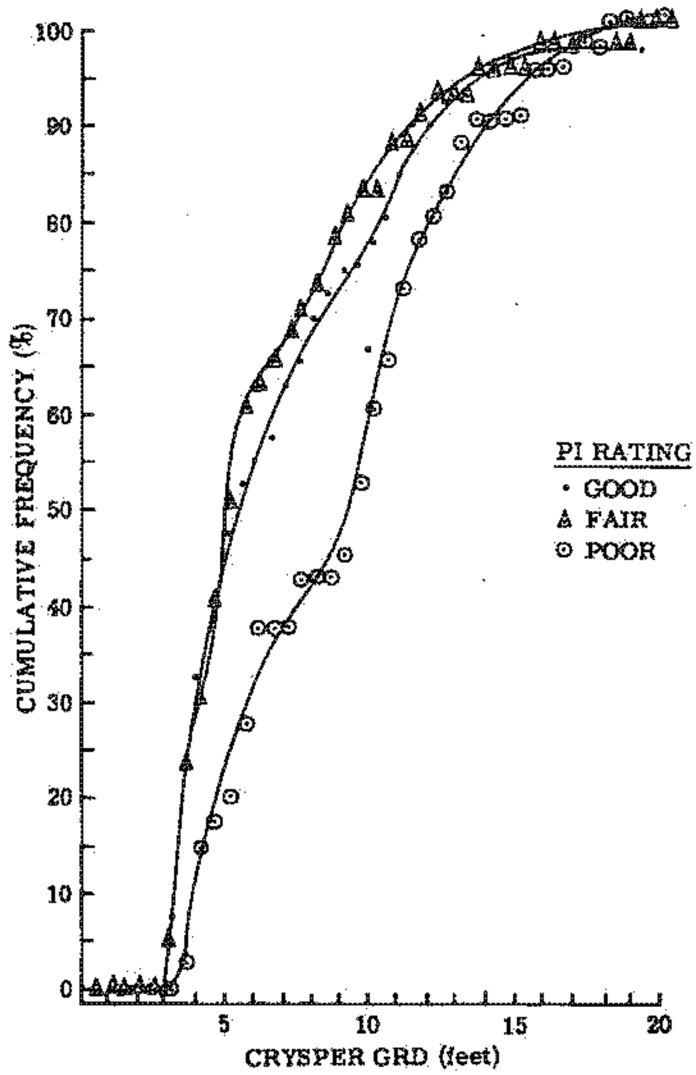


FIGURE 6-14

CUMULATIVE FREQUENCY DISTRIBUTION OF CRYSPER PREDICTED GRD FOR MILITARY INSTALLATIONS

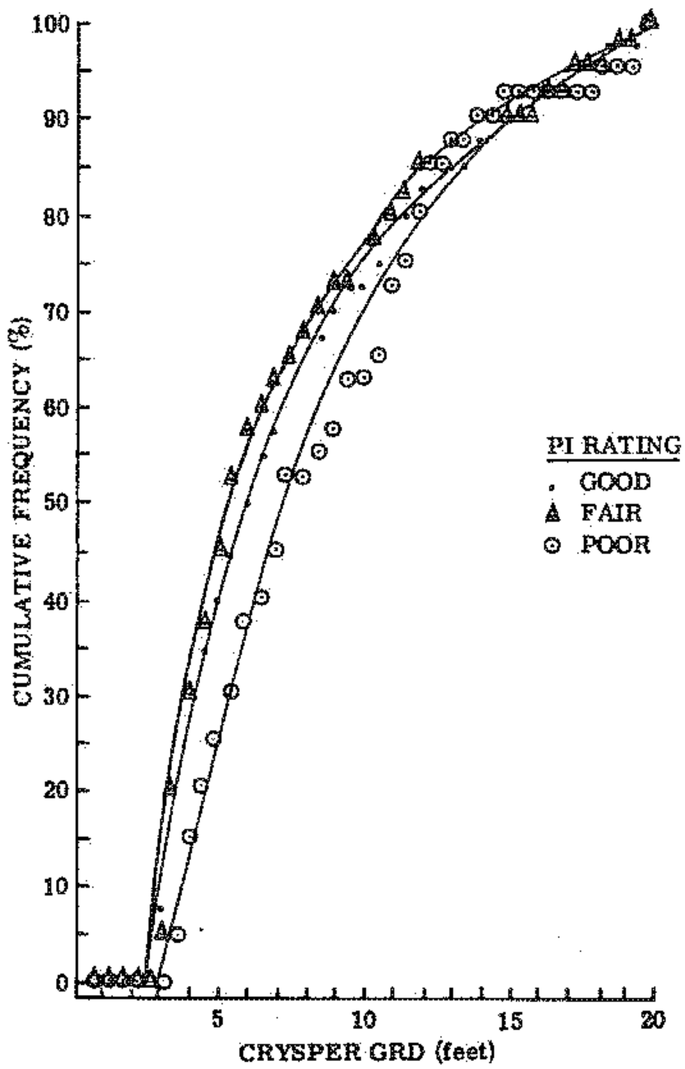


FIGURE 6-15

CUMULATIVE FREQUENCY DISTRIBUTION OF CRYSPER

PREDICTED GRD FOR ALL CATEGORIES

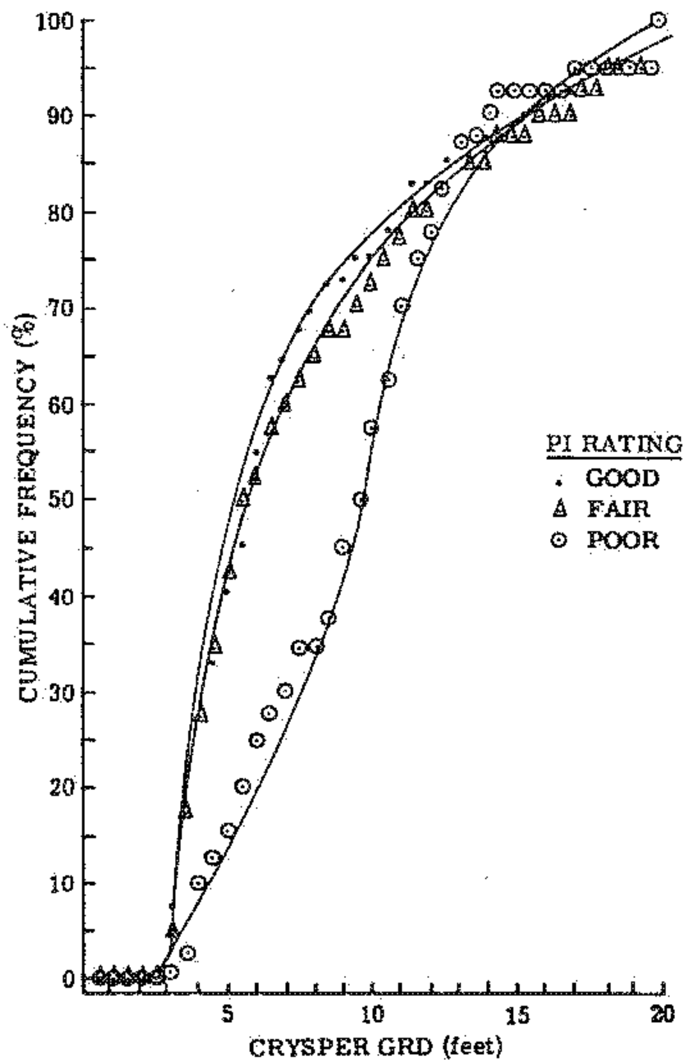


FIGURE 6-16

Notice that there is an orderly relationship between the Good/Poor 50% cumulative frequency points. As the Good values go up in terms of GRD, the Poor values decrease. This gives some indication of the quality sensitivity associated with the various target types. It also may suggest the ranges in size of objects of interest for the target types. It also generally indicates that the threshold GRD values have a similar relationship when using targets at either end of the scale. For some reason, the cumulative frequency distribution for the aircraft data has an unusual shape at the low values of cumulative frequency, and does not fit in the later relationship. The Poor 50% frequency GRD values are of particular interest since they suggest quality limits which may be applicable to acquisition decision making logic. That is, it appeared to be difficult for the PIs to distinguish Goods from Fairs, when the system was performing reasonably well. However, when the system produced GRD values worse than some certain level, it meant the target would indeed be inadequate for his needs and rated as Poor. It appears that this certain GRD value is a function of the target type and perhaps also of the current requirements for readout. More work needs to be done on future KH-9 missions in order to clearly define these relationships so that "take/no take decisions" can be aided by estimates of the performance relative to the readout requirements.

### 6.2.4 CORN Target Comparisons

Mobile and fixed CORN tribar targets are acquired for engineering purposes on KH missions. These targets provide direct estimates of GRD and take into account actual camera operation as well as scale factors and atmospherics. Although tribar resolution readings are somewhat subjective, they are not as subjective as the PI ratings. The locations of the usable mobile CORN targets, target reflectance, and field angle were used as input to CRYSPER. These are significant acquisition characteristics that are necessary to obtain a point-to-point correlation with actual results. During the course of the mission, several changes were made in the operating mode that had a bearing on the flight performance. An exposure change of .2 Stop (.06 log E) was made for acquisitions above 10° solar altitude and three focus changes were made, one to the Aft Camera and two to the Forward. In order to accurately simulate the CORN targets these input parameters were changed at the appropriate times during the CRYSPER run.

Figures 6-17 and 6-18 illustrate a comparison between the CRYSPER predictions and the mobile CORN target readings. There appears to be a very strong correlation between the two values in the in-track direction. In the cross-track direction, the correlation is fair in that it appears as though the camera experienced more smear than preflight tests had indicated. This correlates with the findings of the line target analysis. There is, however, one very interesting fact that must be considered, CRYSPER predictions are for the 96% probable resolutions, i.e., worse case. Ordinarily, one would expect the correlation to be stronger with mean predictions. This has been typical of predictions made during preflight testing. It has been a perplexing phenomenon since the beginning of KH-9 testing over a year ago.

CRYSPER TWO SIGMA LOW RESOLUTION PREDICTIONS

VERSUS CORN TRIBAR RESOLUTION FOR FORWARD CAMERA

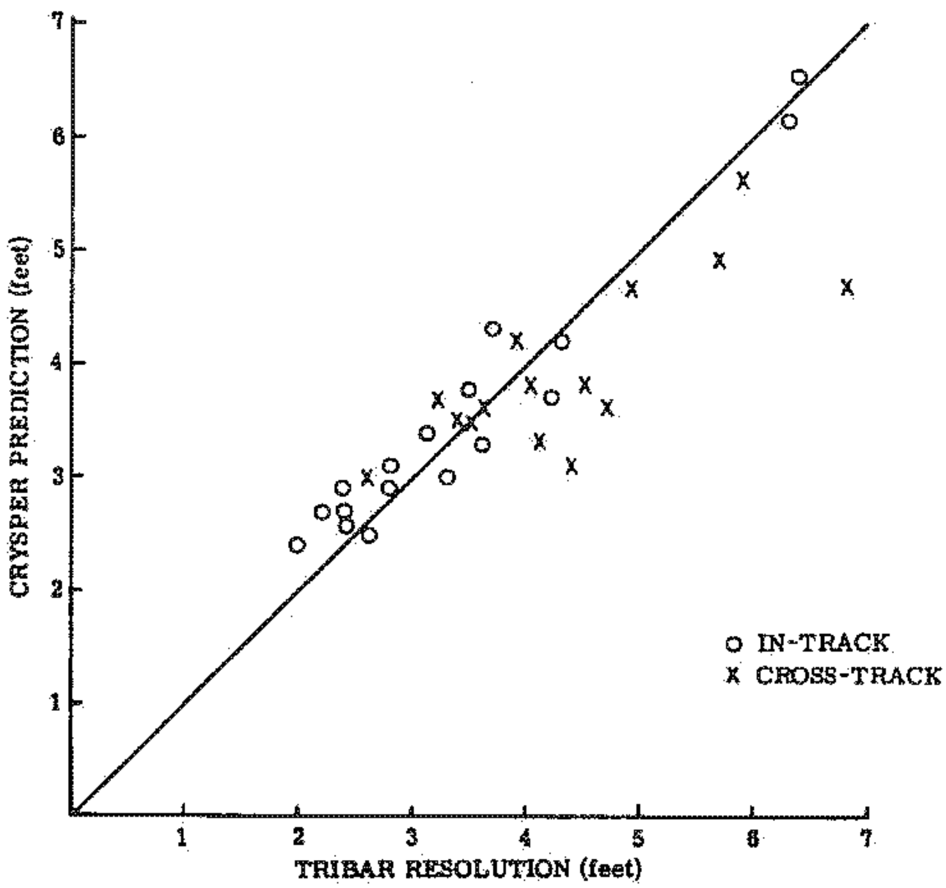


FIGURE 6-17

CRYSPER TWO SIGMA LOW RESOLUTION PREDICTIONS
VERSUS CORN TRIBAR RESOLUTION FOR AFT CAMERA

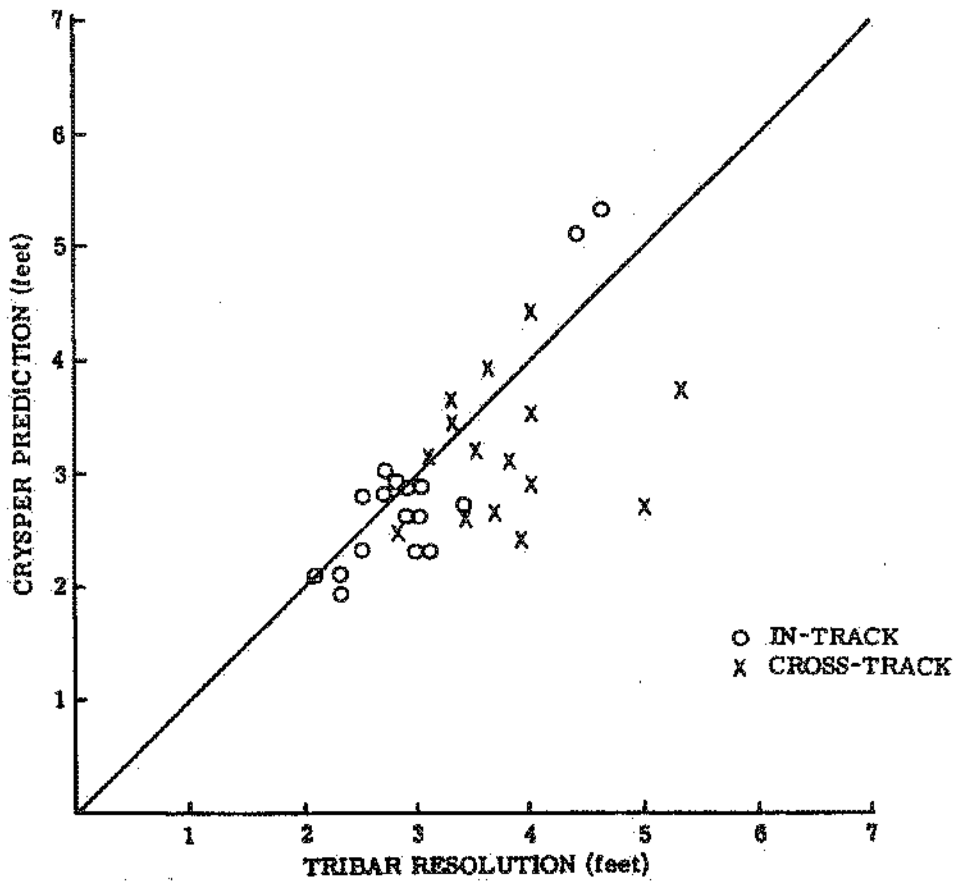


FIGURE 6-18

However, it is a consistent bias in that what is actually achieved corresponds to the predictions as we currently perform them.

6.2.5 Conclusions

A. The CRYSPER Program can be used to compute reasonable approximations of system performance.

B. The two sigma low resolution predictions correlate well with the actual results achieved from the CORN tribar targets in the in-track direction but are low in the cross-track direction.

C. CRYSPER predictions relate on a statistical basis to the Good/Poor photointerpreter ratings.

D. The CRYSPER Program has a potential for aiding in preflight and on-orbit take/no take decisions. It should be noted, however, that it will not necessarily work on an individual target-by-target basis but will work well statistically.

## 6.3 VISUAL EDGE MATCHING (VEM)

### 6.3.1 Background

Image quality evaluation of reconnaissance photography has a long history of various attempts to quantify camera system performance. Performance assessment has always been accomplished primarily by microscopic examination of a mission's operational photography by experienced image analysts. Memory, perception, and preferential judgment are the variables used to probe the causes of disturbed imagery and to decide which operational parameters might optimize the product. Of all the techniques developed and applied, only the tribar resolution method has achieved general community-wide acceptance. The fact that ground targets are required for the application of this evaluation method precludes its use in denied area photography. The purpose of the VEM technique is to microscopically examine cultural detail and characterize its edge sharpness in terms of equivalent standard tribar resolution.

Not all of the film footage returned from a mission is amenable to image quality analysis. Cloud cover and gross density patterns contain no detail information. Potential target areas are all man-made urban/industrial/military complexes. This is the type of imagery utilized in the analysis leading to a system performance assessment. Edges constitute the elemental structure of this type of imagery. Most evaluation techniques historically have been centered about mathematical analyses of microdensitometric edge traces. In terms of practical utilization, these approaches have not proven useful.

In 1963, a study was made to determine whether a visual evaluation of edges, akin to normal photointerpretation tasks, could be of practical use. After several years of work this feasibility was demonstrated. Basically, the technique involved comparing an operational edge with an array of standard edges in a split-field microscope. Subjective judgment produced a matched pair so that some psychophysical quality value could then be assigned to the previously unknown edge. In 1968, a workable breadboard model of a VEM Comparator was completed which utilized a two-dimensional standard array of edges (VEM matrix) varying both in sharpness and contrast. The first operational test was on the ONs from Mission 1105. This mission was the one and only KH-4 System which utilized a full load of ultra-thin base (UTB) film and its resultant photography was characterized by an extreme degree of image quality variability. Not only did the VEM data relatively quantify the degree of variability, but also revealed the time-based quality trends identified by the evaluation team's experienced image analysts.

With the success of the experiment on Mission 1105, the development and production of four operational VEM Comparators was authorized for use on the KH-9 Program. VEM technology continued to develop utilizing the breadboard model for KH-4 missions. At this time, the KH-4 System instituted a two-position focus adjust capability. As part of first bucket engineering operations photography was acquired at both focal positions. Tests were evaluated during the breakdown to select which position to use for the subsequent bucket. VEM data gathered at these exercises always agreed with the subjective assessment as to which focus position was better. Also in 1969, the VEM technology was developing through research on the KH-9 Program. Thru focus chamber test runs were being VEM analyzed and good correlations were attained between edge quality and tribar resolution trends.

The VEM technique was implemented by the PFA Team as an analysis procedure for Mission 1201. This analysis was performed at BRIDGEHEAD in the Mission Analysis Area (MAA). The results were that subjective analyses of focus adequacy were confirmed with the VEM, and the amount of resolution falloff from center to edges of format was sampled. In addition, an extensive VEM resolution data baseline was established at AFSPPF by SSC and AFSPPF personnel. The first phase (VEM/MES) of this work produced VEM resolution values for incorporation into the calculation of Mission Evaluation Score (MES). The second phase (VEM/PAS) produced replicate samplings designed for performance assessment (PAS).

### 6.3.2 Equipment and Procedures

#### 6.3.2.1 VEM Comparator

A VEM Comparator is basically a split-field comparison microscope on a carriage over a light table with power rewinds, see Figure 6-19. The frames are scanned using normal scanning procedures. When a potential target cluster is found, the vertical microscope is centered over the area and clutches activated. Hand cranks then precisely control X- and Y- movement. A fiber optics bundle beneath the microscope objective provides adjustable illumination. Medium power magnification (40X) is used to locate a particular edge suitable for matching. Rotating prisms in the microscope head permit alignment to the horizontal target edge regardless of its orientation on the film. A switch is made to high power magnification (100X) and the field is then split to bring in the horizontal microscope at 100X.

VISUAL EDGE MATCH COMPARATOR

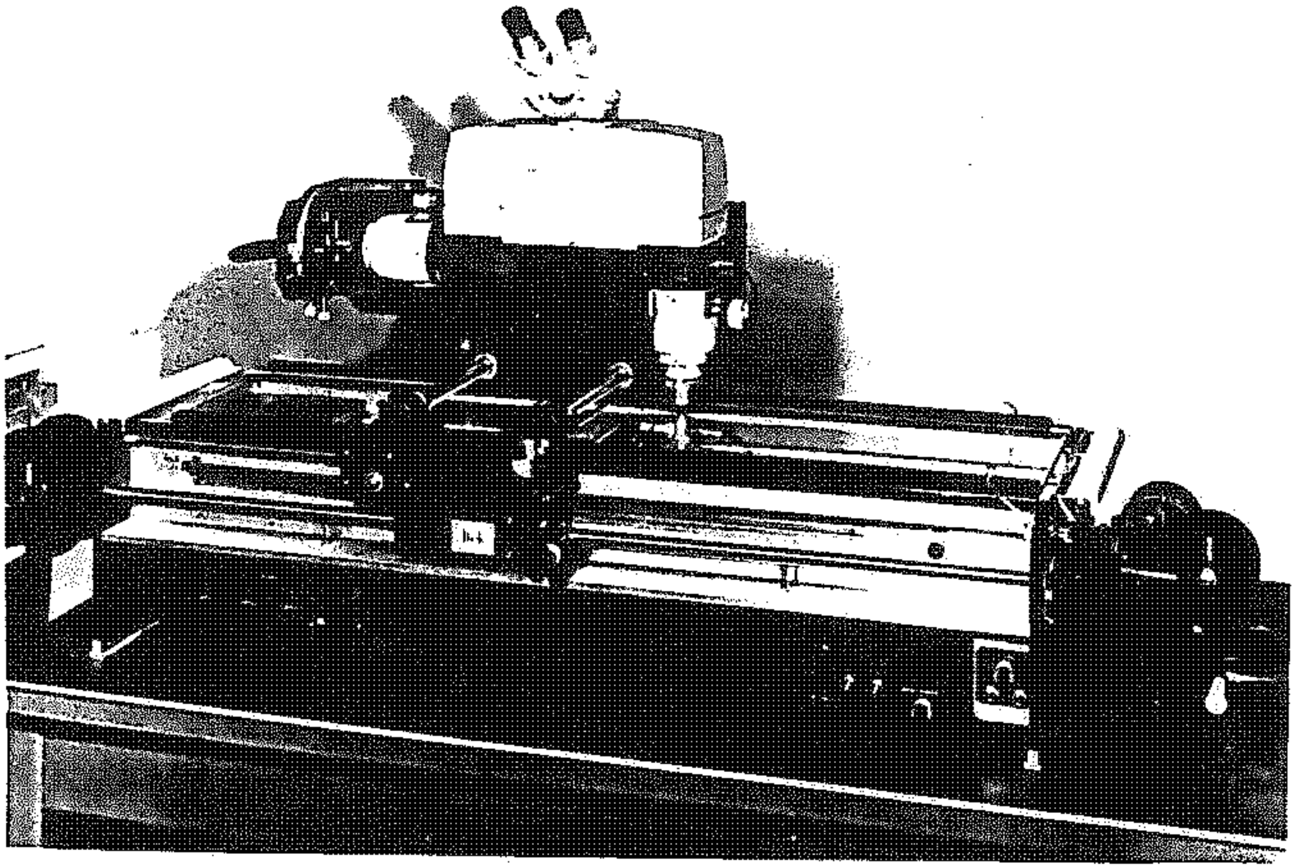

FIGURE 6-19

6.3.2.2 Edge Matching

One half of the field fixes the edge to be measured, while the other half views a standard "known" edge in the VEM matrix. Longitudinal matrix movement and horizontal microscope illumination adjustments permit selection of a reasonable contrast and density match. Lateral matrix movement then allows a match in sharpness. Upon completion of the match, the previously "unknown" edge is identified in terms of an equivalent tribar resolution quality level in cycles per millimeter.

6.3.2.3 VEM Matrices

When matching this array of controlled edges to unknown edges in the mission photography, the Comparator operator decides if the best match is with a particular edge or would fall between two adjacent edges. In this way, measurement capability is quantized to 15 possible levels. That these levels constitute just noticeable differences is evidenced by the following two facts: (a) reader variability is on the order of ±1 quantum level; and (b) thru focus analysis work done on a normal matrix and repeated with an experimental matrix of finer progressions produced statistically equivalent means and standard deviations. With reticle test edges, VEM resolution has the same or perhaps even better measurement accuracy as tribar resolution.

The VEM matrix is a two-dimensional 64 element array of standard "known" edges, see Figure 6-20. For each column in the matrix, sharpness is constant and contrast ranges in 8 steps from high to low. For each row, contrast is constant and sharpness progresses in 8 steps from high to low.

It is essential that the graininess of the matrix edges be the same as that of the mission target edges. To assure this condition for KH-9 mission applications, ON matrices were produced directly on 1414 Film and processed by dual gamma. Similarly, DP matrices were duped onto SO-192 Film using Niagara Printers and viscous processing. All of the matrix production procedures simulated operational parameters. Therefore, a matrix capability now exists to work with either DPs or ONs. In addition, the comparators have been modified with phenallic rollers to accept ONs as well as DPs.

6.3.2.4 Matrix Calibration

Each matrix comes supplied with individual calibrations for resolution. These resolution values are unique to each matrix and reflect the averages of actual readings made from 2:1 contrast tribar targets exposed with the edges during production on a defocusing microcamera. For relative measures this is perfectly adequate when applied to image quality assessment of a camera system's product. But because of user's camera spatial frequency, modulation transfer characteristics are unlike those of the manufacturer's microcamera, interpretation of VEM results in an absolute sense would be incorrect. To be a more powerful analysis tool in the KH-9 program, calibration was carried out in four phases. First, procedures were defined and methodology established using SN-002, Chamber A, Test 14, thru focus ONs and DPs. Second, absolute values were determined specifically for SV-1 using SN-003, Chamber A-2, thru focus ONs and DPs. Third, calibration was verified with mobile CORN

VISUAL EDGE MATCH MATRIX

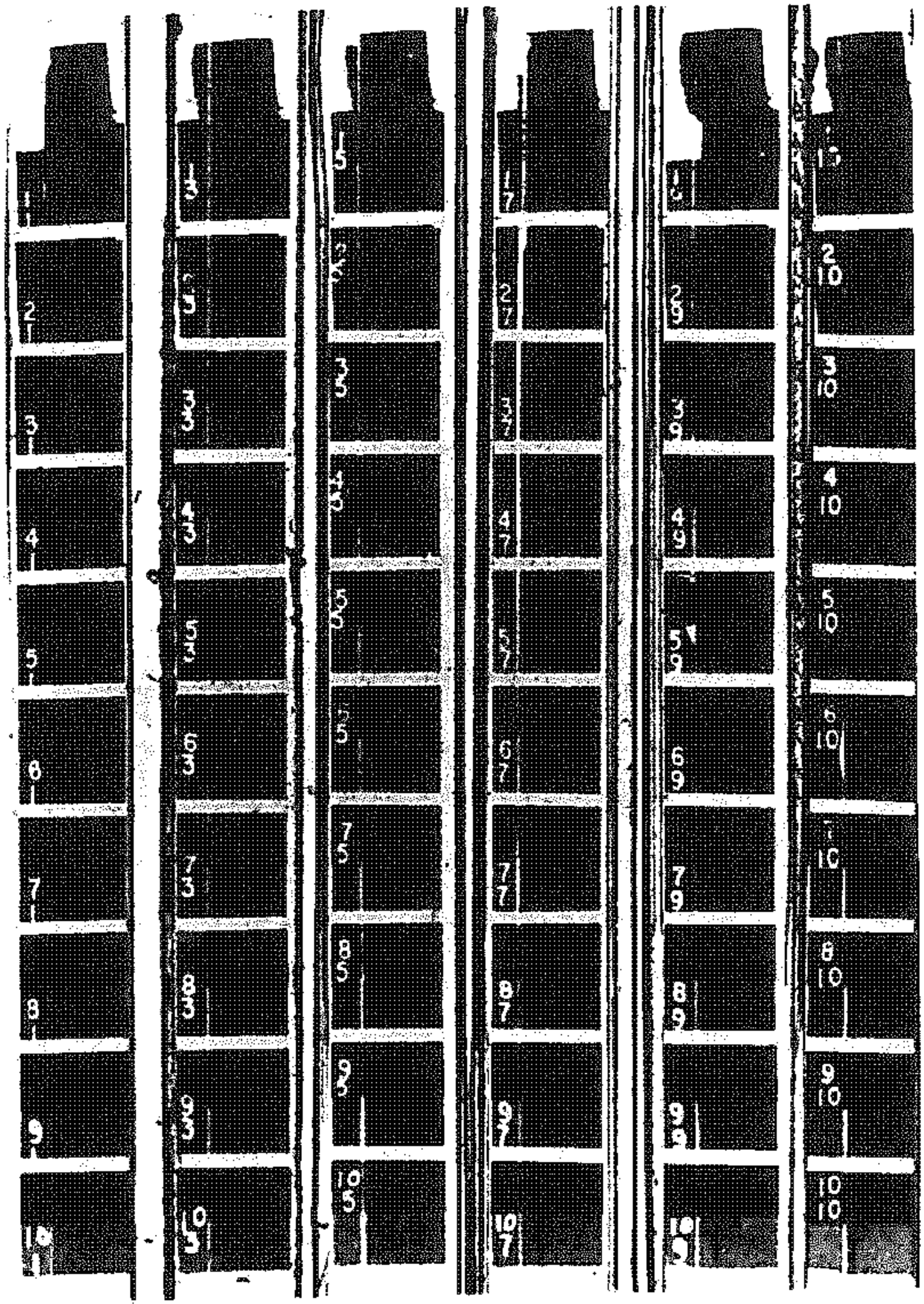

FIGURE 6-20

tribar target acquisitions on Mission 1201 ONs and DPs. Fourth, cross-calibration between matrices was done during the VEM/PAS data baseline buildup.

A test reticle was used which contained a 2:1 contrast tribar target, along with an in-track and cross-track series of seven edges tilted through the normal plane of the reticle itself, see Figure 6-21. Only the one edge closest to being in the same plane as the tribar target was utilized for matching purposes. Because the image motion velocity profiles across the target reticle were unknown, the lateral separation of the cross-track edge from the tribar target precluded its use in the calibration work. Thus, calibration was limited to the in-track direction.

The basic procedure was to read the in-track tribar targets on the ON and then match the corresponding edge on its DP. By both replicating and exploring different focal positions, variation in the apparent quality of a DP edge is related in a functional way to tribar resolution rendition on the ON, taking into account quality degradation inherent in the duplication process. It was found that three readers and three replicates at each focal position produced the minimum adequate statistical sampling for both resolution reading and edge matching to establish correlation confidence. Because only seven focal positions over a fairly narrow range were available and because the largest tribar element available was 71 c/mm, the entire matrix sharpness range could not be calibrated directly. There was sufficient data to establish some confidence in the mid-range, but both extremes had to be calibrated via extrapolation. Actual data points from sequences, K1, K3 and L3 of the Chamber A-2 test are plotted in Figure 6-22 for the Forward-looking Camera and Figure 6-23 for the Aft-looking Camera. In comparing the two sets of data, it is evident that there is a calibration difference between the two cameras, although why this should be so is not yet understood. The calibration check carried out on Mission 1201 photography with mobile CORN tribar acquisitions revealed that whereas the Forward Camera data clearly correlated, the Aft Camera data was more scattered. In addition, most of the data points fall below the calibration curve, indicating an error in calibration. Investigation is underway to determine the influence of exposure level on the calibration procedures. In any event, the advantage of working with DPs and being able to make reliable inferences regarding resolution on the ON is a significant advancement.

In order to overcome the calibration limitations described above, a new reticle has been designed and is being fabricated. This reticle contains both orthogonal edges (in and cross-track) and a 2:1 contrast $12\sqrt{2}$ tribar target which will image in collimator camera tests a dynamic range of 25 to 377 c/mm. In conjunction with a wide range of platen positions, this is expected to satisfy the VEM calibration needs of the KH-9 Program. Until this new reticle is completed and the calibration data formulated, the following data from three DP matrices is being used, see Table 6-5.

EDGE AND TRIBAR TARGETS IN TEST RETICLE

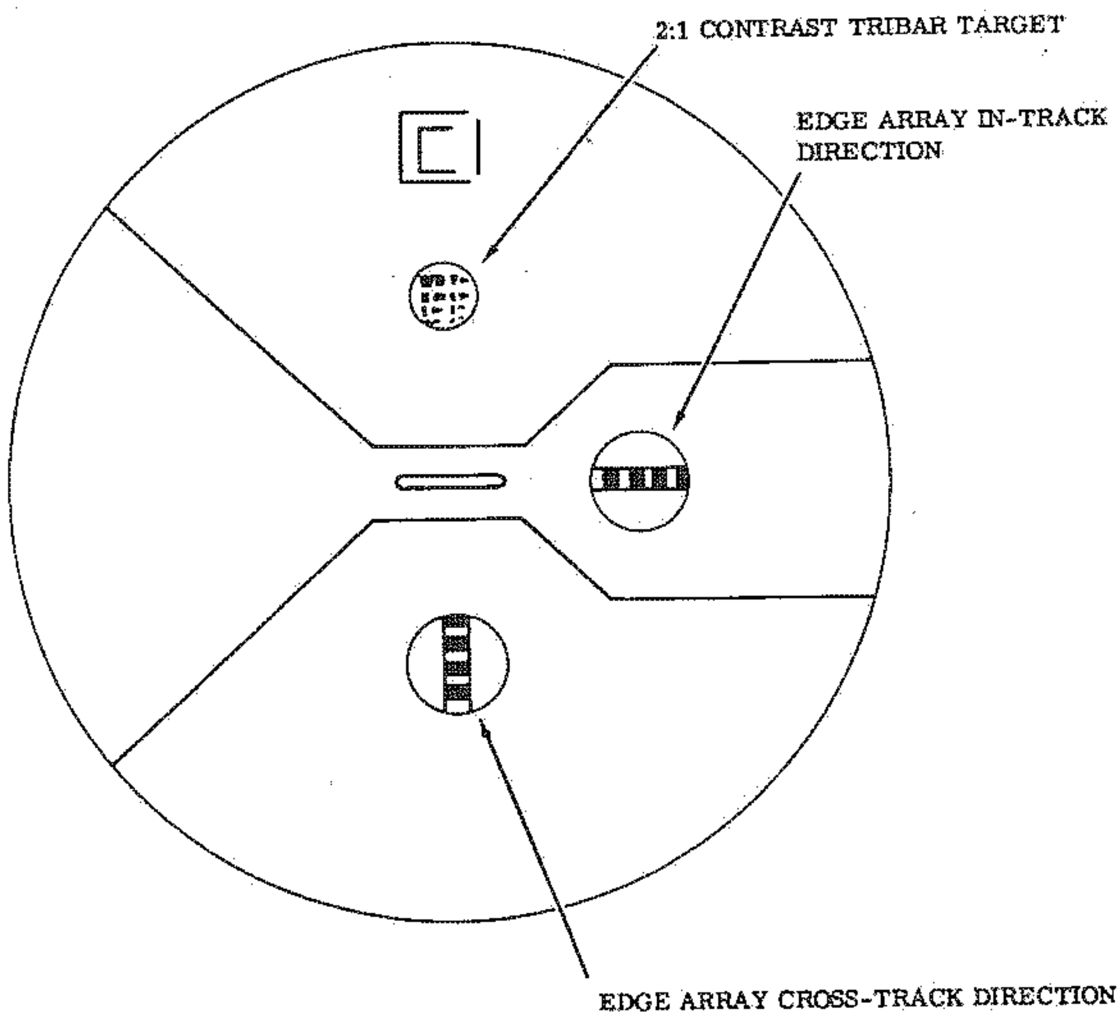


FIGURE 6-21

SN-003, CHAMBER A-2, SEQUENCES K1, K3, & L3 DP EDGE MATRIX CALIBRATION DATA

FORWARD-LOOKING CAMERA

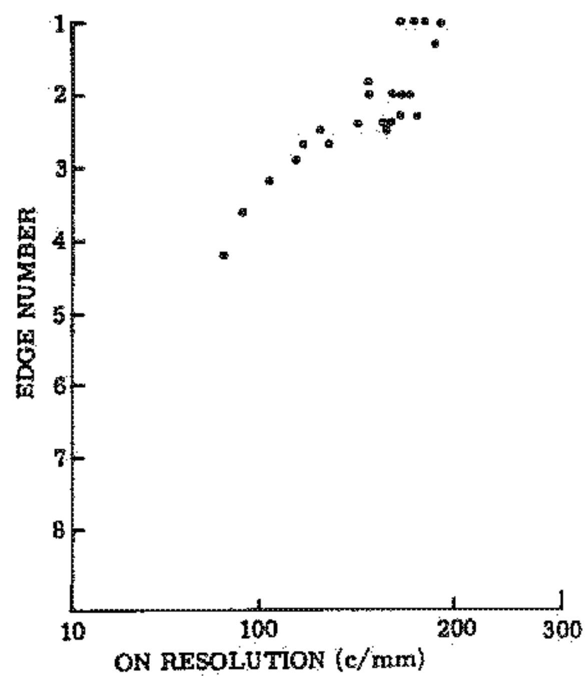


FIGURE 6-22

AFT-LOOKING CAMERA

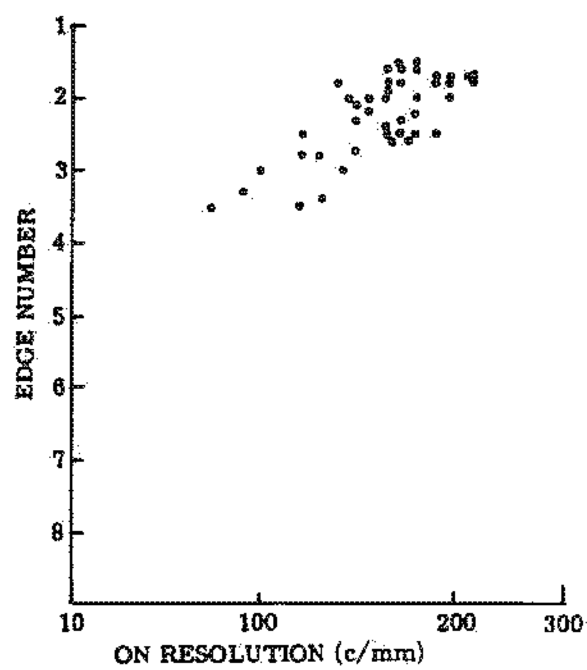


FIGURE 6-23

TABLE 6-5

PRESENT DP MATRIX CALIBRATION DATA

| | Forward Camera | | | Aft Camera | | |
|---|---|---|---|---|---|---|
| | Matrices | | | | | |
| Edge | 1 | 2 | 4 | 1 | 2 | 4 |
| 1 | 270 | 263 | 252 | 305 | 305 | 287 |
| | 215 | 239 | 226 | 250 | 276 | 261 |
| 2 | 170 | 215 | 200 | 200 | 250 | 233 |
| | 140 | 181 | 167 | 165 | 208 | 200 |
| 3 | 115 | 150 | 140 | 137 | 177 | 165 |
| | 100 | 124 | 110 | 121 | 145 | 129 |
| 4 | 88 | 97 | 81 | 103 | 114 | 95 |
| | 76 | 74 | 69 | 92 | 91 | 80 |
| 5 | 66 | 54 | 55 | 80 | 65 | 67 |
| | 50 | 38 | 37 | 60 | 46 | 48 |
| 6 | 35 | 27 | 25 | 44 | 33 | 31 |
| | 28 | 23 | 22 | 36 | 29 | 27 |
| 7 | 23 | 20 | 18 | 28 | 25 | 23 |
| | 18 | 18 | 17 | 23 | 23 | 22 |
| 8 | 16 | 16 | 16 | 21 | 21 | 21 |

6.3.2.5 VEM/PAS Data Collection

Approximately 5,000 edges from Mission 1201 were matched for the quantitative assessment of the camera system performance. To facilitate this effort, three VEM comparators were utilized full time during this operation. The search for edges in cultured detail was restricted to VEM cells. These cells, covering an area of six inches by one half inch on the format, were centered at each 15° of scan and at 0, ±1.0 and ±2.5 inches of field. With these cells, edge population densities could be conveniently grouped together to produce statistically stronger samples than purely random point samplings.

As readers scanned through the photography, cells were located containing cultural detail. Edge matchings within these cells were simply recorded and passed on to data control. Here the edge readings were combined with pertinent identification and operational data for storage in computer memory. Programs were written to retrieve, process, and print this data. The types of analysis questions addressed were:

A. What is the overall comparison of performance between the two cameras?

B. What was the effect of operational changes in the platen position?

C. What are the minor and major axis format resolution profiles?

D. What is the quantitative characterization of the thru focus runs?

It is the intent of the PFA Team to utilize this approach not only in the analysis of upcoming missions, but also to maintain an accumulative data base from which mission performance trends can be established.

The prime difficulty with the VEM/PAS data is the fact that replicate variability is far greater than it was with the laboratory test data. The excessive noise level reduces the reliability of the VEM analysis done on this mission. The average standard deviation for a group of six edge matchings in one cell is 17% of the mean value in lines/mm. Although VEM analysis in fine increments along the format major axis suggests possible camera variability within a cell length, it could also be attributed to variability in the structure of the edges themselves. A study is underway to more adequately define the nature of edge suitability to minimize this potential source of error. It is hoped that we can learn how to establish guidelines for operational edge selection to decrease VEM/PAS variability.

6.3.2.6 Conclusions

A. The VEM technique was used successfully in the analysis of Mission 1201 and shows promise of becoming a primary analysis tool.

B. The VEM resolution calibration needs to be performed over a wider resolution range and in both the flight and scan directions.

C. Improvement in both the VEM Comparator accessories and matrix structure would enhance the utility of the technique.

D. More sophistication in the VEM/PAS software would reduce analysis time.

E. Work should be undertaken to define the suitability of edges to be used for VEM.

# Conclusions and Recommendations

# SECTION VII

## CONCLUSIONS AND RECOMMENDATIONS

### 7.1 CONCLUSIONS/RECOMMENDATIONS

The following conclusions and recommendations are made by the PFA Team:

A. Camera performance on Mission 1201 was good and the camera system met all launch objectives.

B. The KH-9 Camera appears capable of meeting design goals for resolution and coverage.

C. The majority of requirements for first phase intelligence readouts were met. Interpretability was considered good by the NPIC photointerpreters.

D. Area search requirements were met at all scan angles, however, in many instances order of battle readout was difficult beyond plus or minus 45 degrees.

E. The Aft Camera performance was superior to that of the Forward Camera throughout most of Mission 1201.

F. The cause of the large initial out-of-focus condition on the Forward Camera is not understood. Possible causes identified include errors in collimator focus and/or the difference between collimator light source spectrum and daylight. It is recommended that the light source and collimator focus settings at both test facilities be evaluated and modified, if necessary, before Mission 1202.

G. The engineering thru focus runs proved to be extremely useful in optimizing camera performance on-orbit. There were some inadequacies with these tests, however, i.e., some were run over areas of little cultural detail, and sufficient focus increments were not employed. For Mission 1202, greater attention must be placed to the planning for the thru focus engineering tests.

H. Based on on-orbit assessment and post mission evaluation of the telemetry data, it is concluded that the KH-9 functioned as designed and correlated quite closely to the electromechanical signatures established during ground testing.

I. The line target analysis technique is a new approach to quantify image smear from flight photography. Line analysis indicated a higher average smear than expected, particularly on the Forward Camera, in the cross-track direction. Based on the line analysis the Aft Camera performed as expected.

J. Reduction of smear appears to offer the greatest potential for short term improvements in camera system performance. Starting with the SV-3 cameras, modifications are being incorporated which will enable an on-orbit assessment of smear by an ability to incremently adjust the film synchronization. It is recommended that the command software be modified to allow for the full advantage of this capability to be realized.

K. The photography and TM indicated an excessive in-track smear on one first frame of the Forward-looking Camera. The camera was operating in a negative scan sector and a short scan angle. A logic error was identified in the sensor sequencer that improperly generated the skew angle correction when both cameras were operating at negative scan centers and short scan angles. It is recommended that the magnitude of hardware modifications to the sequencer be defined in order to trade-off costs versus operational constraints.

L. Dendritic-like electrostatic discharge plus-density markings were observed on the Aft Camera photography. Operational imagery, however, was not seriously degraded by these markings.

M. No loss of contrast or image quality was noted due to the Wratten 2E Type Filter employed on the Forward Camera. Further flights utilizing the Wratten 2E are recommended.

N. Some mission imagery from the Forward-looking Camera was seriously degraded by specular reflections. This could be particularly harmful with monoscopic operations. It is recommended that mission planners examine the effects of specular reflections before scheduling launch times for future flights.

O. Evaluation of ICD conformance indicates that most ICD requirements are extremely conservative. No changes are warranted at this time.

P. The camera exposure, after a reduction of .2 Stop (.06 log E), was optimum for the mission for photography acquired above a solar altitude of 10 degrees. Sparsity of acquisition at low solar altitudes precluded a thorough exposure analysis of that imagery.

Q. Post recovery original negative handling and reproduction were accomplished without difficulty.

R. Accurate camera performance TM data permitted very successful operation of the Optical Titling System and the efficient breakdown/reproduction of the original negative.

S. Although specialized duplication aided the photointerpreters, in most instances the standard SO-192 reproductions were found to be satisfactory for first phase readout.

T. The image quality of the SO-192 duplicate positives delivered to the photointerpreters were comparable to that of the original negative.

U. Good correlation exists between CRYSPER ground resolved distance predictions, CORN readings, and PI suitability ratings.

V. Visual edge matching (VEM) offers promise as an effective photo-evaluation technique. However, further work with matrix calibration and the nature of edge suitability is required. It is recommended that Mission 1201 photography be further evaluated to resolve some of the unanswered questions and give a further insight to the applicability of this technique, its calibration, and its measurement accuracy.

# APPENDIX A

## GLOSSARY OF TERMS

| | |
|---|---|
| Aft | Aft-looking Camera and Associated Film |
| ACS | Attitude Control System |
| AFSPPF | Air Force Special Projects Production Facility |
| AIM | Aerial Image Modulation |
| aprx | Approximately |
| AUGIE | Acronym for Data Compression Technique Used for RTS to STC Data Transmission |
| BRIDGEHEAD | Primary Film Processing and Immediate Post Flight Evaluation Facility |
| BV | Booster Vehicle |
| C- | Camera Power Off Command |
| C+ | Camera Power On Command |
| CG | Center of Gravity |
| Chamber A | Photographic Vacuum Test Chamber Located at East Coast SSC Facility |
| Chamber A-2 | Photographic Vacuum Test Chamber Located at West Coast Facility |
| c/mm | Cycles Per Millimeter |
| CORN | Controlled Range Network |
| CV | Constant Velocity |
| DIU | Data Interface Unit |
| D log E | Sensitometric Response of Density to Logarithm of Exposure |
| DN | Duplicate Negative |
| DP | Duplicate Positive |
| EM | Electromechanical |
| ESD | Emergency Shut Down |
| ESO | Emergency Shut Down Override |
| FP | Focal Plane |
| FPA | Flight Profile Addendum |
| FP-A | Focal Plane - Forward Camera |
| FP-B | Focal Plane - Aft Camera |
| FT | Film Transport |
| FTF | Field Test Force |
| Forward/FWD | Forward-looking Camera and Associated Film |
| g | Gravity |
| GMT | Greenwich Mean Time |
| GRD | Ground Resolved Distance (bar plus space) |

APPENDIX A (CONT'D)

GLOSSARY OF TERMS

| | |
|---|---|
| Hz | Cycles Per Second (Hertz) |
| HOPE | Computer Program for Evaluating TM Data |
| ICD | Interface Control Document |
| ID | Input Drive Capstan |
| ips | Inch(es) Per Second |
| LSFS | Lateral Separation Focus Sensor |
| MAA | Mission Analysis Area |
| MC | Metering Capstan |
| MCSE | Metering Capstan Summed Error |
| MES | Mission Evaluation Score |
| MFA | Measurement Filter Assembly |
| MIP | Mission Information Potential |
| MONO | Monoscopic Operation |
| MOP | Manual Operation |
| MPR | Mission Performance Review |
| MTF | Modulation Transfer Function |
| NM | Nautical Miles |
| NPIC | National Photographic Interpretation Center |
| OA | Orbit Adjust |
| OB | Optical Bar/Order of Battle |
| OD | Output Drive Capstan |
| ON | Original Negative |
| OP/Op | Camera System Operation |
| PAS | Performance Assessment |
| PCM | Pulse Code Modulation |
| PFA | Post Flight Analysis |
| P-MODE | Photographic Mode |
| PMU | Programmable Memory Unit |
| PN/PNU | Pneumatics |
| PN Plus (+) | Pneumatics On |
| psi | Pounds per Square Inch |
| rad/sec | Radians Per Second |

APPENDIX A (CONT'D)

GLOSSARY OF TERMS

| | |
|---|---|
| REV | Orbital Revolution |
| RMS | Root Mean Square |
| RTS | Remote Tracking Station |
| RV | Reentry/Recovery Vehicle |
| RWC | Rewind Constant |
| RWV | Rewind Velocity |
| SAL | Scan Angle Length |
| SBA | Satellite Basic Assembly |
| SC | Scan Center |
| SCC | System Command and Control |
| SCF | Satellite Control Facility |
| Seq | Sequence |
| SLC-4E | Space Launch Complex - 4 East |
| SOF | Start of Frame |
| Solo | System Engineering Test after Fourth RV Separation |
| SPEC | Specification |
| SS | Sensor Subsystem |
| SSC | Sensor Subsystem Contractor |
| STC | Satellite Test Center |
| SU | Supply Unit |
| SV | Satellite Vehicle |
| SVT | Satellite Vehicle Time |
| SWT | Slit Width Tests |
| $\bar{T}$ | Mean Temperature |
| TCA | Two Camera Assembly |
| TM | Telemetry |
| TU | Take Up Unit |
| UTB | Ultra Thin Base Film |
| VAFB | Vandenberg Air Force Base |
| VBE | Variable Block Erase |
| VDP | Vehicle Disturbance Program |
| VEM | Visual Edge Match |

APPENDIX A (CONT'D)

GLOSSARY OF TERMS

| | |
|---|---|
| Vs | Coarse Film Path Velocity |
| Vx/h | Orbital Angular Rate, In-Track |
| Vy/h | Orbital Angular Rate, Cross-Track |
| WCFO | West Coast Field Office |
| WCPO | West Coast Project Office |

DEFINITIONS

**Acutance** — Acutance is an objective measure of sharpness. It is determined from the average slope of a microdensitometer edge trace.

**ANDING** — Logic operation with two or more inputs, all of which must be TRUE for the output to be TRUE.

**Crystal Ball** — This program is a photometric orbital acquisition model which includes computations of most geometric quantities of interest.

**Defilming** — This operation consists of despooling the original negative from the RV and preparing it for processing.

**Exploitation** — Exploitation is the act of extracting from imagery the full measure of information that can be derived which is of value to finished intelligence producers and related activities, at any given point in time. It is also considered the act of converting images as a result of imagery interpretation, into useful information about the objects, installations, activities, and areas which these images represent. Exploitation is divided into the following three phases:

(1) First Phase - The preliminary, rapid interpretation of newly acquired imagery for the purpose of extracting, organizing, and communicating information to satisfy immediate priority needs.

(2) Second Phase - The systematic review of newly acquired reconnaissance imagery for the purpose of providing a succinct, organized, comprehensive summary of the information extracted, or available for extraction, from the imagery obtained by a mission.

(3) Third Phase - The in-depth exploitation of reconnaissance imagery for the purpose of extracting and coherently organizing the accurate, detailed, and comprehensive information required in the production of intelligence. This analysis may involve more than one mission and is oriented toward specific targets and functional categories.

**Granularity** — Granularity is the objective quality of an image associated with the non-uniformity of a uniformly exposed and processed area.

**Identification Qualifiers** — Identification qualifiers are used by photointerpeters to designate varying degrees of confidence in the identification of targets and their functions. The qualifiers listed below are on the sufficiency of evidence.

(1) Firm - The evidence is sufficient to permit a definite identification.

(2) Probable - The evidence for the identification is strong.

APPENDIX A (CONT'D)

GLOSSARY OF TERMS

(3) Possible - The evidence indicates that the identification is reasonable and more likely than others considered.

(4) Suspect - The evidence is insufficient to permit identification with any degree of certainty, but photography or other information provides some indications of what the function may be.

**Interpretability** — Interpretability is defined as the suitability of the imagery for answering requirements on a given type of target. Some of the factors that affect interpretability are camera performance, natural and man-made atmospheric conditions, scale, and lighting conditions during acquisition. The following are the four levels of interpretability:

(1) Excellent - Suitable for interpretation to answer requirements on a given type of target in complete detail.

(2) Good - Suitable for interpretation to answer requirements on a given type of target in considerable detail.

(3) Fair - Suitable for interpretation to answer requirements on a given type of target, but with only average detail.

(4) Poor - Unsuitable for interpretation to adequately answer requirements on a given type of target.

**OAK** — An OAK is an NPIC publication that presents the results of the first phase exploitation of satellite imagery.

**OAK Supplement** — An OAK Supplement is an NPIC publication that presents the results of the second-phase exploitation of satellite imagery.

**Order of Battle** — Order of Battle is an inventory or count of military capabilities which fall into three basic categories, Air, Naval, and Ground.

THIS PAGE
INTENTIONALLY
LEFT BLANK

## APPENDIX B

### BASIC ORBITAL PARAMETERS

| Day | Rev | Eccentricity $x10^{-3}$ | Period (min/sec) | Min Alt (NM) | Perigee Loc (°N Lat) |
|---|---|---|---|---|---|
| Case 103F | Ref | 9.051 | 89:22 | 99.9 | 21 |
| Injection | 0 | 9.076 | 89:22 | 99.6 | 20 |
| 1 | 16 | 9.210 | 89:22 | 98.7 | 18 |
| 2 | 33 | 9.149 | 89:20 | 98.4 | 23 |
| 3 | 49 | 9.118 | 89:18 | 98.2 | 27 |
| 4 | 65 | 9.055 | 89:17 | 98.1 | 31 |
| 5 | 81 | 8.970 | 89:15 | 98.1 | 35 |
| 6 | 96 | 8.899 | 89:13 | 98.0 | 39 |
| 7 | 112 | 8.826 | 89:12 | 98.0 | 43 |
| OA | 127 | | | | |
| 8 | 128 | 10.042 | 89:20 | 98.1 | 46 |
| 9 | 145 | 9.910 | 89:18 | 98.2 | 50 |
| 10 | 162 | 9.788 | 89:15 | 98.3 | 54 |
| 11 | 178 | 9.648 | 89:14 | 98.4 | 58 |
| OA | 190 | | | | |
| 12 | 192 | 9.969 | 89:18 | 99.1 | 56 |
| 13 | 209 | 9.790 | 89:16 | 99.5 | 61 |
| 14 | 223 | 9.710 | 89:14 | 99.5 | 64 |
| 15 | 242 | 9.948 | 89:11 | 99.7 | 68 |
| 16 | 254 | 9.370 | 89:09 | 99.6 | 71 |
| OA | 256 | | | | |
| 17 | 270 | 8.789 | 89:19 | 99.5 | 20 |
| 18 | 286 | 8.716 | 89:17 | 99.2 | 25 |
| 19 | 303 | 8.663 | 89:16 | 98.8 | 29 |
| 20 | 319 | 8.582 | 89:14 | 98.6 | 33 |
| OA | 336 | | | | |
| 21 | 338 | 8.785 | 89:15 | 98.6 | 36 |
| 22 | 352 | 8.713 | 89:13 | 98.4 | 40 |
| 23 | 368 | 8.624 | 89:11 | 98.4 | 43 |
| 24 | 384 | 8.510 | 89:09 | 98.3 | 47 |
| OA | 385 | | | | |

APPENDIX B (CONT'D)

BASIC ORBITAL PARAMETERS

| Day | Rev | Eccentricity $x10^{-3}$ | Period (min/sec) | Min Alt (NM) | Perigee Loc (°N Lat) |
|---|---|---|---|---|---|
| 25 | 400 | 10.140 | 89:21 | 98.6 | 50 |
| 26 | 415 | - | 89:20 | 98.9 | 54 |
| 27 | 432 | 9.88 | 89:17 | 98.9 | 58 |
| 28 | 448 | 9.749 | 89:14 | 99.0 | 61 |
| 29 | 464 | 9.584 | 89:12 | 99.2 | 65 |
| 30 | 480 | 9.424 | 89:10 | 99.3 | 69 |
| 31 | 496 | 9.240 | 89:07 | 99.4 | 72 |



Approved for Release: 2022/03/03 C05132845

# APPENDIX C

## CAMERA OPERATIONS SUMMARY

| | Rev | Rev Op No. | Mission Op No. | Scan Angle (degrees) | Scan Center (degrees) | Forward (frames) | Aft (frames) |
|---|---|---|---|---|---|---|---|
| RV-1 | 8 | 1 | 1 | 90 | 0 | 6 | 6 |
| | 8 | 2 | 2 | 30 | -15 | 6 | 6 |
| | 8 | 3 | 3 | 60 | 30 | 6 | 6 |
| | 14 | 1 | 4 | 90 | 0 | 50 | 50 |
| | 16 | 1 | 5 | 90 | 0 | 58 | 58 |
| | 20 | 1 | 6 | 90 | 15 | 28 | 28 |
| | 21 | 1 | 7 | 90 | 0 | 52 | 52 |
| | 22 | 1 | 8 | 90 | 0 | 58 | 58 |
| | 23 | 1 | 9 | 120 | 0 | 102 | 102 |
| | 24 | 1 | 10 | 60 | 0 | 6 | 6 |
| | 24 | 2 | 11 | 90 | 0 | 13 | 13 |
| | 25 | 1 | 12 | 90 | 0 | 16 | 16 |
| | 26 | 1 | 13 | 90 | 0 | 27 | 27 |
| | 29 | 1 | 14 | 90 | 0 | 28 | 28 |
| | 31 | 1 | 15 | 90 | 0 | 11 | 11 |
| | 31 | 2 | 16 | 120 | 0 | 80 | 80 |
| | 32 | 1 | 17 | 120 | 0 | 75 | 75 |
| | 33 | 1 | 18 | 90 | -15 | 6 | 6 |
| | 36 | 1 | 19 | 90 | 0 | 53 | 53 |
| | 37 | 1 | 20 | 60 | -15 | 47 | 47 |
| | 38 | 1 | 21 | 90 | 0 | 22 | 22 |
| | 38 | 2 | 22 | 90 | 0 | 32 | 32 |
| | 38 | 3 | 23 | 60 | -15 | 62 | 62 |
| | 39 | 1 | 24 | 90 | 0 | 33 | 33 |
| | 39 | 2 | 25 | 90 | 0 | 67 | 67 |
| | 40 | 1 | 26 | 60 | 0 | 6 | 6 |
| | 40 | 2 | 27 | 90 | 0 | 37 | 37 |
| | 41 | 1 | 28 | 60 | 15 | 67 | 67 |
| | 42 | 1 | 29 | 60 | 0 | 22 | 22 |
| | 42 | 2 | 30 | 120 | 0 | 17 | 17 |

APPENDIX C (CONT'D)

CAMERA OPERATIONS SUMMARY

| | Rev | Rev Op No. | Mission Op No. | Scan Angle (degrees) | Scan Center (degrees) | Forward (frames) | Aft (frames) |
|---|---|---|---|---|---|---|---|
| RV-1 | 42 | 3 | 31 | 90 | 0 | 21 | 21 |
| | 46 | 1 | 32 | 60 | 15 | 6 | 6 |
| | 47 | 1 | 33 | 60 | -15 | 6 | 6 |
| | 47 | 2 | 34 | 90 | 0 | 55 | 55 |
| | 48 | 1 | 35 | 120 | 0 | 72 | 72 |
| | 49 | 1 | 36 | 60 | -30 | 6 | 6 |
| | 51 | 1 | 37 | 60 | -30 | 8 | 8 |
| | 52 | 1 | 38 | 90 | 0 | 18 | 18 |
| | 53 | 1 | 39 | 60 | -15 | 47 | 47 |
| | 54 | 1 | 40 | 90 | 0 | 47 | 47 |
| | 54 | 2 | 41 | 90 | 0 | 33 | 33 |
| | 55 | 1 | 42 | 60 | 15 | 16 | 16 |
| | 55 | 2 | 43 | 60 | 15 | 27 | 27 |
| | 55 | 3 | 44 | 90 | 0 | 72 | 72 |
| | 56 | 1 | 45 | 60 | 15 | 41 | 41 |
| | 57 | 1 | 46 | 90 | -15 | 27 | 27 |
| | 57 | 2 | 47 | 60 | 15 | 12 | 12 |
| | 58 | 1 | 48 | 60 | 15 | 18 | 18 |
| | 58 | 2 | 49 | 90 | 0 | 16 | 16 |
| | 61 | 1 | 50 | 60 | 0 | 11 | 11 |
| | 62 | 1 | 51 | 60 | 15 | 6 | 6 |
| | 63 | 1 | 52 | 60 | 15 | 6 | 6 |
| | 63 | 2 | 53 | 90 | 15 | 38 | 38 |
| | 70 | 1 | 54 | 90 | 0 | 77 | 77 |
| | 70 | 2 | 55 | 60 | -15 | 47 | 47 |
| | 71 | 1 | 56 | 60 | 15 | 47 | 47 |
| | 71 | 2 | 57 | 90 | 0 | 31 | 31 |
| | 72 | 1 | 58 | 60 | 15 | 27 | 27 |
| | 72 | 2 | 59 | 60 | 15 | 42 | 42 |
| | 73 | 1 | 60 | 60 | 0 | 6 | 6 |

APPENDIX C (CONT'D)

CAMERA OPERATIONS SUMMARY

| | Rev | Rev Op No. | Mission Op No. | Scan Angle (degrees) | Scan Center (degrees) | Forward (frames) | Aft (frames) |
|---|---|---|---|---|---|---|---|
| RV-1 | 73 | 2 | 61 | 90 | -15 | 17 | 17 |
| | 74 | 1 | 62 | 90 | 0 | 37 | 37 |
| | 75 | 1 | 63 | 30 | 15 | 6 | 6 |
| RV-2 | 77 | 1 | 64 | 60 | 15 | 17 | 17 |
| | 84 | 1 | 65 | 90 | 0 | 8 | 8 |
| | 85 | 1 | 66 | 30 | -15 | 6 | 6 |
| | 86 | 1 | 67 | 90 | 0 | 57 | 57 |
| | 86 | 2 | 68 | 60 | -15 | 21 | 21 |
| | 87 | 1 | 69 | 60 | -15 | 22 | 22 |
| | 87 | 2 | 70 | 30 | -15 | 12 | 12 |
| | 87 | 3 | 71 | 30 | 30 | 7 | 7 |
| | 88 | 1 | 72 | 60 | 0 | 6 | 6 |
| | 88 | 2 | 73 | 90 | 0 | 67 | 67 |
| | 88 | 3 | 74 | 30 | 15 | 17 | 17 |
| | 89 | 1 | 75 | 60 | 15 | 41 | 41 |
| | 90 | 1 | 76 | 30 | -30 | 11 | 11 |
| | 90 | 2 | 77 | 90 | 0 | 37 | 37 |
| | 90 | 3 | 78 | 90 | 0 | 27 | 27 |
| | 90 | 4 | 79 | 90 | 0 | 33 | 33 |
| | 90 | 5 | 80 | 30 | -30 | 22 | 22 |
| | 91 | 1 | 81 | 30 | 15 | 11 | 11 |
| | 93 | 1 | 82 | 30 | 30 | 26 | 26 |
| | 94 | 1 | 83 | 90 | 0 | 17 | 17 |
| | 95 | 1 | 84 | 90 | 0 | 6 | 6 |
| | 96 | 1 | 85 | 60 | -30 | 46 | 46 |
| | 100 | 1 | 86 | 90 | 0 | 42 | 42 |
| | 101 | 1 | 87 | 90 | 0 | 11 | 11 |
| | 102 | 1 | 88 | 90 | 0 | 107 | 107 |
| | 102 | 2 | 89 | 60 | 15 | 22 | 22 |
| | 102 | 3 | 90 | 30 | -30 | 22 | 22 |

APPENDIX C (CONT'D)

CAMERA OPERATIONS SUMMARY

| | Rev | Rev Op No. | Mission Op No. | Scan Angle (degrees) | Scan Center (degrees) | Forward (frames) | Aft (frames) |
|---|---|---|---|---|---|---|---|
| RV-2 | 102 | 4 | 91 | 90 | 0 | 51 | 51 |
| | 103 | 1 | 92 | 90 | 0 | 37 | 37 |
| | 103 | 2 | 93 | 30 | 30 | 27 | 27 |
| | 103 | 3 | 94 | 30 | 30 | 7 | 7 |
| | 103 | 4 | 95 | 90 | 0 | 57 | 57 |
| | 103 | 5 | 96 | 30 | 30 | 32 | 32 |
| | 104 | 1 | 97 | 60 | 0 | 6 | 6 |
| | 104 | 2 | 98 | 60 | 15 | 36 | 36 |
| | 104 | 3 | 99 | 90 | 0 | 97 | 97 |
| | 106 | 1 | 100 | 90 | 0 | 21 | 21 |
| | 106 | 2 | 101 | 30 | 15 | 6 | 6 |
| | 106 | 3 | 102 | 60 | 15 | 32 | 32 |
| | 106 | 4 | 103 | 90 | 0 | 17 | 17 |
| | 107 | 1 | 104 | 30 | -15 | 11 | 11 |
| | 109 | 1 | 105 | 30 | 30 | 11 | 11 |
| | 109 | 2 | 106 | 30 | 30 | 21 | 21 |
| | 110 | 1 | 107 | 90 | 0 | 21 | 21 |
| | 110 | 2 | 108 | 30 | -30 | 13 | 13 |
| | 113 | 1 | 109 | 30 | 30 | 6 | 6 |
| | 116 | 1 | 110 | 30 | -30 | 42 | 42 |
| | 118 | 1 | 111 | 90 | 0 | 42 | 42 |
| | 118 | 2 | 112 | 90 | 0 | 107 | 107 |
| | 119 | 1 | 113 | 90 | 0 | 87 | 87 |
| | 119 | 2 | 114 | 90 | 0 | 97 | 97 |
| | 120 | 1 | 115 | 90 | 0 | 202 | 202 |
| | 121 | 1 | 116 | 60 | 0 | 6 | 6 |
| | 121 | 2 | 117 | 90 | 0 | 92 | 92 |
| | 122 | 1 | 118 | 90 | 0 | 46 | 46 |
| | 123 | 1 | 119 | 60 | 15 | 16 | 16 |
| | 129 | 1 | 120 | 90 | 15 | 33 | 33 |

APPENDIX C (CONT'D)

CAMERA OPERATIONS SUMMARY

| | Rev | Rev Op No. | Mission Op No. | Scan Angle (degrees) | Scan Center (degrees) | Forward (frames) | Aft (frames) |
|---|---|---|---|---|---|---|---|
| RV-2 | 133 | 1 | 121 | 60 | -15 | 37 | 37 |
| | 134 | 1 | 122 | 30 | -30 | 57 | 57 |
| | 134 | 2 | 123 | 30 | 30 | 16 | 16 |
| | 134 | 3 | 124 | 30 | -30 | 8 | 8 |
| | 135 | 1 | 125 | 90 | 0 | 25 | 25 |
| | 135 | 2 | 126 | 30 | 30 | 12 | 12 |
| | 135 | 3 | 127 | 30 | 30 | 16 | 16 |
| | 135 | 4 | 128 | 30 | -30 | 12 | 12 |
| | 135 | 5 | 129 | 30 | 30 | 17 | 17 |
| | 136 | 1 | 130 | 30 | 30 | 16 | 16 |
| | 136 | 2 | 131 | 30 | 15 | 22 | 22 |
| | 136 | 3 | 132 | 60 | 15 | 87 | 87 |
| | 136 | 4 | 133 | 30 | -30 | 27 | 27 |
| | 137 | 1 | 134 | 60 | 0 | 6 | 6 |
| | 137 | 2 | 135 | 30 | -30 | 11 | 11 |
| | 137 | 3 | 136 | 30 | 15 | 12 | 12 |
| | 138 | 1 | 137 | 30 | 45 | 16 | 16 |
| | 138 | 2 | 138 | 60 | -15 | 11 | 11 |
| | 139 | 1 | 139 | 30 | -15 | 13 | 13 |
| | 139 | 2 | 140 | 30 | 0 | 21 | 21 |
| | 139 | 3 | 141 | 30 | 30 | 6 | 6 |
| | 139 | 4 | 142 | 30 | 30 | 16 | 16 |
| | 143 | 1 | 143 | 30 | 15 | 11 | 11 |
| | 143 | 2 | 144 | 30 | 15 | 6 | 6 |
| | 145 | 1 | 145 | 60 | 15 | 34 | 34 |
| | 150 | 1 | 146 | 90 | 0 | 52 | 52 |
| | 151 | 1 | 147 | 90 | 0 | 16 | 16 |
| | 151 | 2 | 148 | 30 | -30 | 26 | 26 |
| | 152 | 1 | 149 | 30 | 15 | 11 | 11 |
| | 152 | 2 | 150 | 30 | -30 | 22 | 22 |
| | 152 | 3 | 151 | 90 | 0 | 52 | 52 |

APPENDIX C (CONT'D)

CAMERA OPERATIONS SUMMARY

| | Rev | Rev Op No. | Mission Op No. | Scan Angle (degrees) | Scan Center (degrees) | Forward (frames) | Aft (frames) |
|---|---|---|---|---|---|---|---|
| RV-2 | 152 | 4 | 152 | 30 | 15 | 22 | 22 |
| | 153 | 1 | 153 | 60 | 0 | 6 | 6 |
| | 153 | 2 | 154 | 30 | -30 | 32 | 32 |
| | 153 | 3 | 155 | 30 | -30 | 77 | 77 |
| | 154 | 1 | 156 | 90 | 0 | 31 | 31 |
| | 154 | 2 | 157 | 30 | 30 | 6 | 6 |
| | 154 | 3 | 158 | 30 | -30 | 11 | 11 |
| | 155 | 1 | 159 | 60 | -15 | 6 | 6 |
| | 155 | 2 | 160 | 30 | -30 | 17 | 17 |
| | 155 | 3 | 161 | 60 | 15 | 17 | 17 |
| | 155 | 4 | 162 | 60 | 15 | 11 | 11 |
| | 159 | 1 | 163 | 30 | -45 | 6 | 6 |
| | 160 | 1 | 164 | 30 | -30 | 7 | 7 |
| | 160 | 2 | 165 | 60 | -30 | 29 | 29 |
| | 165 | 1 | 166 | 30 | -30 | 16 | 16 |
| | 165 | 2 | 167 | 60 | -30 | 38 | 38 |
| | 166 | 1 | 168 | 30 | -30 | 21 | 21 |
| | 166 | 2 | 169 | 30 | -30 | 23 | 23 |
| | 166 | 3 | 170 | 90 | 0 | 55 | 55 |
| | 167 | 1 | 171 | 90 | -15 | 42 | 42 |
| | 167 | 2 | 172 | 120 | 0 | 52 | 52 |
| | 167 | 3 | 173 | 60 | 15 | 46 | 46 |
| | 167 | 4 | 174 | 60 | -30 | 32 | 32 |
| | 168 | 1 | 175 | 60 | 15 | 36 | 36 |
| | 168 | 2 | 176 | 60 | 30 | 37 | 37 |
| | 169 | 1 | 177 | 60 | 0 | 6 | 6 |
| | 169 | 2 | 178 | 60 | 30 | 36 | 36 |
| | 169 | 3 | 179 | 90 | -15 | 13 | 13 |
| | 169 | 4 | 180 | 90 | 15 | 18 | 18 |
| | 170 | 1 | 181 | 30 | -30 | 11 | 11 |

APPENDIX C (CONT'D)

CAMERA OPERATIONS SUMMARY

| | Rev | Rev Op No. | Mission Op No. | Scan Angle (degrees) | Scan Center (degrees) | Forward (frames) | Aft (frames) |
|---|---|---|---|---|---|---|---|
| RV-2 | 170 | 2 | 182 | 90 | -15 | 27 | 27 |
| | 170 | 3 | 183 | 30 | 15 | 11 | 11 |
| | 171 | 1 | 184 | 30 | -15 | 11 | 11 |
| | 171 | 2 | 185 | 30 | -30 | 6 | 6 |
| | 171 | 3 | 186 | 120 | 0 | 42 | 42 |
| | 172 | 1 | 187 | 30 | 30 | 37 | 37 |
| RV-3 | 180 | 1 | 188 | 30 | -30 | 6 | 6 |
| | 181 | 1 | 189 | 30 | 0 | 11 | 11 |
| | 182 | 1 | 190 | 30 | 0 | 6 | 6 |
| | 183 | 1 | 191 | 90 | 0 | 37 | 37 |
| | 183 | 2 | 192 | 30 | -30 | 27 | 27 |
| | 183 | 3 | 193 | 60 | -15 | 57 | 57 |
| | 184 | 1 | 194 | 30 | -30 | 47 | 47 |
| | 184 | 2 | 195 | 30 | -30 | 42 | 42 |
| | 185 | 1 | 196 | 60 | 0 | 6 | 6 |
| | 185 | 2 | 197 | 30 | 30 | 21 | 21 |
| | 186 | 1 | 198 | 30 | 30 | 6 | 6 |
| | 187 | 1 | 199 | 30 | -30 | 11 | 11 |
| | 188 | 1 | 200 | 30 | 30 | 6 | 6 |
| | 190 | 1 | 201 | 30 | 15 | 8 | 8 |
| | 192 | 1 | 202 | 30 | -30 | 8 | 8 |
| | 193 | 1 | 203 | 30 | -30 | 6 | 6 |
| | 197 | 1 | 204 | 30 | 30 | 21 | 21 |
| | 198 | 1 | 205 | 90 | 0 | 32 | 32 |
| | 198 | 2 | 206 | 30 | -45 | 16 | 16 |
| | 199 | 1 | 207 | 90 | 0 | 52 | 52 |
| | 199 | 2 | 208 | 30 | -30 | 16 | 16 |
| | 199 | 3 | 209 | 90 | 0 | 48 | 48 |
| | 200 | 1 | 210 | 30 | 30 | 6 | 6 |
| | 200 | 2 | 211 | 30 | -30 | 18 | 18 |

APPENDIX C (CONT'D)

CAMERA OPERATIONS SUMMARY

| | Rev | Rev Op No. | Mission Op No. | Scan Angle (degrees) | Scan Center (degrees) | Forward (frames) | Aft (frames) |
|---|---|---|---|---|---|---|---|
| RV-3 | 200 | 3 | 212 | 30 | 15 | 11 | 11 |
| | 201 | 1 | 213 | 60 | 0 | 6 | 6 |
| | 201 | 2 | 214 | 90 | 0 | 26 | 26 |
| | 202 | 1 | 215 | 90 | 0 | 31 | 31 |
| | 203 | 1 | 216 | 30 | 30 | 6 | 6 |
| | 205 | 1 | 217 | 30 | -30 | 8 | 8 |
| | 208 | 1 | 218 | 30 | 30 | 8 | 8 |
| | 209 | 1 | 219 | 30 | -30 | 13 | 13 |
| | 213 | 1 | 220 | 60 | 15 | 21 | 21 |
| | 214 | 1 | 221 | 90 | 0 | 32 | 32 |
| | 215 | 1 | 222 | 60 | 15 | 77 | 77 |
| | 215 | 2 | 223 | 90 | 0 | 46 | 46 |
| | 216 | 1 | 224 | 30 | -30 | 16 | 16 |
| | 216 | 2 | 225 | 30 | 30 | 11 | 11 |
| | 216 | 3 | 226 | 30 | 30 | 26 | 26 |
| | 217 | 1 | 227 | 60 | 0 | 6 | 6 |
| | 217 | 2 | 228 | 90 | 0 | 67 | 67 |
| | 218 | 1 | 229 | 90 | 0 | 27 | 27 |
| | 219 | 1 | 230 | 30 | 30 | 16 | 16 |
| | 219 | 2 | 231 | 30 | 30 | 11 | 11 |
| | 219 | 3 | 232 | 30 | 30 | 11 | 11 |
| | 220 | 1 | 233 | 60 | -15 | 21 | 21 |
| | 221 | 1 | 234 | 30 | 15 | 18 | 18 |
| | 225 | 1 | 235 | 30 | 15 | 13 | 13 |
| | 226 | 1 | 236 | 60 | 30 | 47 | 47 |
| | 229 | 1 | 237 | 30 | -15 | 16 | 16 |
| | 230 | 1 | 238 | 30 | 15 | 6 | 6 |
| | 231 | 1 | 239 | 90 | 0 | 42 | 42 |
| | 231 | 2 | 240 | 60 | -15 | 46 | 46 |
| | 232 | 1 | 241 | 90 | 0 | 27 | 27 |

## APPENDIX C (CONT'D)

## CAMERA OPERATIONS SUMMARY

| | Rev | Rev Op No. | Mission Op No. | Scan Angle (degrees) | Scan Center (degrees) | Forward (frames) | Aft (frames) |
|---|---|---|---|---|---|---|---|
| RV-3 | 232 | 2 | 242 | 30 | -30 | 16 | 16 |
| | 232 | 3 | 243 | 60 | 15 | 7 | 7 |
| | 232 | 4 | 244 | 60 | 15 | 11 | 11 |
| | 233 | 1 | 245 | 30 | -30 | 62 | 62 |
| | 233 | 2 | 246 | 60 | -15 | 12 | 12 |
| | 234 | 1 | 247 | 60 | 0 | 6 | 6 |
| | 234 | 2 | 248 | 60 | 0 | 11 | 11 |
| | 234 | 3 | 249 | 30 | 45 | 12 | 12 |
| | 234 | 4 | 250 | 90 | 0 | 27 | 27 |
| | 235 | 1 | 251 | 60 | -15 | 11 | 11 |
| | 235 | 2 | 252 | 90 | 0 | 60 | 60 |
| | 236 | 1 | 253 | 60 | 15 | 6 | 6 |
| | 237 | 1 | 254 | 60 | 15 | 12 | 12 |
| | 242 | 1 | 255 | 60 | 15 | 26 | 26 |
| | 248 | 1 | 256 | 30 | -30 | 22 | 22 |
| | 248 | 2 | 257 | 60 | 15 | 22 | 22 |
| | 249 | 1 | 258 | 30 | 30 | 26 | 26 |
| | 249 | 2 | 259 | 60 | -15 | 21 | 21 |
| | 250 | 1 | 260 | 60 | 0 | 6 | 6 |
| | 250 | 2 | 261 | 30 | -30 | 26 | 26 |
| | 250 | 3 | 262 | 30 | 30 | 66 | 66 |
| | 251 | 1 | 263 | 30 | 30 | 31 | 31 |
| | 251 | 2 | 264 | 30 | -15 | 11 | 11 |
| | 251 | 3 | 265 | 30 | -15 | 6 | 6 |
| | 252 | 1 | 266 | 60 | -15 | 7 | 7 |
| | 258 | 1 | 267 | 30 | -15 | 19 | 19 |
| | 262 | 1 | 268 | 30 | 15 | 8 | 8 |
| | 263 | 1 | 269 | 60 | -15 | 26 | 26 |
| | 264 | 1 | 270 | 60 | 15 | 31 | 31 |
| | 264 | 2 | 271 | 90 | 0 | 18 | 18 |

## APPENDIX C (CONT'D)

### CAMERA OPERATIONS SUMMARY

| | Rev | Rev Op No. | Mission Op No. | Scan Angle (degrees) | Scan Center (degrees) | Forward (frames) | Aft (frames) |
|---|---|---|---|---|---|---|---|
| RV-3 | 264 | 3 | 272 | 30 | -30 | 32 | 32 |
| | 264 | 4 | 273 | 90 | 0 | 17 | 17 |
| | 265 | 1 | 274 | 60 | -15 | 6 | 6 |
| | 266 | 1 | 275 | 60 | 0 | 6 | 6 |
| | 266 | 2 | 276 | 30 | -15 | 13 | 13 |
| | 266 | 3 | 277 | 60 | -15 | 11 | 11 |
| | 267 | 1 | 278 | 60 | 15 | 62 | 62 |
| | 268 | 1 | 279 | 30 | 0 | 11 | 11 |
| | 269 | 1 | 280 | 30 | 30 | 6 | 6 |
| | 271 | 1 | 281 | 30 | 30 | 6 | 6 |
| | 274 | 1 | 282 | 60 | -15 | 20 | 20 |
| | 278 | 1 | 283 | 30 | -15 | 8 | 8 |
| | 279 | 1 | 284 | 90 | 0 | 22 | 22 |
| | 280 | 1 | 285 | 30 | 30 | 31 | 31 |
| | 280 | 2 | 286 | 30 | 0 | 19 | 19 |
| | 280 | 3 | 287 | 30 | 30 | 36 | 36 |
| | 280 | 4 | 288 | 30 | -30 | 7 | 7 |
| | 280 | 5 | 289 | 30 | 30 | 37 | 37 |
| | 280 | 6 | 290 | 90 | 0 | 72 | 72 |
| | 281 | 1 | 291 | 30 | -30 | 23 | 23 |
| | 281 | 2 | 292 | 90 | 0 | 16 | 16 |
| | 282 | 1 | 293 | 60 | 0 | 6 | 6 |
| | 282 | 2 | 294 | 60 | 15 | 17 | 17 |
| | 283 | 1 | 295 | 90 | 0 | 82 | 82 |
| | 283 | 2 | 296 | 30 | 30 | 17 | 17 |
| | 284 | 1 | 297 | 60 | -15 | 17 | 17 |
| | 285 | 1 | 298 | 30 | -30 | 6 | 6 |
| | 286 | 1 | 299 | 30 | 30 | 11 | 11 |
| | 287 | 1 | 300 | 30 | -30 | 11 | 11 |
| | 290 | 1 | 301 | 30 | -15 | 21 | 21 |

APPENDIX C (CONT'D)

CAMERA OPERATIONS SUMMARY

| | Rev | Rev Op No. | Mission Op No. | Scan Angle (degrees) | Scan Center (degrees) | Forward (frames) | Aft (frames) |
|---|---|---|---|---|---|---|---|
| RV-3 | 293 | 1 | 302 | 30 | -30 | 8 | 8 |
| | 295 | 1 | 303 | 60 | -15 | 16 | 16 |
| | 296 | 1 | 304 | 30 | 30 | 37 | 37 |
| | 296 | 2 | 305 | 30 | 15 | 11 | 11 |
| | 296 | 3 | 306 | 30 | -30 | 7 | 7 |
| | 296 | 4 | 307 | 30 | 30 | 17 | 17 |
| | 296 | 5 | 308 | 30 | 15 | 6 | 6 |
| | 296 | 6 | 309 | 90 | 0 | 12 | 12 |
| | 297 | 1 | 310 | 60 | -30 | 17 | 17 |
| | 298 | 1 | 311 | 60 | 0 | 6 | 6 |
| | 298 | 2 | 312 | 30 | -15 | 6 | 6 |
| | 299 | 1 | 313 | 90 | 0 | 17 | 17 |
| | 299 | 2 | 314 | 60 | 0 | 25 | 25 |
| | 300 | 1 | 315 | 90 | 0 | 11 | 11 |
| | 301 | 1 | 316 | 30 | -30 | 6 | 6 |
| | 302 | 1 | 317 | 30 | -30 | 11 | 11 |
| | 303 | 1 | 318 | 30 | 30 | 6 | 6 |
| | 304 | 1 | 319 | 30 | 15 | 6 | 6 |
| | 305 | 1 | 320 | 60 | 0 | 6 | 6 |
| | 306 | 1 | 321 | 60 | 0 | 29 | 29 |
| | 310 | 1 | 322 | 30 | 30 | 18 | 18 |
| | 311 | 1 | 323 | 30 | -15 | 8 | 8 |
| | 312 | 1 | 324 | 90 | 0 | 37 | 37 |
| | 312 | 2 | 325 | 30 | 0 | 11 | 11 |
| | 312 | 3 | 326 | 90 | 0 | 77 | 77 |
| | 313 | 1 | 327 | 30 | -30 | 18 | 18 |
| | 313 | 2 | 328 | 30 | -45 | 12 | 12 |
| | 314 | 1 | 329 | 60 | 0 | 6 | 6 |
| | 314 | 2 | 330 | 30 | 30 | 31 | 31 |
| | 314 | 3 | 331 | 30 | 0 | 7 | 7 |

APPENDIX C (CONT'D)

CAMERA OPERATIONS SUMMARY

| | Rev | Rev Op No. | Mission Op No. | Scan Angle (degrees) | Scan Center (degrees) | Forward (frames) | Aft (frames) |
|---|---|---|---|---|---|---|---|
| RV-3 | 314 | 4 | 332 | 30 | 30 | 7 | 7 |
| | 314 | 5 | 333 | 30 | -30 (ESD CAM B) | | |
| | 323 | 1 | 334 | 60 | 0 | 6 | 6 |
| | 327 | 1 | 335 | 60 | -15 | 7 | 7 |
| | 328 | 1 | 336 | 60 | -15 | 22 | 22 |
| | 328 | 2 | 337 | 90 | 0 | 72 | 72 |
| | 329 | 1 | 338 | 90 | 0 | 16 | 16 |
| | 330 | 1 | 339 | 60 | 15 | 21 | 21 |
| | 330 | 2 | 340 | 60 | 15 | 11 | 11 |
| | 331 | 1 | 341 | 60 | 0 | 6 | 6 |
| | 331 | 2 | 342 | 60 | -15 | 6 | 6 |
| | 332 | 1 | 343 | 60 | 15 | 27 | 27 |
| | 332 | 2 | 344 | 60 | -15 | 11 | 11 |
| | 333 | 1 | 345 | 90 | 0 | 31 | 31 |
| | 335 | 1 | 346 | 90 | 0 | 6 | 6 |
| | 344 | 1 | 347 | 90 | 0 | 57 | 57 |
| | 345 | 1 | 348 | 60 | 15 | 11 | 11 |
| | 345 | 2 | 349 | 60 | 0 | 27 | 27 |
| | 345 | 3 | 350 | 60 | 15 | 16 | 16 |
| | 346 | 1 | 351 | 60 | 0 | 6 | 6 |
| | 346 | 2 | 352 | 60 | -15 | 11 | 11 |
| | 346 | 3 | 353 | 60 | -15 | 16 | 16 |
| | 347 | 1 | 354 | 60 | 15 | 11 | 11 |
| | 348 | 1 | 355 | 60 | 0 | 11 | 11 |
| | 349 | 1 | 356 | 90 | 0 | 37 | 37 |
| | 360 | 1 | 357 | 60 | -30 | 11 | 11 |
| | 361 | 1 | 358 | 90 | 0 | 11 | 11 |
| | 361 | 2 | 359 | 60 | -30 | 7 | 7 |
| | 363 | 1 | 360 | 60 | 0 | 6 | 6 |
| | 363 | 2 | 361 | 60 | -15 | 6 | 6 |

APPENDIX C (CONT'D)

CAMERA OPERATIONS SUMMARY

| | Rev | Rev Op No. | Mission Op No. | Scan Angle (degrees) | Scan Center (degrees) | Forward (frames) | Aft (frames) |
|---|---|---|---|---|---|---|---|
| RV-3 | 364 | 1 | 362 | 60 | -15 | 11 | 11 |
| | 365 | 1 | 363 | 90 | 0 | 72 | 72 |
| | 368 | 1 | 364 | 60 | -15 | 6 | 6 |
| | 376 | 1 | 365 | 60 | -15 | 36 | 36 |
| | 377 | 1 | 366 | 60 | 0 | 16 | 16 |
| | 378 | 1 | 367 | 60 | 0 | 11 | 11 |
| | 379 | 1 | 368 | 60 | 0 | 6 | 6 |
| | 379 | 2 | 369 | 60 | -15 | 11 | 11 |
| | 381 | 1 | 370 | 90 | 0 | 67 | 67 |
| | 392 | 1 | 371 | 90 | 0 | 26 | 26 |
| | 393 | 1 | 372 | 60 | -15 | 21 | 21 |
| | 393 | 2 | 373 | 60 | 15 | 11 | 11 |
| | 394 | 1 | 374 | 60 | -15 | 6 | 6 |
| | 396 | 1 | 375 | 60 | 15 | 6 | 6 |
| | 397 | 1 | 376 | 90 | 0 | 39 | 39 |
| RV-4 | 420 | 1 | 377 | 60 | 15 | 10 | 10 |
| | 423 | 1 | 378 | 60 | 15 | 6 | 6 |
| | 425 | 1 | 379 | 60 | -15 | 16 | 16 |
| | 426 | 1 | 380 | 60 | -30 | 6 | 6 |
| | 427 | 1 | 381 | 60 | 15 | 36 | 36 |
| | 429 | 1 | 382 | 60 | 15 | 6 | 6 |
| | 429 | 2 | 383 | 90 | 0 | 48 | 48 |
| | 435 | 1 | 384 | 60 | 0 | 8 | 8 |
| | 441 | 1 | 385 | 90 | 0 | 52 | 52 |
| | 441 | 2 | 386 | 30 | 30 | 11 | 11 |
| | 441 | 3 | 387 | 90 | 0 | 37 | 37 |
| | 442 | 1 | 388 | 60 | -15 | 11 | 11 |
| | 443 | 1 | 389 | 90 | 0 | 26 | 26 |
| | 444 | 1 | 390 | 60 | -30 | 12 | 12 |
| | 445 | 1 | 391 | 30 | -15 | 6 | 6 |

APPENDIX C (CONT'D)

CAMERA OPERATIONS SUMMARY

| | Rev | Rev Op No. | Mission Op No. | Scan Angle (degrees) | Scan Center (degrees) | Forward (frames) | Aft (frames) |
|---|---|---|---|---|---|---|---|
| RV-4 | 445 | 2 | 392 | 30 | 30 | 7 | 7 |
| | 445 | 3 | 393 | 60 | 0 | 12 | 12 |
| | 445 | 4 | 394 | 60 | 0 (ESD CAM B) | | |
| | 470 | 1 | 395A | 60 | 0 | 6 | 0 |
| | 472 | 1 | 396A | 90 | 0 | 26 | 0 |
| | 472 | 2 | 397B | 60 | 0 | 0 | 6 |
| | 473 | 1 | 398A | 90 | 0 | 26 | 0 |
| | 473 | 2 | 399A | 90 | 0 | 42 | 0 |
| | 473 | 3 | 400A | 90 | 0 | 53 | 0 |
| | 474 | 1 | 401A | 90 | 0 | 8 | 0 |
| | 474 | 2 | 402A | 90 | 0 | 25 | 0 |
| | 476 | 1 | 403 | 60 | 0 | 6 | 6 |
| | 476 | 2 | 404A | 60 | 0 | 39 | 0 |
| | 477 | 1 | 405 | 90 | 0 | 45 | 45 |
| | 477 | 2 | 406 | 120 | 0 | 51 | 51 |
| | 478 | 1 | 407 | 60 | 15 | 16 | 16 |
| | 479 | 1 | 408 | 60 | 15 | 11 | 11 |
| | 484 | 1 | 409 | 60 | 0 | 9 | 9 |
| | 488 | 1 | 410 | 60 | -15 | 11 | 11 |
| | 489 | 1 | 411 | 60 | -15 | 27 | 27 |
| | 489 | 2 | 412 | 60 | -15 | 14 | 14 |
| | 489 | 3 | 413 | 90 | 0 | 53 | 53 |
| | 490 | 1 | 414 | 90 | 0 | 55 | 55 |
| | 490 | 2 | 415 | 120 | 0 | 127 | 127 |
| | 491 | 1 | 416 | 60 | 30 | 16 | 16 |
| | 492 | 1 | 417 | 60 | 15 | 36 | 36 |
| | 492 | 2 | 418 | 120 | 0 | 1 | 0 |
| | | | | | | (ESD BOTH CAMERAS) | |
| | 492 | 3 | ESD | 60 | 15 | 0 | 0 |
| | 492 | 4 | 419 | 60 | 15 | 12 | 12 |

APPENDIX C (CONT'D)

CAMERA OPERATIONS SUMMARY

| | Rev | Rev Op No. | Mission Op No. | Scan Angle (degrees) | Scan Center (degrees) | Forward (frames) | Aft (frames) |
|---|---|---|---|---|---|---|---|
| RV-4 | 493 | 1 | 420 | 120 | 0 | 132 | 132 |
| | 493 | 2 | 421 | 60 | -15 | 28 | 28 |
| | 493 | 3 | 422 | 60 | -15 | 35 | 35 |
| | 493 | 4 | 423 | 60 | -30 | 6 | 6 |
| | 494 | 1 | 424 | 120 | 0 | 9 | 9 |
| | 494 | 2 | 425 | 120 | 0 | 82 | 82 |
| | 494 | 3 | 426 | 90 | 0 | 21 | 21 |
| | 495 | 1 | 427 | 60 | 15 | 6 | 6 |
| | 497 | 1 | 428B | 120 | 0 | 0 | 58 |
| | 497 | 2 | 429B | 90 | 0 | 0 | 84 |
| | 497 | 3 | 430B | 60 | 0 | 0 | 61 |

THIS PAGE
INTENTIONALLY
LEFT BLANK